

# **Microbial community ecology of marine methane seeps**

Dissertation

zur Erlangung des Doktorgrades der Naturwissenschaften

- Dr. rer. nat.-

Dem Fachbereich 2 Biologie/Chemie

der Universität Bremen

vorgelegt von

**S. Emil Ruff**

Bremen, November 2013

1. Gutachter: Prof. Dr. Antje Boetius

2. Gutachter: Prof. Dr. Rudolf Amann

1. Prüfer: Prof. Dr. Ulrich Fischer

2. Prüfer: Dr. Katrin Knittel

*« You know, if I could have my time again,*

*I think I would be a microbial ecologist. »*

Edward O. Wilson

## Summary

The detailed investigation of microbial communities, e.g. of soil or hydrothermal vent ecosystems, greatly improved our understanding of the diversity, habitat preferences and functions of microorganisms and their impact on global element cycles. The aim of this thesis was a detailed analysis of the diversity, abundance and distribution of microorganisms at marine methane seeps and the mechanisms that govern community assembly at these sites. The seep ecosystems were investigated using geochemical analyses, gene libraries, pyrosequencing, community fingerprinting and fluorescence *in situ* hybridization. Cold seep ecosystems hosted distinct microbial communities that differed from those of the surrounding seabed and were unique microbial habitat patches in the deep sea. The communities also greatly differed between seeps, covered broad ranges of richness and evenness and showed high degrees of endemism. However, despite the differences all seeps were inhabited by certain organisms – the cold seep microbiome - including key functional clades of anaerobic methane oxidizing archaea (ANME) and sulfate-reducing bacteria. Additionally, aerobic methanotrophs and thiotrophs were found at all seeps where oxygen was present. These key functional clades seemed to be influenced by environmental parameters, such as temperature, fluid flux, sediment depth and faunal activity. Bioirrigation by ampharetid tubeworms, for instance, created a habitat for aerobic *Methylococcales*, whereas vesicomid clams seemed to favor the establishment of the clade ANME-2c. Thus, niche-based processes played an important role for the community assembly at seep ecosystems. However, most of the seeps seemed to be clearly dominated by a few, globally distributed operational taxonomic units at 97% 16S rRNA gene identity (OTU<sub>0.03</sub>) of each key functional clade. Some of these OTU<sub>0.03</sub> were rare at some seep ecosystems and abundant at others. Moreover, some findings suggested that rare organisms became abundant because the environmental conditions at the seep changed supporting the importance of species sorting at seep communities. Finally, the succession of microbial communities and the emergence of ecosystem function at a cold seep were monitored showing that it may take years to develop fully functioning communities that efficiently remove the potential greenhouse gas methane. Overall this work may help to resolve the mysteries of microbial community ecology at cold seep ecosystems.

## Zusammenfassung

Die ausführliche Erforschung mikrobieller Lebensgemeinschaften, z.B. in Böden oder an Hydrothermalquellen, erweiterte unsere Kenntnisse hinsichtlich der Vielfalt und der Stoffwechsellleistungen von Mikroorganismen und ihrem Einfluss auf globale Stoffkreisläufe erheblich. Gegenstand dieser Dissertation war die Untersuchung der Vielfalt, Häufigkeit und Verteilung der Mikroorganismen an kalten Methanquellen, sowie der ökologischen Mechanismen, welche diese Gemeinschaften beeinflussten. Die Ökosysteme wurden mittels geochemischer Analysen, Genbanken, Pyrosequenzierung, *Community Fingerprinting* und Fluoreszenz *in situ* Hybridisierung beschrieben. Die mikrobiellen Gemeinschaften an Methanquellen unterschieden sich stark von jenen im umliegenden Meeresboden. Zudem unterschieden sich die Gemeinschaften einzelner Methanquellen deutlich bezüglich ihres Artenreichtums und der Artengleichheit und waren stark endemisch. Trotz der Unterschiede fanden sich an allen Standorten bestimmte Organismen – das Methanquellen-Mikrobiom – darunter waren anaerobe methanoxidierende Archaeen und sulfatreduzierende Bakterien, sowie aerobe Methan- und Schwefeloxidierer, sofern Sauerstoff vorhanden war. Diese funktionellen Gruppen schienen von Umweltfaktoren wie Temperatur, Fluidflüssen, Sedimenttiefe und Makrofauna-Aktivität beeinflusst zu werden. Bioturbation durch bestimmte Röhrenwürmer, beispielsweise, schaffte einen Lebensraum für aerobe Methanotrophe, während die Aktivität von *Calyptogena*-Muscheln scheinbar das Ansiedeln anaerober Methanoxidierer begünstigte. Ökologische Nischen spielten also eine wichtige Rolle für die Entwicklung der Ökosysteme. Die meisten Methanquellen wurden von wenigen, weltweit vorkommenden taxonomischen Einheiten (OTU<sub>0.03</sub> - mit zu 97% identischen 16S rRNA Genen) aus jeder funktionellen Gruppe dominiert. Einige dieser OTU<sub>0.03</sub> traten an manchen Standorten häufig und an anderen selten auf und schienen durch bestimmten Umweltveränderungen beeinflusst zu werden, was die Bedeutung des *Species-sorting* Prinzips für die Entstehung der Lebensgemeinschaften bestätigte. Überdies wurde die Sukzession mikrobieller Gemeinschaften beobachtet und gezeigt, dass es möglicherweise Jahre dauert bis voll funktionsfähige Biozönosen entstehen, die das Klimagas Methan effizient entfernen. Insgesamt trug diese Arbeit dazu bei, die ökologischen Prozesse, welche für die Entstehung der Lebensgemeinschaften verantwortlich sind, besser zu verstehen.

## Table of contents

|                                |           |
|--------------------------------|-----------|
| <b>Table of contents</b> ..... | <b>1</b>  |
| <b>Chapter 1</b> .....         | <b>3</b>  |
| General Introduction.....      | 4         |
| Thesis Objectives.....         | 21        |
| <b>Chapter 2</b> .....         | <b>22</b> |
| Abstract.....                  | 24        |
| Introduction.....              | 25        |
| Material and Methods.....      | 27        |
| Results and Discussion.....    | 29        |
| Conclusion.....                | 36        |
| Acknowledgements.....          | 36        |
| Figures and Tables.....        | 37        |
| References.....                | 43        |
| <b>Chapter 3</b> .....         | <b>48</b> |
| Abstract.....                  | 50        |
| Introduction.....              | 50        |
| Material and Methods.....      | 51        |
| Results.....                   | 54        |
| Discussion.....                | 61        |
| Conclusion.....                | 63        |
| Acknowledgements.....          | 63        |
| References.....                | 64        |
| <b>Chapter 4</b> .....         | <b>66</b> |
| Abstract.....                  | 68        |
| Introduction.....              | 69        |
| Material and Methods.....      | 71        |
| Results.....                   | 75        |
| Discussion.....                | 79        |
| Conclusion.....                | 83        |
| Acknowledgements.....          | 83        |
| Figures.....                   | 84        |
| References.....                | 89        |

|  |            |
|--|------------|
| <b>Chapter 5.....</b>  | <b>93</b>  |
| Abstract.....  | 95         |
| Introduction.....  | 96         |
| Material and Methods.....                                    | 99         |
| Results.....   | 103        |
| Discussion.....  | 107        |
| Conclusion.....  | 114        |
| Acknowledgements.....  | 114        |
| Figures.....   | 115        |
| References.....  | 123        |
| <b>Chapter 6.....</b>  | <b>130</b> |
| General Discussion.....                                      | 131        |
| Microbial communities at methane seep ecosystems.....        | 131        |
| Environmental heterogeneity at methane seep ecosystems.....  | 138        |
| Microbial community assembly at methane seep ecosystems..... | 140        |
| Conclusion.....  | 145        |
| Outlook.....   | 146        |
| References.....  | 147        |
| Acknowledgements.....  | 162        |
| <b>Appendix.....</b>   | <b>163</b> |
| Supporting Information Chapter 2.....                        | 164        |
| Supporting Information Chapter 3.....                        | 183        |
| Supporting Information Chapter 4.....                        | 204        |
| Miscellaneous.....   | 212        |
| Statement.....   | 216        |

# Chapter 1

## General Introduction

The description and classification of all living organisms may be one of mankind's oldest yet unaccomplished ambitions. It is the tremendous opulence of life that has fascinated generations of naturalists and researchers alike, yet we do not fully comprehend its complexity and meaning to this day. It was estimated that there are around 8.7 million eukaryotic species on Earth of which we classified around 20% (Mora et al., 2011). To complicate the matter this large number is dwarfed by the estimated number of prokaryotic species, as one ton of soil could already harbor as many as 4 million different prokaryotic species (Curtis et al., 2002). Hence, given the roughly 9000 prokaryotic species that have been described so far (Sutcliffe et al., 2012), at least 99% of prokaryotic diversity remains unknown. The need to determine the species diversity of ecosystems and how it is generated and maintained, however, has increased since ecosystems all over the world are being destroyed (Hoekstra et al., 2005). Some ecosystems were threatened by human activities before they were even discovered, for instance in the deep sea of Hikurangi continental margin off the coast of New Zealand (Baco et al., 2010). As diversity is often positively correlated with the productivity and resilience of an ecosystem, both for macroscopic (Walker et al., 1999; Folke et al., 2004; Worm et al., 2006) as well as microscopic organisms (Horner-Devine et al., 2003; Allison and Martiny, 2008; Bienhold et al., 2011) we need to foster surveys of biodiversity in general and surveys of microbial diversity in particular. Or to put it with the words of Noah Fierer and Jay Lennon (2011): *“Although the fields of ecology and biogeography have traditionally ignored microorganisms, there are no longer valid excuses for neglecting microorganisms in surveys of biodiversity”*. This thesis includes the first large survey of microbial diversity at marine methane seeps, which are widespread biodiversity hotspots of global importance. It attempts to give insights into the complexity of those communities and possible mechanisms of their assembly.

### Species diversity

Species are the most fundamental units that are used to describe and classify biodiversity. Species diversity, which consists of the two components richness and evenness, serves as a central measure and concept in ecology. Species richness refers to the number of species in a community and species evenness to the similarity of their proportional abundances (Whittaker, 1972; Tuomisto, 2012). Two very common measures to describe

and compare species diversity are the Shannon and the Simpson diversity indices. Both indices take richness and evenness into account while Shannon is more sensitive towards the rare and Simpson gives more weight to abundant taxa (Hill et al., 2003). However, it has to be considered for their interpretation that both are indices of diversity and not diversity itself (Jost, 2006).

A common drawback in ecological studies is caused by the different numbers of individuals per sample, which makes a direct comparison of the diversity found in the samples or ecosystems problematic. Species rarefaction was established to circumvent this problem of unequal sampling effort by repeated random sub-sampling of the pool of individuals (Sanders, 1968). As a result of rarefaction, each sample produces a curve with a certain slope. These curves can be used to compare richness, if certain precautions were met, which include sufficient sample sizes and equal sampling methods (Gotelli and Colwell, 2001). Another popular method is the extrapolation of observed species richness to estimate the number of species that are expected if the sampling effort would be unlimited. A very common species estimator is Chao1, which extrapolates species richness based on rare taxa in the dataset and is especially appropriate for microbial ecology (Chao, 1984).

Species diversity can be measured on different scales. Alpha diversity, also termed local or within-habitat diversity, refers to the smallest scale and describes the number of species that is found at one site or one sample (Whittaker, 1972). Beta diversity is the variation of species between sites and describes the change in community composition (Whittaker, 1972). Beta diversity is also termed species turnover or between-habitat diversity. It is either a directional variation along a gradient, such as light intensity or temperature or a non-directional variation (Anderson et al., 2011). Beta diversity can be measured based on presence/absence of species using a binary dissimilarity coefficient, such as Jaccard (Cheetham and Hazel, 1969), or based on relative abundance of species using, for instance, the Bray-Curtis dissimilarity coefficient (Bray and Curtis, 1957). Gamma diversity is the number of species found in a range of sites, such as a geographic area (Whittaker, 1972) and is the product of alpha and beta diversity.

### **Species niche**

In most ecological theories and models species diversity is inseparably connected to the number of available species niches. Although the species niche is a central concept in ecology its precise definition has been subjected to continuous debate, since its first

introduction almost one century ago (Grinnell, 1917; Whittaker et al., 1973; Leibold, 1995; Colwell and Rangel, 2009). As most of the confusion was caused by the usage of the terms niche and habitat it is necessary to clearly distinguish those two concepts (Whittaker et al., 1973). A habitat is defined as the position of a species along the physical and chemical gradients within an environment, whereas a niche is defined as the position of a species within an interacting community (Whittaker et al., 1973). Niche partitioning, or niche differentiation, leads to the coexistence of different species as they have different positions in the community. It is generally assumed that species that occupy different niches coexist whereas species that have an identical niche compete (Whittaker, 1972). The number of species that can be packed along environmental gradients is in principle very large as long as the species are in a competitive equilibrium (MacArthur, 1970).

### **Prokaryotic species definition**

The debate on the definition of a prokaryotic species is as old as microbiology itself and still in progress. So far the most reliable, but at the same time most tedious way to classify a species is the phylo-phenetic approach based on a detailed genotypic and phenotypic characterization of the organism (Rosselló-Móra and Amann, 2001, and references therein). This approach, however, is only applicable to a very small proportion of organisms as the majority of prokaryotes defy cultivation (Rappé and Giovannoni, 2003; Epstein, 2013). A major breakthrough was achieved by using ribosomal RNA as a molecular marker for evolutionary relatedness (Woese and Fox, 1977; Lane et al., 1985). It was shown that the ribosomal RNA is highly conserved throughout evolution, and that 97% 16S ribosomal RNA identity can be used as a threshold to distinguish prokaryotic species (Rosselló-Móra and Amann, 2001, and references therein), which is widely accepted until now. However, it was proposed that the species threshold may be at 98-99% 16S identity (Yarza et al., 2008, and references therein; Mende et al., 2013). During this thesis I used a threshold of 97% 16S rRNA identity and I am aware that this might not be a genuine species threshold but rather in the upper level for genus distinction. However, for the hypotheses put forward here, for the results obtained and conclusions drawn, this value has a sufficient resolution and moreover is still most widely used for comparisons of microbial diversity.

## **Concepts in community ecology**

There are four fundamental processes that create, maintain and shape the species diversity of ecosystems. These are dispersal, selection, speciation and ecological drift (Vellend, 2010). Dispersal is the movement of organisms across space, selection represents deterministic fitness differences among species, speciation creates new species and ecological drift are stochastic changes in species abundance. All ecological theories and concepts concerning community assembly are based on these processes, but differ in the relative contribution of each of them (Nemergut et al., 2013). The simplest concepts in community ecology assume that the diversity of a community is purely based on stochastic or neutral processes. All individuals in a community are strictly equivalent regarding their prospects of reproduction and extinction (Chave, 2004). Theories based on neutral processes were developed over the last decades and culminated in the unified neutral theory (Hubbell, 1997). This theory suggests that deterministic processes become ineffective over large spatial and temporal scales and thus diversity is governed by speciation and dispersal. Contrastingly, niche-based theories rely on the assumption that diversity is not shaped randomly, but caused by deterministic factors such as environmental requirements of the organisms and species interactions (Leibold, 1995). It is widely accepted among ecologists that these two fundamentally different concepts are not conflicting, but rather complementary, since both seem to be involved in the mechanisms that govern community assembly (Gaston and Chown, 2005; Leibold and McPeck, 2006; Dumbrell et al., 2010).

One possible way to combine neutral and niche-based processes on local and regional scales of diversity is realized by the metacommunity concept (Leibold et al., 2004). This concept identifies four major perspectives on metacommunities: the neutral view, the species-sorting view, the patch-dynamic view and the mass effects view, that each emphasizes different processes of potential importance in metacommunities. In the neutral view all species are similar in their competitive ability, movement and fitness. Species diversity is then derived both from probabilities of species loss (extinction, emigration) and gain (immigration, speciation). The species-sorting view emphasizes that the resource gradients or patch types cause sufficiently strong differences in the local species diversity so that patch quality and dispersal jointly affect local community composition. The patch dynamic view assumes that habitat patches are identical and that each patch is capable of containing populations. Local species diversity is limited by dispersal and dominated by local extinction and colonization. The mass-effect view

focuses on the effect of immigration and emigration on local population dynamics. In such a system species can be rescued from local competitive exclusion in communities where they are bad competitors, by immigration from communities where they are good competitors.

Most ecological theories and concepts are derived from studies and datasets concerning plant and/or animal communities. However, in spite of the four to seven orders of magnitude size difference between microbial and macrobial populations, it has been shown that microbial diversity seems to be shaped by similar processes as macrobial diversity and can be investigated using the same measures (Astorga et al., 2012). These include for instance the distance decay of community similarity (Nekola and White, 1999), which is caused by either a decrease in environmental similarity with distance (e.g. climatic gradients) or by limits to dispersal and niche width differences among taxa. The taxa-area relationship seems to be another universal concept (Arrhenius, 1921; García Martín and Goldenfeld, 2006), which relates the area of an ecosystem to the number of species it supports. Both the distance decay (Bell, 2010) and taxa-area relationships (Bell et al., 2005) have been shown to occur likewise in certain microbial communities. However, oftentimes the two concepts are not clearly separated and used analogous (Green et al., 2004; Horner-Devine et al., 2004), which is a problem for disentangling the underlying processes (L. Zinger, pers. comm.). Finally, even the latitudinal diversity gradient (Willig et al., 2003) a phenomenon that describes the decline of species diversity from the equator to the poles, was shown to apply to microbial populations of oceanic surface waters (Fuhrman et al., 2008).

In contrast microbial ecologists have described biogeographical patterns that were poorly explained by classical concepts, for instance for microbial communities of salt marshes (Martiny et al., 2011). It was claimed that classical concepts can be applied to microorganisms once we reconcile the scale of our analyses to the scale of the organisms being observed (Fierer and Lennon, 2011). However, as the dispersal of many microorganisms indeed appears to be unlimited, it seems as though we need to think about reconciling both ends of the scale and not just the small scale. Advances in microbial ecology need new conceptual and theoretical frameworks that go beyond the mainly descriptive studies (Prosser et al., 2007). With increasingly powerful survey tools, creative experiments, temporal data sets and new theoretical models, the next era of microbial biogeography promises to transform our understanding of the processes shaping all biodiversity (Hanson et al., 2012).

## Microbial biogeography

Microbial biogeography documents the spatial distribution of microbial taxa in the environment at local, regional, and continental scales (Ramette and Tiedje, 2007). For a long time it was assumed that microbial taxa do not show biogeographic patterns, due to their small size, high dispersal rate and large population sizes, following Baas-Becking's theorem of "everything is everywhere" (O'Malley, 2007). It was claimed that organisms smaller than 2 mm have a worldwide distribution (Finlay, 2002). However, in recent years evidence accumulated that some microbial populations, such as hyperthermophilic archaea of terrestrial hot-springs (Whitaker et al., 2003) and freshwater diatoms (Telford et al., 2006) show very strong endemism and dispersal limitations. Microbial biogeography was reported on all spatial scales from microhabitats such as soil pores (Ruamps et al., 2011) to global patterns such as the preferential occurrence of taxa in polar water masses (Sul et al., 2013). It was shown that endemism of microbial taxa seems to be increasing with increasing phylogenetic resolution (Nemergut et al., 2011) as bacterial taxa on phylum level were much more widespread as taxa on species level (Figure 1). Furthermore, large surveys of microbial diversity based on deep sequencing techniques revealed that in most ecosystems there are few abundant taxa, but a majority of species that occur with very low relative abundances. These rare organisms were termed the rare biosphere (Sogin et al., 2006).

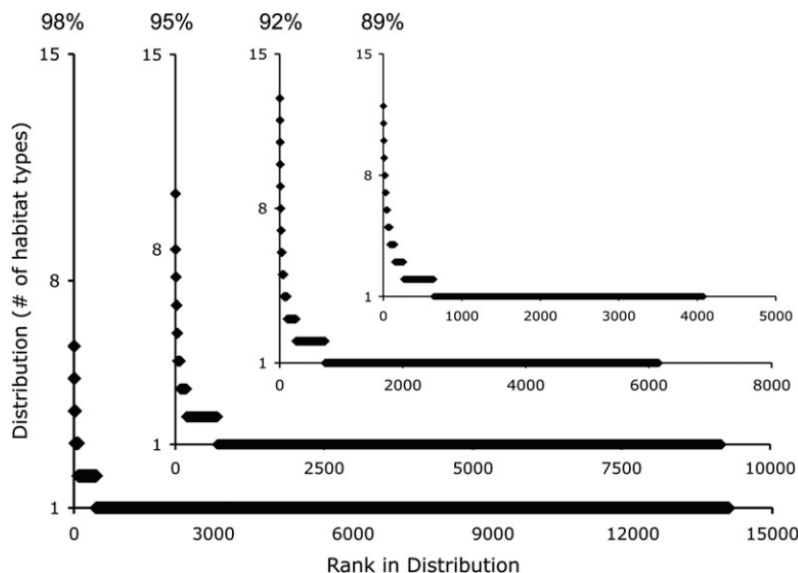


**Figure 1: Rank distribution**  
Rank distribution plots displaying the presence of OTUs in different numbers of habitat types. At all OTU definitions, the vast majority of lineages were observed in only a single habitat type. Adapted from (Nemergut et al., 2011).

## **Rare Biosphere**

Since the first description of the rare biosphere in surface waters of the North Atlantic (Sogin et al., 2006) this phenomenon was repeatedly shown also in other ecosystems including soil (Elshahed et al., 2008), sediments (Hamdan et al., 2013), coastal sands (Gobet et al., 2012), hydrothermal vent fluids (Huber et al., 2007) and sea water (Galand et al., 2009; Caporaso et al., 2012; Gibbons et al., 2013). Those studies show that around 30% of all microbial OTU<sub>0.03</sub> (operational taxonomic units at a 97% 16S rRNA identity cut-off) are present only once in a given dataset, regardless of the realm of origin. These OTU<sub>0.03</sub> are referred to as absolute single sequence OTUs (SSO<sub>abs</sub>) (Gobet et al., 2012). Organisms that occur once in one sample, but are more common in other samples of the dataset are termed relative single sequence OTUs (SSO<sub>rel</sub>) (Gobet et al., 2012). SSO<sub>abs</sub> are permanently rare organisms and thus may represent inactive cells, fossil DNA, spores or contaminations. Contrastingly, SSO<sub>rel</sub> are organisms that are rare in one ecosystem, but very common or even dominant in another ecosystem. These organisms belong to a seed bank (Gibbons et al., 2013) and may spawn when the conditions change, which was shown for pelagic communities where rare organisms became abundant after disturbance (Sjöstedt et al., 2012) or showed seasonal patterns (Hugoni et al., 2013). Remarkably, these dynamics between rare and abundant were also shown for plants (Murray et al., 1999). Furthermore, despite their low abundance rare microbial organisms were disproportionally active in surface waters of the ocean (Campbell et al., 2011; Hunt et al., 2013) and contributed significantly to ecosystem functions, such as sulfate reduction in peat soils (Pester et al., 2010). In addition it was shown that dormant cells that often belong to the rare biosphere contribute to the maintenance of diversity especially in nutrient-poor ecosystems (Jones and Lennon, 2010) such as ecosystems in the deep-sea. These ecosystems, however, are very hard to access due to their remoteness and thus in general are poorly understood, despite their global significance.

## **Marine benthic ecosystems**

The ocean is the largest environment on Earth and is divided into pelagic (referring to the water column) and benthic (sedimentary) ecosystems (Figure 2). Marine benthic ecosystems comprise a multitude of microbial habitats and harbor roughly one third of Earth's microbial biomass (Kallmeyer et al., 2012). Most of the biomass is found in the deep biosphere, which is generally applied to marine sediments deeper than one meter below the seafloor. The subsurface harbors around  $3 \times 10^{29}$  cells (Kallmeyer et al., 2012)

and seems to be dominated largely by heterotrophic organisms, especially of the phylum *Crenarchaeota* (Lipp et al., 2008; Kubo et al., 2012; Lloyd et al., 2013). Most of this hidden life is active and seems to be sustained by large amounts of buried organic carbon (Parkes et al., 2007). It was shown that despite decreasing cell numbers with increasing depth life extends down to kilometers below the seafloor with temperature being likely the only limit of microbial life. Carbon turnover and growth are extremely slow which results in microbial generation times of up to millennia (Hoehler and Jørgensen, 2013). Although some subsurface organisms have been successfully cultivated little is known about microbial community structure and function (D'Hondt et al., 2004). Microbial community size however, is controlled by the total energy flux that is available in these sediments (Roy et al., 2012).

The most diverse marine microbial communities are found in surface sediments of coasts, coral reefs and the deep sea (Gaidos et al., 2010; Bolhuis and Stal, 2011; Zinger et al., 2011; Gobet et al., 2012). The majority of deep sea surface microorganisms also has heterotrophic lifestyles (Lloyd et al., 2013) and lives on particulate organic matter (POM) that was produced in the photic zone being slowly exported to the deep sea (Witte et al., 2003; Bienhold et al., 2011; Jacob et al., 2013). In addition to the sedimentation of POM there are large organic matter pulses to the oligotrophic deep-sea, such as whale falls and wood falls. These materials are quickly colonized, profoundly change the surrounding seafloor and sustain complex microbial and faunal communities for decades (Treude et al., 2009; Goffredi and Orphan, 2010; Bienhold et al., 2013).

However, not all ecosystems of the dark ocean are fuelled by photosynthesis, as there are patches of reduced habitats driven by inorganic compounds derived from the Earth's interior (Jørgensen and Boetius, 2007). The most spectacular of these ecosystems are hydrothermal vents that occur along spreading zones, such as Mid-oceanic ridges. Super-heated, reduced fluids that form by the interaction of sea water and hot mantle rock, are discharged from the crust and fuel complex ecosystems (Tivey, 2007). At the base of these ecosystems are chemoautotrophic microorganisms that convert chemical energy, mainly hydrogen, methane and reduced sulfur compounds into biomass (Sievert and Vetriani, 2012). These microorganisms are either free-living and colonize the chimneys (Brazelton et al., 2010; Flores et al., 2012) and surrounding sediments (Schauer et al., 2011) or they are symbionts of marine invertebrates (Dubilier et al., 2008). The faunal communities are characterized by extremely high densities of biomass and a high degree of endemism (Rogers et al., 2012). Less spectacular, but as widespread and fascinating

as hydrothermal vents are cold seep ecosystems that are driven by fluids enriched in methane and other hydrocarbons from the subsurface. These cold seeps have received much attention from the scientific community due to their importance in the global carbon cycle and their impact on climate change.

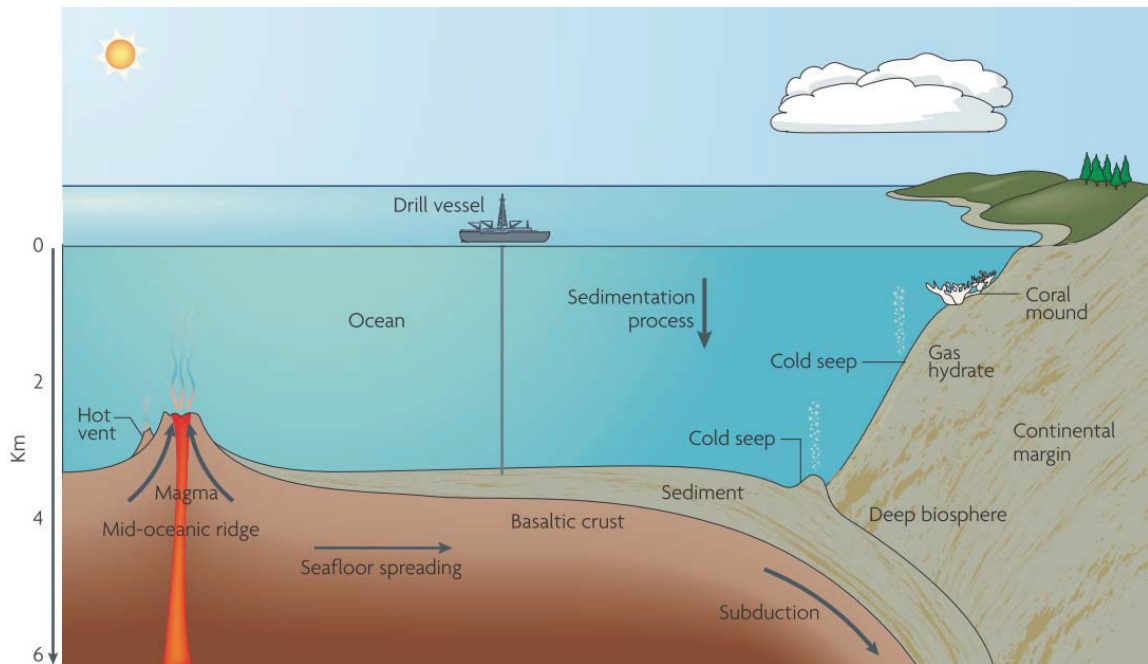


**Figure 2: Vertical section of the seabed and seafloor structures**

Hydrothermal vents and cold seeps, which are typically found at mid-oceanic ridges or continental margins, respectively, are driven by reduced inorganic compounds. In contrast, benthic communities of normal deep sea sediments and the deep biosphere are mainly fuelled by sedimenting organic matter from the ocean surface. Adapted from (Jørgensen and Boetius, 2007).

### **Cold seep ecosystems**

Oceanic sediments contain around 550 gigatons of carbon (Gt C) in the form of methane hydrates (Pinero et al., 2013) and at least 200,000 Gt C as buried organic matter in the deep sediment layers of continental margins (Boetius and Wenzhöfer, 2013). A very small fraction of the oceanic carbon reservoir of around 0.03 Gt C per year is released via cold seeps (Boetius and Wenzhöfer, 2013). Cold seeps occur at areas of the seabed, where methane from the subsurface is released to the water column via conduits in the sediment. Methane seepage is a globally significant process that occurs in all oceans and seas mainly along continental margins (Figure 3) (Judd, 2003).

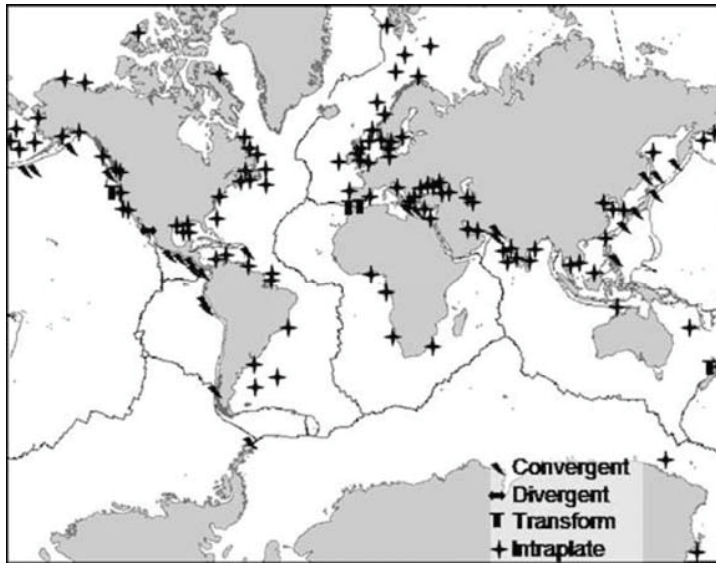


**Figure 3: Seabed fluid flow**

This map shows the sites with seabed fluid flow and their relation to tectonic settings. Occurrences of seabed fluid flow are identified by the following features: Gas seeps, cold seep communities, methane-derived authigenic carbonate, pockmarks, shallow gas, gas hydrates. Adapted from (Judd, 2003).

Between 20% and 80% of the methane (in total 0.01 Gt C per year) is consumed by methanotrophic microorganisms at the sediment water interface and around 0.02 Gt of carbon are released to the water column (Boetius and Wenzhöfer, 2013), where it is oxidized by pelagic methanotrophs (Schubert et al., 2006; Lesniewski et al., 2012). The amount of methane that is released to the water column increases with increasing size of the seepage site and fluid flux rate (Figure 4) (Reeburgh, 2007).

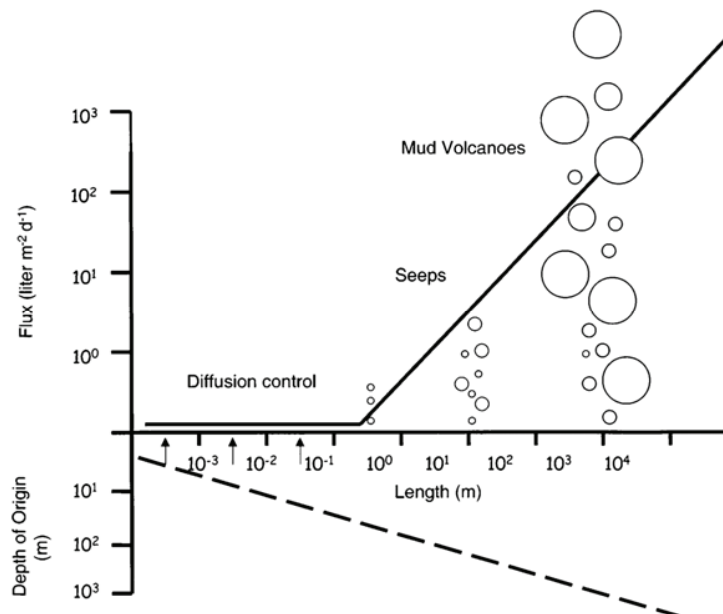


**Figure 4: Seepage intensity**

Schematic diagram showing the length, depth, and flux scales of methane additions from a range of sources to the ocean water column (Reeburgh, 2007).

The first cold seeps were discovered in the Gulf of Mexico around 30 years ago (Paull et al., 1984; Kennicutt et al., 1985) and turned out to be oases of life that support some of the most diverse and biomass-rich faunal assemblages in the oceans (Baker et al., 2010). Common cold seeps are small patches of several square meters that are covered by either bacterial mats or seep-associated marine invertebrates and are very widespread on continental margins. Mud volcanoes are the largest cold seep structures in the ocean seabed and it was estimated that up to 100.000 submarine mud volcanoes exist worldwide (Milkov, 2000). They can be up to a few kilometers wide, exist over long time periods and are formed by upwards migrating fluidized mud from the subsurface (Niemann and Boetius, 2010). These muds can originate from several kilometers depth and persistently discharge for several hundred thousand years (Perez-Garcia et al., 2009). Mud volcanoes generally feature very high fluid fluxes in their center that are gradually decreasing towards the periphery (De Beer et al., 2006; Foucher et al., 2010; Lichtschlag et al., 2010) and are often highly dynamic (Feseker et al., 2009). At tens or hundreds of meters diameter pockmarks are smaller than mud volcanoes, but even more frequent. Pockmarks are crater-like depressions that likely form by the rapid eruption of gas and porewater (Hovland et al., 2002). Methane seepage in the anoxic Black Sea results in remarkable features that were termed microbial reefs. Here, oxygen-sensitive, methanotrophic microorganisms which usually occur only in the sulfidic sediments build carbonate structures of several meters height (Michaelis et al., 2002).

### **Seep-associated fauna**

The seep-associated fauna at cold seeps relies in most cases on chemosynthetic microorganisms at the base of the food chain that convert the chemical energy into organic compounds that are available for higher trophic levels (Levin, 2005). The most common and well-studied cold seep animals are vesicomyid clams (Decker et al., 2013) (Figure 5A), mytilid mussels (Duperron et al., 2011) (Figure 5B) and siboglinid tubeworms (Lösekann et al., 2008; Sommer et al., 2009; Hilário et al., 2011) (Figure 5C). These animals harbor chemosynthetic endosymbionts that convert reduced inorganic compounds, such as methane, sulfide and hydrogen into organic molecules that the host is able to metabolize (Dubilier et al., 2008; Petersen et al., 2011). However, seep-associated fauna does not always depend on symbionts, since there are heterotrophic animals that feed upon the lithotrophy-derived microbial biomass. Among those are copepods and nematodes (Van Gaever et al., 2009b), arthropods (Niemann et al., 2013),

dorvilleid polychaetes (Thurber et al., 2012) and ampharetid polychaetes (Thurber et al., 2010). Ampharetids were often found at seeps, but were only recently found to be the dominant fauna at seeps of the Hikurangi and Makran margins (Sommer et al., 2010; Fischer et al., 2012).

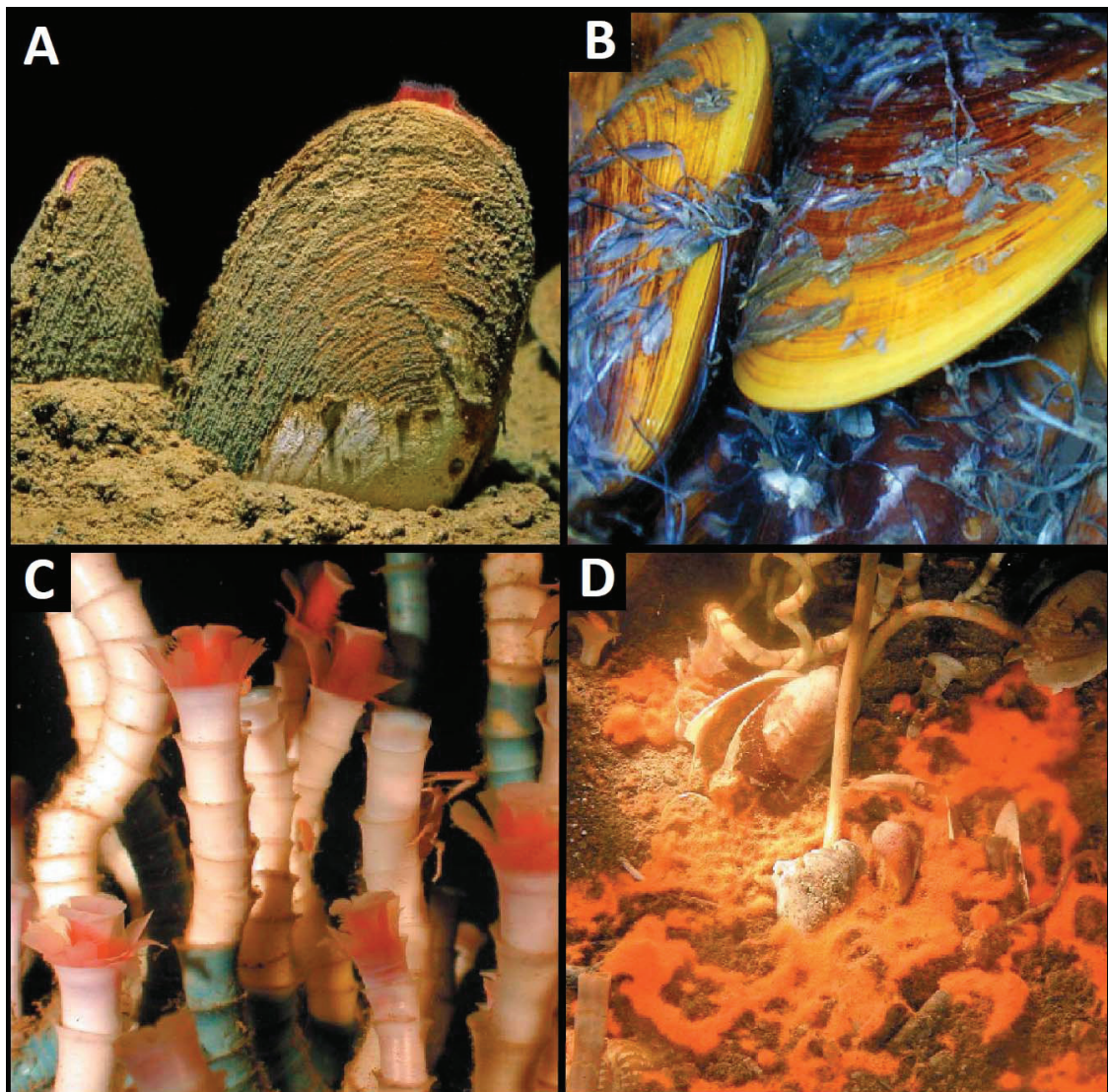


**Figure 5: Seep-associated organisms**

A: Vesicomyid clams dig with their foot into the seep sediment to take up sulfide that is used by their thiotrophic endosymbionts (Image courtesy MBARI). B: Mytilid mussels of the genus *Bathymodiolus* live on the sediment surface and harbor thio- and methanotrophic endosymbionts (Image courtesy NOAA). C: *Lamellibrachia* tubeworms within the family *Siboglinidae* can live for centuries, which was determined by staining their chitin tube (blue part). They deeply “root” in the seep sediment and contain thiotrophic endosymbionts. D: Orange mats of large sulfur bacteria that oxidize sulfide at the sediment-water interface (C and D adapted from (Boetius, 2005)).

The diversity of seep-associated animals is influenced by habitat heterogeneity due to biotic and abiotic factors (Cordes et al., 2010). These factors include trophic niches (Levin et al., 2013), sulfide fluxes (Barry and Kochevar, 1998; Levin et al., 2003), methane fluxes (Olu-Le Roy et al., 2007; Pop Ristova et al., 2012), the substrate on which the organisms grow (Ritt et al., 2011), the sediment disturbance (Van Gaever et al., 2009a) and the water depth (Sibuet and Olu, 1998). In contrast, the seep fauna also causes habitat heterogeneity and greatly impacts the seep ecosystem by altering the geochemistry and thus creating niches. It was proposed that siboglinid tubeworms release internally produced sulfate to the sediment through extensions of their body and thus influence the sulfur cycle by replenishing the sulfate pool (Arvidson et al., 2004; Cordes et al., 2005; Dattagupta et al., 2008). Additionally, they alter the physical environment of the sediment water interface due to the protrusion of their bodies into the water column (Sommer et al., 2009). Clams and mussels irrigate their immediate environment and influence benthic fluxes (Wallmann et al., 1997; Menot et al., 2009).

### **Microbial communities at cold seep ecosystems**

Microorganisms are at the base of the food chain at all cold seep ecosystems because they are the primary producers of biomass and catalyze vital ecosystem functions such as aerobic and anaerobic methanotrophy, sulfate reduction and sulfide oxidation.

Aerobic methanotrophic bacteria are found in the oxic sediment layers (Yan et al., 2006; Lösekann et al., 2007; Tavormina et al., 2008; Wasmund et al., 2009) and as symbionts of mussels (Duperron et al., 2008; Duperron et al., 2011) and siboglinids (Sommer et al., 2009). The aerobic methanotrophs at cold seeps belong to the order *Methylococcales* within the *Gammaproteobacteria*. They seem to play a major role at mud volcanoes, where sulfate is limiting due to high fluid fluxes and the sediment is disturbed frequently (Lösekann et al., 2007; Felden et al., 2010; Felden et al., 2013). At most cold seeps the oxic sediment layer is usually very thin. Thus, although the diversity of aerobic methanotrophs can be high, they do not appear to have a major impact on the overall removal of methane (Yan et al., 2006; Wasmund et al., 2009; Roalkvam et al., 2011). An exception is found at Hikurangi margin ampharetid seeps. Here, very high rates of methane oxidation and total oxygen uptake indicated the presence of an active and biomass-rich community of aerobic methanotrophs in the sediment (Sommer et al., 2010).

Anaerobic methanotrophic archaea (ANME) predominate the anoxic sulfidic sediment and mainly occur in consortia with sulfate-reducing bacteria (SRB). These

consortia perform the anaerobic oxidation of methane (AOM) coupled to sulfate reduction (SR) (Knittel and Boetius, 2009). ANME belong to the class *Methanomicrobia* and are subdivided in the major clades ANME-1, ANME-2 and ANME-3 (Hinrichs et al., 1999; Orphan et al., 2002; Niemann et al., 2006) (Figure 6), which are subdivided into the subgroups ANME-1a, ANME-1b, thermophilic ANME-1, ANME-2a-c and the newly described *Cand. Methanoperedenaceae* (Orphan et al., 2001; Teske et al., 2002; Holler et al., 2011; Biddle et al., 2012; Merkel et al., 2012; Haroon et al., 2013).

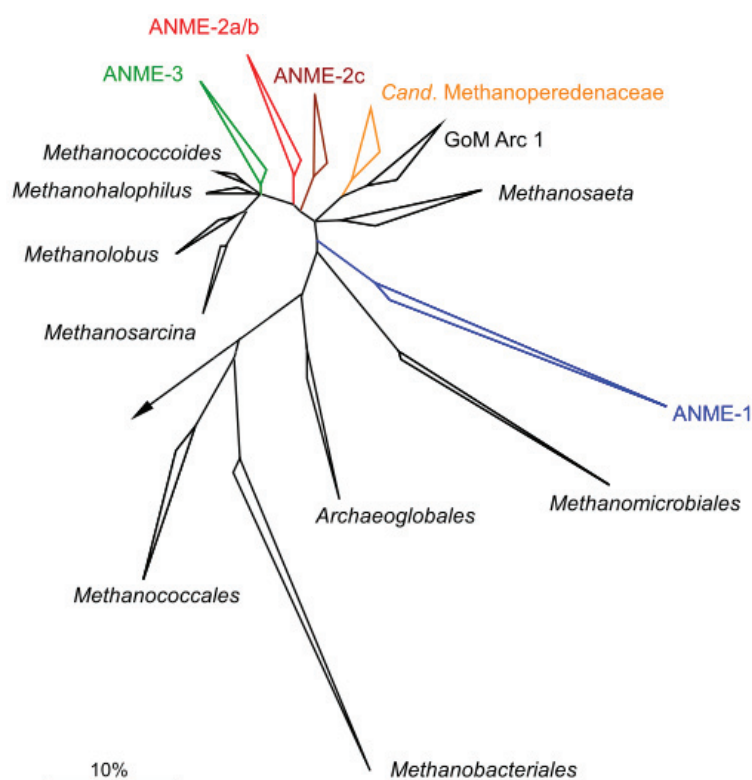


**Figure 6: ANME Phylogeny**  
Phylogenetic tree showing the affiliations of ANME 16S rRNA gene sequences to selected reference sequences of the domain *Archaea*. Bar, 10% estimated sequence divergence. Modified after (Knittel and Boetius, 2009).

Sulfate reducers are commonly found in anoxic sediments, since sulfate is a ubiquitous electron acceptor commonly used for the degradation of hydrocarbons or organic matter (Muyzer and Stams, 2008). The SRB involved in AOM belong to the class *Deltaproteobacteria* and are subdivided into several clades being related to either *Desulfosarcina* (DSS) or *Desulfobulbus* (DBB) (Schreiber et al., 2010; Kleindienst et al., 2012) (Figure 7). At the majority of seep sites ANME-1 and ANME-2 tend to aggregate with the DSS relatives SEEP-SRB-1 (Schreiber et al., 2010), whereas ANME-3 aggregates with DBB relatives (Niemann et al., 2006).

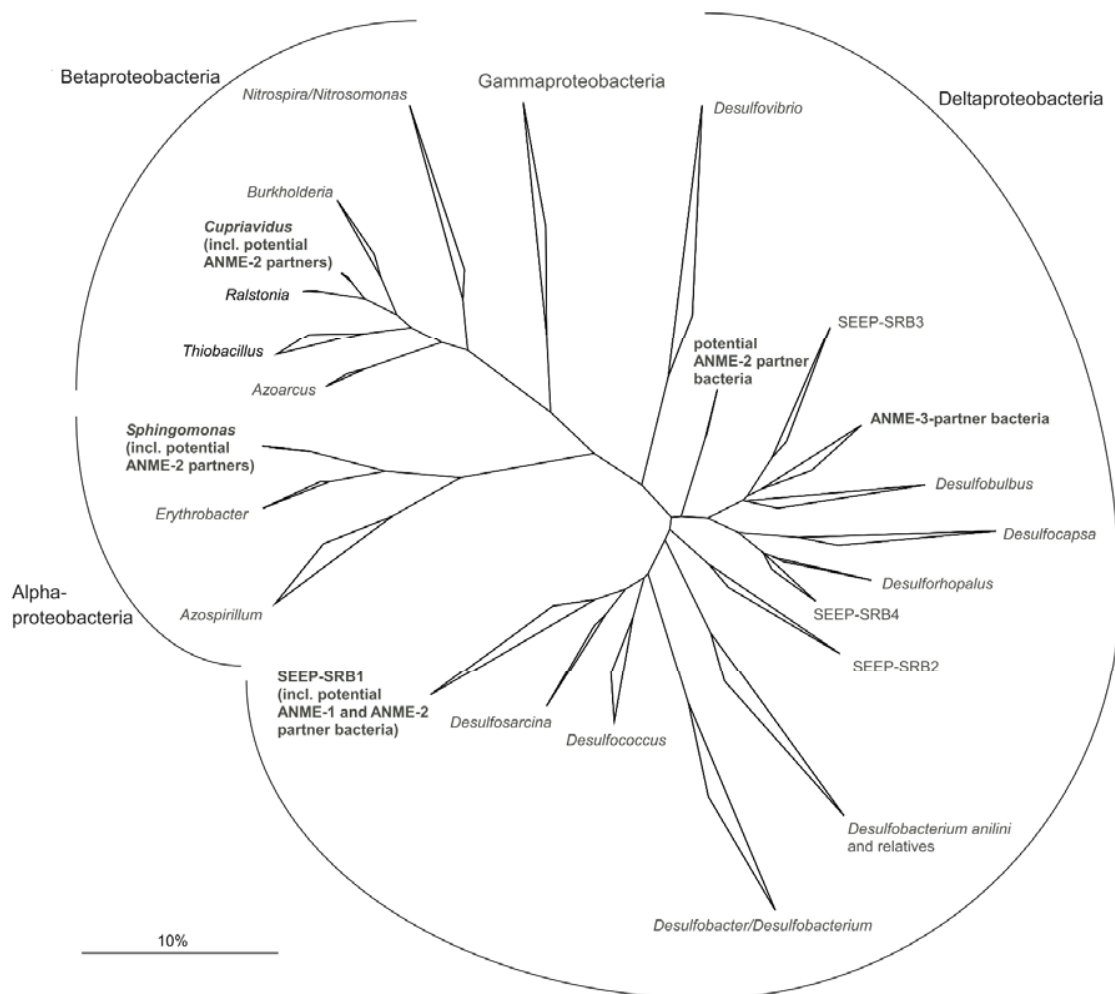


**Figure 7: Phylogeny of ANME-associated bacteria**

Phylogenetic tree showing the affiliations of 16S rRNA gene sequences of ANME partner bacteria to selected reference sequences. *Desulfosarcina* relatives of the SEEP-SRB1 cluster and *Desulfobulbus* relatives have been repeatedly shown to be associated with ANME-1/ ANME-2 and ANME-3, respectively. Other potential partner bacteria from different proteobacterial lineages are indicated. Bar, 10% estimated sequence divergence (Knittel and Boetius, 2009).

Sulfide oxidizers at seeps mainly belong to the gammaproteobacterial family *Beggiatoaceae* and form mats of white, yellow or orange color that cover areas of up to one hundred square meters (Joye et al., 2004; Mills et al., 2004; Knittel et al., 2005; Lloyd et al., 2010; Grünke et al., 2012; Meyer et al., 2013) (Figure 5D). *Beggiatoa* spp. are large, filamentous bacteria that oxidize the sulfide that is produced during AOM using oxygen or nitrate (Preisler et al., 2007). *Thiomargarita* are spherical cell and are less widespread at seeps (Girnth et al., 2011). Some seeps also feature mats of epsilonproteobacterial

*Campylobacteriales*, such as *Arcobacter* (Omoregie et al., 2008; Grünke et al., 2011) and *Sulfurovum* (Roalkvam et al., 2011). Sulfide oxidizers are also common symbionts of marine invertebrates, such as mussels, clams and siboglinids (Dubilier et al., 2008, and references therein).

Moreover, cold seeps frequently harbor other archaeal and bacterial clades with as yet unknown functions. These commensals include archaea of Marine Benthic Group B, *Thermoplasmatales* and GoM Arc1, as well as bacteria of the candidate phylum JS1, *Planctomycetes*, *Alphaproteobacteria*, *Betaproteobacteria* (Figure 7) and *Chloroflexi* (Mills et al., 2005; Pernthaler et al., 2008; Harrison et al., 2009; Knittel and Boetius, 2009; Chevalier et al., 2013). It was suspected that these organisms might have a direct or indirect role for important ecosystem functions, such as JS1 was suspected to be involved in methane-derived carbon metabolism (Chevalier et al., 2013), however the role of all of these clades remains elusive and is an important research topic.

### **Habitats of methanotrophs at cold seep ecosystems**

It has been shown that microbial communities often differ substantially between cold seeps, which is especially well-documented for the methanotrophic clades (Boetius and Knittel, 2010), however their niche preferences are still largely unknown. Aerobic *Methylococcales* are often found in the oxic sediment layers of mud volcanoes (Niemann et al., 2006; Pachiadaki et al., 2010; Felden et al., 2013). This may be because the aerobic methylootrophs outcompete the anaerobic methanotrophs in hot or disturbed sediments of high fluid flow regimes due to their faster growth rates (Felden et al., 2013). It was also indicated that aerobic methanotrophy was a major pathway in bioirrigated sediments inhabited by tubeworms (Fischer et al., 2012) and the occurrence of aerobic methanotrophs was reported in deeper sediment layers (Pachiadaki et al., 2010; Roalkvam et al., 2011).

Although evidence for niche preferences of ANME are accumulating they are not resolved yet and in some cases even contradictory. ANME-1 seems to be adapted to deeper sediment layers, often featuring high sulfide and low sulfate concentrations (Elvert et al., 2005; Knittel et al., 2005; Niemann et al., 2005; Wegener et al., 2008; Roalkvam et al., 2011; Yanagawa et al., 2011; Vigneron et al., 2013). A thermophilic subgroup of ANME-1 occurs in hydrothermal sediments (Teske et al., 2002; Biddle et al., 2012) and hydrothermal fluids (Merkel et al., 2012). Another subgroup ANME-1b was found to dominate hypersaline sediments (Lloyd et al., 2006), however other hypersaline sediments

harbored different ANME-1 and also ANME-2 (Lazar et al., 2011). ANME-2 seems to be a versatile clade that occurs preferentially at sulfate-penetrated sulfide-rich surface sediments (Elvert et al., 2005; Knittel et al., 2005; Wegener et al., 2008; Rossel et al., 2011; Yanagawa et al., 2011). Its subclade ANME-2a is found often in high methane fluid regimes and above hydrates (Elvert et al., 2005; Knittel et al., 2005; Lösekann et al., 2007; Wegener et al., 2008), whereas ANME-2c seems to prefer low methane fluxes or bioturbated sediments (Elvert et al., 2005; Knittel et al., 2005; Wegener et al., 2008). However ANME-2 were found in the deep biosphere (Roussel et al., 2008) and ANME-2c were also reported from deep sulfidic, sulfate-depleted sediments (Roalkvam et al., 2011). Finally ANME-3 seems to be fairly widespread in surface sediments at cold seeps, but mostly rare (Knittel et al., 2005; Lazar et al., 2011; Vigneron et al., 2013), except at seeps that are influenced by very cold water masses from polar regions (Niemann et al., 2006; Niemann et al., 2009). Contrastingly, ANME-3 were also found in the deep subsurface (Roussel et al., 2008). These contradicting results underline that the ecological niches of these key functional organisms are far from being resolved and emphasize the need for more comprehensive and large-scale studies. Ideally, these studies should investigate not only the diversity, but also the abundance and distribution of organisms as well as environmental data that can be correlated to the emerging patterns.

## Thesis objectives

The overall aim of this thesis was to thoroughly describe the microbial communities of globally distributed cold seep ecosystems to deduce possible niches of the key functional organisms and infer mechanisms that establish and shape their diversity. I investigated the ecosystems using community fingerprinting, gene libraries and pyrosequencing to describe the microbial lineages. In addition, I determined the in situ abundance of some major clades using cell staining methods and finally analyzed biogeochemical and environmental data to describe the major processes. Subsequently, the large amount of data was integrated to elucidate the following hypotheses:

1. Despite the large differences in microbial community structure found at methane seeps on a local level there are distinct microbial populations that are shared between the ecosystems, due to the outstanding biogeochemistry of methane seeps.

I investigated the microbial communities of 50 sediment samples from 23 cold seep sites of 15 areas and compared them to each other and previously described ecosystems (Chapter 1-4).

2. Niche differences and the extent of local diversity at cold seeps are strongly impacted by biogeochemistry and the seep-associated fauna.

I analyzed the impact of environmental parameters on community structure (Chapter 1, 2) as well as the interaction between microorganisms, biogeochemistry and fauna (Chapter 2-4).

3. The diversity of microbial communities at marine methane seeps is shaped by niche-based and neutral processes.

I integrated the results and patterns of all Chapters based on classical ecological theory and discussed ecological concepts that are potentially involved in community assembly at cold seep ecosystems.

## Chapter 2

**The cold seep microbiome:  
Bacterial and archaeal diversity of methane-fueled seafloor  
systems compared to other marine benthic environments**

S. Emil Ruff<sup>1, 2</sup>, Jennifer F. Biddle<sup>3</sup>, Andreas Teske<sup>4</sup>,  
Katrin Knittel<sup>2</sup>, Alban Ramette<sup>1</sup>, Antje Boetius<sup>1,5,6</sup>

- 1: HGF MPG Group for Deep Sea Ecology and Technology;  
Max Planck Institute for Marine Microbiology, Bremen
- 2: Department of Molecular Ecology;  
Max Planck Institute for Marine Microbiology, Bremen
- 3: College of Earth, Ocean and Environment, University of Delaware
- 4: Department of Marine Sciences, University of North Carolina
- 5: Alfred Wegener Institute Helmholtz Center for Polar and Marine  
Research, Bremerhaven, Germany
- 6: FB5 Geosciences, University of Bremen

Relevant contributions:

I have developed the concepts and ideas together with A. Ramette, K. Knittel and A. Boetius. I processed the data, optimized the bioinformatics routine, analyzed and visualized the data and wrote the manuscript with assistance from all co-authors

## Abstract

Methane seeps are distinct seafloor ecosystems shaped by the emission of methane from seabed reservoirs and its consumption by methanotrophic archaea and bacteria providing the primary source of energy and carbon to proliferous seep communities. Here we tested the hypothesis that methane-fueled seafloor habitats host a microbiome distinct from that of hydrothermal vents, coastal sediments and deep-sea surface and subsurface sediments. Using pyrosequencing of the hypervariable V6 region of the bacterial and archaeal 16S rRNA gene, we found that seafloor microbiomes overlap at phylum level, but show a high diversity and increasing specificity at and below class level, analogous to human, animal and plant microbiomes. Methane seep and vent communities showed the highest degree of endemism. Global methane seep communities varied substantially in diversity, richness and community structure, but the ubiquitous occurrence and high relative sequence abundance of taxa such as *Methanosarcinales*, *Desulfobacterales* and candidate phylum JS1 distinguished the methane seep microbiome from other seafloor microbiomes. The globally distributed metacommunity of key functional clades, including methanotrophs, sulfate reducers and thiotrophs consisted of relatively few microbial taxa, which seem to be responsible for most of the microbial biomass at methane seeps worldwide. Heterotrophic groups overlapped between seeps and other deep-sea sediments at the class to order level, but comprised different taxa at a higher phylogenetic resolution. Between different seeps, the relative abundance of the key taxa varied from rare to dominant, indicating a strong effect of environmental filtering according to the species-sorting paradigm in community ecology.

## Introduction

The assessment and comparison of microbial assemblages of different environments such as air (Bottos et al., 2013), soils (Fierer et al., 2012), oceans (Gibbons et al., 2013), plants (Turner et al., 2013), animals (Ezenwa et al., 2012) and humans (Le Chatelier et al., 2013) has become a major challenge in microbial ecology. Global surveys showed that each of these different realms was found to host distinct communities of bacteria and archaea, also coined “microbiome”. A core microbiome comprises microbial taxa which are commonly represented across a range of variables such as space, time, physicochemical conditions and biological interactions (Shade and Handelsman, 2012). It is assumed that such global associations are based on adaptations and specific interactions of microbial taxa with each other and their specific habitat or host, and that the represented taxa contribute relevant functions to their ecosystem (Hamady and Knight, 2009; Turnbaugh et al., 2009; Huse et al., 2012). A key question in the definition of microbiomes concerns the role of environmental forces and assembly rules structuring community composition (Levy and Borenstein, 2013), such as habitat-filtering by selection of organisms according to their niche preferences, biological interaction such as competition and cooperation, phylogenetic co-occurrence or stochastic dispersal processes (Fierer and Lennon, 2011; Hanson et al., 2012).

Insight into the microbial diversity of marine seafloor ecosystems has increased tremendously in recent years with the use of high-throughput sequencing methods and global databases (Zinger et al., 2011) (<http://icomm.mbl.edu/>). Analyses of seafloor archaeal and/or bacterial communities included hydrothermal vents (Huber et al., 2007; Campbell et al., 2013), subsurface sediments (Biddle et al., 2011; Briggs et al., 2012; Jørgensen et al., 2012), deep-sea sediments (Bienhold et al., 2011; Durbin and Teske, 2011; Hamdan et al., 2013; Jacob et al., 2013), coastal sediments (Gaidos et al., 2010; Gobet et al., 2012) and cold seep sediments (Pernthaler et al., 2008; Stokke et al., 2012). It has been found that marine sediments host as diverse communities as soils (Torsvik et al., 2002), and that they are also characterized by high turnover on small (decimeter to kilometer) to intermediate (hundreds of kilometers) spatial scales (Martiny et al., 2006; Ruff et al., 2013). Community turnover was also related to water depth (Hewson et al., 2007; Bienhold et al., 2011), or sediment depth (Urakawa et al., 2000; Böer et al., 2009; Ruff et al., 2013). Generally benthic (seafloor-hosted) microbial communities of the ocean are distinct from pelagic (seawater-hosted) communities (Zinger et al., 2011) and were found

to vary with energy availability in the form of deposited organic matter (Bienhold et al., 2011; Jacob et al., 2013; Jamieson et al., 2013).

Here we have investigated the composition of archaeal and bacterial communities of a distinct type of benthic ecosystem called “methane seep”, defined by the upward advection of methane from the subsurface seabed to the seafloor (Boetius and Wenzhöfer, 2013). Methane seep ecosystems are found around the world at all continental margins. Typically, the sediments of methane seeps are highly reduced, and oxygen availability is often limited to a few millimeters to centimeters. They are characterized by rich benthic communities fueled by the microbial conversion of methane to different energy sources (Levin, 2005). At the seafloor, where the electron donor methane meets microbial electron acceptors such as oxygen, sulfate, iron or manganese, the sediments host diverse types of methanotrophs, which convert the chemical energy in methane to a range of products utilized by other functional taxa such as thiotrophs, ferrotrophs and organotrophs (Orphan et al., 2002; Knittel et al., 2005; Niemann et al., 2006; Omoregie et al., 2008; Tavormina et al., 2008; Beal et al., 2009; Holler et al., 2011; Milucka et al., 2012; Ruff et al., 2013).

In this study we analyzed the microbial diversity of 23 globally distributed methane seeps and compared it to five other seafloor realms (deep sulfate methane transition zones (SMTZ), hydrothermal vents, coastal sediments and deep sea surface and subsurface sediments) represented by 50 sites. These different seafloor realms are distinct in their faunal composition showing little to no species overlap (Baker et al., 2010). However, it is yet unknown if their microbial communities are as distinct and to what extent they overlap. In this study, pyrosequencing of DNA samples extracted by standardized protocols was used to gain insight into the diversity, distribution and biogeography of microorganisms (Zinger et al., 2011; Amend et al., 2012). The main objectives were to compare richness, evenness,  $\beta$ -diversity parameters and community composition across different seep ecosystems and other seafloor environments. The main hypotheses tested were: i) methane seeps host distinct microbiomes that differ from those of other benthic ecosystems ii) microbial communities of methane seeps and SMTZ are similar and share a core microbiome iii) the diversity of key functional organisms at methane seeps is low since environmental filtering in this extreme seafloor habitat is high.

## Material and Methods

### Dataset specification

This study is based on a sample set obtained from 23 globally distributed methane seeps and four SMTZ provided to the International Census of Marine Microbes (ICOMM) pipeline (<http://icomm.mbl.edu>). The seep samples originate from the Atlantic, North Pacific and the Southern Ocean, the Gulf of Mexico and the Black Sea (Figure S1, Table S1). For a comparison with other seafloor realms, we additionally analyzed 14 hydrothermal vent samples, 17 coastal sediment samples, 14 deep-sea surface and 5 deep subsurface sediment samples, provided by the ICOMM project (Figure S1, Tables S2, S3). For 29 of the additional samples archaeal information was lacking. The full ICOMM 454 microbial 16S pyrotag dataset and contextual geospatial parameters are available on the web (VAMPS site: <http://vamps.mbl.edu>, MICROBIS site: <http://icomm.mbl.edu/microbis>).

### Generation of pyrotags, quality control and taxonomic annotation

DNA extraction was carried out by a standardized protocol as described on the MICROBIS project pages (<http://icomm.mbl.edu/microbis>) using commercial extraction kits. The hypervariable V6 region of the 16S rRNA gene was PCR amplified using one forward and two reverse primers for archaea (Arch958F/Arch1048R<sub>mix</sub>) and four forward and four reverse primers for bacteria (Bac967F<sub>mix</sub>/Bac1064R<sub>mix</sub>). Details for primer are provided under (<http://vamps.mbl.edu/resources/prim.php>). Massively parallel tag sequencing of the PCR products was carried out on a 454 Life Sciences GS FLX sequencer at Marine Biological Laboratory, Woods Hole, MA. The sequence reads were submitted to a rigorous quality control procedure based on mothur v24 (Schloss et al., 2009), which includes denoising of the flow grams using an algorithm based on PyroNoise (Quince et al., 2009), removal of PCR errors and a chimera check using uchime (Edgar et al., 2011). Archaeal and bacterial reads longer than 79 and 74 bases, respectively, were clustered at 97% sequence identity (OTU<sub>0.03</sub>) and taxonomically assigned based on the SILVA taxonomy implemented in mothur. To minimize biases all steps were performed according to the same protocols using the same infrastructure. OTU<sub>0.03</sub> that occurred only once in the whole dataset are termed absolute single sequence OTU<sub>0.03</sub> (SSO<sub>abs</sub>) (Gobet et al., 2012). OTU<sub>0.03</sub> that occurred only once in at least one sample, but are more frequent in other samples are termed relative single sequence OTU (SSO<sub>rel</sub>) (Gobet et al., 2012).

## Statistical analyses

The sequence abundance tables were used to calculate diversity indices and Chao1 richness (Chao, 1984) using *mothur* v24. Chao1 richness was calculated 100 times per sample, with each calculation based on the rarefaction of 3000 randomly chosen sequences without replacement. Dissimilarities between all samples were calculated using the Bray-Curtis dissimilarity coefficient (Bray and Curtis, 1957). The resulting beta-diversity matrices were used for 2-dimensional non metric multidimensional scaling (NMDS) ordinations with 20 random starts (Kruskal, 1964). Stress values below 0.2 indicate that the multidimensional dataset is well represented by the 2D ordination. To test whether the inclusion of singletons affected further statistical tests we generated NMDS ordinations with and without singletons and compared them using Procrustes correlation analysis (Gower, 1975). Since the correlation of the two archaeal (Procrustes correlation coefficient=0.999,  $p=0.001$ ) and the two bacterial ordinations (0.998,  $p=0.001$ ) was highly significant, we decided to include the singletons in our analyses, to be able to identify types of microorganisms which can switch from rare to dominant modes of distribution. RDA (Redundancy Analyses) based on Hellinger transformed OTU<sub>0.03</sub> datasets (Legendre and Legendre, 1998) were carried out to evaluate the combined effects of sediment depth, sediment temperature, water depth and ranges of methane and sulfate concentrations on the microbial community composition in methane seep habitats (see supplementary information). The significance of combined and pure effects was assessed by analysis of variance (ANOVA). Indicator taxa of the different seafloor microbiomes were calculated based on relative abundance tables (Dufrène and Legendre, 1997). Distance decay was based on pairwise community dissimilarities using the Sørensen index and assessed in a logarithmic transformed space to enhance the linear fitting (Nekola and White, 1999). Log-transformations were done using the natural logarithm, which gives the same results than log<sub>10</sub> transformations (Rosenzweig, 1995). Because some values were zero in the similarity and distance tables, a small value (0.01) was added before log-transformation (Zinger et al., *in prep*). The significance of  $\beta$  was tested by 1000 Monte Carlo permutations of the residuals under the full regression model (Legendre and Legendre, 1998). All analyses were carried out with the R statistical environment and the packages *vegan* (Oksanen et al., 2012), *labdsv* (Roberts, 2012), *gmt* (Magnusson, 2011), as well as with custom R scripts.

## Results and Discussion

### Diversity of seafloor communities

We examined 77 bacterial and 48 archaeal communities from as different seafloor realms as methane seeps, SMTZ, hydrothermal vents, coastal sediments, deep-sea surface and subsurface sediments (Figure S1, for details see supporting information Table S1-S3). After rigorous denoising and quality control of the 125 datasets we obtained a total of 1,486,735 bacterial and 796,544 archaeal sequences (Table S4, S5). Clustering of the sequences yielded 174,820 bacterial and 16,896 archaeal operational taxonomic units at 97% sequence identity level (OTU<sub>0.03</sub>). The archaeal dataset contained 55% SSO<sub>abs</sub> and 19% SSO<sub>rel</sub> and the bacterial dataset contained 58% SSO<sub>abs</sub> and 22% SSO<sub>rel</sub>. Richness and the number of SSO<sub>rel</sub> per sampling site were similar to values reported before in local studies of benthic habitats (Gaidos et al., 2010; Gobet et al., 2012; Jacob et al., 2013). SSO<sub>rel</sub> do not overlap with SSO<sub>abs</sub> and are particularly interesting for the investigation of community assembly rules, since they comprise rare organisms that may become abundant due to environmental filtering when conditions change as predicted by the species sorting view (Leibold et al., 2004).

### *Richness and evenness of seafloor communities*

The observed (S) and estimated (Chao1) richness of microbial communities from methane seeps and other ecosystems spanned more than two orders of magnitude (Figure 1, supporting information Table S4, S5), with distinct differences between the seafloor realms. The average contribution of archaeal OTU<sub>0.03</sub> to total richness was also largely different between the microbiomes and ranged from 17% in the subsurface and around 30% at methane seeps and vents to 54% in coastal sands. Microbial diversity was further assessed using the inverse Simpson diversity index (D), which takes both richness and evenness into account and basically describes the probability that two reads chosen at random will be of the same OTU (Hill et al., 2003). The minimal value D can take is 1, i.e. a pure culture, the maximal D is equal to the observed richness S of that sample and means that every OTU is present exactly once. Archaeal diversity was lowest at two deep seafloor habitats, the gas and mud emitting Håkon Mosby mud volcano (HMMV) (D=1.2) and the Lost City hydrothermal vents (S=54 OTU<sub>0.03</sub>; Chao1=91 OTU<sub>0.03</sub>). It peaked in intertidal microbial mats of the North Sea coast (S=812 OTU<sub>0.03</sub>; Chao1=2617 OTU<sub>0.03</sub>; D=64). Bacterial diversity was lowest at hydrothermal chimneys of Lost City (S=173

OTU<sub>0.03</sub>; Chao1=337 OTU<sub>0.03</sub>) and the Lau Vent Field (D=3.9). The highest diversity was retrieved from non-methane deep-sea surface sediments in the southeast Pacific off New Zealand (S=1978 OTU<sub>0.03</sub>; Chao1=8848 OTU<sub>0.03</sub>; D=719). Across all benthic realms, archaeal diversity was lower than bacterial diversity as previously observed for microbiomes of temperate (Fierer et al., 2007) and cold soils (Hamilton et al., 2013), mangrove sediments (Andreote et al., 2012) and the human skin (Probst et al., 2013). The observed richness (S) was on average 4-fold lower, estimated richness (Chao1) was on average 6-fold lower and evenness (D) was on average 15-fold lower. However, archaeal and bacterial diversity showed a highly significant positive correlation, as determined by Spearman's rank correlation ( $R_S=0.68$ ,  $p_S<0.001$ ;  $R_{Chao1}=0.62$ ,  $p_{Chao1}<0.001$ ;  $R_D=0.55$ ,  $p_D<0.001$ ). This strongly suggests that the diversity of bacteria and archaea is shaped by similar ecological mechanisms and environmental factors.

#### *Community shifts at seafloor realms*

Beta diversity at OTU<sub>0.03</sub> level differed greatly between all seafloor realms (Figure 2). Community dissimilarity between sampling sites, as defined by OTU<sub>0.03</sub> turnover, was highest in hydrothermal vent and methane seep ecosystems, both showing a substantial degree of endemism, and lowest in deep-sea surface sediments (Table 1). The differences between realms ranged from 1% – 7% shared OTU<sub>0.03</sub> for the archaea and from <1% – 6% shared OTU<sub>0.03</sub> for the bacteria (Figure S4). No single OTU<sub>0.03</sub> was found in all seafloor samples. Based on redundancy analysis (RDA) by random subsampling, all microbiomes were significantly different from each other ( $p<0.05$ ) using ten tests, 200 permutations each and correction of the false discovery rate of  $p$  (Benjamini and Hochberg, 1995). As to the key environmental factors determining sequence abundance cross all realms, *Archaea* and *Bacteria* were influenced by water depth and sediment depth (Figure S5A, B). Water depth affects the flux of organic material to the seafloor by particle sedimentation from surface waters, and thereby energy availability (Jørgensen and Boetius, 2007). Previous studies described linear relationships between water depth, bacterial abundance and community composition (Hewson et al., 2007; Bienhold et al., 2011; Jacob et al., 2013). Sediment depth is a proxy both for redox gradients, but also for the age of deposited matter, and is another crucial factor shaping microbial community structure (Urakawa et al., 2000; Böer et al., 2009; Ruff et al., 2013). Methane and sulfate concentration ranges (Hamdan et al., 2013), as well as sediment temperature across all realms impacted mostly bacterial composition and had a minor influence on archaea. Together the five tested

parameters explained 15% ( $p=0.001$ ) of archaeal and 11% ( $p=0.001$ ) of bacterial community variation across all marine ecosystems.

#### *Composition of seafloor communities*

At phylum level, all seafloor realms investigated here shared a high proportion of taxa. The three major archaeal phyla *Euryarchaeota*, *Crenarchaeota* and *Thaumarchaeota* (Brochier-Armanet et al., 2008) were found at all realms. Of the 53 bacterial phyla that we retrieved, the seafloor realms shared between 80 and 98% (Figure S4), with *Proteobacteria* (44% of all bacterial reads) and *Bacteroidetes* (9% of all bacterial reads) being the most sequence-abundant taxa. The ten most abundant bacterial phyla accounted for 84% of all bacterial reads and eight of those ten were found at all investigated sites. Thus, the cosmopolitan taxa were also the most abundant, which supports an earlier Sanger-based study (Nemergut et al., 2011).

However, substantial differences in community composition between the seafloor realms were detected at the class (Table 2, Table S6) and order level (Figure S2), confirming earlier studies based on Sanger-type 16S rRNA sequencing. We defined indicator taxa for each realm (Table 2) using a method that is based on the relative abundance and relative frequency of occurrence of a given taxon within each realm (Dufrene and Legendre, 1997). Most of the indicator taxa that we found are explained by selection according to biogeochemical function, determined by available energy sources and electron acceptors. For instance, at methane seeps, *Methanomicrobia* and *Deltaproteobacteria* are the dominant clades (Knittel and Boetius, 2009) performing AOM, while at hydrothermal vents the sequence-abundance of *Epsilonproteobacteria* can be related to environmental selection of diverse sulfide-oxidizing bacteria in this class (Campbell et al., 2006). *Gemmatimonadetes* and *Acidobacteria* (Durbin and Teske, 2011) are common in oxic deep-sea surface sediments, whereas heterotrophic MCG archaea (Lloyd et al., 2013) and *Chloroflexi* (Nunoura et al., 2013) are typical for organic-rich subsurface ecosystems.

Species sorting according to biogeochemical function may also explain some of the observed overlap at the class level as, for instance, the microbial community of deep sulfate methane transition zones shared many taxa with deep-sea subsurface samples (ODP1-4), such as MCG archaea, *Bacilli* and *Chloroflexi* (Biddle et al., 2006). Microbial communities of methane seeps at high seafloor temperature were similar to chimney

samples from the Lau hydrothermal vent field (LV1-6) and contained clades such as *Thermodesulfobacteria*, *Thermoprotei* and *Archaeoglobi* (Flores et al., 2012).

### **The methane seep microbiome**

#### *Richness and evenness at methane seeps and SMTZ*

The microbial community analyses support the hypothesis that methane seeps host distinct communities to those of other marine seafloor realms. Our analysis comprised a broad range of observed richness (S), estimated richness (Chao1) and evenness (D) for both archaea and bacteria (Figure 1, 2, Table S4). Of 23 methane seeps and four SMTZ, archaeal diversity was lowest at Håkon Mosby mud volcano (D=1.2) and at a microbial reef in the Black Sea (S=57 OTU<sub>0.03</sub>; Chao1=128) and highest in the SMTZ of the White Oak River estuary (S=421 OTU<sub>0.03</sub>; D=20) and at a cold seep of Quepos Slide near the coast of Costa Rica (Chao1=1106 OTU<sub>0.03</sub>). Bacterial diversity was lowest in sediments of a quiescent seep in Antarctica (S=355 OTU<sub>0.03</sub>; D=4.5) and in hot sediments at Guaymas Basin (Chao1=583 OTU<sub>0.03</sub>), and peaked at the cold seep of Quepos Slide (S=1613 OTU<sub>0.03</sub>; Chao1=5145 OTU<sub>0.03</sub>; D=462). Accumulation curves (Figure S3) and richness estimates revealed that by analyzing these 27 globally distributed communities at the order level, we captured 100% of the expected phylogenetic diversity of archaea and 98% of bacteria at methane-impacted ecosystems. However, at OTU<sub>0.03</sub> level we retrieved only 55% of the archaeal and 47% of the bacterial diversity, indicating that a large part of the global phylogenetic diversity remained untapped. Thus, in marine sedimentary habitats where methane serves as key energy source to a few taxa capable of metabolizing this C1 compound, the entire microbial communities were much more diverse and distinct as expected from the predominant biogeochemistry.

#### *Community shifts at methane seeps*

We also detected a large range of beta diversity, regardless of whether we kept or discarded the SSO<sub>abs</sub> from the dataset (Figure 3). Two samples from the same area at Guaymas Basin (GB1 and GB2), for instance, were less similar in community structure than deep-sea sediments from different hemispheres (NZS and SMS samples) or sands from a Hawaiian coral reef and the North Sea (e.g. CR2 and MM3). The maximum percentage of shared archaeal OTU<sub>0.03</sub> between any two AOM habitats was 66%, but several habitats did not share any OTU<sub>0.03</sub> at all (0% species overlap). Bacterial OTU<sub>0.03</sub>

turnover was even more pronounced with a maximum of 36% shared and a minimum of 0% shared OTU<sub>0.03</sub>. These differences in community structure were partially explained by dispersal in space, as shown by the analysis of distance decay of community similarity (Figure S6). However, the high degree of endemism at methane-impacted sites seemed to be mainly due to other mechanisms (Martiny et al., 2011; Hanson et al., 2012), such as spatial isolation or environmental filtering, which was tested using RDA. The RDA analysis (Figure S5C, D) showed that the archaeal community at methane seeps was shaped by sediment temperature ( $p_{\text{Species}}=0.02$ ;  $p_{\text{Order}}=0.01$ ) and sediment depth ( $p_{\text{Species}}=0.05$ ), whereas the bacterial community was shaped mainly by sediment depth ( $p_{\text{Species}}=0.05$ ;  $p_{\text{Order}}=0.02$ ). Neither water depth nor the prevailing ranges of methane concentrations significantly impacted the communities, since the supply of electron acceptors may be more relevant than the supply of methane at many types of seeps when a minimum of methane is available (De Beer et al., 2006; Boetius and Wenzhöfer, 2013). Altogether the five tested parameters explained 16% ( $p=0.018$ ) of the archaeal community variation on order level and 24% ( $p=0.001$ ) on OTU<sub>0.03</sub> level and 10% ( $p=0.049$ ) of bacterial community variation on order and 21% ( $p=0.003$ ) on OTU<sub>0.03</sub> level.

To further explore the role of environmental filtering, we tested if the microbial communities of cold seeps, hot seeps and SMTZ were significantly different from each other using pairwise comparisons of either archaeal or bacterial communities. Moreover, we tested if each of those communities differed from vents, subsurface, surface and coastal sediments. Indeed, for nearly all tested combinations both the archaeal and bacterial community structures differed significantly ( $p<0.05$ ) as determined by RDA. Only the bacterial communities of SMTZ were not significantly different from those of hot and cold seeps confirming earlier observations (Harrison et al., 2009).

#### *Composition of methane seep communities*

Indicator clades of the methane seep microbiome at class level were *Methanomicrobia*, *Deltaproteobacteria*, candidate phylum JS1, candidate division Hyd24.12, *Deferribacteres* and *Spirochaetes* (Figure 3, Table S6). *Gammaproteobacteria*, *Flavobacteria*, *Thermoplasmatales* and Marine Benthic Group B were also frequently found, but they were also important at coastal and deep-sea sediments or the deep subsurface. At order level we discovered two archaeal and ten bacterial taxa that were present at all methane seeps and SMTZ (Table S8) at an average relative abundance of over 1%, here defined as the seep metacommunity. Two of the 12 taxa, *Methanosarcinales* and

*Desulfobacterales*, comprise those organisms, which degrade methane and other hydrocarbons anaerobically (Kniemeyer et al., 2007; Widdel et al., 2010; Kellermann et al., 2012; Milucka et al., 2012). The aerobic methanotrophs *Methylococcales* (Tavormina et al., 2008; Ruff et al., 2013) and the conspicuous members of the *Thiotrichales* often forming thiotrophic bacterial mats at methane seeps (Grünke et al., 2012) were also found at most, but not all seep sites, potentially due to the limitation by oxygen supply in several of the investigated habitats. The majority of the heterotrophic core clades of methane seeps were also commonly found in detritus-fueled deep-sea sediments, such as the *Actinobacteridae*, *Flavobacteriales*, *Sphingobacteriales* and *Caldilineales*. However, at OTU<sub>0.03</sub> level, the methane seep heterotrophs showed little overlap with deep-sea sediments, indicating that the composition and availability of organic matter and electron acceptors could differ between both seafloor realms (Pohlman et al., 2010).

In addition to these key functional groups we found other archaeal and bacterial clades at methane seeps with unknown function as described previously (Mills et al., 2005; Knittel and Boetius, 2009; Roalkvam et al., 2011). These clades included *Thermoplasmatales*, which were shown to comprise methane-metabolizing organisms (Paul et al., 2012) and *Firmicutes* that include sulfate reducers (Hubert et al., 2009). The *Spirochaetes* may be favored by the sulfide enriched methane seeps, since they contain sulfide-oxidizers that live in consortia with sulfate-reducing bacteria (Dubinina et al., 2011). Candidate phylum JS1 was present at all sites and the dominant clade at some hot seeps and deep mud volcano sediments (DS1-3). This candidate phylum is suspected to contain sulfate reducers (Mori et al., 2003) and to be involved in the methane-derived carbon cycle at seeps (Chevalier et al., 2013). Remarkably, in our data set JS1 correlated negatively with deltaproteobacterial SRB based on Spearman's rank correlation ( $R=-0.49$ ,  $p<0.01$ ), indicating that JS1 may compete with SRB. Despite the dominance of these functional groups at methane seeps in sequence abundance, none of the individual taxa (OTU<sub>0.03</sub>) were cosmopolitans. Hence, ecosystem functions such as microbial oxidation of methane, sulfate reduction and sulfide oxidation are redundant and provided by a suite of related microorganisms, which are selected by environmental conditions and may further diversify by environmental isolation.

### **Diversity and distribution of key functional groups at methane seeps**

We assessed the diversity and global distribution of the orders and key indicator types for methane seeps *Methanosarcinales*, ANME-1, *Desulfobacterales* and *Methylococcales*.

The distribution of the major clades of marine ANME (ANME-1, ANME-2 and ANME-3 (Hinrichs et al., 1999; Orphan et al., 2002; Niemann et al., 2006) and associated sulfate-reducing bacteria (Niemann et al., 2006; Schreiber et al., 2010) differ between seep ecosystems, but niche preferences of ANME clades and the sulfate-reducing subgroups are not resolved yet. The relative sequence abundance of all ANME clades matched well with relative cell abundances determined by fluorescence in-situ hybridization (FISH) (Table S7), thus it is likely that the following considerations can be extended to the *in situ* abundance of ANME clades. ANME-2a was the most widespread and sequence-abundant clade and dominated many cold seep sites, but was less abundant or even absent at hot seeps (Figure 3A). ANME-2c was found predominantly at sites inhabited by vesicomid clams (HRC, JAP, KO) (Knittel et al., 2005; Pop Ristova et al., 2012) (Felden et al 2013 *in review*). The recently described *Cand. Methanoperedenaceae* (also referred to as AOM-associated archaea - AAA), which use nitrate as electron acceptor, (Haroon et al., 2013) were found at hot seeps and a quiescent seep in Antarctica (Figure 3A). ANME-3 was also widespread, but dominated only the cold, vigorously methane emitting seeps such as HMMV (Felden et al., 2010) and the REGAB pockmark (KO) in the Kongo Basin (Pop Ristova et al., 2012). ANME-1b was rare at most sites but dominated anoxic settings such as the Black Sea microbial mats (BS2) (Knittel et al., 2005). ANME-1a and other unclassified ANME-1 seemed to inhabit preferably hot seeps (Holler et al., 2011; Biddle et al., 2012). Sequences of *Cand. Methyloirabilis oxyfera*, which perform the nitrite-dependent AOM (Ettwig et al., 2010) occurred at one Guaymas Basin hot seep (Figure 3B).

#### *The role of species-level phylotypes*

To examine the relevance of species-level phylotypes within the seep microbiome we looked at the ten most abundant OTU<sub>0.03</sub> of the major functional clades. Despite the pronounced environmental differences between seep habitats, the 10 most frequent ANME OTU<sub>0.03</sub> were responsible for 86% of all ANME reads, but represented only 0.6% of their global diversity (1765 ANME OTU<sub>0.03</sub>). Each of those 10 OTU<sub>0.03</sub> was found on average at 13 out of 23 methane seep habitats worldwide. Interestingly, 5 of these 10 frequent ANME were SSO<sub>rel</sub>, meaning that they occurred as only one sequence in at least one seep, but highly dominated other seeps (Table S9). We observed a similar trend for the 10 most frequent *Desulfobacterales* OTU<sub>0.03</sub>, which represented 0.3% of the total diversity of that clade (3146 OTU<sub>0.03</sub>), but comprised 38% of all *Desulfobacterales* reads. Each of those OTU<sub>0.03</sub> was found on average at 12 seeps. Here again, 6 were SSO<sub>rel</sub>.

Similarly, The 10 most frequent OTU<sub>0.03</sub> of aerobic methanotrophic *Methylococcales* comprised 3% of the diversity, but 96% of the reads. 8 of those organisms were SSO<sub>rel</sub> and they occurred on average at 10 seeps. Finally, the 10 most frequent *Thiotrichales* OTU<sub>0.03</sub> (9 SSO<sub>rel</sub>) corresponded to 3% of the diversity (294 OTU<sub>0.03</sub>) and were responsible for 76% of total reads. This suggests that environmental filtering may play a crucial role for the distribution of key functional groups (Bowen et al., 2012; Gibbons et al., 2013).

## **Conclusion**

According to the species-sorting view (Leibold et al., 2004), our results indicate that the core microbiome of cold seeps comprises a metacommunity of key functional organisms that are globally distributed and locally selected and diversifying, which was shown to be the case for other microbial assemblages (Martiny et al., 2011). Analogous to the human gut microbiome (Turnbaugh et al., 2009) this metacommunity is phylogenetically diverse, but functionally consistent and carries out key ecosystem functions like methanotrophy, thiotrophy and sulfate reduction with global relevance to methane emission from the ocean. Although its diversity at order level has been relatively well captured by recent surveys of seafloor habitats worldwide, many more ecotypes with specific niche preferences and biotic interactions remain to be discovered.

## **Acknowledgements**

We thank Mitchell Sogin and Linda Amaral-Zettler for their assistance concerning the preparation of sequencing data and Angelique Gobet, Lucie Zinger and Pier L. Buttigieg for support in statistical analyses. This study is a contribution to the International Census of Marine Microbes (ICoMM) funded by the Alfred P. Sloan Foundation. Further support for this study was supplied by the Max Planck Society and the DFG Leibnitz program to A.B.

## Figures and Tables

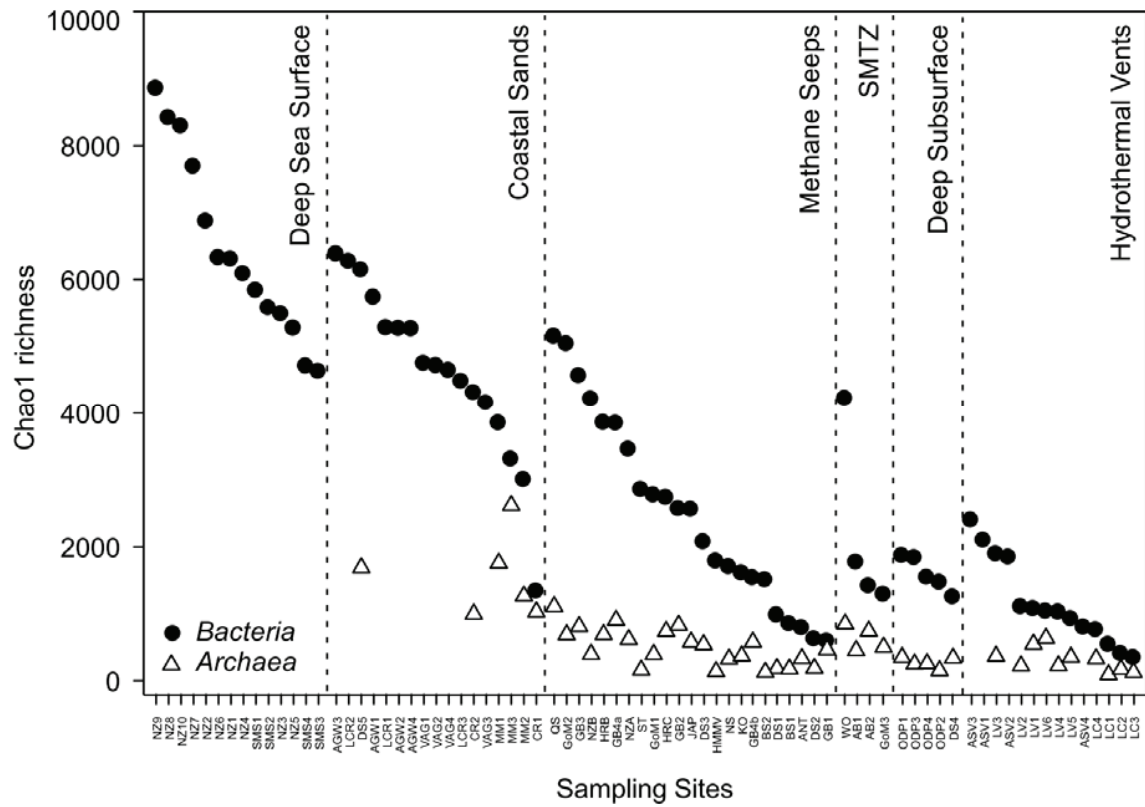


**Figure 1: Chao1 richness estimates**

The symbols represent the mean of 100 Chao1 calculations per sampling site, with each calculation based on rarefaction of 3000 randomly chosen sequences without replacement. No archaeal data were available for deep-sea surface sediments.

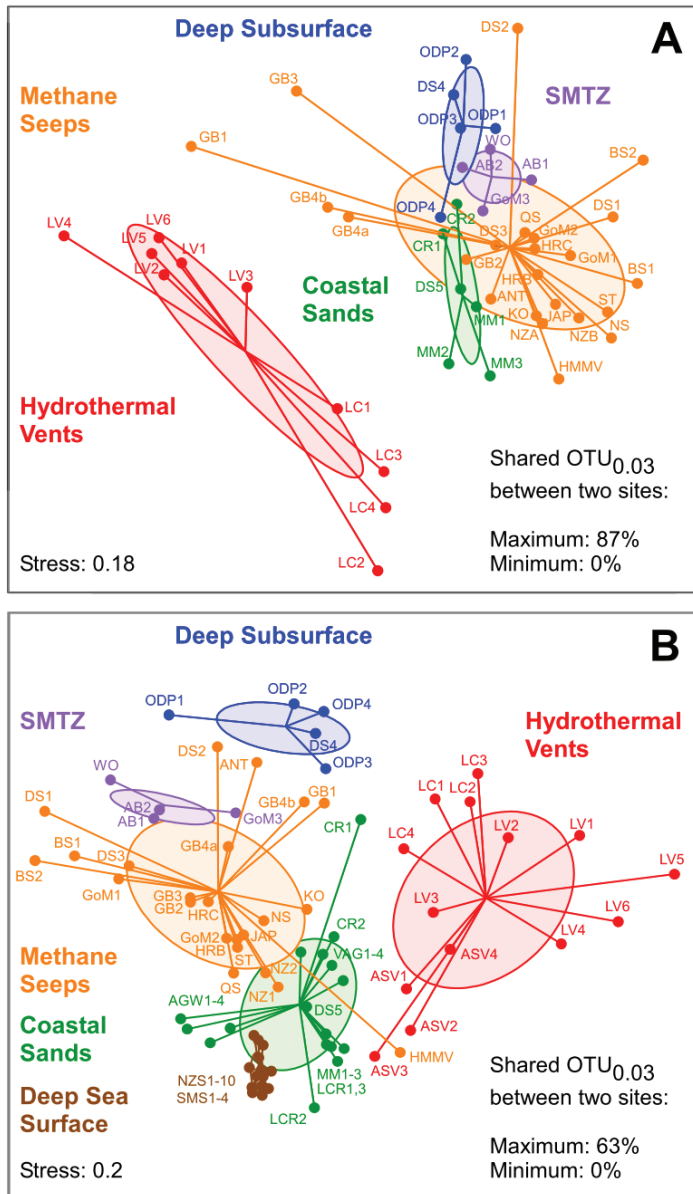


**Figure 2: NMDS ordination based on archaeal and bacterial OTU<sub>0.03</sub>**

Beta diversity of archaeal (A: 48 samples) and bacterial (B: 77 samples) communities visualized by non-metric multidimensional scaling (NMDS). Each sample is connected to the group centroid, which is the weighted averaged mean of the within group distances. Ellipses represent one standard deviation of the mean. All groups were significantly different as tested with a subsampling based RDA approach. Procrustes correlation of the microbial community structure with and without absolute singletons (SSO<sub>abs</sub>) had a value of  $R = 0.998$  ( $p = 0.001$ ) for both domains, showing that these had a minor effect on beta diversity patterns.

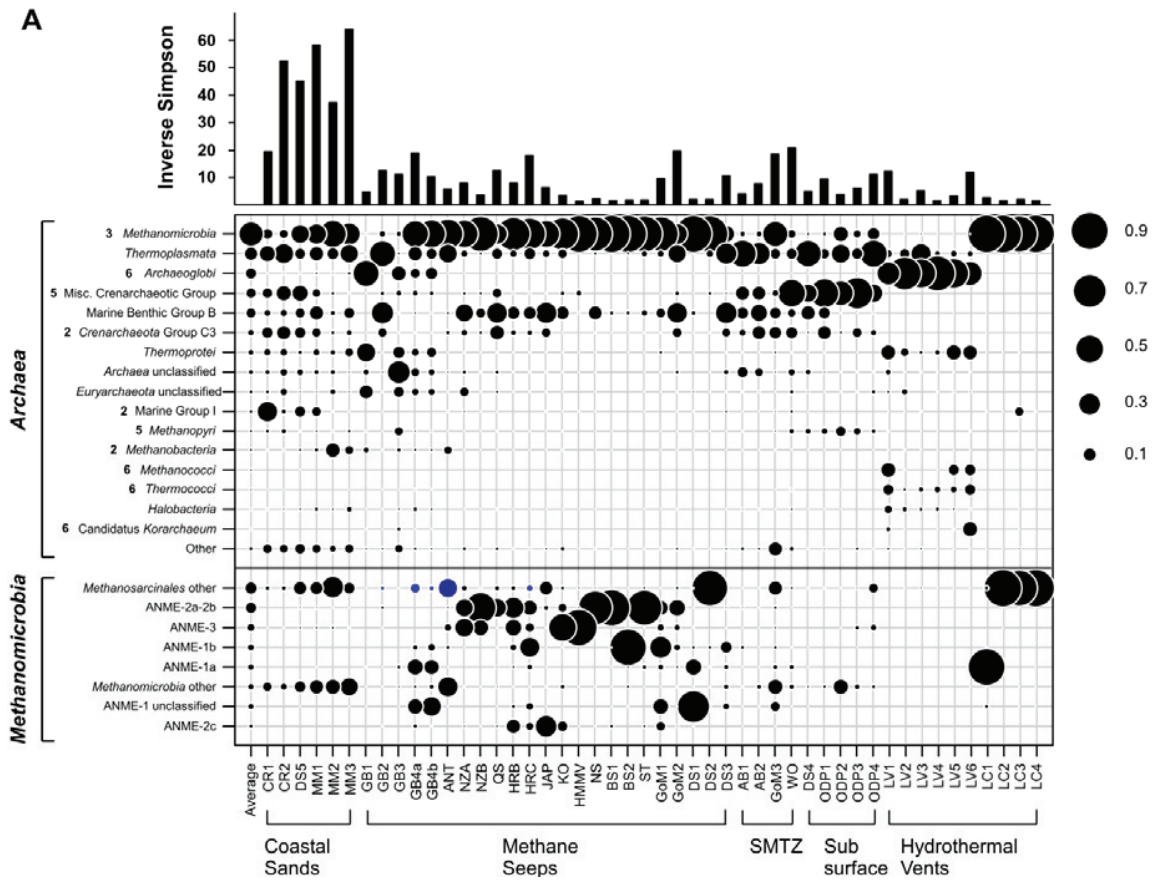


**Figure 3: Relative sequence abundance of archaeal and bacterial classes in different seafloor realms**

These plots show the relative sequence abundance of the most abundant archaeal (**A**) and bacterial (**B**) classes in different seafloor realms. The evenness of microbial clades in each ecosystem is given above by the inverse Simpson diversity index. Significant indicator taxa for each of the realms (archaea:  $p < 0.05$ ; bacteria:  $p < 0.01$ ) are marked with numbers left to their names. 1: Deep-sea surface 2: Coastal sands 3: Methane seeps, 4: SMTZ, 5: Subsurface, 6: Hydrothermal vents. (**A**) The methane-cycling archaeal class *Methanomicrobia* is shown in more detail, with subdivisions for the major methanotrophic clades. The blue dots show a relative sequence abundance of more than one percent of the recently described (Haroon et al., 2013) nitrate-respiring *Cand. Methanoperedenaceae* (ANME-2d clade). (**B**) The red dots show a relative sequence abundance of more than one percent of nitrite-respiring clade of methanotrophic *Cand. Methyloirabilis oxyfera* (Ettwig et al., 2010). Figure 3 continues on next page.

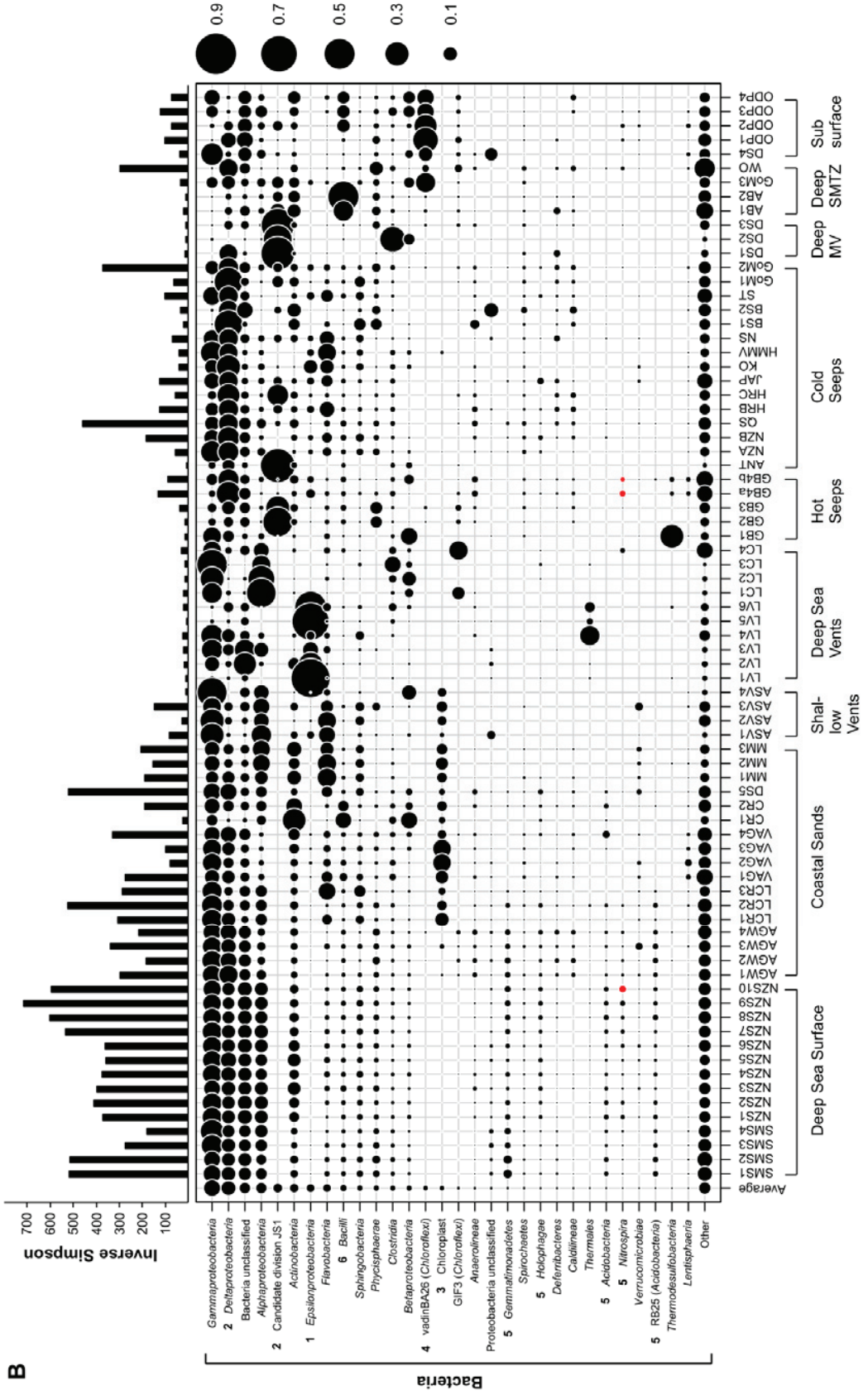


**Table 1: Percent shared OTU<sub>0.03</sub> between samples of marine realms**

| Seafloor realm     | Number of samples | Domain          | Max shared OTU <sub>0.03</sub> (%) | Mean shared OTU <sub>0.03</sub> (%) | Min shared OTU <sub>0.03</sub> (%) |
|--------------------|-------------------|-----------------|------------------------------------|-------------------------------------|------------------------------------|
| Hydrothermal Vents | 14                | <i>Bacteria</i> | 29                                 | 3                                   | 0                                  |
|                    | 10                | <i>Archaea</i>  | 78                                 | 14                                  | 0                                  |
| Methane seeps      | 23                | <i>Bacteria</i> | 36                                 | 5                                   | <0.1                               |
|                    | 23                | <i>Archaea</i>  | 66                                 | 8                                   | 0                                  |
| SMTZ               | 4                 | <i>Bacteria</i> | 33                                 | 7                                   | 1                                  |
|                    | 4                 | <i>Archaea</i>  | 49                                 | 13                                  | 4                                  |
| Coastal Sands      | 17                | <i>Bacteria</i> | 38                                 | 6                                   | <0.01                              |
|                    | 6                 | <i>Archaea</i>  | 25                                 | 10                                  | <0.01                              |
| Subsurface         | 5                 | <i>Bacteria</i> | 18                                 | 10                                  | 6                                  |
|                    | 5                 | <i>Archaea</i>  | 28                                 | 18                                  | 13                                 |
| Deep Sea Surface   | 14                | <i>Bacteria</i> | 34                                 | 19                                  | 8                                  |
|                    | 0                 | <i>Archaea</i>  | NA                                 | NA                                  | NA                                 |

Table 2: Characteristics of benthic microbiomes

| Archaea  |                         |                     |                         |                         |                      |                    |
|--|-------------------------|---------------------|-------------------------|-------------------------|----------------------|--------------------|
|  | Methane Seeps (23) *    | SMTZ (4)            | Coastal Sands (6)       | Hydrothermal Vents (10) | Deep-Sea Surface (0) | Sub surface (5)    |
| <b>Most frequent class **</b>                                  | <i>Methanococcoides</i> | <i>Thermoplasma</i> | <i>Methanococcoides</i> | <i>Methanococcoides</i> | n.a.                 | MCG                |
| <b>Most frequent order</b>                                     | <i>Methanococcales</i>  | MBGE                | <i>Thermoplasmales</i>  | <i>Archaeoglobales</i>  | n.a.                 | MCG                |
| <b>Indicator class</b>   | <i>Methanococcoides</i> | SCG                 | Marine Group 1          | <i>Thermococci</i>      | n.a.                 | <i>Methanopyri</i> |
| <b>Beta dispersion</b>   | 0.62                    | 0.68                | 0.55                    | 0.56                    | n.a.                 | 0.44               |
| <b>Evenness</b>  |                         |                     |                         |                         |                      |                    |
| <b>Mean / Median</b>   | 7.5 / 6.1               | 13 / 13             | 46 / 49                 | 4.2 / 2.1               | n.a.                 | 7.0 / 6.0          |
| <b>Chao1 Richness</b>  |                         |                     |                         |                         |                      |                    |
| <b>Mean / Median</b>   | 492 / 436               | 635 / 620           | 1558 / 1476             | 307 / 276               | n.a.                 | 269 / 257          |
| <b>SSO<sub>abs</sub> (in %)</b>                                |                         |                     |                         |                         |                      |                    |
| <b>Mean / Median</b>   | 28 / 27                 | 31 / 32             | 43 / 44                 | 34 / 33                 | n.a.                 | 33 / 32            |
| <b>SSO<sub>rel</sub> (in%)</b>                                 |                         |                     |                         |                         |                      |                    |
| <b>Mean / Median</b>   | 24 / 25                 | 19 / 20             | 14 / 14                 | 20 / 21                 | n.a.                 | 18 / 17            |
| <b>Mean contribution to total richness of S / Chao1 (in %)</b> | 26 / 23                 | 44 / 34             | 54 / 49                 | 30 / 36                 | n.a.                 | 17 / 17            |

| Bacteria   |                             |                             |                                      |                               |                                |                                  |
|--|-----------------------------|-----------------------------|--------------------------------------|-------------------------------|--------------------------------|----------------------------------|
|  | Methane Seeps (23)          | SMTZ (4)                    | Coastal Sands (17)                   | Hydrothermal Vents (14)       | Deep-Sea Surface (14)          | Sub surface (5)                  |
| <b>Most frequent class</b>                                     | <i>Delta-proteobacteria</i> | <i>Bacilli</i>              | <i>Gamma-proteobacteria</i>          | <i>Gamma-proteobacteria</i>   | <i>Gamma-proteobacteria</i>    | vadinBA ( <i>Chloroflexi</i> )   |
| <b>Most frequent order</b>                                     | Candidate phylum JS1        | <i>Lactobacillales</i>      | <i>Flavobacteriales</i> ***          | <i>Nautiliales</i>            | <i>Alteromonadales</i>         | vadinBA26 ( <i>Chloroflexi</i> ) |
| <b>Indicator class</b>   | <i>Delta-proteobacteria</i> | GIF9 ( <i>Chloroflexi</i> ) | OPB35 *** ( <i>Verrucomicrobia</i> ) | <i>Epsilon-proteobacteria</i> | SAR 202 ( <i>Chloroflexi</i> ) | vadinBA ( <i>Chloroflexi</i> )   |
| <b>Beta dispersion</b>   | 0.64                        | 0.68                        | 0.62                                 | 0.65                          | 0.47                           | 0.52                             |
| <b>Evenness</b>  |                             |                             |                                      |                               |                                |                                  |
| <b>Mean / Median</b>   | 87 / 51                     | 87 / 23                     | 247 / 214                            | 28 / 16                       | 78 / 70                        | 445 / 405                        |
| <b>Chao1 Richness</b>  |                             |                             |                                      |                               |                                |                                  |
| <b>Mean / Median</b>   | 2499 / 2549                 | 2166 / 1583                 | 4634 / 4710                          | 1152 / 1021                   | 6447 / 6187                    | 1585 / 1536                      |
| <b>SSO<sub>abs</sub> (in%)</b>                                 |                             |                             |                                      |                               |                                |                                  |
| <b>Mean / Median</b>   | 34 / 35                     | 38 / 37                     | 35 / 36                              | 33 / 36                       | 30 / 30                        | 35 / 35                          |
| <b>SSO<sub>rel</sub> (in%)</b>                                 |                             |                             |                                      |                               |                                |                                  |
| <b>Mean / Median</b>   | 24 / 27                     | 18 / 18                     | 26 / 26                              | 21 / 22                       | 34 / 35                        | 16 / 17                          |
| <b>Mean contribution to total richness of S / Chao1 (in %)</b> | 74 / 77                     | 56 / 66                     | 46 / 51                              | 70 / 64                       | n.a.                           | 83 / 83                          |

\* The brackets denote the number of samples used, \*\* based on relative 454 V6 sequence abundance, n.a. - not analyzed

\*\*\* Chloroplast sequences were targeted by the primers we used and originally showed up as the most frequent order and highly significant indicator for coastal sands, but were discarded as they originate from algae and plants.

MCG: Miscellaneous Crenarchaeotic Group, MBGE: Marine Benthic Group E, SCG: Soil Crenarchaeotic Group  
Taxonomic assignment is based on ARB/SILVA (Quast et al. 2013)

Indicator taxa are based on relative abundance and relative frequency of occurrence (Dufréne and Legendre 1997)

SSO: Single sequence OTU, S: Standardized observed richness, Chao1: Estimated richness, Beta dispersion: Average within group dissimilarity

## References

- Amend, A. S., Oliver, T. A., et al. (2012). "Macroecological Patterns of Marine Bacteria on a Global Scale." *J Biogeogr* **40**: 800-811.
- Andreote, F. D., Jiménez, D. J., et al. (2012). "The Microbiome of Brazilian Mangrove Sediments as Revealed by Metagenomics." *PLoS ONE* **7**: e38600.
- Baker, M. C., Ramirez-Llodra, E. Z., et al. (2010). Biogeography, Ecology, and Vulnerability of Chemosynthetic Ecosystems in the Deep Sea. *Life in the World's Oceans: Diversity, Distribution, and Abundance*. McIntyre, A. D., Wiley-Blackwell: 161-183.
- Beal, E. J., House, C. H., et al. (2009). "Manganese- and Iron-Dependent Marine Methane Oxidation." *Science* **325**: 184-187.
- Benjamini, Y. and Hochberg, Y. (1995). "Controlling the False Discovery Rate: A Practical and Powerful Approach to Multiple Testing." *J Roy Stat Soc B Met* **57**: 289-300.
- Biddle, J. F., Cardman, Z., et al. (2012). "Anaerobic Oxidation of Methane at Different Temperature Regimes in Guaymas Basin Hydrothermal Sediments." *ISME J* **6**: 1018-1031.
- Biddle, J. F., Lipp, J. S., et al. (2006). "Heterotrophic Archaea Dominate Sedimentary Subsurface Ecosystems Off Peru." *Proc Natl Acad Sci USA* **103**: 3846-3851.
- Biddle, J. F., White, J. R., et al. (2011). "Metagenomics of the Subsurface Brazos-Trinity Basin (Iodp Site 1320): Comparison with Other Sediment and Pyrosequenced Metagenomes." *ISME J* **5**: 1038-1047.
- Bienhold, C., Boetius, A., et al. (2011). "The Energy-Diversity Relationship of Complex Bacterial Communities in Arctic Deep-Sea Sediments." *ISME J* **6**: 724-732.
- Böer, S. I., Hedtkamp, S. I. C., et al. (2009). "Time- and Sediment Depth-Related Variations in Bacterial Diversity and Community Structure in Subtidal Sands." *ISME J* **3**: 780-791.
- Boetius, A. and Wenzhöfer, F. (2013). "Seafloor Oxygen Consumption Fuelled by Methane from Cold Seeps." *Nature Geosci* **6**: 725-734.
- Bottos, E. M., Woo, A. C., et al. (2013). "Airborne Bacterial Populations above Desert Soils of the McMurdo Dry Valleys, Antarctica." *Microb Ecol*: 1-9.
- Bowen, J. L., Morrison, H. G., et al. (2012). "Salt Marsh Sediment Diversity: A Test of the Variability of the Rare Biosphere among Environmental Replicates." *ISME J* **6**: 2014-2023.
- Bray, J. R. and Curtis, J. T. (1957). "An Ordination of the Upland Forest Communities of Southern Wisconsin." *Ecol Monogr* **27**: 326-349.
- Briggs, B. R., Inagaki, F., et al. (2012). "Bacterial Dominance in Subseafloor Sediments Characterized by Methane Hydrates." *FEMS Microbiol Ecol* **81**: 88-98.
- Brochier-Armanet, C., Boussau, B., et al. (2008). "Mesophilic Crenarchaeota: Proposal for a Third Archaeal Phylum, the Thaumarchaeota." *Nat Rev Microbiol* **6**: 245-252.
- Campbell, B. J., Polson, S. W., et al. (2013). "Diffuse Flow Environments within Basalt- and Sediment-Based Hydrothermal Vent Ecosystems Harbor Specialized Microbial Communities." *Front Microbiol* **4**.
- Campbell, B. J., Summers Engel, A., et al. (2006). "The Versatile E-Proteobacteria: Key Players in Sulphidic Habitats." *Nat Rev Micro* **4**: 458-468.
- Chao, A. (1984). "Nonparametric Estimation of the Number of Classes in a Population." *Scand J Stat* **11**: 265-270.
- Chevalier, N., Bouloubassi, I., et al. (2013). "Microbial Methane Turnover at Marmara Sea Cold Seeps: A Combined 16s Rrna and Lipid Biomarker Investigation." *Geobiology* **11**: 55-71.

- De Beer, D., Sauter, E., et al. (2006). "In Situ Fluxes and Zonation of Microbial Activity in Surface Sediments of the Håkon Mosby Mud Volcano." *Limnol Oceanogr* **51**: 1315-1331.
- Dubinina, G., Grabovich, M., et al. (2011). "Spirochaeta Perfilievii Sp. Nov., an Oxygen-Tolerant, Sulfide-Oxidizing, Sulfur- and Thiosulfate-Reducing Spirochaete Isolated from a Saline Spring." *Int J Syst Evol Microbiol* **61**: 110-117.
- Dufrène, M. and Legendre, P. (1997). "Species Assemblages and Indicator Species: The Need for a Flexible Asymmetrical Approach." *Ecol Monogr* **67**: 345-366.
- Durbin, A. M. and Teske, A. (2011). "Microbial Diversity and Stratification of South Pacific Abyssal Marine Sediments." *Environ Microbiol* **13**: 3219-3234.
- Edgar, R. C., Haas, B. J., et al. (2011). "Uchime Improves Sensitivity and Speed of Chimera Detection." *Bioinformatics* **27**: 2194-2200.
- Ettwig, K. F., Butler, M. K., et al. (2010). "Nitrite-Driven Anaerobic Methane Oxidation by Oxygenic Bacteria." *Nature* **464**: 543-548.
- Ezenwa, V. O., Gerardo, N. M., et al. (2012). "Animal Behavior and the Microbiome." *Science* **338**: 198-199.
- Felden, J., Wenzhöfer, F., et al. (2010). "Transport and Consumption of Oxygen and Methane in Different Habitats of the Håkon Mosby Mud Volcano (Hmmv)." *Limnol Oceanogr* **55**: 2366-2380.
- Fierer, N., Breitbart, M., et al. (2007). "Metagenomic and Small-Subunit Rna Analyses Reveal the Genetic Diversity of Bacteria, Archaea, Fungi, and Viruses in Soil." *Appl Environ Microbiol* **73**: 7059-7066.
- Fierer, N., Leff, J. W., et al. (2012). "Cross-Biome Metagenomic Analyses of Soil Microbial Communities and Their Functional Attributes." *Proc Natl Acad Sci USA* **109**: 21390-21395.
- Fierer, N. and Lennon, J. T. (2011). "The Generation and Maintenance of Diversity in Microbial Communities." *Am J Bot* **98**: 439-448.
- Flores, G. E., Shakya, M., et al. (2012). "Inter-Field Variability in the Microbial Communities of Hydrothermal Vent Deposits from a Back-Arc Basin." *Geobiology* **10**: 333-346.
- Gaidos, E., Rusch, A., et al. (2010). "Ribosomal Tag Pyrosequencing of DNA and Rna from Benthic Coral Reef Microbiota: Community Spatial Structure, Rare Members and Nitrogen-Cycling Guilds." *Environ Microbiol* **13**: 1138-1152.
- Gibbons, S. M., Caporaso, J. G., et al. (2013). "Evidence for a Persistent Microbial Seed Bank Throughout the Global Ocean." *Proc Natl Acad Sci USA* **110**: 4651-4655.
- Gobet, A., Boer, S. I., et al. (2012). "Diversity and Dynamics of Rare and of Resident Bacterial Populations in Coastal Sands." *ISME J* **6**: 542-553.
- Gower, J. C. (1975). "Generalized Procrustes Analysis." *Psychometrika* **40**: 33-51.
- Grünke, S., Lichtschlag, A., et al. (2012). "Mats of Psychrophilic Thiotrophic Bacteria Associated with Cold Seeps of the Barents Sea." *Biogeosciences* **9**: 2947-2960.
- Hamady, M. and Knight, R. (2009). "Microbial Community Profiling for Human Microbiome Projects: Tools, Techniques, and Challenges." *Genome Res* **19**: 1141-1152.
- Hamdan, L. J., Coffin, R. B., et al. (2013). "Ocean Currents Shape the Microbiome of Arctic Marine Sediments." *ISME J* **7**: 685-696.
- Hamilton, T. L., Peters, J. W., et al. (2013). "Molecular Evidence for an Active Endogenous Microbiome beneath Glacial Ice." *ISME J* **7**: 1402-1412.
- Hanson, C. A., Fuhrman, J. A., et al. (2012). "Beyond Biogeographic Patterns: Processes Shaping the Microbial Landscape." *Nat Rev Micro* **10**: 497-506.
- Haroon, M. F., Hu, S., et al. (2013). "Anaerobic Oxidation of Methane Coupled to Nitrate Reduction in a Novel Archaeal Lineage." *Nature* **500**: 567-570.

- Harrison, B. K., Zhang, H., et al. (2009). "Variations in Archaeal and Bacterial Diversity Associated with the Sulfate-Methane Transition Zone in Continental Margin Sediments (Santa Barbara Basin, California)." *Appl Environ Microbiol* **75**: 1487-1499.
- Hewson, I., Jacobson-Meyers, M. E., et al. (2007). "Diversity and Biogeography of Bacterial Assemblages in Surface Sediments across the San Pedro Basin, Southern California Borderlands." *Environ Microbiol* **9**: 923-933.
- Hill, T. C. J., Walsh, K. A., et al. (2003). "Using Ecological Diversity Measures with Bacterial Communities." *FEMS Microbiol Ecol* **43**: 1-11.
- Hinrichs, K.-U., Hayes, J. M., et al. (1999). "Methane-Consuming Archaeobacteria in Marine Sediments." *Nature* **398**: 802-805.
- Holler, T., Widdel, F., et al. (2011). "Thermophilic Anaerobic Oxidation of Methane by Marine Microbial Consortia." *ISME J* **5**: 1946-1956.
- Huber, J. A., Mark Welch, D. B., et al. (2007). "Microbial Population Structures in the Deep Marine Biosphere." *Science* **318**: 97-100.
- Hubert, C., Loy, A., et al. (2009). "A Constant Flux of Diverse Thermophilic Bacteria into the Cold Arctic Seabed." *Science* **325**: 1541-1544.
- Huse, S. M., Ye, Y., et al. (2012). "A Core Human Microbiome as Viewed through 16s Rrna Sequence Clusters." *PLoS ONE* **7**: e34242.
- Jacob, M., Soltwedel, T., et al. (2013). "Biogeography of Deep-Sea Benthic Bacteria at Regional Scale (Lter Hausgarten, Fram Strait, Arctic)." *PLoS ONE* **8**: e72779.
- Jamieson, R. E., Heywood, J. L., et al. (2013). "Bacterial Biodiversity in Deep-Sea Sediments from Two Regions of Contrasting Surface Water Productivity near the Crozet Islands, Southern Ocean." *Deep-Sea Res Pt I* **75**: 67-77.
- Jørgensen, B. B. and Boetius, A. (2007). "Feast and Famine - Microbial Life in the Deep-Sea Bed." *Nat Rev Micro* **5**: 770-781.
- Jørgensen, S. L., Hannisdal, B., et al. (2012). "Correlating Microbial Community Profiles with Geochemical Data in Highly Stratified Sediments from the Arctic Mid-Ocean Ridge." *Proc Natl Acad Sci USA* **109**: 2846-2855.
- Kellermann, M. Y., Wegener, G., et al. (2012). "Autotrophy as a Predominant Mode of Carbon Fixation in Anaerobic Methane-Oxidizing Microbial Communities." *Proc Natl Acad Sci USA* **109**: 19321-19326.
- Kniemeyer, O., Musat, F., et al. (2007). "Anaerobic Oxidation of Short-Chain Hydrocarbons by Marine Sulphate-Reducing Bacteria." *Nature* **449**: 898-901.
- Knittel, K. and Boetius, A. (2009). "Anaerobic Oxidation of Methane: Progress with an Unknown Process." *Annu Rev Microbiol* **63**: 311-334.
- Knittel, K., Lösekann, T., et al. (2005). "Diversity and Distribution of Methanotrophic Archaea at Cold Seeps." *Appl Environ Microbiol* **71**: 467-479.
- Kruskal, J. B. (1964). "Nonmetric Multidimensional Scaling: A Numerical Method." *Psychometrika* **29**: 115-129.
- Le Chatelier, E., Nielsen, T., et al. (2013). "Richness of Human Gut Microbiome Correlates with Metabolic Markers." *Nature* **500**: 541-546.
- Legendre, P. and Legendre, L. (1998). *Numerical Ecology*. Amsterdam, Elsevier Science B.V.
- Leibold, M. A., Holyoak, M., et al. (2004). "The Metacommunity Concept: A Framework for Multi-Scale Community Ecology." *Ecol Lett* **7**: 601-613.
- Levin, L. A. (2005). Ecology of Cold Seep Sediments: Interactions of Fauna with Flow, Chemistry and Microbes. *Oceanography and Marine Biology: An Annual Review*. Gibson, R. N., Atkinson, R. J. A., et al., Taylor & Francis. **43**: 1-46.

- Levy, R. and Borenstein, E. (2013). "Metabolic Modeling of Species Interaction in the Human Microbiome Elucidates Community-Level Assembly Rules." *Proc Natl Acad Sci USA* **110**: 12804-12809.
- Lloyd, K. G., Schreiber, L., et al. (2013). "Predominant Archaea in Marine Sediments Degrade Detrital Proteins." *Nature* **496**: 215-218.
- Magnusson, A. (2011). "Interface between Gmt Map-Making Software and R."
- Martiny, J. B. H., Bohannan, B. J. M., et al. (2006). "Microbial Biogeography: Putting Microorganisms on the Map." *Nat Rev Micro* **4**: 102-112.
- Martiny, J. B. H., Eisen, J. A., et al. (2011). "Drivers of Bacterial B-Diversity Depend on Spatial Scale." *Proc Natl Acad Sci USA* **108**: 7850-7854.
- Mills, H. J., Martinez, R. J., et al. (2005). "Characterization of Microbial Community Structure in Gulf of Mexico Gas Hydrates: Comparative Analysis of DNA- and Rna-Derived Clone Libraries." *Appl Environ Microbiol* **71**: 3235-3247.
- Milucka, J., Ferdelman, T. G., et al. (2012). "Zero-Valent Sulphur Is a Key Intermediate in Marine Methane Oxidation." *Nature* **491**: 541-546.
- Mori, K., Kim, H., et al. (2003). "A Novel Lineage of Sulfate-Reducing Microorganisms: Thermodesulfobiaceae Fam. Nov., Thermodesulfobium Narugense, Gen. Nov., Sp. Nov., a New Thermophilic Isolate from a Hot Spring." *Extremophiles* **7**: 283-290.
- Nekola, J. C. and White, P. S. (1999). "The Distance Decay of Similarity in Biogeography and Ecology." *J Biogeogr* **26**: 867-878.
- Nemergut, D. R., Costello, E. K., et al. (2011). "Global Patterns in the Biogeography of Bacterial Taxa." *Environ Microbiol* **13**: 135-144.
- Niemann, H., Lösekann, T., et al. (2006). "Novel Microbial Communities of the Haakon Mosby Mud Volcano and Their Role as a Methane Sink." *Nature* **443**: 854-858.
- Nunoura, T., Hirai, M., et al. (2013). "Isolation and Characterization of a Thermophilic, Obligately Anaerobic and Heterotrophic Marine *Chloroflexi* Bacterium from a *Chloroflexi*-Dominated Microbial Community Associated with a Japanese Shallow Hydrothermal System, and Proposal for *Thermomarinilinea Lacunofontalis* Gen. Nov., Sp. Nov." *Microbes Environ* **28**: 228-235.
- Oksanen, J., Blanchet, F. G., et al. (2012). "Vegan: Community Ecology Package."
- Omoregie, E. O., Mastalerz, V., et al. (2008). "Biogeochemistry and Community Composition of Iron- and Sulfur-Precipitating Microbial Mats at the Chefren Mud Volcano (Nile Deep Sea Fan, Eastern Mediterranean)." *Appl Environ Microbiol* **74**: 3198-3215.
- Orphan, V. J., House, C. H., et al. (2002). "Multiple Archaeal Groups Mediate Methane Oxidation in Anoxic Cold Seep Sediments." *Proc Natl Acad Sci USA* **99**: 7663 - 7668.
- Paul, K., Nonoh, J. O., et al. (2012). ""Methanoplasmatales," Thermoplasmatales-Related Archaea in Termite Guts and Other Environments, Are the Seventh Order of Methanogens." *Appl Environ Microbiol* **78**: 8245-8253.
- Pernthaler, A., Dekas, A. E., et al. (2008). "Diverse Syntrophic Partnerships from Deep-Sea Methane Vents Revealed by Direct Cell Capture and Metagenomics." *Proc Natl Acad Sci USA* **105**: 7052-7057.
- Pohlman, J. W., Bauer, J. E., et al. (2010). "Methane Hydrate-Bearing Seeps as a Source of Aged Dissolved Organic Carbon to the Oceans." *Nat Geosci* **4**: 37-41.
- Pop Ristova, P., Wenzhöfer, F., et al. (2012). "Bacterial Diversity and Biogeochemistry of Different Chemosynthetic Habitats of the Regab Cold Seep (West African Margin, 3160 M Water Depth)." *Biogeosciences* **9**: 5031-5048.
- Probst, A. J., Auerbach, A. K., et al. (2013). "Archaea on Human Skin." *PLoS ONE* **8**: e65388.

- Quast, C., Pruesse, E., et al. (2013). "The Silva Ribosomal Rna Gene Database Project: Improved Data Processing and Web-Based Tools." *Nucleic Acids Res* **41**: D590-D596.
- Quince, C., Lanzen, A., et al. (2009). "Accurate Determination of Microbial Diversity from 454 Pyrosequencing Data." *Nat Meth* **6**: 639-641.
- Roalkvam, I., Jørgensen, S. L., et al. (2011). "New Insight into Stratification of Anaerobic Methanotrophs in Cold Seep Sediments." *FEMS Microbiol Ecol* **78**: 233-243.
- Roberts, D. W. (2012). *Labdsv: Ordination and Multivariate Analysis for Ecology*.
- Rosenzweig, M., L. (1995). *Species Diversity in Space and Time*, Cambridge University Press.
- Ruff, S. E., Arnds, J., et al. (2013). "Microbial Communities of Deep-Sea Methane Seeps at Hikurangi Continental Margin (New Zealand)." *PLoS ONE* **8**: e72627.
- Schloss, P. D., Westcott, S. L., et al. (2009). "Introducing Mothur: Open-Source, Platform-Independent, Community-Supported Software for Describing and Comparing Microbial Communities." *Appl Environ Microbiol* **75**: 7537-7541.
- Schreiber, L., Holler, T., et al. (2010). "Identification of the Dominant Sulfate-Reducing Bacterial Partner of Anaerobic Methanotrophs of the Anme-2 Clade." *Environ Microbiol* **12**: 2327-2340.
- Shade, A. and Handelsman, J. (2012). "Beyond the Venn Diagram: The Hunt for a Core Microbiome." *Environ Microbiol* **14**: 4-12.
- Stokke, R., Roalkvam, I., et al. (2012). "Integrated Metagenomic and Metaproteomic Analyses of an Anme-1-Dominated Community in Marine Cold Seep Sediments." *Environ Microbiol* **14**: 1333-1346.
- Tavormina, P. L., Ussler, W., III, et al. (2008). "Planktonic and Sediment-Associated Aerobic Methanotrophs in Two Seep Systems Along the North American Margin." *Appl Environ Microbiol* **74**: 3985-3995.
- Torsvik, V., Øvreås, L., et al. (2002). "Prokaryotic Diversity--Magnitude, Dynamics, and Controlling Factors." *Science* **296**: 1064-1066.
- Turnbaugh, P. J., Hamady, M., et al. (2009). "A Core Gut Microbiome in Obese and Lean Twins." *Nature* **457**: 480-484.
- Turner, T., James, E., et al. (2013). "The Plant Microbiome." *Genome Biol* **14**: 209.
- Urakawa, H., Yoshida, T., et al. (2000). "Characterization of Depth-Related Population Variation in Microbial Communities of a Coastal Marine Sediment Using 16s Rdna-Based Approaches and Quinone Profiling." *Environ Microbiol* **2**: 542-554.
- Widdel, F., Knittel, K., et al. (2010). Anaerobic Hydrocarbon-Degrading Microorganisms: An Overview. *Handbook of Hydrocarbon and Lipid Microbiology*. Timmis, K. N., Springer. **3**: 1997-2021.
- Zinger, L., Amaral-Zettler, L. A., et al. (2011). "Global Patterns of Bacterial Beta-Diversity in Seafloor and Seawater Ecosystems." *PLoS ONE* **6**: e24570.

## Chapter 3

## **Microbial communities of deep-sea methane seeps at Hikurangi continental margin (New Zealand)**

S. Emil Ruff<sup>1,2,#</sup>, Julia Arnds<sup>2</sup>, Katrin Knittel<sup>2</sup>, Rudolf Amann<sup>2</sup>,  
Gunter Wegener<sup>1,3</sup>, Alban Ramette<sup>1</sup>, Antje Boetius<sup>1,3,4,#</sup>

- 1: HGF MPG Group for Deep Sea Ecology and Technology,  
Max Planck Institute for Marine Microbiology, Bremen, Germany
  - 2: Department of Molecular Ecology,  
Max Planck Institute for Marine Microbiology, Bremen, Germany
  - 3: MARUM Center for Marine Environmental Sciences,  
University of Bremen, Germany
  - 4: Alfred Wegener Institute Helmholtz Center  
for Polar and Marine Research, Bremerhaven, Germany
- #: Corresponding author: [eruff@mpi-bremen.de](mailto:eruff@mpi-bremen.de)

Published at PLoS ONE

DOI: [10.1371/journal.pone.0072627](https://doi.org/10.1371/journal.pone.0072627)

### Relevant contributions:

I developed the concepts and ideas together with K. Knittel, A. Ramette, R. Amann and A. Boetius. I constructed gene libraries, designed probes, performed CARD-FISH and ARISA, analyzed and visualized the data and wrote the manuscript with assistance from all co-authors.

# Microbial Communities of Deep-Sea Methane Seeps at Hikurangi Continental Margin (New Zealand)

S. Emil Ruff<sup>1,2\*</sup>, Julia Arnds<sup>2</sup>, Katrin Knittel<sup>2</sup>, Rudolf Amann<sup>2</sup>, Gunter Wegener<sup>1,3</sup>, Alban Ramette<sup>1</sup>, Antje Boetius<sup>1,3,4</sup>

**1** HGF MPG Group for Deep Sea Ecology and Technology, Max Planck Institute for Marine Microbiology, Bremen, Germany, **2** Department of Molecular Ecology, Max Planck Institute for Marine Microbiology, Bremen, Germany, **3** MARUM Center for Marine Environmental Sciences, University of Bremen, Bremen, Germany, **4** Alfred Wegener Institute Helmholtz Center for Polar and Marine Research, Bremerhaven, Germany

## Abstract

The methane-emitting cold seeps of Hikurangi margin (New Zealand) are among the few deep-sea chemosynthetic ecosystems of the Southern Hemisphere known to date. Here we compared the biogeochemistry and microbial communities of a variety of Hikurangi cold seep ecosystems. These included highly reduced seep habitats dominated by bacterial mats, partially oxidized habitats populated by heterotrophic ampharetid polychaetes and deeply oxidized habitats dominated by chemosynthetic frenulate tubeworms. The ampharetid habitats were characterized by a thick oxic sediment layer that hosted a diverse and biomass-rich community of aerobic methanotrophic *Gammaproteobacteria*. These bacteria consumed up to 25% of the emanating methane and clustered within three deep-branching groups named Marine Methylotrophic Group (MMG) 1-3. MMG1 and MMG2 methylotrophs belong to the order *Methylococcales*, whereas MMG3 methylotrophs are related to the *Methylophaga*. Organisms of the groups MMG1 and MMG3 are close relatives of chemosynthetic endosymbionts of marine invertebrates. The anoxic sediment layers of all investigated seeps were dominated by anaerobic methanotrophic archaea (ANME) of the ANME-2 clade and sulfate-reducing *Deltaproteobacteria*. Microbial community analysis using Automated Ribosomal Intergenic Spacer Analysis (ARISA) showed that the different seep habitats hosted distinct microbial communities, which were strongly influenced by the seep-associated fauna and the geographic location. Despite outstanding features of Hikurangi seep communities, the organisms responsible for key ecosystem functions were similar to those found at seeps worldwide. This suggests that similar types of biogeochemical settings select for similar community composition regardless of geographic distance. Because ampharetid polychaetes are widespread at cold seeps the role of aerobic methanotrophy may have been underestimated in seafloor methane budgets.

**Citation:** Ruff SE, Arnds J, Knittel K, Amann R, Wegener G, et al. (2013) Microbial Communities of Deep-Sea Methane Seeps at Hikurangi Continental Margin (New Zealand). PLoS ONE 8(9): e72627. doi:10.1371/journal.pone.0072627

**Editor:** Lucas J. Stal, Royal Netherlands Institute of Sea Research (NIOZ), Netherlands

**Received:** March 26, 2013; **Accepted:** July 11, 2013; **Published:** September 30, 2013

**Copyright:** © 2013 Ruff et al. This is an open-access article distributed under the terms of the Creative Commons Attribution License, which permits unrestricted use, distribution, and reproduction in any medium, provided the original author and source are credited.

**Funding:** Cruise SO191 was part of the COMET/MUMM II project within the program GEOTECHNOLOGIEN funded by the German Ministry of Education and Research (Grant No: 03G0608A). Further support was provided by the Max Planck Society, and by the DFG Leibniz program to AB. The funders had no role in study design, data collection and analysis, decision to publish, or preparation of the manuscript.

**Competing interests:** The authors have declared that no competing interests exist.

\* E-mail: eruff@mpi-bremen.de

## Introduction

Hikurangi margin located off northeastern New Zealand is an accretionary margin originating from the subduction of the Pacific plate under the Australian plate. The subduction causes dewatering of Hikurangi trough sediments and forms fluids enriched in hydrocarbons that migrate through the deformation front [1]. Some of the gas transported with the fluids forms gas hydrates in the seabed, but a substantial proportion is emitted to the water column [2,3,4,5]. Hikurangi margin was suggested to be a biogeographically new cold seep province, since many of the local seeps were populated by novel animal species, and the communities showed a high degree of endemism [6]. A new type of seep habitat was described dominated by

heterotrophic ampharetids (*Ampharetidae*, *Polychaeta*) [7], with isotopic signatures revealing a methane-based nutrition of the worms [8]. Ampharetid seep habitats are biogeochemically distinct due to their high methane effluxes [2] and high total oxygen uptake (TOU) rates, indicating that aerobic methanotrophy is a major pathway for methane turnover [7]. Furthermore, it was suggested that ampharetid habitats represent an early stage in the development of seep ecosystems [7]. Hikurangi margin also hosts highly reduced seep ecosystems characterized by mats of sulfur-oxidizing bacteria that scavenge sulfur released by the anaerobic oxidation of methane (AOM) [9]. A third type of seep habitat is inhabited by frenulate tubeworms (*Siboglinidae*, *Polychaeta*), which root in subsurface sediments and harbor bacterial

**Table 1.** Sampling sites included in this study (FS Sonne, cruise SO 191 – New Vents; 11.01. - 23.03.2007).

| Station No. | PANGAEA Event | Area               | Habitat             | Latitude [S] | Longitude [E] | Water depth [m] |
|-------------|---------------|--------------------|---------------------|--------------|---------------|-----------------|
| 45          | SO191/2_045   | Omakere Ridge      | <i>Frenulata</i>    | 40°01.079'   | 177°51.573'   | 1159            |
| 78          | SO191/2_078   | Omakere Ridge      | Reference           | 40°01.399'   | 177°48.944'   | 1182            |
| 124         | SO191/2_124   | Wairarapa N. Tower | <i>Ampharetidae</i> | 41°46.908'   | 175°24.024'   | 1054            |
| 157         | SO191/2_157   | Wairarapa N. Tower | <i>Ampharetidae</i> | 41°46.851'   | 175°24.107'   | 1056            |
| 215         | SO191/3_215   | Rock Garden        | <i>Ampharetidae</i> | 40°02.007'   | 178°09.650'   | 661             |
| 232         | SO191/3_232   | Omakere Ridge      | <i>Ampharetidae</i> | 40°02.150'   | 177°47.950'   | 1172            |
| 258         | SO191/3_258   | Rock Garden        | <i>Ampharetidae</i> | 40°01.890'   | 178°09.650'   | 659             |
| 273         | SO191/3_273   | Wairarapa          | <i>Ampharetidae</i> | 41°46.986'   | 175°24.251'   | 1059            |
| 309         | SO191/3_309   | Wairarapa Takahae  | <i>Ampharetidae</i> | 41°46.350'   | 175°25.690'   | 1057            |
| 315         | SO191/3_315   | Wairarapa Takahae  | SOB                 | 41°46.320'   | 175°25.690'   | 1057            |

endosymbionts [6]. It was shown that these different types of dominating megafauna indicate spatial variations in fluid flow, methane turnover and efflux to the hydrosphere [10,11,12].

In most previously studied methane seeps the biogeochemistry was dominated by AOM in subsurface horizons and sulfide oxidation at the surface. AOM is mediated by consortia of anaerobic methanotrophic archaea (ANME) and sulfate-reducing bacteria (SRB). ANME belong to the class *Methanomicrobia* and comprise the major clades ANME-1, ANME-2 and ANME-3 [9]. The partner SRB are usually *Deltaproteobacteria* closely related to *Desulfosarcina/Desulfococcus* (DSS) and *Desulfobulbus* (DBB) [9,13]. It is generally assumed that aerobic methanotrophy plays a minor role at seeps due to limited oxygen availability in the seafloor [9]. Exceptions are the centers of active mud volcanoes, where high pore water velocities prevent the diffusion of sulfate into the sediment and hence inhibit AOM [10,14], or where other disturbances favor the more rapidly growing aerobic methanotrophs [11]. Typical aerobic methanotrophs at seeps are *Gammaproteobacteria* of the order *Methylococcales* [14,15,16].

A main objective of this study was to compare the microbial communities of the different Hikurangi cold seeps, with a focus on ampharetid habitats, to identify distinct distribution patterns. Given the large geographic distances to other known seep ecosystems, and the previous description of a distinct seep fauna at the Hikurangi margin, another objective of this study was to compare the microbial communities of the Hikurangi region with other seeps worldwide. A detailed description of the new seep habitats is provided based on biogeochemical measurements, comparative sequence analyses of 16S rRNA and the particulate methane monooxygenase subunit A (*pmoA*), and visualization of key methanotrophs using fluorescence in situ hybridization (FISH). Microbial community  $\beta$ -diversity at Hikurangi cold seeps was analyzed by the fingerprinting technique ARISA [17]. We showed that aerobic methanotrophy plays an important role at ampharetid habitats and found distinct microbial communities that differ from other types of seep and non-seep ecosystems.

## Materials and Methods

### Sampling procedure and study sites

The nine investigated cold seep sites were located on the Hikurangi continental margin, east of New Zealand's North Island (Table 1, Figure 1). Seven sites were dominated by heterotrophic ampharetids, one site showed few ampharetids and a white surface, supposedly caused by mat-forming sulfur-oxidizing bacteria (SOB), and one site was densely populated by frenulate tubeworms. The sites 45, 78 and 232 were located at Omakere Ridge and the sites 215 and 258 were located at Rock Garden, on the northern part of Hikurangi margin (Figure 1, Table 1). The sites 124, 157, 273, 309 and 315 were situated at Wairarapa several hundred kilometers further south on Hikurangi margin. The samples were retrieved by TV-guided multicoring during cruise SO-191 leg 2 and 3 on the German research vessel "FS Sonne" in 2007. After retrieval, the cores were transferred to the cold room (4°C) and sectioned at intervals of 1 or 2 cm. Five representative sites were selected for a detailed microbial community analysis. These were site 45 (frenulate habitat), 124, 309 (ampharetid habitat), 315 (SOB habitat) and 78 (reference site). Subsamples for DNA extraction were frozen at -20°C and subsamples for FISH were fixed in 4% formaldehyde for 24 h at 4 °C, washed twice with 1× PBS and stored in 1× PBS/absolute ethanol (1:1) at -20 °C. As a formal process in the preparation of the FS SONNE expedition 191, a diplomatic permission was received from the coastal state (New Zealand) to retrieve samples for scientific purposes from their Exclusive Economic Zone (EEZ, 200 miles offshore). No protected species were harmed by the seafloor sampling activities.

### Concentration of methane and sulfur species and biogeochemical rate measurements

For methane measurements, 2 ml sediment of each horizon was sampled with cut-off plastic syringes immediately after sectioning. Material was transferred into 20 ml butyl-rubber sealed vials filled with 5 ml sodium hydroxide solution (2.5%). From the headspace of these vials methane concentrations were measured using gas chromatography coupled to flame-ionization detection (GC 5890A, Hewlett Packard, Palo Alto, CA, USA). Sulfide was determined colorimetrically from pore

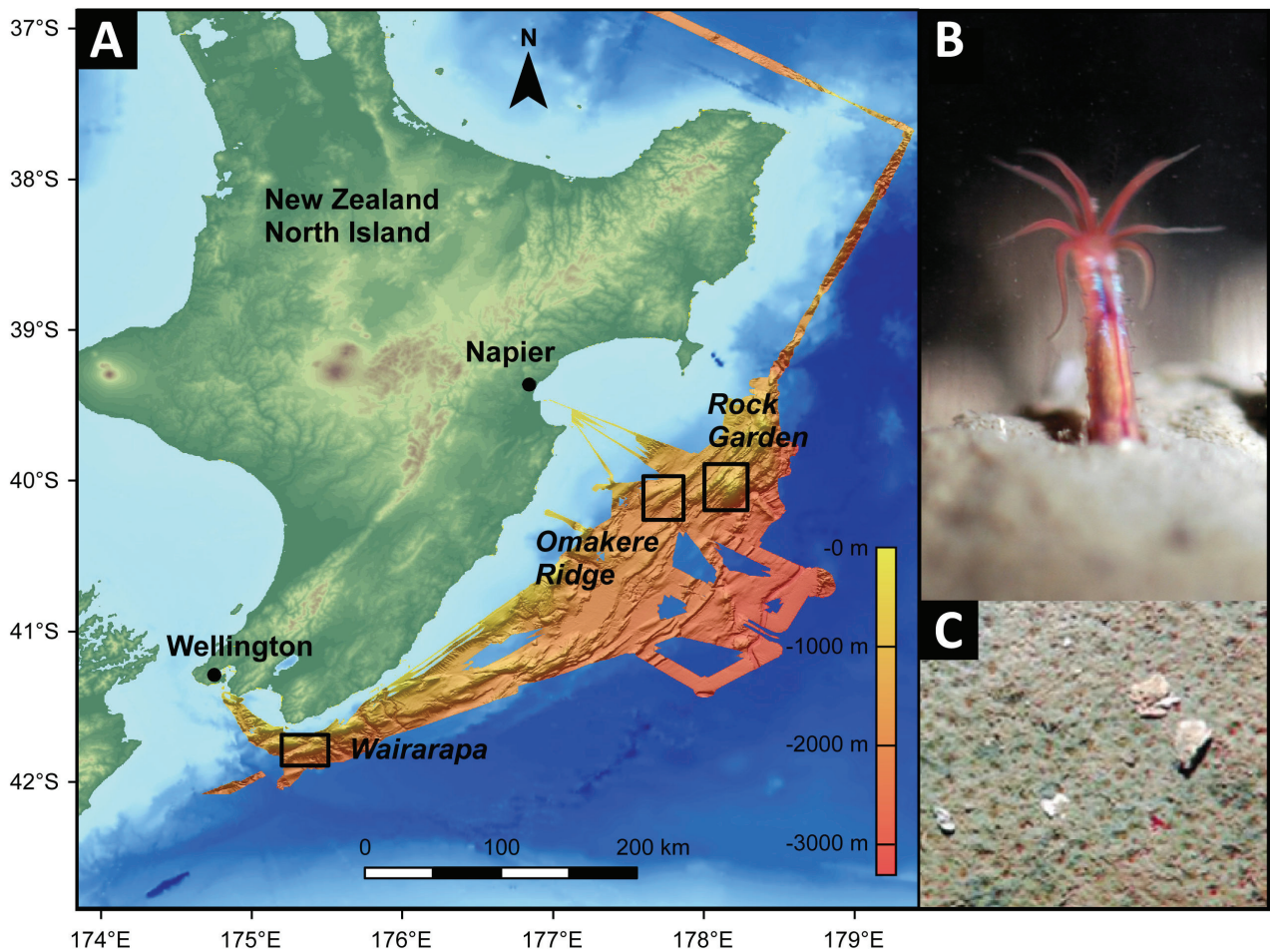


**Figure 1. The sampling sites.** **A:** Bathymetric map of Hikurangi margin, New Zealand. The map was generated using the ESRI ArcGIS software and the General Bathymetric Chart of the Oceans (GEBCO\_09 Grid, version 20091120, <http://www.gebco.net>). Data for the high resolution bathymetry were provided by Jens Greinert. Sampling areas are indicated. **B:** Close-up view of an ampharetid polychaete, the dominant fauna at many Hikurangi seep sites. These polychaetes are between 1 and 2.5 cm long and inhabit tubes which extend 2-3 cm into the sediment (image courtesy of S. Sommer). **C:** Each depression on the sediment surface was created and inhabited by a single polychaete (image courtesy of D. Bowden).

doi: 10.1371/journal.pone.0072627.g001

water samples fixed with zinc acetate (20%) using methylene blue method [18]. Sulfate concentrations were determined by ion chromatography (761 Compact IC,  $\Omega$  Metrohm, Filderstadt, Germany).

Methane oxidation (MOx) and sulfate reduction (SR) rates were determined using the subcore injection method [19]. Three subcores from the sampling sites were treated with carrier-free radiolabeled methane (5 kBq) or sulfate (50 kBq), respectively. Cores were incubated at 4°C for 12 to 36 hours in the dark. For MOx measurements biological activity was stopped by the transfer of 1 cm long sediment sections into gas tight flasks with sodium hydroxide solution (2.5%). To determine MOx rates, concentration of the reactant methane was determined by flame ionization gas chromatography (GC 5890A),  $^{14}\text{C}$ -methane was stripped from the headspace, converted to  $\text{CO}_2$  (via CuO-catalyzed oxidation at 850°C) and

trapped in CarboSorb (PerkinElmer, Waltham, MA, USA). Microbially produced inorganic carbon was released from the sample by acidification and trapping in CarboSorb. To determine SR rates, sediment sections were transferred to zinc acetate solution. Concentration of sulfate was measured via ion chromatography or by barium sulfate precipitation. Activity of added  $^{35}\text{S}$ -sulfate was measured from the supernatant, activity of produced total reduced sulfur was determined after releasing it using cold chromium distillation [20]. To determine activities of  $^{14}\text{C}$  and  $^{35}\text{S}$ , scintillation cocktails Permafluor-E $\text{C}$  or Ultima Gold $\text{C}$  (PerkinElmer) were added and samples measured by scintillation technique (Tricarb 2500 liquid scintillation counter, Packard, Palo Alto, CA, USA). Rates were determined by the ratio of product and reactant activity and the reactant concentration as described before [21].

### DNA extraction

DNA was retrieved from 3 g of sediment (pooled for each 5 cm layer) by chloroform extraction as described before [22] and purified using the Wizard DNA clean-up system (Promega, Madison, WI, USA).

### Gene library construction

PCRs for 16S rRNA gene libraries were carried out using 5–75 ng environmental DNA, 25 cycles and the primers GM3/GM4 and Arch20F/Uni1392R (for details see Table S2 in the Materials and Methods S1). 10 parallel PCRs of each sample were pooled, purified using the PCR Purification Kit (Qiagen, Hilden, Germany) and eluted in 30  $\mu$ l ultrapure water. For the bacterial library of station 315 we used 15 cycles and pooled 20 PCRs. Cloning reactions were performed with vector pCR4 and the TOPO TA Cloning Kit (Invitrogen, San Diego, CA, USA) and inserts sequenced using the BigDye Terminator v 3.1 Cycle Sequencing Kit (Applied Biosystems, Carlsbad, CA, USA) on an ABI PRISM 3130xl Genetic Analyzer. Bacterial libraries of station 45 and 78 and archaeal libraries of station 78 and 315 were constructed alike, except that vector pGEM T-Easy (Promega, Madison, WI, USA) was used and sequencing was performed by LGC Genomics (LGC, Berlin, Germany). The libraries for the particulate methane monooxygenase subunit A gene (*pmoA*) were constructed using 24 cycles and the primers A189F/MB661R (for details see Table S2 in the Materials and Methods S1). Chimeric 16S rRNA sequences were removed using the software Mallard [23].

### Phylogenetic analysis

Phylogenetic classification was carried out with the software package ARB [24] based on the SILVA small subunit rRNA reference sequence database (SSURef v102, release date: 02-15-10) [25]. Sequences were aligned by SINA [26] and manually optimized according to the secondary structure. To build phylogenetic trees our full-length sequences (>1300 bases) were complemented with sequences from the database. Phylogenetic trees were calculated with the maximum likelihood algorithm PHYML (100 bootstraps) as implemented in ARB using a positional variability filter. Nucleotide substitutions were weighted according to the HKY model [27]. Partial sequences were added to the tree using the ARB maximum parsimony algorithm. Redundant sequences were deleted for clarity.

### Clustering of operational taxonomic units (OTUs) and determination of species richness

A lower triangular distance matrix of the sequences of each gene library was calculated using the neighbor-joining method [28] as implemented in ARB. The 16S and *pmoA* matrices were corrected according to Jukes-Cantor [29] and Kimura [30], respectively. OTU clustering, species rarefaction and Chao1 OTU richness estimates [31] were performed based on these matrices using the software mothur v 1.20 [32].

### Automated ribosomal intergenic spacer analysis (ARISA)

ARISA was carried out using 20–25 ng of environmental DNA according to Böer and colleagues [33], with slight modifications (see Materials and Methods S1). To include the maximum number of peaks while excluding background fluorescence, only fragments above a threshold of 50 fluorescence units and between 100 and 1000 bp were taken into consideration [34]. The GeneMapper output file was reformatted and analyzed by custom R scripts [35]. An “interactive” binning strategy with a bin size of 2 bp was applied to the ARISA generated data to account for size calling imprecision [34]. The binning frame that offered the highest pairwise similarities among samples was further subjected to multivariate analyses. An operational taxonomic unit (OTU) was considered present in a given DNA sample only if it was observed at least twice among the set of three replicated PCRs from the DNA extract of that particular sample [35,36]. We processed 26 samples originating from different geographic locations, seep habitats, sampling sites and depth intervals.

### Statistical analyses

Non-metric multidimensional scaling (NMDS) [37] was carried out based on the Bray-Curtis similarity measure [38] using PAST v 1.99 [39]. To reduce the stress value, a three-dimensional (3D) ordination space was chosen of which two axes are shown. Stress values below 0.2 reliably represent the underlying data. Analysis of similarity (ANOSIM) was used to determine significant differences between groups [40] based on a Bray-Curtis similarity measure. Redundancy analysis (RDA) and analysis of variance (ANOVA) was performed using the software package vegan [41] based on the software environment R v 2.15.0.

### Cell enumeration and catalyzed reporter deposition fluorescence in situ hybridization (CARD-FISH)

Total numbers of single cells were determined using acridine orange direct counts [11]. CARD-FISH was carried out as described previously [42] with the following modifications. The samples were ultra-sonicated before filtration and endogenous peroxidases inactivated by incubation in 0.15% H<sub>2</sub>O<sub>2</sub> in methanol for 30 min at room temperature [43]. Archaeal cell walls were permeabilized with Proteinase K solution (15  $\mu$ g ml<sup>-1</sup> (Merck, Darmstadt, Germany) in 0.05 M EDTA (pH 8), 0.1 M Tris-HCl (pH 8), 0.5 M NaCl) for 5 min or HCl (0.1M) for 1 min at room temperature. Bacterial cell walls were permeabilized with lysozyme solution (1000kU/ml) [42] for 30 min at 37°C or HCl (0.1M) for 1 min at room temperature. In case of dual CARD-FISH, probe-coupled peroxidases of the first hybridization were inactivated (see above) prior to the second hybridization. Cells were stained with DAPI (1 $\mu$ g/ml), embedded in mounting medium and counted in 20–60 independent microscopic fields using an Axiophot II epifluorescence microscope (Carl Zeiss, Jena, Germany). Cells in dense aggregates were estimated semi-quantitatively in 100–250 independent microscopic fields [14]. A complete list of probes used in this study is provided (see Table S2 in the Materials and Methods S1).

### Nucleotide sequence accession numbers

The nucleotide sequence data reported in this paper have been archived in the EMBL, GenBank, and DDBJ nucleotide sequence database. The accession numbers JF268327 to JF268425, JN884818 to JN885079 and JQ241648 to JQ241771 refer to 16S rRNA gene sequences, JN990380 to JN990410 and KC751343 to KC751411 refer to *pmoA* gene sequences. Submission was done using the new tool CDinFusion [44]. Contextual data are included according to the MIMARKS standard [45].

### Results

In this study we investigated nine cold seep sites located off the northeast coast of New Zealand at water depths between 660 and 1200 meters (Figure 1, Table 1). Seven of the investigated seep sites (124,157,215,232,258,273,309) were densely populated by heterotrophic ampharetids (*Ampharetidae*, *Polychaeta*). One seep site (315) hosted mainly sulfur-oxidizing bacteria (SOB) with minor co-occurrence of ampharetid polychaetes and one seep site (45) was colonized by chemosynthetic frenulate tubeworms (*Siboglinidae*, *Polychaeta*). A site without see page (78) was analyzed as reference.

### Biogeochemistry of Hikurangi seep ecosystems

Biogeochemical measurements were conducted at all seep sites with a focus on the ampharetid habitats 124 and 309, the SOB habitat 315 and the frenulate habitat 45. We distinguished between oxic/suboxic and sulfidic sediment layers based on sulfide concentration or appearance of the sediment cores. At the frenulate site 45 methane concentrations [ $\text{CH}_4$ ] remained below 3  $\mu\text{M}$  down to 16 cmbsf (centimeter below sea floor) and sulfate [ $\text{SO}_4^{2-}$ ] was nearly constant at 28 mM. Methane oxidation (MOx) was not detected and sulfate reduction (SR) was present at very low rates (Figure 2). At the ampharetid sites 124 and 309, [ $\text{CH}_4$ ] reached up to 600  $\mu\text{M}$  and [ $\text{SO}_4^{2-}$ ] decreased from 28 mM to 0 mM within the upper 20 cmbsf. The sulfide concentration at site 124 was low in the upper sediment horizon (0-7 cm), but increased strongly below. Although sulfide data were not available for site 309, this trend was observed at this and other ampharetid sites (Figure S1), indicating that the upper sediment horizon at ampharetid sites is non-sulfidic. At both ampharetid sites the MOx activity showed a peak in the oxic and anoxic layer (Figure 2), which was also observed at most other ampharetid sites (Figure S1). Within the oxic/suboxic layer methane oxidation rates amounted to  $1.2 \pm 0.5 \text{ mol m}^{-2} \text{ yr}^{-1}$  (mean  $\pm$  standard error) at site 124 and  $1.8 \pm 0.2 \text{ mol m}^{-2} \text{ yr}^{-1}$  at site 309. In the sulfidic layers integrated MOx rates were higher with  $4.3 \pm 1.2 \text{ mol m}^{-2} \text{ yr}^{-1}$  (site 124) and  $6.1 \pm 1.9 \text{ mol m}^{-2} \text{ yr}^{-1}$  (site 309). Integrated SR rates were  $5.0 \pm 1.9 \text{ mol m}^{-2} \text{ yr}^{-1}$  (site 124) and  $2.9 \pm 0.8 \text{ mol m}^{-2} \text{ yr}^{-1}$  (site 309). The average annual methane oxidation rate found in the oxic layer of all ampharetid sites was around  $0.7 \pm 0.2 \text{ mol m}^{-2} \text{ yr}^{-1}$ , as compared to  $3.7 \pm 1.1 \text{ mol m}^{-2} \text{ yr}^{-1}$  in the anoxic zone.

At the SOB site 315 the oxic/suboxic layer was only a few millimeters thick. Methane concentration was up to 400  $\mu\text{M}$  and

sulfate disappeared within the upper 10 cmbsf (Figure 2). Sulfide data were not available for this site. MOx and SR rates peaked between 3 and 5 cmbsf. Integrated MOx rates were  $14.6 \pm 2.2 \text{ mol m}^{-2} \text{ yr}^{-1}$  within the upper 10 cmbsf and  $9.1 \pm 2.7 \text{ mol m}^{-2} \text{ yr}^{-1}$  between 10 and 20 cmbsf. Integrated SR rates were  $21.4 \pm 2.9 \text{ mol m}^{-2} \text{ yr}^{-1}$  and  $3.7 \pm 0.9 \text{ mol m}^{-2} \text{ yr}^{-1}$ , respectively. At the reference site we did not detect methane, sulfide, AOM or SR (Figure S1).

### Archaeal diversity of Hikurangi margin sediments

Sequencing of selected clones from 16S rRNA gene libraries of the upper 10 cmbsf from four sampling sites (45,78,309,315) resulted in a total of 305 partial and 21 full-length, high quality sequences. We found the highest archaeal richness at the reference site with 27 observed and 48 estimated operational taxonomic units (OTUs) using Chao1 at a 97% similarity cut-off. The lowest archaeal richness was present at the SOB site (14 observed and 25 estimated OTUs). At the frenulate and ampharetid sites 16 of 28 and 18 of 46 estimated OTUs were retrieved, respectively.

At the reference site, we detected mostly *Thaumarchaeota* and *Crenarchaeota* of Marine Benthic Group B, whereas sequences of methane-oxidizing groups were absent (Figure 3A). Gene libraries of methane seep sites 45, 309 and 315 contained many sequences related to ANME-2a/2b and ANME-3. ANME-2c was found only at the ampharetid site 309. Interestingly, ANME-1 sequences were absent in all libraries. The diversity of ANME at each site was high, especially at site 309 with 17 different OTUs (97% cut off). A few sequences affiliated to methanogenic *Methanosarcinaceae* were present at all seep sites. A detailed archaeal phylogeny is provided (Figure S2).

### Bacterial diversity of Hikurangi margin sediments

The upper 10 cmbsf of all sampled sites (45,78,309,315) yielded a total of 355 bacterial 16S rRNA partial and 78 full-length sequences. These were distributed widely among the *Bacteria* (Figure 3B). The highest bacterial richness was found at the reference site, with 77 observed and 1355 estimated OTUs at a 97% similarity cut-off. Lowest richness was present at the SOB site (54 observed and 56 estimated OTUs). At the frenulate and ampharetid sites we retrieved 62 of 197 and 54 of 177 estimated OTUs, respectively.

The majority of sequences clustered with the *Alphaproteobacteria*, *Gammaproteobacteria* and *Deltaproteobacteria*, *Planctomycetes* and *Acidobacteria*, which were present in all sediments. *Deltaproteobacteria* was the dominant phylum in all libraries and the majority of the clones was assigned to sulfate reducers (Figure S3). Among those, members of the *Desulfobulbaceae*, such as SEEP-SRB3 and SEEP-SRB4 were only found at active methane seeps, whereas *Desulfobacteraceae* were found in all sediments. Within the *Desulfobacteraceae* the genus *Desulfobacula* was confined to the seep sediments, whereas members of the SEEP-SRB1 were also found at the reference site.

Major differences between the gene libraries were observed for the *Gammaproteobacteria*. Sequences related to *Methylococcales*, *Methylophaga* and *Leucothrix* occurred in

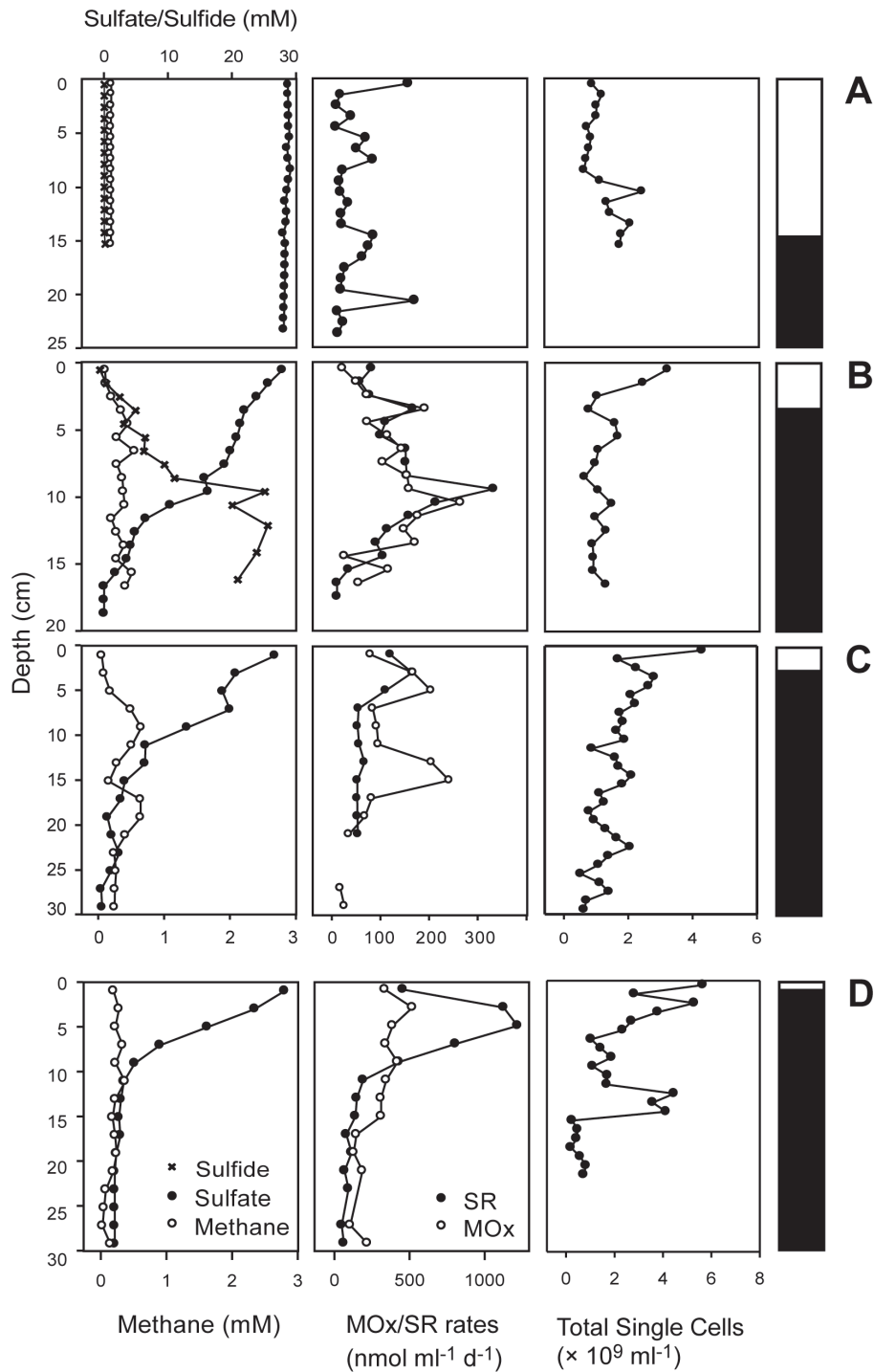


**Figure 2. Biogeochemistry and total single cell numbers.** Methane and sulfate concentrations, rates of methane oxidation (MOx) and sulfate reduction (SR), and total single cell numbers of four sampling sites from the Hikurangi margin. **A:** Frenulate site 45, **B:** Ampharetid site 124, **C:** Ampharetid site 309, **D:** SOB site 315. Note the different scales on x- and y-axes. The bars on the side show the redox state of the sediment: White is oxic/suboxic and black is sulfidic. In the frenulate habitat, methane hardly reached the top 10 cm layer and the suboxic zone extended to 15 cmbsf. In the ampharetid habitat, methane was present throughout the core, but the suboxic zone nevertheless reached 2-4 cm deep. In the bacterial mat habitat, the suboxic zone was limited to a few mm.

doi: 10.1371/journal.pone.0072627.g002

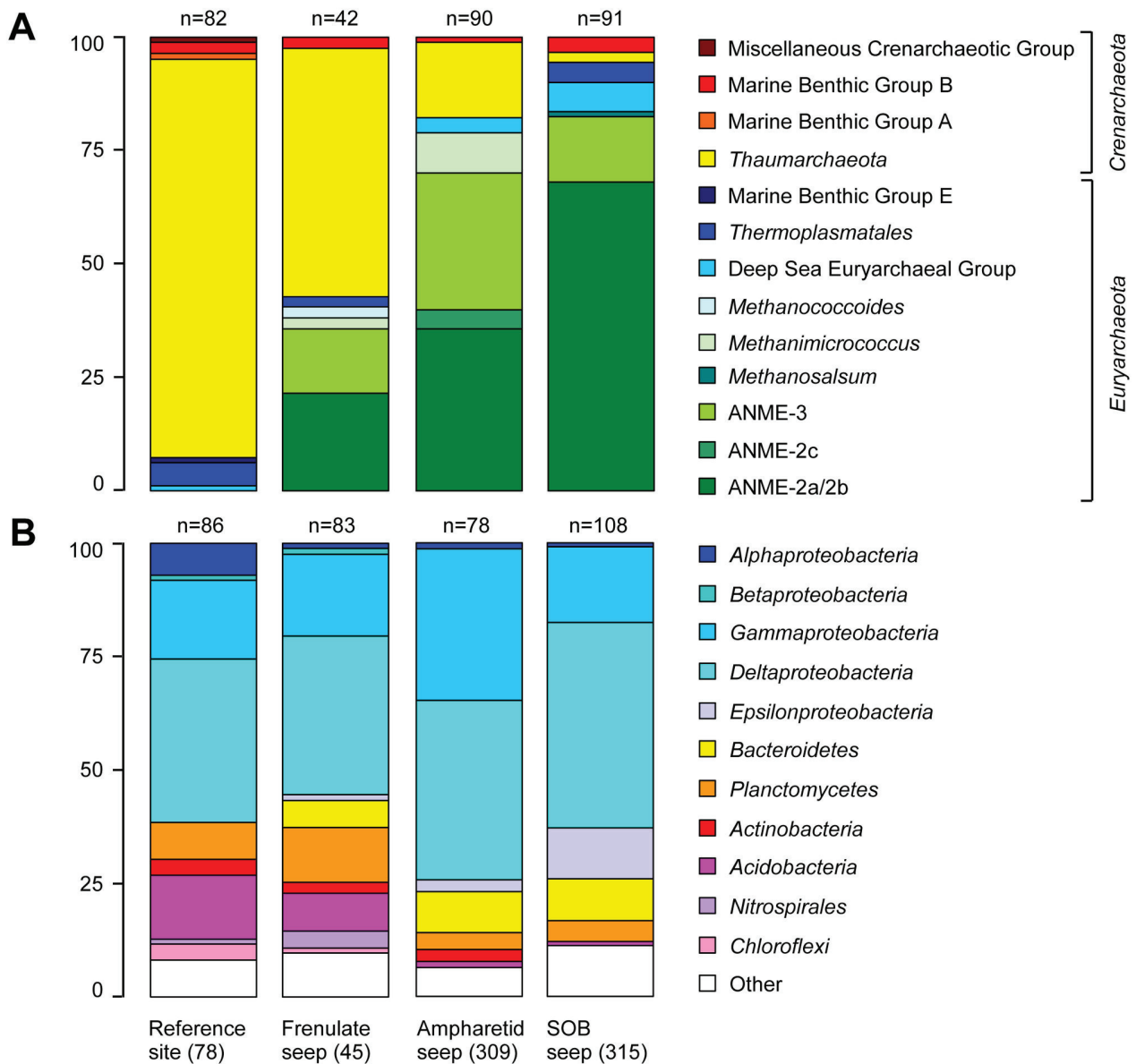


**Figure 3. Relative 16S rRNA clone frequencies.** A: Archaeal and B: bacterial diversity at the frenulate (45), ampharetid (309), SOB (315) and the reference site (78) as determined by 16S rRNA gene analysis. The scale bar represents relative clone frequency in percent. The total number of clones per library is indicated above the respective column.

doi: 10.1371/journal.pone.0072627.g003

high diversity at the ampharetid sites, some were present at the frenulate site, but they were absent at the reference site. Most sequences related to methylotrophs clustered within three distinct groups that we termed Marine Methylotrophic Group 1 to Marine Methylotrophic Group 3 (MMG1-MMG3) (Figure 4). MMG1 and MMG2 are related to *Methylococcales*, while MMG3 is related to the deep-branching *Methylophaga*. Sequences of the MMG1 and MMG2 shared >95% similarity, whereas MMG3 was wider with pairwise similarities above 90%. All MMGs contained only sequences from marine

samples, mostly from cold seep sediments. Additionally, MMG1 and MMG3 contained many sequences from marine methylotrophic endosymbionts of e.g. *Bathymodiolus* spp. and *Idas* spp.

**Diversity of pmoA genes**

To further investigate the diversity of aerobic methanotrophic bacteria, we analyzed *pmoA* genes encoding for subunit A of the particulate methane monooxygenase. This enzyme plays a central role in aerobic methanotrophy as it activates methane

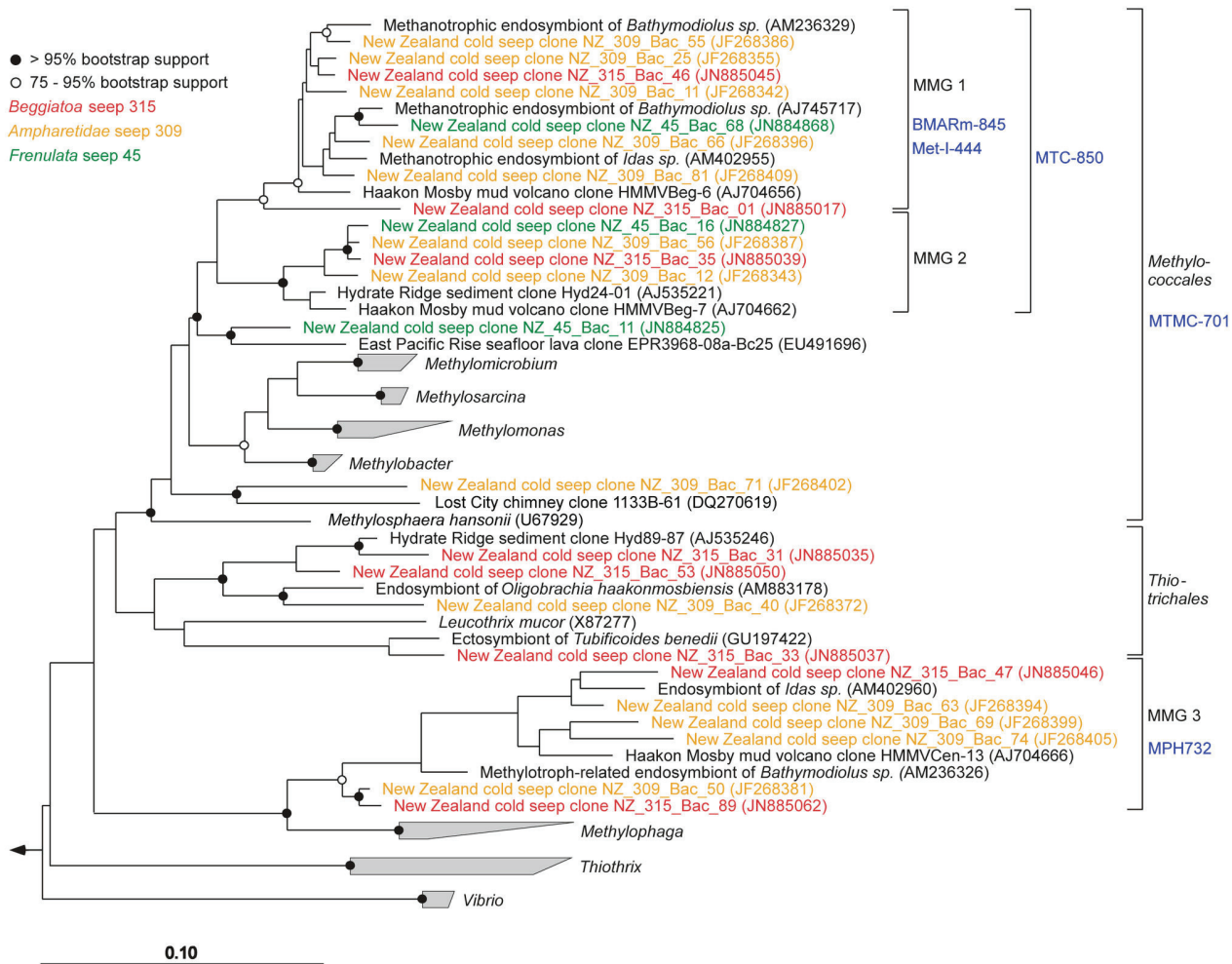


**Figure 4. Phylogenetic affiliation of the Marine Methylotrophic Groups 1-3.** Phylogeny of the Marine Methylotrophic Groups 1-3 within the *Gammaproteobacteria* based on their 16S rRNA genes. The colors indicate the origin of the sequences. Organisms belonging to the depicted groups were only found at cold seeps and not at the reference site. Probes specific for certain groups are marked in blue (see also Table S2 in the Materials and Methods S1).

doi: 10.1371/journal.pone.0072627.g004

by the addition of oxygen. Analysis of the top 10 cm of sediment at sites 45, 309 and 315 yielded 236 sequences and 24 OTUs. The Chao1 estimated richness was 29 OTUs. The OTUs were calculated using a cut-off of 93% amino acid sequence similarity, which corresponds to a 97% 16S rRNA similarity [46]. We found a highly diverse *pmoA* composition at the frenulate site 45 (20 OTUs). Many of the OTUs were related to endosymbionts of *Lamellibrachia* sp. and did not occur at the other seeps. The *pmoA* diversity at the SOB site 315 was also quite high (8 OTUs), but the OTUs mostly differed from the ones present at the frenulate site. Interestingly, at the ampharetid site 309 we discovered only 2 different OTUs. Both OTUs were closely related to methanotrophic endosymbionts. The *pmoA* sequences formed five very distinct monophyletic clusters (Figure S4). All clusters contained sequences exclusively from marine methane-rich

ecosystems. One cluster included the cultured organism *Methylomonas methanica*. Four clusters contained sequences of either methanotrophic endosymbionts of *Bathymodiolus* spp., *Rimicaris* spp. or *Lamellibrachia* spp.

#### In situ abundance and distribution of microorganisms

Abundance and distribution of microbial cells were determined for two ampharetid sites (124,309), for one SOB site (315) and one frenulate site (45). The percentages of subgroups are given relative to the total number of cells, including aggregates. Total single cell numbers (Figure 2) do not contain aggregated cells.

**Frenulate site 45.** At the site populated by frenulates, the highest cell abundance was found at 13.5 cmbsf with  $2.2 \times 10^9$  cells ml<sup>-1</sup> sediment (Figure 2). Single cells of *Bacteria* and

*Archaea* were found throughout the sediment, whereas consortia of archaeal and bacterial cells were only detected between 11 and 12 cm depth. Single cells of ANME-2 and ANME-3 were found in low numbers in the deeper sediment horizons, whereas ANME-1 was not detected at all. *Methylococcales* peaked in the top cmbsf at  $4.9 \times 10^7$  cells ml<sup>-1</sup> sediment, but were found down to 15 cmbsf.

**Ampharetid sites 124 and 309.** The highest total cell numbers at the ampharetid sites were found in the oxic top centimeter. Most cells were identified as *Bacteria* (80-90%, probe EUB338-I-III; LEN338), of which *Methylococcales* (probe MTMC-701 and competitors) dominated the surface sediment at both sites (12-15%). However, as many of the observed *Methylococcales* aggregated in clusters of irregular shape, their total abundance was certainly underestimated. *Methylococcales* aggregates were between 5 and 40  $\mu$ m in diameter (Figure 5A–D). The large aggregates were comprised of large oval cells and appeared to contain also other cell types (Figure 5A). Small aggregates consisted of small densely packed or large loosely packed cocci (Figure 5B,C; see also Movie S1). Many aggregates consisted of cells belonging to clade MMG2 (probe MTC-850), which seemed to be responsible for most of the biomass of aerobic methyloproths at the ampharetid habitats. The *Methylococcales* probe (MTMC-701) also visualized a few up to 30  $\mu$ m long filaments with square-shaped cells (Figure 5D). Single *Methylococcales* cells occurred as rods (<1 $\mu$ m) and oval or round cocci (up to 2 $\mu$ m) showing a high morphological diversity. MMG1 (probe MetI-444) comprised cells that were stained by a probe specific for *Bathymodiolus* spp. endosymbionts (BMARm-845, Figure S5). MMG1 and MMG3 (probe MPH-732) occurred mainly in the top centimeter as single cells and at low abundances (~1-4%). Although the abundance of *Methylococcales* decreased with increasing sediment depth, MMG2 were detected as deep as 7 cmbsf. Organisms likely involved in sulfur cycling included *Epsilonproteobacteria* (~3%, probe EPSI682) and potential sulfur-oxidizing *Gamma*proteobacteria (~3%, probe Gam660) that occurred in the oxic surface layer. Single cells of sulfate-reducing *Desulfosarcina/Desulfococcus* (probe DSS658) occurred throughout the sediment (1-14%) and peaked in the anoxic layer.

*Archaea* were almost absent in the upper oxic centimeters, but their cell numbers increased with depth. At site 124, AOM consortia of ANME-2a (probe ANME2a-647) and SEEP-SRB1a (probe SEEP1a-473) were largest and most abundant between 7 and 13 cmbsf, peaking with  $4.2 \times 10^7$  consortia ml<sup>-1</sup> sediment (see also Movie S2). Consortia of ANME-2c (probe ANME2c-760) and SEEP-SRB1a (Figure 5I) were also detected, but in lower numbers. The diameter of the aggregates ranged from 2  $\mu$ m, harboring as few as 6 cells, to 12  $\mu$ m (about  $10^4$  cells) with an average of  $2.9 \pm 0.3$   $\mu$ m (about 140 cells). Hence, the total number of AOM-mediating archaeal and bacterial cells at this site may have been as high as  $5.9 \times 10^9$  ml<sup>-1</sup>. We found many small AOM aggregates, lesser medium sized ones and only few large aggregates (Figure S6). At site 309, ANME-2c archaea were abundant only in around 15 cmbsf, accounting for up to 25% of all cells. They mostly occurred in small, loosely associated aggregates with DSS

(Figure 5E–H). Although ANME-3 archaea were present in the 16S rRNA gene libraries they were not detected in situ (probe ANME3-1249 and helper probes). In accordance with the gene libraries, ANME-1 archaea (probe ANME1-350) were not detected. Methanogenic archaea were present in low numbers (up to 1%, probe MS1414) only in the upper horizon.

**Sulfide oxidizing mats site 315.** The sulfidic top centimeter of sediment at the SOB site also harbored the largest number of cells with *Bacteria* accounting for around 90%. In contrast to the ampharetid sites *Methylococcales* accounted only for around 1% of the community ( $9 \times 10^7$  cells ml<sup>-1</sup>). Similar to site 309 we again found about 1% MMG1 and 1% MMG3, while MMG2 was almost absent. Cell numbers of aerobic methyloproths decreased within the first 3 cmbsf and were not detected in the deeper sediment. The bacterial community of the top layer included organisms involved in sulfur cycling, such as potential sulfur-oxidizing *Gamma*proteobacteria (up to 3%) and *Epsilon*proteobacteria (up to 4%). Single cells of the DSS group occurred in all depths (up to 12%).

ANME-2 archaea were omnipresent and mostly associated with DSS. Relative abundance of ANME-2 (15% of total cells) and DSS (30%) peaked between 2 and 8 cmbsf. Single cells of ANME-2 (up to 4%) and DSS (up to 15%) were also abundant. We found the highest aggregate numbers at 2 cmbsf, whereas the largest aggregates, with diameters of >16  $\mu$ m, occurred at 6 cmbsf. In the uppermost layers, ANME-2a/DSS aggregates dominated, whereas in the deeper sediment, ANME-2a and ANME-2c were equally abundant. Neither ANME-1 nor ANME-3 archaea were detected. Methanogenic archaea (probe MS1414) made up 2-3% of all cells in the horizon between 2 to 9 cm, but were absent above and below.

### Variation of microbial diversity

To get a broader perspective of the microbial communities on Hikurangi margin we assessed the variation of microbial diversity between different seep sediments by ARISA. In total 385 different OTUs (individual ITS regions of bacteria that differ in length by at least 2 bases) were found (Figure S7). Each 5 cm depth interval contained on average  $149 \pm 15$  OTUs (mean  $\pm$  S.D.). The community structure of the upper oxic/suboxic sediment (0-5 cm) was significantly different from the deeper sediment (5-15 cm) as shown by NMDS ordination and ANOSIM (Figure 6A). However, OTU partitioning according to depth showed that the majority of OTUs (e.g. 80 at ampharetid site 232) was not restricted to a certain layer, but seemed rather dispersed throughout the sediment (Figure S8A). The largest number of layer-specific OTUs always occurred in the oxic top sediment layer, and the top and bottom layers frequently shared the least OTU numbers. 51 OTUs were common to all seep sites, whereas only 7 OTUs were common to all layers at all seep sites.

Grouping the dataset according to the habitats, i.e. the dominant seep-associated fauna, showed the differences between all seep habitats and the reference site (Figure 6B). 169 OTUs were found in all three seep habitats of which 138 might be considered ubiquitous residents of Hikurangi sediments since they were also present at the reference site. Ampharetid sites shared 49 OTUs with the SOB and 69 with

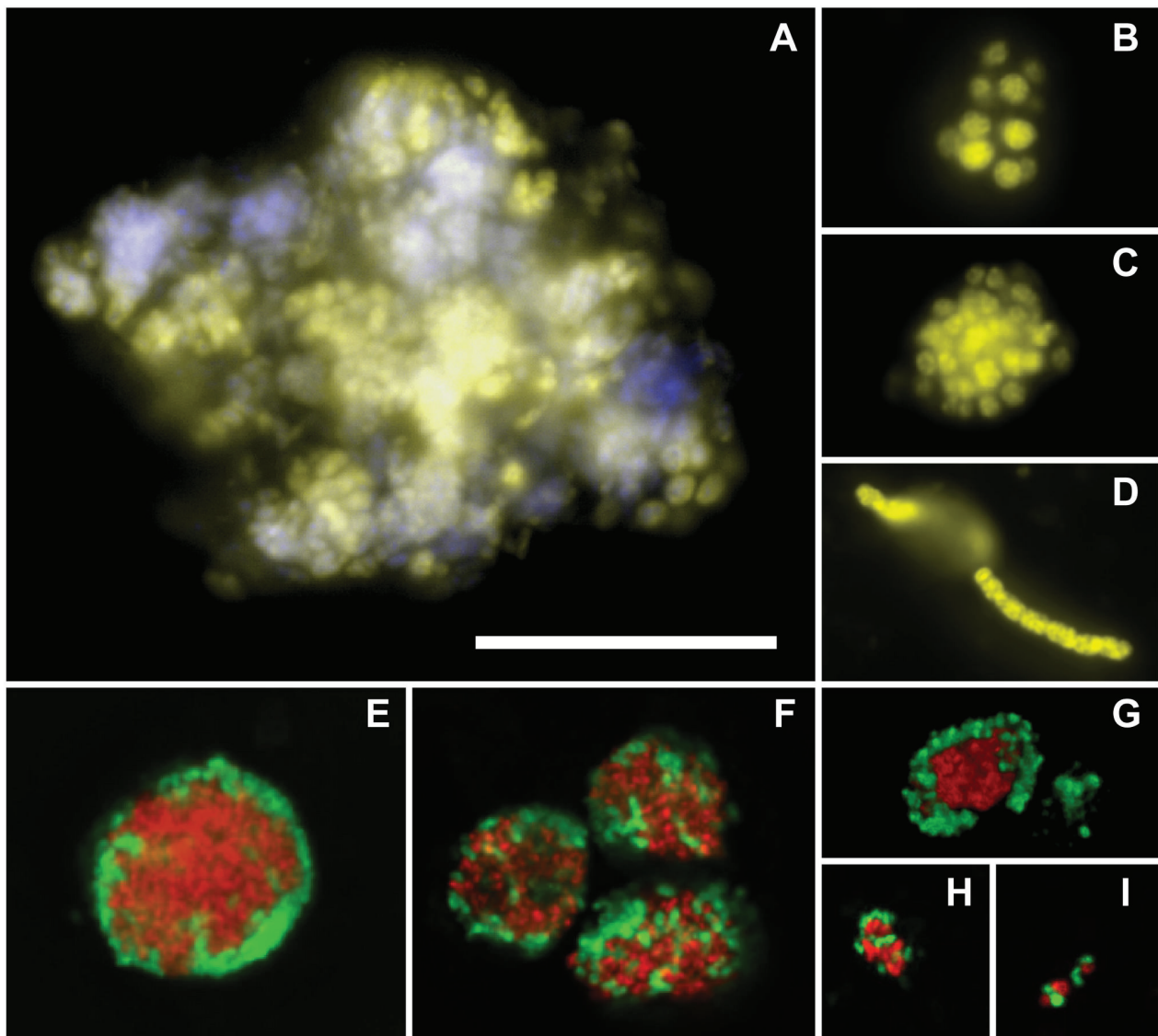


**Figure 5. Micrographs of methylotrophic and methanotrophic organisms in sediments of Hikurangi margin seeps.** A–D: Aerobic methylotrophic organisms of the order *Methylococcales* (probe MTMC-701 - yellow) in surface sediment of the ampharetid site 309. The dual stain with probe and DAPI (blue) shows that the large aggregates contained other cells besides *Methylococcales*. E–I: Consortia of anaerobic methanotrophic archaea of the clade ANME-2a and ANME2c (probe ANME2a-647, ANME2c-760 - red) and sulfate-reducing *Desulfosarcina/Desulfococcus* (DSS) (probe DSS658 - green) in the deeper sediment layers. E,F: Shell-type and mixed-type ANME-2a/DSS consortia at the SOB site 315. G,H: Consortia of ANME-2a and the DSS subgroup SEEP-SRB-1a (probe SEEP1a-473 – green) at the ampharetid site 124. I: ANME-2c/SEEP-SRB-1a consortium at ampharetid site 124. The scale bar represents 20  $\mu\text{m}$ .

doi: 10.1371/journal.pone.0072627.g005

the frenulate site, whereas only 1 OTU was shared between the SOB and the frenulate site (Figure S8B). Thus, ampharetid habitats appear to host communities partially overlapping with those of sulfidic sediments (e.g. SOB site) and non-sulfidic sediments (reference site). Habitat type had a significant impact ( $p=0.02$ ) on the microbial community as calculated by redundancy analysis (Figure S10).

Although each seep ecosystem contained a comparable number of OTUs ( $225 \pm 30$ ), their OTU composition differed significantly (Figure 6C). The high diversity of Hikurangi ecosystems is supported by a pairwise OTU comparison, which showed that only  $55 \pm 4\%$  of OTUs are shared between any two sampling sites (Figure S9). The differences in bacterial communities were also apparent on a larger scale when we

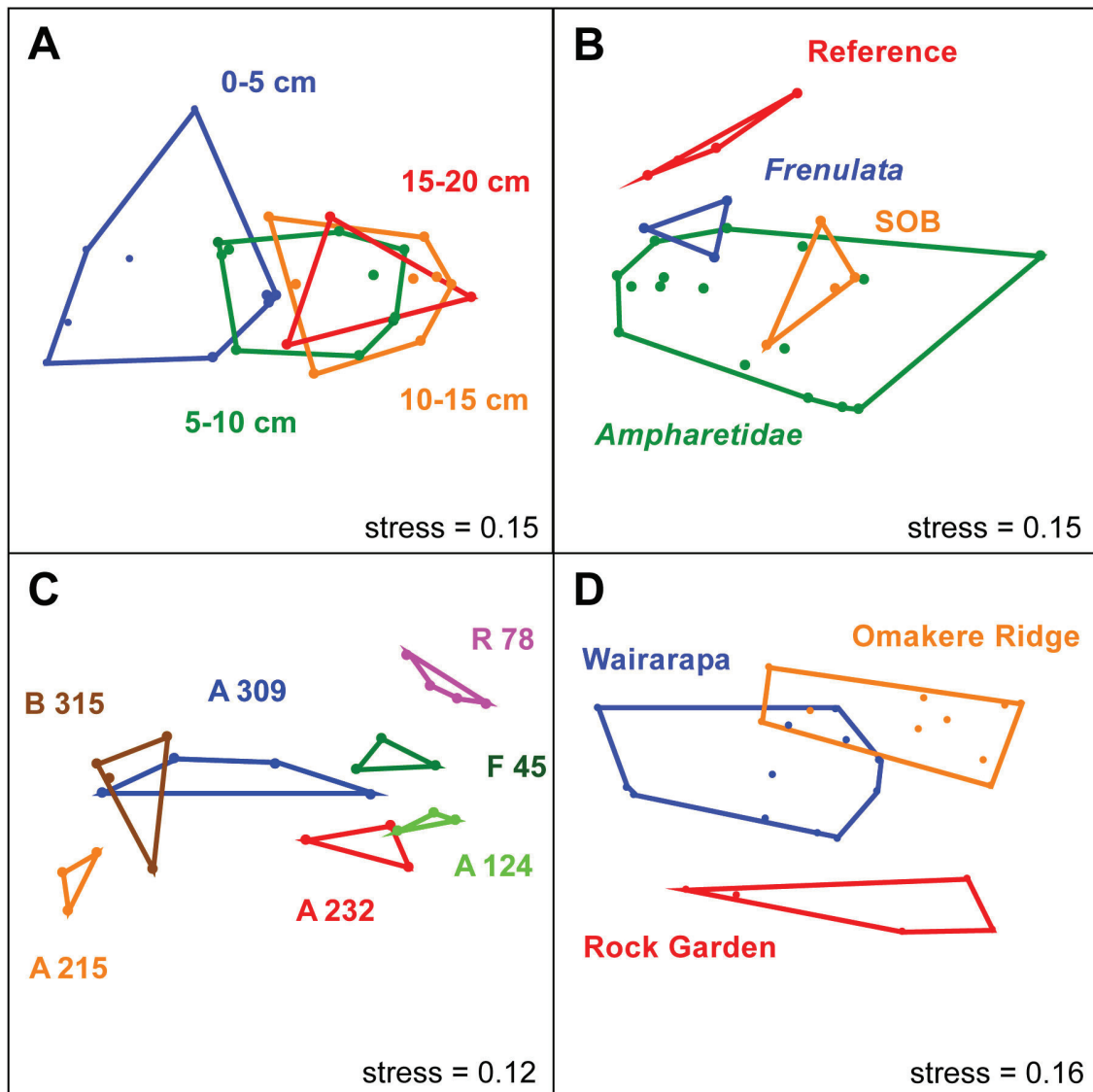


**Figure 6. NMDS ordination plots.** 3D-NMDS ordination plots, shown as 2D graphs (other axes are not shown), visualizing the ARISA dataset. The subgroups that were analyzed for each condition are depicted as colored polygons. **A:** Ordination plot of investigated depth layers. ANOSIM was used to test whether the layers are significantly different. Layer 1 (0-5 cm) was different from layer 2 (5-10 cm;  $R_{1/2} = 0.28$ ,  $p_{1/2} = 0.013$ ) and layer 3 ( $R_{1/3} = 0.6$ ,  $p_{1/3} = 0.001$ ). Layer 2 and 3 were not significantly different. We excluded the deepest layer due to its insufficient number of data points. **B:** Ordination plot of seep-associated microbial or faunal communities. ANOSIM was not performed, due to unequal group sizes. **C:** Ordination plot of sampling sites. A: *Ampharetidae*, B:SOB, F: *Frenulata*, R: Reference. Dissimilarity of the sites is supported by an R value of 0.48 ( $p < 0.001$ ). A 157 and A 258, as well as the bottom layers (15-20 cm) of site R 78, A 309 and B 315 were excluded from the ANOSIM to ensure equal group sizes. **D:** Ordination plot of the sampling areas Omakere Ridge (OR), Wairarapa (W) and Rock Garden (RG). The overall differences between the sampling areas are supported by an ANOSIM R value of 0.542 ( $p < 0.001$ ). R and p values comparing the seep areas are as follows.  $R_{RG/OR} = 0.7$  ( $p < 0.001$ );  $R_{RG/W} = 0.64$  ( $p < 0.001$ ),  $R_{W/OR} = 0.39$  ( $p < 0.001$ ).

doi: 10.1371/journal.pone.0072627.g006

examined the sampling areas Rock Garden, Omakere Ridge and Wairarapa. The areas hosted significantly different microbial communities (Figure 6D), although more than 60% of the OTUs were shared. Interestingly, despite the larger spatial

distance Omakere Ridge seeps shared many more OTUs with Wairarapa, than with Rock Garden seeps (Figure S8C). The differences in microbial diversity between the three seep areas were confirmed by RDA ( $p = 0.003$ ) (Figure S10).

## Discussion

### The role of ampharetid polychaetes for aerobic methanotrophy at Hikurangi margin cold seeps

Many of the cold seeps at Hikurangi margin investigated during expedition SO-191 leg 2 and 3 were densely populated by heterotrophic ampharetid polychaetes [7,8]. These occurred mainly at sites with high fluid fluxes [2,7] and with TOU rates that were among the highest reported from cold seep ecosystems worldwide, peaking at  $118 \text{ mmol m}^{-2} \text{ d}^{-1}$  (mean =  $84 \text{ mmol m}^{-2} \text{ d}^{-1}$ ) [7,10,11,12]. However, in contrast to most other seeps pore water profiles indicated that oxygen consumption was not only coupled to sulfide oxidation, but also to methane oxidation. At ampharetid habitats the bioirrigation by the polychaetes appeared to maintain an oxic/suboxic zone of about 2-4 cm, with low concentrations of sulfide. Hence, both aerobic sulfide- and methane-oxidizing microorganisms are key players in those sediments. We calculated that the aerobic community was responsible for 10-25% of the methane consumption at these seeps.

In turn, the heterotrophic polychaetes seemed to feed mainly on the methanotrophs, since the  $^{13}\text{C}$ -depleted carbon isotopic signature of their tissue clearly revealed a methane-based nutrition [7]. Infaunal density and biomass at the ampharetid habitats were among the highest that have ever been reported for cold seep sediments [47]. Thus, it appears that ampharetids and aerobic methanotrophs mutually benefit from their presence at these high fluid flux seep sites. Due to this close trophic link and the large biomass of aerobic methylotrophs, we presume that ampharetids 'garden' the sediment to reduce oxygen limitation in the sediment and ensure rapid growth of their food source, the aerobic methylotrophs. Formation of large cell aggregates and long filaments by the methanotrophic bacteria might therefore be explained both by a high supply of methane and oxygen, but also as a consequence of reduced grazing pressure on large cell clumps by the suspension feeding ampharetids.

### Aerobic and anaerobic methanotrophs at ampharetid habitats

We confirmed a large community of aerobic methanotrophic bacteria in the uppermost oxic-suboxic sediment layers at ampharetid habitats, whereas anaerobic methane-oxidizing archaea dominated the deeper anoxic and sulfidic layers. The aerobic methanotrophs clustered into three monophyletic clades, which we named Marine Methylotrophic Group (MMG) 1-3, because they contain sequences retrieved from marine methane-rich ecosystems or methanotrophic endosymbionts. Sequences of *Methylococcales* and MMG1 were reported from oxygen-depleted sediment [48] and *pmoA* sequences related to the ones we observed in ampharetid habitats were found in oxygen minimum zones of the Eastern Pacific Ocean [49]. Thus, methylotrophs of these clusters might either be microaerophilic or able to cope with anoxia in the deeper sediment layers. Methylotrophic bacteria affiliated with the MMG clusters have been observed as dominant populations in freshly exposed mud flows of Håkon Mosby mud volcano (HMMV) [14], and were also detected as rare members of cold

seep communities by FISH [50]. MMG1 and MMG2 belong to the order *Methylococcales* while MMG3 is closely related to the deep-branching *Methylophaga*, which are non-methane utilizing methylotrophs. MMG1 are so closely related to endosymbionts of *Bathymodiolus* spp. that we visualized the cells in the sediment with a *Bathymodiolus* endosymbiont specific probe. MMG1-3 occurred also at the SOB habitat, whereas MMG3 was missing at the frenulate habitat.

The analysis of aerobic methanotrophs on a functional level, using the *pmoA* gene, revealed five monophyletic clusters that exclusively contained sequences originating from marine methane-rich ecosystems. The high diversity of *pmoA* sequences present at the SOB and frenulate habitats supported the results of the 16S rRNA gene analysis. We found organisms related to benthic and pelagic methanotrophs at both ecosystems and a high number of OTUs related to siboglinid endosymbionts at the frenulate habitat. However, the ampharetid habitat had a much lower *pmoA* diversity as was expected from the 16S rRNA analysis. All *pmoA* sequences clustered into two OTUs (at a 93% similarity cut-off) forming two distinct clades. One clade contained *pmoA* sequences related to *Bathymodiolus* spp. endosymbionts, while the other contained sequences related to *Rimicaris* sp. epibionts. The OTUs likely belonged to MMG1 or MMG2, since members of the MMG3 might lack a *pmoA* gene like their close relatives of the genus *Methylophaga* [51]. The low *pmoA* diversity might be due to a PCR bias caused by a clear dominance of these two OTUs in the sediment. MMG2 strongly dominated the methylotrophic community and contributed by far most of the biomass in the form of large aggregates. Thus, only two taxa seem to be responsible for most of the aerobic methanotrophy at ampharetid habitats despite the high diversity of methylotrophic communities found in Hikurangi ecosystems. This low diversity could be the result of a natural enrichment of aggregate-forming organisms of MMG2 caused by the polychaete activity. The existence of a specific niche at ampharetid habitats is supported by the absence of alphaproteobacterial type-II methanotrophs. We did not find them in 16S rRNA and *pmoA* gene libraries from the investigated cold seeps, although they are abundant in nearby methane-bearing sediments [52].

The anaerobic microbial communities at ampharetid habitats were confined to sulfidic sediment layers below the oxygenated zone. They were dominated by ANME-2/DSS consortia known to mediate AOM [9]. Although we found ANME-3 in the gene libraries of all seeps, in situ hybridization was only successful at frenulate site 45, which indicates that ANME-3 cells might be inactive under given conditions. ANME-1 archaea were not detected with either method. The absence of ANME-1 in bioirrigated sediments supports the hypothesis that this clade might be more sensitive to oxygen than other types [53] or it could be a result of the remoteness of the Hikurangi seep sites. Archaeal diversity and aggregate numbers as well as AOM rates were comparable to other seeps with medium to high fluid fluxes [53,54,55]. However, the AOM zone was shifted downwards compared to most other active seep sites, which is presumably due to bioirrigation by the ampharetids. An even deeper shift of the AOM zone, up to several decimeters, was

**Table 2.** Biogeochemical and physical characteristics of Hikurangi margin, Hydrate Ridge, Black Sea and Håkon Mosby mud volcano seep sites.

|  | MOx rates<br>( $\mu\text{mol cm}^{-3}$<br>$\text{day}^{-1}$ ) | SR rates ( $\mu\text{mol}$<br>$\text{cm}^{-3} \text{day}^{-1}$ ) | Water<br>Temp. ( $^{\circ}\text{C}$ ) | depth (m) | Oxygen<br>penetration<br>(mm) | Sulfate<br>conc. (mM) | Sulfide<br>conc. (mM) | Methane<br>conc. ( $\mu\text{M}$ ) | Methane flux<br>( $\text{mmol m}^{-2}$<br>$\text{day}^{-1}$ ) |
|--|---|--|---------------------------------------|-----------|-------------------------------|-----------------------|-----------------------|------------------------------------|---|
| Hikurangi <i>Frenulata</i> site 45             | n.a.  | <0.15  | 4-5                                   | 1159      | n.a.                          | 29                    | 0                     | 2-4                                | n.a.  |
| Hikurangi <i>Ampharetidae</i> site 124         | 0.02-0.2  | 0.05-0.35  | 4-5                                   | 1054      | 1-4 <sup>#</sup>              | 5-29                  | 0-15                  | 80-530                             | >200 <sup>#</sup>   |
| Hikurangi <i>Ampharetidae</i> site 309         | 0.1-0.25  | 0.05-0.2   | 4-5                                   | 1057      | 1-4 <sup>#</sup>              | 3-26                  | n.a.                  | 10-600                             | >200 <sup>#</sup>   |
| Hikurangi <i>Beggiatoa</i> site 315            | 0.1-0.5   | 0.1-1.2  | 4-5                                   | 1057      | n.a.                          | 0-23                  | n.a.                  | 15-360                             | n.a.  |
| Hydrate Ridge <i>Beggiatoa</i>                 | <3  | <2.1   | 2-4                                   | 777       | 1                             | <18                   | 10-26                 | n.a.                               | 30-90   |
| Hydrate Ridge <i>Calyptogena</i>               | <2.7  | <3.6   | 2-4                                   | 787       | 10                            | 18-26                 | 0-10                  | n.a.                               | <1  |
| Black Sea sediment P817                        | 0.4-0.7   | 1.4-2.1  | 8-9                                   | 192       | anoxic                        | 10-13                 | 1                     | 80-150                             | n.a.  |
| Black Sea P822 microbial mat<br>inside chimney | 300*  | n.a.   | 8-9                                   | 191       | anoxic                        | 6                     | 3                     | 4000                               | n.a.  |
| HMMV <i>Beggiatoa</i> site                     | 0.1-0.6   | 0.1-1  | -1                                    | 1250      | 1-2                           | 0-30                  | 0-4                   | 0.3**                              | 50-150***   |
| HMMV tubeworm site                             | 0-0.25  | 0-0.25   | -1                                    | 1250      | 30-100                        | 25-30                 | 0                     | 0.7**                              | 50-150***   |

average for ampharetid sites  $\mu\text{mol g dry weight}^{-1} \text{day}^{-1}$  measured above sediment mud volcano average n.a. not assessed

References[7,14,52,56,69,70,71,72,7]:

observed at the frenulate habitat and other seep sediments populated by thin siboglinid tubeworms [56,57]. In contrast, at the more sulfidic habitat covered by SOB and only very few ampharetids, the diversity and abundance of aerobic methyloprophs was lower and the anaerobic methanotrophic community extended to the top sediment horizon. For comparison, at the SOB habitat anaerobic oxidation of methane and sulfate reduction rates were about 7-fold higher than at the ampharetid habitats. Biogeochemical profiles as well as diversity and biomass of ANME clades were very similar to previously described SOB sites [53,58,59]. The relationship between abundance and bioirrigation activity of ampharetids and the biogeochemical zonation of underlying sediments is an interesting future research subject.

### Comparison of Hikurangi margin seeps to previously described ecosystems

Hikurangi margin cold seeps are far away from all studied seep areas and only few deep-sea chemosynthetic ecosystems are known from the Southern Hemisphere [60,61,62]. Previous studies have found very strong and long lasting seepage activity [63] and substantial differences concerning the composition and diversity of the local seep fauna [6]. Here we investigated the seep microbial communities and compared them to those from the Northern Hemisphere. Representatives of the main functional groups, such as aerobic and anaerobic methanotrophs, sulfide oxidizers and sulfate reducers of Hikurangi margin were closely related to those known from other seeps described before. However, the biogeochemistry and occurrence of methyloprophic groups was different. Especially the diversity and abundance of aerobic methyloprophs is to our knowledge unprecedented. Another outstanding feature of these seeps is the absence of ANME-1 at all investigated sediments. To understand whether this is a result of geographic remoteness or due to metabolic constraints of this clade we need detailed analyses of other

ampharetid habitats, such as the ones recently discovered at the Makran margin [56]. An overview of important biogeochemical and microbial characteristics of Hikurangi margin cold seeps, compared to sites from Hydrate Ridge, HMMV and the Black Sea is provided (Table 2 and Table S1).

### Drivers of biodiversity at Hikurangi margin seep ecosystems

ARISA data revealed a comparable richness of abundant bacterial types at each site and in the four depth layers investigated. However,  $\beta$ -diversity was considerably different at all spatial scales from a few centimeters to hundreds of kilometers. For example, microbial communities in two depth layers of the same ecosystem frequently shared as little or less OTUs as two seep ecosystems from different geographical regions. The observed increasing dissimilarity of the community with increasing sediment depth was already described in previous studies [33,64]. This effect was also present at the reference site, and is not unique to seep ecosystems. Our results support the hypothesis that availability of electron acceptors, especially oxygen, is a main driver influencing chemosynthetic communities and biodiversity of cold seep sediments [53,56]. In contrast, no direct link was observed between methane oxidation rates, sulfate reduction rates and community composition or richness, probably because of the relatively similar range of biogeochemical activity across the different seeps investigated. However, the presence of different fauna had a significant impact on the underlying bacterial community. This supports the finding that the presence and activity of the polychaete worms shape the underlying microbial communities at ampharetid habitats. In addition, the seep area had a significant influence on the microbial communities. This might be due to a number of factors, such as differences in the geochemistry, water currents or distance to the coast. In contrast to earlier findings from the San Pedro Basin and the Laptev Sea [65,66], water depth did

not shape the communities at Hikurangi. This study shows that at least for the key environmental functions like methano- and thiotrophy at cold seeps, similar types of biogeochemical settings select for similar community composition, despite the large geographical distance to known environments covered here.

## Conclusion

Hikurangi margin harbors cold seep ecosystems with unique features concerning seep-associated fauna and methanotrophic communities. Bioirrigation by the ampharetid polychaetes maintains a habitat suitable for aerobic methylotrophic bacteria in the top sediment, contributing to about 25% of total methane consumption, while anaerobic methanotrophic archaea dominate the deeper anoxic layers. Dense polychaete communities such as the ones formed by ampharetids investigated here are present also at other seepage sites [56,66,67]. Accordingly, the role of aerobic oxidation of methane in seafloor methane budgets may be underestimated.

## Supporting Information

**Figure S1. Biogeochemistry of additional Hikurangi ecosystems.**

(PDF)

**Figure S2. Phylogeny of archaeal 16S rRNA.**

(PDF)

**Figure S3. Phylogeny of deltaproteobacterial 16S rRNA.**

(PDF)

**Figure S4. Phylogeny of *pmoA* protein.**

(PDF)

**Figure S5. Micrographs of organisms related to *Bathymodiolus* spp. Endosymbionts.**

(PDF)

**Figure S6. Abundance and size distribution of AOM aggregates.**

(PDF)

**Figure S7. Number of operational taxonomic units at each site.**

(PDF)

**Figure S8. Partitioning of operational taxonomic units.**

(PDF)

**Figure S9. Shared operational taxonomic units between sites.**

(PDF)

**Figure S10. Redundancy analysis of ARISA data and environmental parameters.**

(PDF)

**Movie S1. 3D animated methylococci aggregate.** The methylococci aggregate originates from the oxic layer at ampharetid site 124. The cells are hybridized with the *Methylococcales* specific probe (MTMC-701, green) and nucleic acid is stained with DAPI (blue). The aggregate consists of large oval cells that are loosely packed. For details concerning the animation see Materials and Methods S1.

(MPG)

**Movie S2. 3D animated AOM aggregate.** The AOM aggregate was found in the anoxic layer of ampharetid site 124. The diameter was 12  $\mu\text{m}$ , total cell volume of the aggregate (excluding intercellular space), based on the DAPI signal, was 76  $\mu\text{m}^3$ , the volume of the archaeal core (ANME-2a-647 - red) was 20  $\mu\text{m}^3$  and the bacterial shell (SEEP1a-473 - green) was 25  $\mu\text{m}^3$ . For details concerning animation and volume calculation see Supporting Material and Methods.

(AVI)

**Table S1. Total cell counts and relative abundance of methanotrophs at Hikurangi margin, Hydrate Ridge, Black Sea and Håkon Mosby mud volcano seep sites.**

(PDF)

**Materials and Methods S1.** (PDF)

## Acknowledgements

The officers and crew of FS SONNE, as well as the coworkers aboard the ship are gratefully acknowledged for their support during cruise SO191 leg 2 and 3. We thank Viola Beier, Gabriele Schüßler, Tina Treude, Helge Niemann, Daniel Santillano for help with rate measurements, Nicole Rödiger for assistance in the molecular lab, Wiebke Rentzsch and Feyza Selçuk for support with AODC and CARD-FISH, Christina Bienhold and Petra Pop Ristova for advice concerning the statistical analyses, Dennis Fink for assistance with 3D animation, Stefan Sommer and David Bowden for the permission to use their images and Janine Felden, Jens Greinert and Paul Wintersteller for their input in the production of the bathymetric map.

## Author Contributions

Conceived and designed the experiments: SER KK RA AB AR. Performed the experiments: SER JA GW. Analyzed the data: SER JA GW. Wrote the manuscript: SER KK AB GW.

## References

- Lewis KB, Marshall BA (1996) Seep faunas and other indicators of methane-rich dewatering on New Zealand convergent margins. *N Z J Geol Geophys* 39: 181-200. doi:10.1080/00288306.1996.9514704.
- Naudts L, Greinert J, Poort J, Belza J, Vangampelaere E et al. (2010) Active venting sites on the gas-hydrate-bearing Hikurangi Margin, off New Zealand: Diffusive- versus bubble-released methane. *Mar Geol* 272: 233-250. doi:10.1016/j.margeo.2009.08.002.
- Klaucke I, Weinrebe W, Petersen CJ, Bowden D (2010) Temporal variability of gas seeps offshore New Zealand: Multi-frequency geoaoustic imaging of the Wairarapa area, Hikurangi margin. *Mar Geol* 272: 49-58. doi:10.1016/j.margeo.2009.02.009.
- Krabbenhoft A, Netzeband GL, Bialas J, Papenberg C (2010) Episodic methane concentrations at seep sites on the upper slope Opuawe Bank, southern Hikurangi Margin, New Zealand. *Mar Geol* 272: 71-78. doi:10.1016/j.margeo.2009.08.001.
- Jones AT, Greinert J, Bowden DA, Klaucke I, Petersen CJ et al. (2010) Acoustic and visual characterisation of methane-rich seabed seeps at Omakere Ridge on the Hikurangi Margin, New Zealand. *Mar Geol* 272: 154-169. doi:10.1016/j.margeo.2009.03.008.
- Baco AR, Rowden AA, Levin LA, Smith CR, Bowden DA (2010) Initial characterization of cold seep faunal communities on the New Zealand Hikurangi margin. *Mar Geol* 272: 251-259. doi:10.1016/j.margeo.2009.06.015.
- Sommer S, Linke P, Pfannkuche O, Niemann H, Treude T (2010) Benthic respiration in a seep habitat dominated by dense beds of ampharetid polychaetes at the Hikurangi Margin (New Zealand). *Mar Geol* 272: 223-232. doi:10.1016/j.margeo.2009.06.003.
- Thurber AR, Kröger K, Neira C, Wiklund H, Levin LA (2010) Stable isotope signatures and methane use by New Zealand cold seep benthos. *Mar Geol* 272: 260-269. doi:10.1016/j.margeo.2009.06.001.
- Knittel K, Boetius A (2009) Anaerobic Oxidation of Methane: Progress with an Unknown Process. *Annu Rev Microbiol* 63: 311-334. doi:10.1146/annurev.micro.61.080706.093130. PubMed: 19575572.
- Felden J, Wenzhöfer F, Feseker T, Boetius A (2010) Transport and consumption of oxygen and methane in different habitats of the Håkon Mosby Mud Volcano (HMMV). *Limnol Oceanogr* 55: 2366-2380. doi:10.4319/l.o.2010.55.6.2366.
- Felden J, Lichtschlag A, Wenzhöfer F, de Beer D, Feseker T et al. (2013) Limitations of microbial hydrocarbon degradation at the Amon Mud Volcano (Nile Deep Sea Fan). *Biogeosciences Discuss* 10: 335-370. doi:10.5194/bgd-10-335-2013.
- Pop Ristova P, Wenzhöfer F, Ramette A, Zabel M, Fischer D et al. (2012) Bacterial diversity and biogeochemistry of different chemosynthetic habitats of the REGAB cold seep (West African margin, 3160 m water depth). *Biogeosciences* 9: 5031-5048. doi:10.5194/bg-9-5031-2012.
- Schreiber L, Holler T, Knittel K, Meyerdierts A, Amann R (2010) Identification of the dominant sulfate-reducing bacterial partner of anaerobic methanotrophs of the ANME-2 clade. *Environ Microbiol* 12: 2327-2340. PubMed: 21966923.
- Lösekann T, Knittel K, Nadalig T, Fuchs B, Niemann H et al. (2007) Diversity and Abundance of Aerobic and Anaerobic Methane Oxidizers at the Håkon Mosby Mud Volcano, Barents Sea. *Appl Environ Microbiol* 73: 3348-3362. doi:10.1128/AEM.00016-07. PubMed: 17369343.
- Roalkvam I, Jørgensen SL, Chen Y, Stokke R, Dahle H et al. (2011) New insight into stratification of anaerobic methanotrophs in cold seep sediments. *FEMS Microbiol Ecol* 78: 233-243. doi:10.1111/j.1574-6941.2011.01153.x. PubMed: 21676010.
- Inagaki F, Tsunogai U, Suzuki M, Kosaka A, Machiyama H et al. (2004) Characterization of C1-Metabolizing Prokaryotic Communities in Methane Seep Habitats at the Kuroshima Knoll, Southern Ryukyu Arc, by Analyzing pmoA, mmoX, mxoF, mcrA, and 16S rRNA Genes. *Appl Environ Microbiol* 70: 7445-7455. doi:10.1128/AEM.70.12.7445-7455.2004. PubMed: 15574947.
- Fisher MM, Triplett EW (1999) Automated Approach for Ribosomal Intergenic Spacer Analysis of Microbial Diversity and Its Application to Freshwater Bacterial Communities. *Appl Environ Microbiol* 65: 4630-4636. PubMed: 10508099.
- Cline JD (1969) Spectrophotometric determination of hydrogen sulfide in natural waters. *Limnol Oceanogr* 14: 454-458. doi:10.4319/l.o.1969.14.3.0454.
- Jørgensen BB, Cohen Y (1977) Solar Lake (Sinai). 5. The Sulfur Cycle of the Benthic Cyanobacterial Mats. *Limnology and Oceanography* 22: 657-666.
- Kallmeyer J, Ferdelman TG, Weber A, Fossing H, Jørgensen BB (2004) A cold chromium distillation procedure for radiolabeled sulfide applied to sulfate reduction measurements. *Limnol Oceanogr Meth* 2: 171-180. doi:10.4319/lom.2004.2.171.
- Thang NM, Brüchert V, Formolo M, Wegener G, Ginters L et al. (2012) The Impact of Sediment and Carbon Fluxes on the Biogeochemistry of Methane and Sulfur in Littoral Baltic Sea Sediments (Himmerfjärden, Sweden). *Estuar Coast* 36: 98-115.
- Zhou J, Bruns MA, Tiedje JM (1996) DNA recovery from soils of diverse composition. *Appl Environ Microbiol* 62: 316-322. PubMed: 8593035.
- Ashelford KE, Chuzhanova NA, Fry JC, Jones AJ, Weightman AJ (2006) New Screening Software Shows that Most Recent Large 16S rRNA Gene Clone Libraries Contain Chimeras. *Appl Environ Microbiol* 72: 5734-5741. doi:10.1128/AEM.00556-06. PubMed: 16957188.
- Ludwig W, Strunk O, Westram R, Richter L, Meier H et al. (2004) ARB: a software environment for sequence data. *Nucleic Acids Res* 32: 1363-1371. doi:10.1093/nar/gkh293. PubMed: 14985472.
- Quast C, Pruesse E, Yilmaz P, Gerken J, Schweer T et al. (2013) The SILVA ribosomal RNA gene database project: improved data processing and web-based tools. *Nucleic Acids Res* 41: D590-D596. doi:10.1093/nar/gks1219. PubMed: 23193283.
- Pruesse E, Peplies J, Glöckner FO (2012) SINA: accurate high throughput multiple sequence alignment of ribosomal RNA genes. *Bioinformatics*.
- Hasegawa M, Kishino H, Yano T-a (1985) Dating of the human-ape splitting by a molecular clock of mitochondrial DNA. *J Mol Evol* 22: 160-174. doi:10.1007/BF02101694. PubMed: 3934395.
- Saitou N, Nei M (1987) The neighbor-joining method: a new method for reconstructing phylogenetic trees. *Mol Biol Evol* 4: 406-425. PubMed: 3447015.
- Jukes TH, Cantor CR (1969) Evolution of Protein Molecules; HN Munro. New York: Academic Press. pp. 566.
- Kimura M (1983) The Neutral Theory of Molecular Evolution. Cambridge: Cambridge University Press. pp. 369.
- Chao A (1984) Nonparametric Estimation of the Number of Classes in a Population. *Scand J Stat* 11: 265-270.
- Schloss PD, Westcott SL, Ryabin T, Hall JR, Hartmann M et al. (2009) Introducing mothur: Open-Source, Platform-Independent, Community-Supported Software for Describing and Comparing Microbial Communities. *Appl Environ Microbiol* 75: 7537-7541. doi:10.1128/AEM.01541-09. PubMed: 19801464.
- Böer SI, Hedtkamp SIC, van Beusekom JEE, Fuhrman JA, Boetius A et al. (2009) Time- and sediment depth-related variations in bacterial diversity and community structure in subtidal sands. *ISME J* 3: 780-791. doi:10.1038/ismej.2009.29. PubMed: 19340087.
- Hewson I, Fuhrman JA (2006) Improved Strategy for Comparing Microbial Assemblage Fingerprints. *Microb Ecol* 51: 147-153. doi:10.1007/s00248-005-0144-9. PubMed: 16437287.
- Ramette A (2009) Quantitative Community Fingerprinting Methods for Estimating the Abundance of Operational Taxonomic Units in Natural Microbial Communities. *Appl Environ Microbiol* 75: 2495-2505. doi:10.1128/AEM.02409-08. PubMed: 19201961.
- Bent SJ, Forney LJ (2008) The tragedy of the uncommon: understanding limitations in the analysis of microbial diversity. *ISME J* 2: 689-695. doi:10.1038/ismej.2008.44. PubMed: 18463690.
- Kruskal JB (1964) Nonmetric multidimensional scaling: A numerical method. *Psychometrika* 29: 115-129. doi:10.1007/BF02289694.
- Bray JR, Curtis JT (1957) An Ordination of the Upland Forest Communities of Southern Wisconsin. *Ecol Monogr* 27: 326-349.
- Hammer Ø, Harper DAT, Ryan PD (2001) Past: paleontological statistics software package for education and data analysis. *Palaeontol Electron* 4: 1-9.
- Clarke KR (1993) Non-parametric multivariate analyses of changes in community structure. *Austral Ecol* 18: 117-143. doi:10.1111/j.1442-9993.1993.tb00438.x.
- Oksanen J, Blanchet FG, Kindt R, Legendre P, Minchin PR et al. (2012) *vegan: Community Ecology Package*.
- Pernthaler A, Pernthaler J, Amann R (2002) Fluorescence In Situ Hybridization and Catalyzed Reporter Deposition for the Identification of Marine Bacteria. *Appl Environ Microbiol* 68: 3094-3101. doi:10.1128/AEM.68.6.3094-3101.2002. PubMed: 12039771.
- Ishii K, Mußmann M, MacGregor BJ, Amann R (2004) An improved fluorescence in situ hybridization protocol for the identification of bacteria and archaea in marine sediments. *FEMS Microbiol Ecol* 50: 203-213. doi:10.1016/j.femsec.2004.06.015. PubMed: 19712361.
- Hankeln W, Wendel NJ, Gerken J, Waldmann J, Buttigieg PL et al. (2011) CDinFusion - Submission-Ready, On-Line Integration of

- Sequence and Contextual Data. PLOS ONE 6: e24797. doi:10.1371/journal.pone.0024797. PubMed: 21935468.
45. Yilmaz P, Kottmann R, Field D, Knight R, Cole JR et al. (2011) Minimum information about a marker gene sequence (MIMARKS) and minimum information about any (x) sequence (MlxS) specifications. *Nat Biotechnol* 29: 415-420. doi:10.1038/nbt.1823. PubMed: 21552244.
  46. Degelmann DM, Borcken W, Drake HL, Kolb S (2010) Different Atmospheric Methane-Oxidizing Communities in European Beech and Norway Spruce Soils. *Appl Environ Microbiol* 76: 3228-3235. doi: 10.1128/AEM.02730-09. PubMed: 20348309.
  47. Bernardino AF, Levin LA, Thurber AR, Smith CR (2012) Comparative Composition, Diversity and Trophic Ecology of Sediment Macrofauna at Vents, Seeps and Organic Falls. PLOS ONE 7: e33515. doi:10.1371/journal.pone.0033515. PubMed: 22496753.
  48. Walsh DA, Zaikova E, Howes CG, Song YC, Wright JJ et al. (2009) Metagenome of a Versatile Chemolithoautotroph from Expanding Oceanic Dead Zones. *Science* 326: 578-582. doi:10.1126/science.1175309. PubMed: 19900896.
  49. Hayashi T, Obata H, Gamo T, Sano Y, Naganuma T (2007) Distribution and Phylogenetic Characteristics of the Genes Encoding Enzymes Relevant to Methane Oxidation in Oxygen Minimum Zones of the Eastern Pacific Ocean. *Res J Environ Sci* 1: 275-284. doi:10.3923/rjes.2007.275.284.
  50. Tavormina PL, Ussler W III, Orphan VJ (2008) Planktonic and Sediment-Associated Aerobic Methanotrophs in Two Seep Systems along the North American Margin. *Appl Environ Microbiol* 74: 3985-3995. doi:10.1128/AEM.00069-08. PubMed: 18487407.
  51. Villeneuve C, Martineau C, Mauffrey F, Villemur R (2012) Complete Genome Sequences of *Methylophaga* sp. Strain JAM1 and *Methylophaga* sp. Strain JAM7. *J Bacteriol* 194: 4126-4127.
  52. Hamdan LJ, Gillevet PM, Pohman JW, Sikaroodi M, Greinert J et al. (2011) Diversity and biogeochemical structuring of bacterial communities across the Porangahau ridge accretionary prism, New Zealand. *FEMS Microbiol Ecol* 77: 518-532. doi:10.1111/j.1574-6941.2011.01133.x. PubMed: 21595727.
  53. Knittel K, Lösekann T, Boetius A, Kort R, Amann R (2005) Diversity and Distribution of Methanotrophic Archaea at Cold Seeps. *Appl Environ Microbiol* 71: 467-479. doi:10.1128/AEM.71.1.467-479.2005. PubMed: 15640223.
  54. Wegener G, Shovtini M, Knittel K, Niemann H, Hovland M et al. (2008) Biogeochemical processes and microbial diversity of the Gullfaks and Tommeliten methane seeps (Northern North Sea). *Biogeosciences* 5: 1127-1144. doi:10.5194/bg-5-1127-2008.
  55. Boetius A, Ravenschlag K, Schubert CJ, Rickert D, Widdel F et al. (2000) A marine microbial consortium apparently mediating anaerobic oxidation of methane. *Nature* 407: 623-626. doi:10.1038/35036572. PubMed: 11034209.
  56. Fischer D, Sahling H, Nöthen K, Bohrmann G, Zabel M et al. (2011) Interaction between hydrocarbon seepage, chemosynthetic communities and bottom water redox at cold seeps of the Makran accretionary prism: insights from habitat-specific pore water sampling and modeling. *Biogeosciences Discuss* 8: 9763-9811. doi:10.5194/bgd-8-9763-2011.
  57. Niemann H, Lösekann T, de Beer D, Elvert M, Nadalig T et al. (2006) Novel microbial communities of the Håkon Mosby mud volcano and their role as a methane sink. *Nature* 443: 854-858. doi:10.1038/nature05227. PubMed: 17051217.
  58. Lichtschlag A, Felden J, Brüchert V, Boetius A, de Beer D (2010) Geochemical processes and chemosynthetic primary production in different thiotrophic mats of the Håkon Mosby Mud Volcano (Barents Sea). *Limnol Oceanogr* 55: 931-949. doi:10.4319/lo.2009.55.2.0931.
  59. Grünke S, Lichtschlag A, de Beer D, Felden J, Salman V et al. (2012) Mats of psychrophilic thiotrophic bacteria associated with cold seeps of the Barents Sea. *Biogeosciences* 9: 2947-2960. doi:10.5194/bg-9-2947-2012.
  60. Rogers AD, Tyler PA, Connelly DP, Copley JT, James R et al. (2012) The Discovery of New Deep-Sea Hydrothermal Vent Communities in the Southern Ocean and Implications for Biogeography. *PLOS Biol* 10: e1001234. PubMed: 22235194.
  61. Niemann H, Fischer D, Graffe D, Knittel K, Montiel A et al. (2009) Biogeochemistry of a low-activity cold seep in the Larsen B area, western Weddell Sea, Antarctica. *Biogeosciences* 6: 2383-2395. doi: 10.5194/bg-6-2383-2009.
  62. Sellanes J, Quiroga E, Neira C (2008) Megafauna community structure and trophic relationships at the recently discovered Concepción Methane Seep Area, Chile, ~36°S. *ICES J Mar Sci* 65: 1102-1111. doi: 10.1093/icesjms/fsn099.
  63. Greinert J, Lewis KB, Bialas J, Pecher IA, Rowden A et al. (2009) Methane seepage along the Hikurangi Margin, New Zealand: Overview of studies in 2006 and 2007 and new evidence from visual, bathymetric and hydroacoustic investigations. *Mar Geol* 272: 6-25.
  64. Urakawa H, Yoshida T, Nishimura M, Ohwada K (2000) Characterization of depth-related population variation in microbial communities of a coastal marine sediment using 16S rDNA-based approaches and quinone profiling. *Environ Microbiol* 2: 542-554. doi: 10.1046/j.1462-2920.2000.00137.x. PubMed: 11233162.
  65. Hewson I, Jacobson Meyers ME, Fuhrman JA (2007) Diversity and biogeography of bacterial assemblages in surface sediments across the San Pedro Basin, Southern California Borderlands. *Environ Microbiol* 9: 923-933. doi:10.1111/j.1462-2920.2006.01214.x. PubMed: 17359264.
  66. Bienhold C, Boetius A, Ramette A (2011) The energy-diversity relationship of complex bacterial communities in Arctic deep-sea sediments. *ISME J* 6: 724-732. PubMed: 22071347.
  67. Carlier A, Ritt B, Rodrigues CF, Sarrazin J, Olu K et al. (2010) Heterogeneous energetic pathways and carbon sources on deep eastern Mediterranean cold seep communities. *Mar Biol* 157: 2545-2565. doi:10.1007/s00227-010-1518-1.
  68. Levin LA, Mendoza GF (2007) Community structure and nutrition of deep methane-seep macrobenthos from the North Pacific (Aleutian) Margin and the Gulf of Mexico (Florida Escarpment). *Mar Ecol* 28: 131-151. doi:10.1111/j.1439-0485.2006.00131.x.
  69. Arnds J (2009) Molecular characterization of microbial populations in methane-rich marine habitats. Bremen: Universität Bremen. pp. 158.
  70. Knittel K, Boetius A, Lemke A, Eilers H, Lochte K et al. (2003) Activity, distribution, and diversity of sulfate reducers and other bacteria in sediments above gas hydrate (Cascadia Margin, Oregon). *Geomicrobiol J* 20: 269-294. doi:10.1080/01490450303896.
  71. Jørgensen BB, Weber A, Zopf J (2001) Sulfate reduction and anaerobic methane oxidation in Black Sea sediments. *Deep Sea Res* 48: 2097-2120. doi:10.1016/S0967-0637(01)00007-3.
  71. Ridgway NM (1969) Temperature and salinity of seawater at the ocean floor in the New Zealand region. *New Zeal J Mar Fresh* 3: 57-72. doi: 10.1080/00288330.1969.9515278.
  73. Bialas J, Greinert J, Linke P, Pfannkuche O (2007) FS Sonne Cruise Report SO 191 New Vents. Kiel: Leibniz-Institute of Marine Sciences. pp. 190.

## Chapter 4

**Microbial community assembly  
and the development of ecosystem functions  
at a deep-sea mud volcano**

S. Emil Ruff<sup>1,2,#</sup>, Janine Felden<sup>3</sup>, Dirk de Beer<sup>4</sup>  
Katrin Knittel<sup>2</sup>, Antje Boetius<sup>1,3,5</sup>, Alban Ramette<sup>1</sup>

- 1: HGF MPG Group for Deep Sea Ecology and Technology,  
Max Planck Institute for Marine Microbiology, Bremen
  - 2: Department of Molecular Ecology,  
Max Planck Institute for Marine Microbiology, Bremen
  - 3: MARUM Center for Marine Environmental Sciences,  
University of Bremen, Germany
  - 4: Department of Biogeochemistry,  
Max Planck Institute for Marine Microbiology, Bremen
  - 5: Alfred Wegener Institute Helmholtz Center  
for Polar and Marine Research, Bremerhaven, Germany
- #: Corresponding author: [eruff@mpi-bremen.de](mailto:eruff@mpi-bremen.de)

Relevant contributions:

I developed the concepts and ideas together with K. Knittel, A. Ramette and A. Boetius. I processed the sequences, analyzed and visualized data from pyrosequencing, CARD-FISH and biogeochemical experiments and wrote the manuscript with assistance from all co-authors.

## Abstract

Underwater mud volcanoes are dynamic geological systems that can erupt subsurface minerals and muds to form new seafloor. Yet, little is known about the microbial colonization of such new surfaces and the development of community functions such as methanotrophy, thiotrophy and carbon fixation. Here we have assessed the development of archaeal and bacterial communities in freshly exposed subsurface mud flows after gas eruptions of the Håkon Mosby mud volcano (HMMV, Barents Sea, 1250 m water depth). Combining biogeochemical measurements, Next Generation Sequencing and fluorescence *in situ* hybridization, we show that the diversity and abundance of deep subsurface clades, such as the Miscellaneous Crenarchaeotic Group (MCG) and candidate phylum JS1 declined with increasing exposure time to surface conditions. Aerobic methanotrophs were the first to colonize exposed subsurface muds within less than a year, followed by anaerobic methane oxidizers, sulfate reducers and thiotrophs. Within a few years rare anaerobic methane-oxidizing archaea (ANME) became abundant members of the microbial community and dominated biogeochemical processes at the HMMV. However, comparisons with stable sediments above gas hydrates at HMMV suggest that it may take even longer before an efficient benthic filter can develop to consume a significant proportion of the rising methane. The rapid changes in community structure associated with important shifts in ecosystem functions such as removal of methane and sulfide provide key insights on the evolution of microbial life at the interface of marine realms.

## Introduction

Marine mud volcanoes are seabed structures formed by upward migration of gasses and muds from the subsurface (Niemann and Boetius, 2010). Active mud volcanoes with repeating outbursts of gas and mud flows are important sources of the greenhouse gas methane (Milkov et al., 2003). Depending on the extent of the fluid flow, a part of the emitted methane is consumed by seafloor microorganisms comprising free-living or symbiotic methanotrophs (Lösekann et al., 2008; Felden et al., 2010). Mud volcanoes are considered “windows to the deep biosphere” due to the discharge of subsurface sediments, fluids and gasses from hundreds of meters to several kilometers depth (Kopf, 2002). Such subsurface sediments are dominated by different archaea and bacteria including the Miscellaneous Crenarchaeotic Group (MCG) (Kubo et al., 2012), *Chloroflexi* and candidate phylum JS1 (Blazejak and Schippers, 2010). These subsurface communities are viable, and heterotrophy by fermentation, sulfate reduction, methanotrophy and methanogenesis, are the major metabolic pathways of the microbes living in the deep biosphere (Parkes et al., 2005; Biddle et al., 2006; Morono et al., 2011). The subsurface is a huge microbial realm, and its members may be introduced to the surface by various processes, including fluid seepage, fluid venting and mud eruptions (Huber et al., 2007; Hubert et al., 2009; Schrenk et al., 2010).

This study focused on the exposure of subsurface muds to the deep sea floor by mud volcanism, to investigate microbial colonization and the development of new communities and their biogeochemical functions. Previously, microbial colonization and succession was monitored using colonization devices in various marine environments such as hydrothermal sediments (Callac et al., 2013), high- and low-temperature hydrothermal vents (Pagé et al., 2008; Rassa et al., 2009) and young oceanic crust (Orcutt et al., 2011). On land and in the sea it may take months to years before fully functional microbial communities develop at freshly exposed surfaces such as volcanic deposits (King, 2003) and nascent hydrothermal vents (McCliment et al., 2006; Wang et al., 2009). Especially for deep-sea habitats, the time scales and processes of colonization and succession of natural marine communities remain poorly understood, because of the technical and logistical challenges of establishing microbial observatories in the ocean. Here we addressed this issue by repeated sampling of an active mud volcano for a detailed analysis of its microbial diversity, abundance and distribution as well as important ecosystem functions such as methane and sulfide consumption.

Håkon Mosby mud volcano (HMMV) is located northeast of Norway (72°N, 14°44'E) on the Barents Sea continental slope at a water depth of around 1250 m. The present structure of the HMMV is approximately 30,000 years old and is formed by centrally focused upward migration of gas-charged muds from several kilometers depth (Perez-Garcia et al., 2009). HMMV has three distinct morphological areas. A flat center formed by gassy muds, a hummocky rim of consolidated muds overlying thick gas hydrate layers and a surrounding moat formed by older eruptions and collapses of mud (Jerosch et al., 2007). Subsurface heat flux measurements indicated that mud and gas are expelled at the geometrical center of the structure and that mud moves southward along the slope (Kaul et al., 2006; Feseker et al., 2008). This leads to a zonation of the HMMV landscape, from freshly exposed subsurface muds marked by high temperatures (up to 26°C at 0.5 m below the sea floor) and high upward fluid flow rates (3 – 6 m yr<sup>-1</sup>) to increasingly consolidated muds marked by low upward fluid flow rates (0.3 – 0.6 m yr<sup>-1</sup>) towards the outer, stabilized zone overlying gas hydrates (De Beer et al., 2006; Feseker et al., 2008). These form a hilly landscape around the HMMV center and are densely populated by chemosynthetic siboglinid tubeworms (Lösekann et al. 2008). It was previously found that the inner, gas-emitting center is populated by aerobic methanotrophs inhabiting the sediment-water interface, whereas the outer center is colonized by mats of sulfur-oxidizing bacteria (Lichtsschlag et al., 2010; Grünke et al., 2012) above anaerobic methanotrophic microbial consortia performing the anaerobic oxidation of methane (AOM) coupled to sulfate reduction (SR) (Niemann et al., 2006; Lösekann et al., 2007; Felden et al., 2010),

This marked zonation of HMMV was ideal for investigating the diversity of freshly exposed subsurface muds, the microbial colonization patterns and the development of key ecosystem functions. To address these objectives we used biogeochemical measurements, pyrosequencing and fluorescence in situ hybridization. The main hypotheses tested were: i) HMMV discharges subsurface muds to the seafloor which host deep biosphere microbial communities; ii) microbial diversity increases with exposure time of the gassy subsurface muds, due to their colonization by surface microorganisms iii) With time the environment selects for key functional clades which provide the main ecosystem functions such as methane consumption.

## Material and Methods

### Sampling sites

Visual and acoustic observations, temperature recordings and microbathymetric mapping during the expeditions in 2003, 2006, 2009 and 2010 showed that HMMV was highly active in this period, marked by vigorous gas emissions, high fluid flow and heat flux as well as bathymetric and geographical shifts of physical markers and of mapped habitats at the seafloor (Feseker et al., 2008; Foucher et al., 2010). The first long-term observation of sediment temperatures from September 2005 to June 2006 yielded evidence of several eruptive events, indicated by abrupt temperature increases of several °C within a few days. High-resolution bathymetric maps and video observations of the seafloor also showed changes in the morphology of HMMV at that time (Feseker et al., 2008). Geochemical data from 2003 - 2007 have been published (Niemann et al., 2006; Felden et al., 2010) and are available at PANGAEA (doi:10.1594/PANGAEA.744547). In 2009 an observatory for continuous observation of heat flux, bathymetry and geochemical signatures was deployed (LOOME, Feseker, pers. comm.), which recorded further eruptions in autumn 2009. In 2010 the observations were completed by sampling along a new mud flow that had emerged from the 2009 eruption and had moved southward.

Here, we analyzed 10 surface and 5 subsurface sediment samples across HMMV mud flows from most recently discharged subsurface muds towards old consolidated muds (Figure 1) as well as one reference site (REF) located approximately 0.5 km outside of the HMMV (Table 1). Surface samples obtained in 2003, 2009 and 2010 are indicated with (S1), (S2) and (S3), respectively, and deep samples are indicated with (D). The surface of the new mud flows (New Flow Surface – NFS2-3) at the geographical center was sampled in 2009 and 2010. Around 100 m south of the center, we sampled more consolidated mud in 2003 and 2010 that were termed aged mud flows (Aged Flow Surface – AFS1-3). Old mud flows (Old Flow Surface – OFS1-3) were sampled around 300 m southeast and 100 m north of the geographical center in 2003, 2009 and 2010. The stabilized sediments above hydrate deposits (Hydrate Surface – HS1) were sampled in 2003. Surface sediment samples (0-20 cm) were recovered either by TV-guided Multicorer or by push cores using the remotely operated vehicle Quest (Marum, University Bremen).

To compare surface and deep subsurface microbial communities, we also analyzed subsurface sediments (>2 m below sea floor) obtained in 2003 by gravity corer, including the new flow (New Flow Deep – NFD with an in situ temperature of ~20°C; aged

flow (AFD – ~6°C); old flow (OFD1-2 – ~3°C) and hydrate zone ca (HD – 0°C). All cores except the reference site were degassing after retrieval. After recovery, sediments were immediately subsampled in a refrigerated container (0°C) and further processed for biogeochemical analyses or preserved at -20°C for later DNA analyses. Further details as to the geographic locations and dates of sampling and the archive of all environmental data are provided in the supporting information Table S1 and in the earth system data archive PANGAEA ([www.pangaea.de](http://www.pangaea.de)).

### **Biogeochemistry**

Pore water and turnover rates were determined for surface sediment cores obtained in 2009 and 2010. The pore water was extracted with Rhizons (Rhizon CSS: length 5 cm, pore diameter 0.15 µm; Rhizosphere Research Products, Wageningen, Netherlands) in 1 cm-resolution and immediately fixed in 5% zinc acetate (ZnAc) solution for sulfate, and sulfide analyses. The samples were diluted, filtered and the concentrations measured with non-suppressed anion exchange chromatography (Waters IC-Pak anion exchange column, waters 430 conductivity detector). The total sulfide concentrations ( $\text{H}_2\text{S} + \text{HS}^- + \text{S}^{2-}$ ) were determined using the diamine complexation method (Cline, 1969). Samples for dissolved inorganic carbon (DIC) and alkalinity measurements were preserved by adding 2 µl saturated mercury chloride ( $\text{HgCl}_2$ ) solution and stored headspace-free in gas-tight glass vials. DIC and alkalinity were measured using the flow injection method (detector VWR scientific model 1054) (Hall and Aller, 1992). Dissolved sulfide was eliminated prior to the DIC measurement by adding 0.5 M molybdate solution (Lustwerk and Burdige, 1995). Nutrient subsamples (10 – 15 ml) were stored at – 20 °C prior to concentration measurements with a Skalar Continuous-Flow Analyzer (Grasshoff et al., 1999). Sulfate reduction (SR) and anaerobic oxidation of methane (AOM) were measured *ex situ* by the whole core injection method (Jørgensen, 1978). We incubated the samples at *in situ* temperature (1.0°C) for 12 hours with either  $^{14}\text{CH}_4$  (dissolved in water, 2.5 kBq) or carrier-free  $^{35}\text{SO}_4$  (dissolved in water, 50 kBq). Sediment was fixed in 25 ml 2.5% sodium hydroxide (NaOH) solution or 20 ml 20% ZnAc solution for AOM or SR, respectively. Turnover rates were measured as previously described (Treude et al., 2003; Kallmeyer et al., 2004).

### **Community analysis by massive parallel tag sequencing and quality control**

DNA extraction was carried out as described on the MICROBIS project pages (<http://icomm.mbl.edu/microbis>) using a commercially available extraction kit. We amplified the hypervariable regions V4-V6 of archaeal and bacterial 16S rRNA genes using PCR and several sets of forward and reverse primers (<http://vamps.mbl.edu/resources/primers.php>). Massively parallel tag sequencing of the PCR products was carried out on a 454 Life Sciences GS FLX sequencer at Marine Biological Laboratory, Woods Hole, MA, following the same experimental conditions for all samples. Sequence reads were submitted to a rigorous quality control procedure based on *mothur* version 24 (Schloss et al., 2009) including denoising of the flow grams using an algorithm based on *PyroNoise* (Quince et al., 2009), removal of PCR errors and a chimera check using *uchime* (Edgar et al., 2011). The reads were taxonomically assigned according to the SILVA taxonomy implemented in *mothur* and clustered at 97% ribosomal sequence identity.

### **Statistical analyses of community diversity patterns**

Sequence abundance tables that were obtained after the taxonomic assignment were used to calculate inverse Simpson diversity indices. Chao1 richness confidence intervals (Chao, 1984) and species rarefaction were calculated 100 times per sample, with each calculation based on 1000 (*Archaea*) and 2300 (*Bacteria*) randomly chosen sequences without replacement using *mothur*. Bray-Curtis dissimilarities (Bray and Curtis, 1957) between all samples were calculated and used for 2-dimensional non metric multidimensional scaling (NMDS) ordinations with 20 random starts (Kruskal, 1964). Stress values below 0.2 indicated that the multidimensional dataset was well represented by the 2D ordination. NMDS ordinations were compared and tested using Procrustes correlation analysis (Gower, 1975). All analyses were carried out with the R statistical environment and the packages *vegan* (Oksanen et al., 2012), *labdsv* (Roberts, 2012), as well as with custom R scripts. Operational taxonomic units at 97% sequence identity ( $OTU_{0.03}$ ) that occurred only once in the whole dataset were termed absolute single sequence OTUs ( $SSO_{abs}$ ) (Gobet et al., 2012).  $OTU_{0.03}$  sequences that occurred only once in at least one sample, but may occur more often in other samples were termed relative single sequence OTUs ( $SSO_{rel}$ ) (Gobet et al., 2012).  $SSO_{rel}$  are particularly interesting for community ecology, since they comprise rare organisms that might become abundant when conditions change.

### **Cell enumeration and catalyzed reporter deposition fluorescence in situ hybridization (CARD-FISH)**

Total numbers of single cells were determined using acridine orange direct counts according to the protocol published in (Meyer-Reil, 1983). CARD-FISH was performed as previously described (Ruff et al., 2013) with the following modifications. 4-6  $\mu\text{l}$  of 25-fold diluted sediment were used for filtration. Archaeal cell walls were permeabilized with 0.1M HCl for 2 min to detect ANME-3 cells, or Proteinase K solution ( $15 \mu\text{g ml}^{-1}$  (Merck, Darmstadt, Germany) in 0.05 M EDTA (pH 8), 0.1 M Tris-HCl (pH 8), 0.5 M NaCl) for 2-4 min at room temperature for all other archaea. Bacterial cell walls were permeabilized with lysozyme solution (1000kU/ml) for 60 min at 37°. Cells were stained with DAPI ( $1\mu\text{g/ml}$ ), embedded in mounting medium and counted in 40-60 independent microscopic fields using an Axiophot II epifluorescence microscope (Carl Zeiss, Jena, Germany). Cells numbers of dense aggregates were estimated semi-quantitatively as previously described (Lösekann et al., 2007). A complete list of probes used in this study is provided (supporting information Table S3).

## Results

### Visual and biogeochemical habitat characterization

The new mud flow appeared in an area of about 4500 qm end of 2009 after an eruption (Figure 1). It was characterized by a strongly disturbed surface with cracks from degassing. High concentrations of DIC and ammonium, alkalinity, but no sulfide were detected. Methane oxidation (MOx) rates were low and sulfate reduction (SR) was absent, although sulfate was diffusing into the sediment (Figure 2B). The aged mud flow about 20-80 m from the active central site was characterized by a smooth surface, with slightly rippled sediments, MOx rates had increased but SR rates remained barely detectable and sulfide was below the detection limit, while the concentration of ammonium decreased (Figure 2C). The surfaces of new and aged mud flows lacked visible macrofauna or bacterial mats. Sulfide production due to the anaerobic oxidation of methane (AOM) was only detected at old mud flows (Figure 2D) that were marked by the presence of thin microbial mats located 50-150m away from the active center. At the reference site, DIC, sulfate and alkalinity showed typical background concentrations, ammonium, methane and sulfide were absent, and there was no MOx and SR activity (Figure 2A).

### Overall microbial diversity

To assess microbial diversity of HMMV mud flows we extracted environmental DNA and sequenced the hypervariable regions V4-V6 of microbial 16S rRNA genes. After denoising and quality control of the 32 datasets (16 archaeal and 16 bacterial samples) we obtained a total of 320,019 archaeal and 317,482 bacterial sequences. The average length ( $\pm$  S.D.) of the sequences was  $290 \pm 15$  (*Archaea*) and  $284 \pm 9$  nucleotides (*Bacteria*). Clustering of the sequences at 97% sequence identity (OTU<sub>0.03</sub>) yielded 809 archaeal and 17,981 bacterial OTU<sub>0.03</sub>. The numbers of OTU<sub>0.03</sub> per sample were very different, spanning more than two orders of magnitude for both microbial domains (Figure 3, Table S1).

The five most frequent archaeal OTU<sub>0.03</sub> belonged to the clades MCG, ANME-3, Marine Group 1, *Methanosaeta* and ANME-2a/2b and accounted for over 91% of all archaeal reads. The five most frequent bacterial OTU<sub>0.03</sub> belonged to the *Methylococcales*, *Aquificales*, candidate phylum JS1, *Flavobacteriales* and *Burkholderiales* and accounted for 25% of all bacterial reads. (Figure 4, Figure S1). Between 5 and 15% of archaeal OTU<sub>0.03</sub> were shared between the mud flows, but each mud flow shared only 1% with the reference site. The bacterial communities of the mud flows shared between 13 and 15% of

OTU<sub>0.03</sub> and also 18-19% with the reference (Table S4). The surface and subsurface layers of HMMV were very different and shared only 4% archaeal and 3% bacterial OTU<sub>0.03</sub>. As far as rare organisms are concerned, the archaeal dataset contained 55% SSO<sub>abs</sub> (sequences occurring only once in the data set) and 24% SSO<sub>rel</sub> (sequences occurring once in at least one sample). The bacterial dataset contained 59% SSO<sub>abs</sub> and 24% SSO<sub>rel</sub>.

The time of exposure at sediment surface, determined by the distance from the actively gas emitting center (NS area, Figure 1) significantly shaped the microbial community structure of mud flows as tested with ANOSIM ( $R=0.7$ ,  $p<0.01$ ). The sampling year had no influence on the communities ( $R=0.04$ ,  $p=0.35$ ). This is supported by the similarity analysis (Fig. S2) and by CARD-FISH cell counts, since two samples with a similar exposure time, but from different years (e.g. NFS2 and NFS3 or OFS2 and OFS3) show very similar relative cell abundances (Figure 5). Thus, we distinguish in the following between the microbial community structure of subsurface and surface sediments as well as between surface sediments of different exposure time, i.e distance to the active center.

### **Subsurface communities**

In general, we observed an extremely low microbial diversity in deep subsurface sediments of the gassy muds of Håkon Mosby. Subsurface samples of the fresh mud flow (NFD) contained only one archaeal OTU<sub>0.03</sub> of the MCG clade, although DNA quantities obtained were sufficiently high with 1 µg per g sediment. Other subsurface samples from the center muds had a similarly low archaeal richness ranging from 2 to 21 observed OTUs (Figure 3A, Table S2). Most of the samples were so low in archaeal richness that calculation of the diversity index inverse Simpson  $D$  and Chao1 were technically not feasible (Figure 3A, Table S2). The archaeal clades of subsurface muds were the same as those in surface muds, such as MCG, Marine Group 1, methanogenic *Methanosaeta* and methanotrophic ANME clades, but occurred in different proportions (Figure 4A). Richness of the subsurface communities progressively increased with horizontal distance from the central mud flow towards the more stabilized sediments in the hydrate zone (Figure 3A, D; Figure S2A).

Bacterial richness also was extremely low in the deep subsurface samples ranging from 28 to 353 observed OTU<sub>0.03</sub> (Figure 3B, Table S2). Analogous to the archaea, the diversity of bacterial communities was increasing with increasing distance from the center (Figure 3B, E; Figure S2B).  $D$  ranged from very low values (around 10) in the center and

aged muds, to  $D \sim 50$  in the older muds to  $D \sim 250$  in the highly diverse ecosystems found at the surface of the hydrate zone and reference site (Figure 3B). The subsurface muds seemed to be dominated by *Aquificales* and candidate phylum JS1 (Figure 4B) and included *Burkholderiales*, *Anaerolineales*, *Clostridiales* and *Chloroflexi* (Figure S1) differing greatly from the muds exposed at the surface.

### Surface communities

The observed archaeal richness was lowest in the newly exposed muds, highest in the reference sediment and steadily increased with time of sediment exposure (Figure 3A) ranging from 7 - 219 archaeal OTU<sub>0.03</sub> per sample. In parallel, total cell counts increased (Figure 3C) and were accompanied by a pronounced community shift (Figure S2A). All archaeal communities at the HMMV surface had  $D < 2$  and sometimes close to one, except the ones in the hydrate zone ( $D=4.7$ ) (Figure 3D). These extremely low values are remarkable, since one is the lowest possible value of  $D$ , which means that only one organism is present, i.e. a pure culture. Chao1 richness confirmed the overall low richness at HMMV habitats and showed a similar trend (Table S2).

The archaeal community in the newly exposed mud flows contained some methanogens, but seemed to be largely dominated by a single OTU<sub>0.03</sub> of the Miscellaneous Crenarchaeotic Group (MCG). This MCG OTU was responsible for 54% of all archaeal sequences of our dataset and its relative sequence abundance decreased with increasing time of mud exposure (Figure 4A, S1). In the aged and old mud flows, an increasing proportion of sequences of anaerobic methanotrophic archaea (ANME) of the clade ANME-3 were detected. Remarkably, we detected one ANME-3 OTU<sub>0.03</sub> that was absent or rare in new muds, but clearly dominated the datasets of aged and old muds and then declined again in the hydrate zone (Figure 4A, 5). In the hydrate zone ANME-2a seemed to be very abundant. Here too, the archaeal dataset was greatly dominated by one ANME-2a OTU<sub>0.03</sub> that was rare in younger muds. The reference site was populated by *Thaumarchaeota* of Marine Group 1 (Figure 4A), however, a few sequences belonged to the ANME-3 OTU<sub>0.03</sub>. CARD-FISH revealed a decline of archaeal relative cell abundance with time of sediment exposure and confirmed the emergence of ANME-3 in old muds (Figure 5).

Observed bacterial richness also increased with sediment age ranging from 242 to 5788 bacterial OTU<sub>0.03</sub> per sample. However, in contrast to the archaea, bacterial richness peaked in the hydrate zone and not at the reference site (Figure 3B, Table S2). Similarly to

archaea there was a pronounced community shift (Figure S2B) and  $D$  was increasing with sediment age, ranging from  $D=10$  in the fresh muds to  $D=266$  in the hydrate zone (Figure 3E, Table S2). Chao1 estimated richness showed the same trend and ranged from 248 expected species in the new mud flows to 3907 at the reference site (Table S2). The surface of freshly mixed muds seemed to be dominated by aerobic methylotrophic *Methylococcales*, whereas in aged and old mud flows *Flavobacteria* and *Desulfobacterales*, including the sulfate-reducing partner bacteria of the ANME-2 and ANME-3 clades increased in relative abundance (Figure 4B, Figure 5). *Thiotrichales* and *Campylobacterales*, which comprise thiotrophs, appeared together with the *Desulfobacterales* that were likely producing the measured hydrogen sulfide in the old muds.

## **Discussion**

Previous investigations of factors structuring microbial community composition and function at active cold seep ecosystems such as the HMMV have found that upward fluid flow velocity, controlling the supply of electron donors (methane, sulfide) but limiting that of electron acceptors (sulfate, oxygen), is of key influence (Wegener and Boetius, 2009; Felden et al., 2010; Roalkvam et al., 2012; Guan et al., 2013). Furthermore, faunal activity like dwelling and burrowing can have a substantial impact on the structuring of chemosynthetic communities at methane cold seeps (Cordes et al., 2005; Levin, 2005; Fischer et al., 2012; Pop Ristova et al., 2012; Ruff et al., 2013). Here we investigated microbial community shifts and functions in recently exposed subsurface sediments in relation to their biogeochemistry and time of exposure to ambient conditions.

### **Microbial colonization and community succession**

The HMMV expels muds, fluids and gases from a deeply rooted gas chimney (Perez-Garcia et al., 2009). Frequent gas eruptions recorded in the period 2003-2010 led to the deposition of warm subsurface muds around the active center, which were sampled less than a year after their deposition. The long-term observation of gas eruptions and mud movement at HMMV indicated that the frequent eruptions of gas and mud led to a southward transport of the deposited surface muds with approximately 0.1-0.5 m per day (Kaul et al., 2006, Feseker et al. pers. comm.), so that with increasing distance from the active center the time of mud exposure and colonization increases. The hydrogeological model for HMMV suggests that during transit, the muds degas and collapse, except from a few extreme overflow events, which are visible in the bathymetry of HMMV (Foucher et al., 2010). Hence, for this study, we categorized the mud zones visually and by geospatial information into the area of the freshly deposited mud (new flow) in an area of 50x90 m (Fig. 1); in a zone about 20-100 m distance from the active center (aged flow) in which the communities had about a year to develop, and in muds of >100 m distance (old flow) with about 2-5 years of exposure. The surrounding sediments at the HMMV rim are stratified and show no sign of fluid mixing, hence have established over thousands of years.

The archaeal and bacterial communities inhabiting the surface mud flows of HMMV showed marked differences within a distance of a few tens to hundred meters from the active center. Sediments with a similar distance from the center showed a very similar community structure (Figure 3, 4, S1, S2) and similar total and relative cell abundances

(Figure 3C, Figure 5), independent of the year of sampling.. In the center of HMMV the communities of subsurface sediments including these recently exposed were composed of clades that were typical for the deep biosphere (Figure 4, Figure S1), suggesting their recent upward transport. With increasing distance from the center (time of surface exposure) these members of the deep biosphere disappeared from the surface communities. Furthermore, the time of surface exposure of HMMV muds was accompanied by an increase in microbial richness, evenness and total cell numbers (Figure 3) and by a profound shift of community structure (Figure S2). Around 95% of archaeal and around 80% of bacterial OTU<sub>0.03</sub> were replaced with time, across the entire center of the MV. The exposed gassy muds were colonized by *Flavobacteriales*, sulfate-reducing *Desulfobacterales* and different types of methanotrophs. Early colonizers were aerobic *Methylococcales* (first year), followed by an anaerobic methanotrophic community dominated by ANME-3 in muds older than 1-2 years. With the appearance of an anaerobic community producing sulfide, the older muds were colonized by thiotrophic mats of *Beggiatoaceae*. These mats on the mud flows of about 2 years exposure were still substantially thinner than those of the outermost mud zone, before the hydrate-bearing rim of HMMV sampled in 2003 and 2006 (Lichtsschlag et al., 2010; Grünke et al., 2012). Outside of the central mud flows, at the rim of HMMV, ANME-2a dominated the stabilized sediments of the hydrate zone, marking another zone of significant community turnover (Niemann et al., 2006; Lösekann et al., 2007). The observation that ANME OTU<sub>0.03</sub> were members of the rare biosphere in the aged muds (1 yr exposure), but became dominant with time strongly supports the idea that rare organisms may be a seed bank (Gibbons et al., 2013) and provide important functions when favored by the environmental conditions (Sogin et al., 2006; Galand et al., 2009).

The reference site outside the HMMV was characterized by a typical deep-sea sediment community and showed little OTU overlap with the mud flows of HMMV. Most notably, the reference site seemed dominated by *Sinobacteraceae* and *Thaumarchaeota* that are typical for deep sea surface sediment (Durbin and Teske, 2010). Hence, we could support our hypothesis that the mud transport at HMMV leads to the exposure of deep subsurface communities which are overgrown by surface types with time, especially those profiting from the increased availability of energy.

### Succession of ecosystem functions

The freshly exposed subsurface muds were characterized by very low cell numbers and a low microbial diversity. In the warm subsurface muds and fluids transported upwards in the most active center of the HMMV (NFD), methanotrophy seems to play a minor role due to the limitation of electron acceptors likely caused by the high fluid flow of 3-6 myr<sup>-1</sup> (Niemann et al., 2006), and ANME types were absent. Instead, the dominance of subsurface MCG archaea in the center subsurface sediments indicates that heterotrophic activities may dominate (Lloyd et al., 2013). In comparison, the subsurface muds outside of the active central gas chimney (OFD), marked by lower upward fluid flow rates of 0.3-0.6 myr<sup>-1</sup> (Niemann et al., 2006) showed relatively high sequence abundance of *Aquificales* indicating that also hydrogen and/or sulfur oxidation may occur (Sievert and Vetriani, 2012). The presence of JS1, which are common at cold seeps (Ruff et al. unpubl. results) and in methane-rich marine sediments in general (Harrison et al., 2009; Hamdan et al., 2011) needs further investigation. This clade was proposed to be involved in methane-derived carbon cycling (Chevalier et al., 2013).

With increasing distance to the active center of the mud volcano and increasing exposure to surface conditions, the microbial communities and their associated functions changed profoundly (Figure 2). Aerobic methylotrophs colonized the freshly deposited muds rapidly upon exposure of the subsurface muds to the oxygen-rich bottom waters, likely due to their higher energy yield and faster growth rates than that of anaerobes (Dedysh et al., 1998; Nauhaus et al., 2007). The methylotrophs can profit from the high supply of methane in the gassy muds, and are only limited by the cold temperatures at the surface (-1°C) and the availability of oxygen. They may be distributed with the bottom waters, and populate the muds from the surface, because their relative abundance (Figure 5) and cell numbers decreased with sediment depth (not shown). Accordingly, in the freshly exposed samples (NFS) the number of *Methylococcales* cells was very low or below detection limit, while it increased with mud exposure time and peaked at around  $1 \times 10^9$  cells ml<sup>-1</sup> in muds that were between one and two years old (Figure S3). Using a velocity of the mud flow of 0.5 m per day (Feseker, pers. comm.), we estimated a doubling time ( $T_D$ ) of about 90 days, which equals to a growth rate of 0.01 d<sup>-1</sup>. This rate would be consistent with the *in situ* growth rate (0.02 d<sup>-1</sup>) of a boreal, acidophilic methylotroph (Dedysh et al., 1998). The whole bacterial community, to which the methanotrophs contributed between 16 to 33% of cell abundance, was growing at a slower average rate of 0.007 ( $T_D = 103$  d). Our data supported previous evidence for the early colonization by

aerobic methanotrophs of surface sediments of an active mud volcano in the Eastern Mediterranean (Felden et al., 2013). A recent compilation of biogeochemical rates at cold seeps indicate that the activity of aerobic methanotrophs as early colonizers of active seeps has been underestimated (Boetius and Wenzhöfer, 2013).

Interestingly, aerobic and anaerobic methanotrophs were not detected in the subsurface nor surface sediments of the active center. ANME and sulfate-reducing bacteria appeared as members of the rare biosphere in the aged flow outside of the most active zones of mud and fluid transport. Accordingly, anaerobic oxidation of methane (AOM) and sulfide production were detected only in sediments exposed for > 1-2 yrs, where muds were transported away from the active center (e.g. site AFS3, Figure 2B, C). The slow growth of ANME consortia of 3-9 month generation times (Girguis et al., 2005; Nauhaus et al., 2007; Holler et al., 2011) may explain the delayed colonization compared to the aerobic methanotrophs. It is difficult to assess the exact origin of the AOM consortia that colonize the gassy muds, but they may originate from the more consolidated muds outside of the active center by the gas eruptions and mud flow. Furthermore, the emergence of AOM communities preceded the development of the thiotrophs, which accordingly were limited to old mud flows and the hydrate zone. Above the gas hydrates of the outer rim around the HMMV center, the microbial communities may yet be much older, in the range of decades or more. Upward fluid flow can be neglected in this area, and the chemosynthetic community is nourished by the methane release from the gas hydrate layer (De Beer et al., 2006). In this rather stabilized environment we found the communities with the highest diversity and evenness, and the most efficient benthic filter, consuming all of the emitted methane (Felden et al., 2010).

## **Conclusion**

We showed that the succession of microbial communities and the emergence of ecosystem functions at recently erupted subsurface sediments were tightly linked to environmental gradients, which suggested that species sorting seemed to play a major role for the microbial community assembly. The key functions of those microbial communities such as the efficient removal of the potential greenhouse gas methane needed a few years to fully develop. Since deep-sea methanogenic, methanotrophic and thiotrophic clades at large food falls also needed months to years to develop functional communities (Goffredi et al., 2008; Treude et al., 2009; Bienhold et al., 2013) our results indicate that similar time-scales are involved in the colonization of submarine surfaces. Those new insights into colonization patterns, successions and delays in biogeochemical responses are also relevant to impact studies at deep-sea habitats, such as deep-sea oil spills and mining.

## **Acknowledgements**

The officers, crews and coworkers of the Polarstern Cruises PS64, PS74-2, as well as the Maria S. Merian Cruise MSM16-2 are greatly acknowledged for their support. We thank Erika Weiz and Rafael Stiens for their excellent assistance concerning sample preparation and CARD-FISH. We are grateful to Tomas Feseker for sharing knowledge and we thank Boyan Angelov for help with data processing. This work is part of the Census of Deep Life funded by the Alfred P. Sloan Foundation. Further support for this study was supplied by the Max Planck Society and the DFG Leibnitz program to A.B.

## Figures

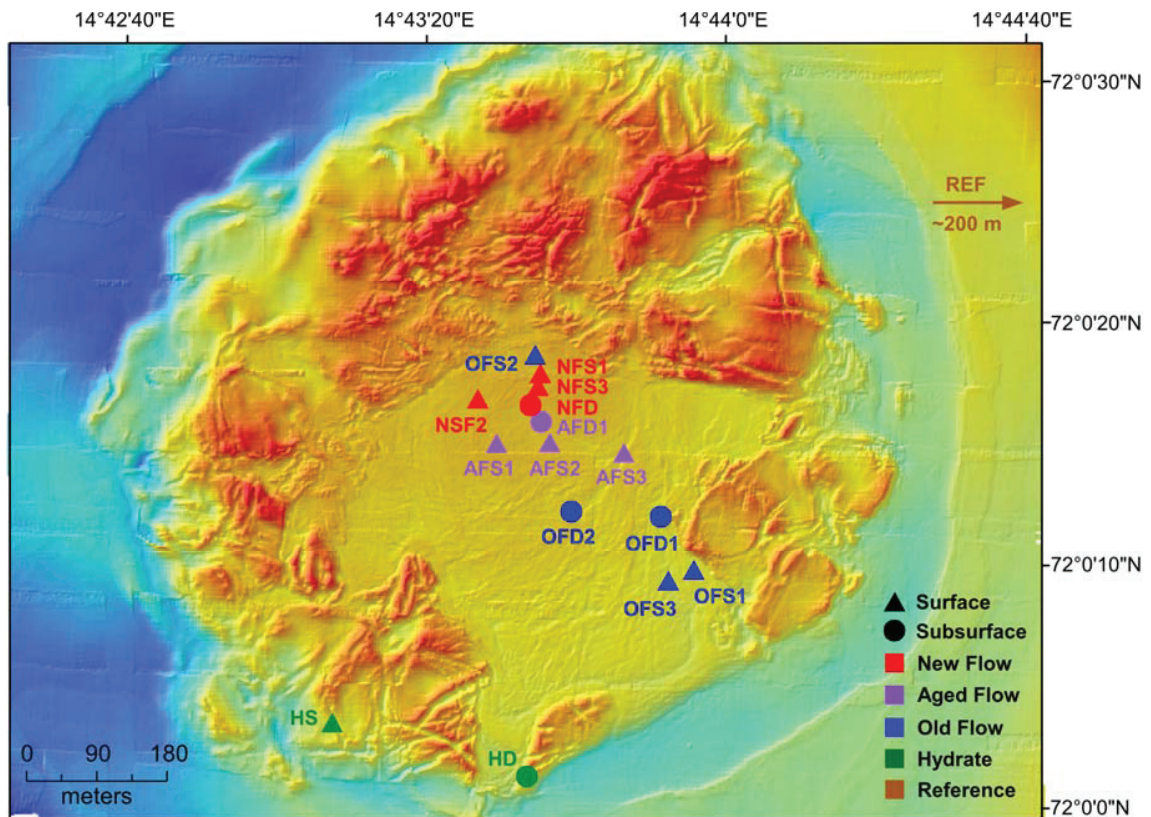


**Figure 1: Map of HMMV and the locations of sampling sites**

The samples originate from the surface and subsurface of recently erupted muds (new flow surface – NFS, new flow deep – NFD), of aged muds (aged flow surface – AFS, aged flow deep – AFD), of consolidated muds (old flow surface – OFS, old flow deep – OFD) and of the stable hydrate zone (hydrate surface – HS, hydrate deep – HD). The reference site is located outside of the mud volcano structure and is not depicted.

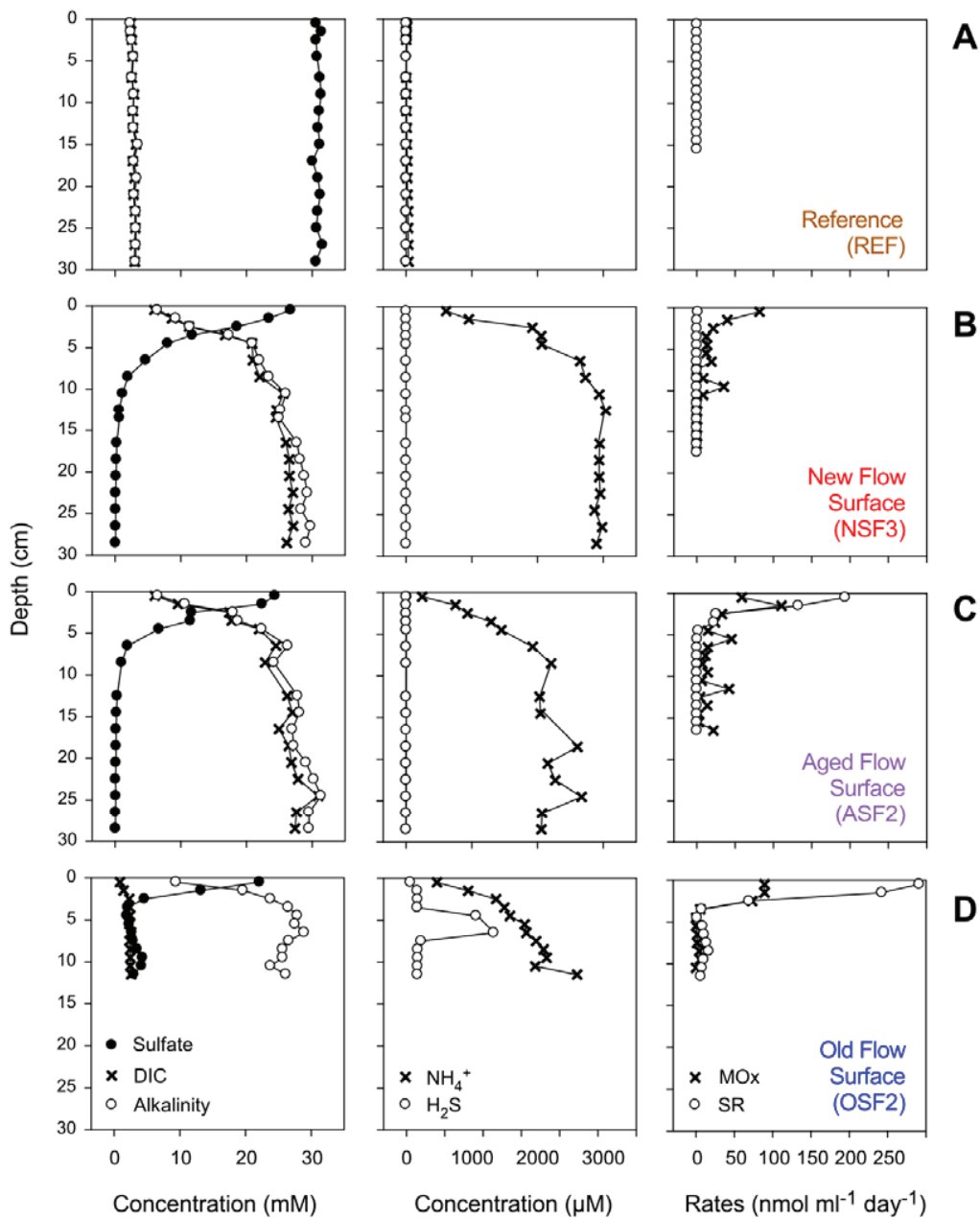


**Figure 2: Biogeochemistry in surface sediments of mud flows**

The porewater chemistry profiles of the mud flows at Håkon Mosby mud volcano show an upward transport of sulfate-depleted subsurface fluids enriched in dissolved inorganic carbon (DIC) and ammonium ( $\text{NH}_4$ ) and microbial consumption the sediment surface.  $\text{H}_2\text{S}$  = hydrogensulfide,  $\text{MOx}$  = methane oxidation, SR = sulfate reduction.

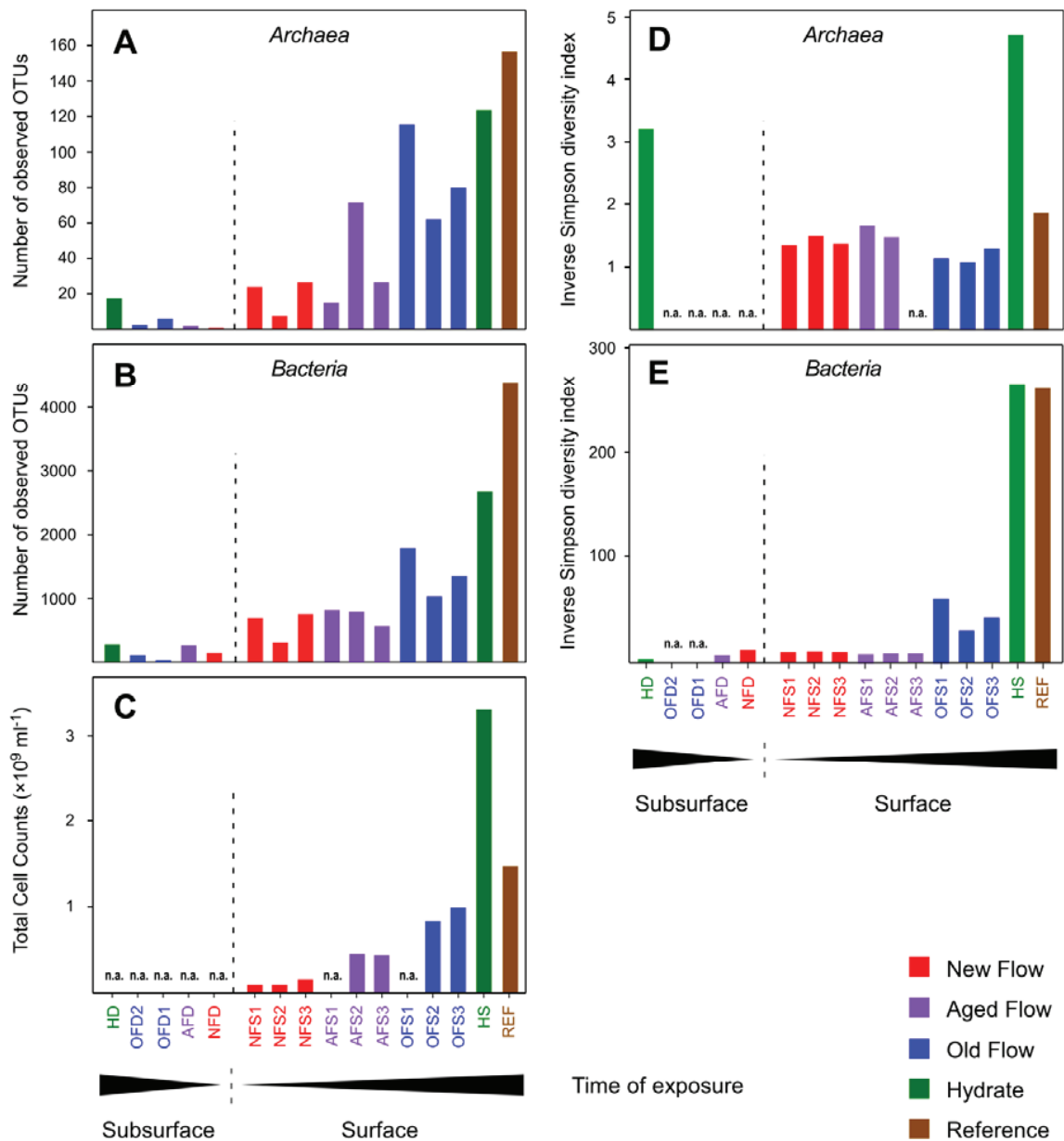


**Figure 3: Observed microbial richness, microbial diversity and total cell abundance**  
 The observed richness of archaea (A) and bacteria (B) in the different mud flows of Håkon Mosby mud volcano is represented as the average number of observed OTU<sub>0.03</sub> of both sequence runs. Richness is very low in the deep subsurface and the fresh surface muds and becomes gradually higher with increasing exposure time of the sediments to ambient conditions and decreasing fluid flow and temperature. The same trend is observed for total cell counts (C) as well as archaeal (D) and bacterial (E) inverse Simpson diversity indices. N.a. not available.

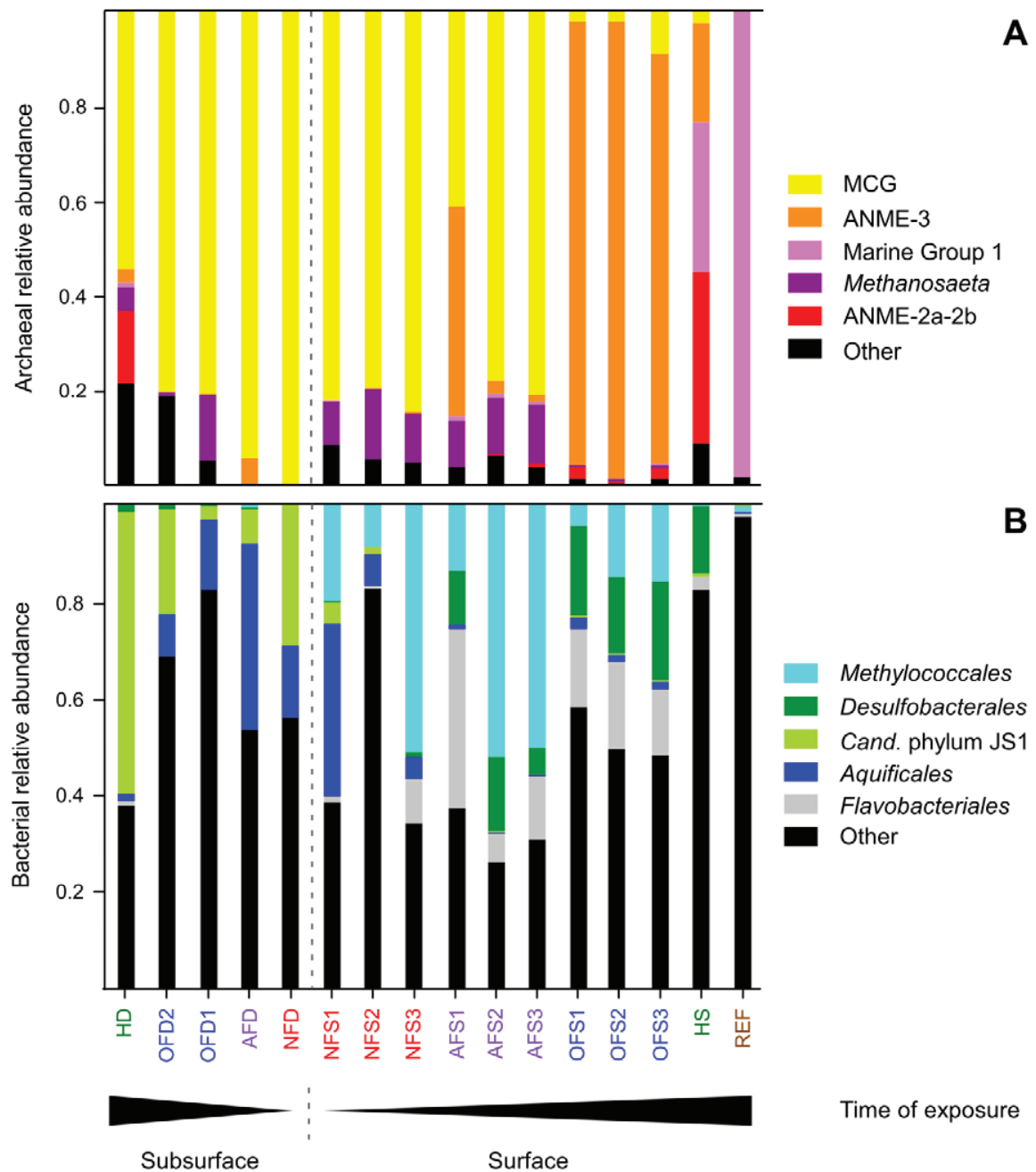


**Figure 4: Succession of microbial clades**

The bar charts are based on relative abundance data obtained by 454 pyrosequencing. The five most abundant archaeal (**A**) and bacterial (**B**) clades are shown and clearly shift with increasing time of exposure and decreasing fluid flux. NF = new flow, AF = aged flow, OF = old flow, H = hydrate zone, REF = reference.

**Figure 5**

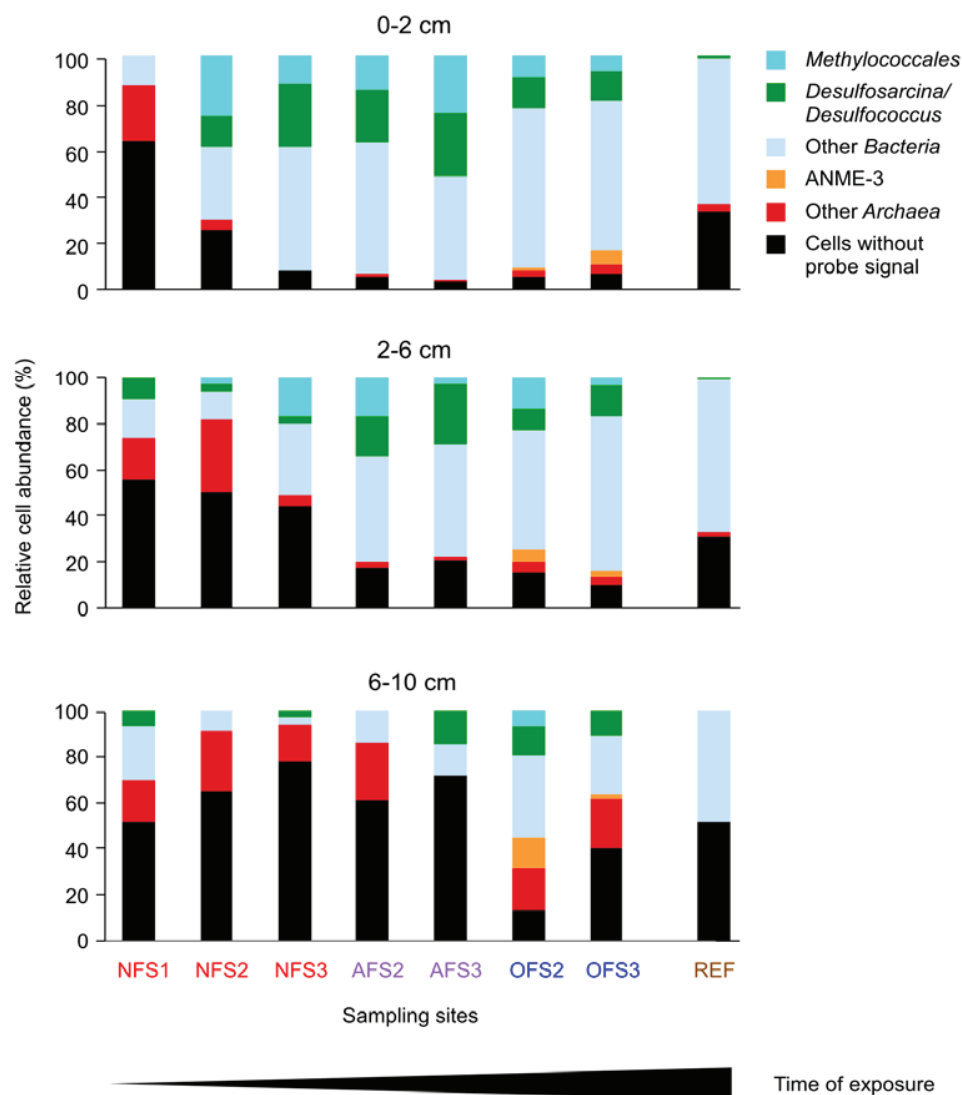


**Figure 5: Relative in situ abundance of microbial clades**

The relative cell abundances were assessed using CARD-FISH with specific probes for *Methylococcales* (probe MTMC-701), *Desulfosarcina/Desulfococcus* (probe DSS658), *Bacteria* (probe EUB338 I-III), ANME-3 (probe ANME3-1249) and *Archaea* (probe Arch915) and show clear shifts with sediment depth and increasing time of exposure. *Bacteria* that did not belong to *Methylococcales* or DSS are denoted as “other *Bacteria*”. *Archaea* that did not belong to ANME-3 are referred to as “other *Archaea*”. “Cells without a probe signal” were only stained by the nucleic acid stain DAPI and not by the general archaeal or bacterial probes.

## References

- Biddle, J. F., Lipp, J. S., et al. (2006). "Heterotrophic Archaea Dominate Sedimentary Subsurface Ecosystems Off Peru." *Proc Natl Acad Sci USA* **103**: 3846-3851.
- Bienhold, C., Pop Ristova, P., et al. (2013). "How Deep-Sea Wood Falls Sustain Chemosynthetic Life." *PLoS ONE* **8**: e53590.
- Blazejak, A. and Schippers, A. (2010). "High Abundance of Js-1- and Chloroflexi-Related Bacteria in Deeply Buried Marine Sediments Revealed by Quantitative, Real-Time Pcr." *FEMS Microbiol Ecol* **72**: 198-207.
- Boetius, A. and Wenzhöfer, F. (2013). "Seafloor Oxygen Consumption Fuelled by Methane from Cold Seeps." *Nature Geosci* **6**: 725-734.
- Bray, J. R. and Curtis, J. T. (1957). "An Ordination of the Upland Forest Communities of Southern Wisconsin." *Ecol Monogr* **27**: 326-349.
- Callac, N., Rommevaux-Jestin, C., et al. (2013). "Microbial Colonization of Basaltic Glasses in Hydrothermal Organic-Rich Sediments at Guaymas Basin." *Front Microbiol* **4**.
- Chao, A. (1984). "Nonparametric Estimation of the Number of Classes in a Population." *Scand J Stat* **11**: 265-270.
- Chevalier, N., Bouloubassi, I., et al. (2013). "Microbial Methane Turnover at Marmara Sea Cold Seeps: A Combined 16s Rrna and Lipid Biomarker Investigation." *Geobiology* **11**: 55-71.
- Cline, J. D. (1969). "Spectrophotometric Determination of Hydrogen Sulfide in Natural Waters." *Limnol Oceanogr* **14**: 454-458.
- Cordes, E. E., Arthur, M. A., et al. (2005). "Modeling the Mutualistic Interactions between Tubeworms and Microbial Consortia." *PLoS Biol* **3**: e77.
- De Beer, D., Sauter, E., et al. (2006). "In Situ Fluxes and Zonation of Microbial Activity in Surface Sediments of the Håkon Mosby Mud Volcano." *Limnol Oceanogr* **51**: 1315-1331.
- Dedysh, S. N., Panikov, N. S., et al. (1998). "Isolation of Acidophilic Methane-Oxidizing Bacteria from Northern Peat Wetlands." *Science* **282**: 281-284.
- Durbin, A. M. and Teske, A. (2010). "Sediment-Associated Microdiversity within the Marine Group I Crenarchaeota." *Environ Microbiol Rep* **2**: 693-703.
- Edgar, R. C., Haas, B. J., et al. (2011). "Uchime Improves Sensitivity and Speed of Chimera Detection." *Bioinformatics* **27**: 2194-2200.
- Felden, J., Lichtschlag, A., et al. (2013). "Limitations of Microbial Hydrocarbon Degradation at the Amon Mud Volcano (Nile Deep-Sea Fan)." *Biogeosciences* **10**: 3269-3283.
- Felden, J., Wenzhöfer, F., et al. (2010). "Transport and Consumption of Oxygen and Methane in Different Habitats of the Håkon Mosby Mud Volcano (Hmmv)." *Limnol Oceanogr* **55**: 2366-2380.
- Feseker, T., Foucher, J. P., et al. (2008). "Fluid Flow or Mud Eruptions? Sediment Temperature Distributions on Håkon Mosby Mud Volcano, Sw Barents Sea Slope." *Mar Geol* **247**: 194-207.
- Fischer, D., Sahling, H., et al. (2012). "Interaction between Hydrocarbon Seepage, Chemosynthetic Communities, and Bottom Water Redox at Cold Seeps of the Makran Accretionary Prism: Insights from Habitat-Specific Pore Water Sampling and Modeling." *Biogeosciences* **9**: 2013-2031.
- Foucher, J.-P., Dupré, S., et al. (2010). "Changes in Seabed Morphology, Mud Temperature and Free Gas Venting at the Håkon Mosby Mud Volcano, Offshore Northern Norway, over the Time Period 2003 - 2006." *Geo-Mar Lett* **30**: 157-167.

- Galand, P. E., Casamayor, E. O., et al. (2009). "Ecology of the Rare Microbial Biosphere of the Arctic Ocean." *Proceedings of the National Academy of Sciences* **106**: 22427-22432.
- Gibbons, S. M., Caporaso, J. G., et al. (2013). "Evidence for a Persistent Microbial Seed Bank Throughout the Global Ocean." *Proc Natl Acad Sci USA* **110**: 4651-4655.
- Girguis, P. R., Cozen, A. E., et al. (2005). "Growth and Population Dynamics of Anaerobic Methane-Oxidizing Archaea and Sulfate-Reducing Bacteria in a Continuous-Flow Bioreactor." *Appl Environ Microbiol* **71**: 3725-3733.
- Gobet, A., Boer, S. I., et al. (2012). "Diversity and Dynamics of Rare and of Resident Bacterial Populations in Coastal Sands." *ISME J* **6**: 542-553.
- Goffredi, S. K., Wilpiseski, R., et al. (2008). "Temporal Evolution of Methane Cycling and Phylogenetic Diversity of Archaea in Sediments from a Deep-Sea Whale-Fall in Monterey Canyon, California." *ISME J* **2**: 204-220.
- Gower, J. C. (1975). "Generalized Procrustes Analysis." *Psychometrika* **40**: 33-51.
- Grasshoff, K., Kremling, K., et al. (1999). *Methods of Seawater Analysis*. Weinheim, Germany, WILEY-VCH.
- Grünke, S., Lichtschlag, A., et al. (2012). "Mats of Psychrophilic Thiotrophic Bacteria Associated with Cold Seeps of the Barents Sea." *Biogeosciences* **9**: 2947-2960.
- Guan, H., Sun, Y., et al. (2013). "Factors Controlling the Types of Microbial Consortia in Cold-Seep Environments: A Molecular and Isotopic Investigation of Authigenic Carbonates from the South China Sea." *Chem Geol* **354**: 55-64.
- Hall, P. O. J. and Aller, R. C. (1992). "Rapid, Small-Volume, Flow Injection Analysis for  $\Sigma\text{CO}_2$  and  $\text{NH}_4^+$  in Marine and Freshwaters." *Limnol Oceanogr* **37**: 1113-1119.
- Hamdan, L. J., Gillevet, P. M., et al. (2011). "Diversity and Biogeochemical Structuring of Bacterial Communities across the Porangahau Ridge Accretionary Prism, New Zealand." *FEMS Microbiol Ecol* **77**: 518-532.
- Harrison, B. K., Zhang, H., et al. (2009). "Variations in Archaeal and Bacterial Diversity Associated with the Sulfate-Methane Transition Zone in Continental Margin Sediments (Santa Barbara Basin, California)." *Appl Environ Microbiol* **75**: 1487-1499.
- Holler, T., Widdel, F., et al. (2011). "Thermophilic Anaerobic Oxidation of Methane by Marine Microbial Consortia." *ISME J* **5**: 1946-1956.
- Huber, J. A., Mark Welch, D. B., et al. (2007). "Microbial Population Structures in the Deep Marine Biosphere." *Science* **318**: 97-100.
- Hubert, C., Loy, A., et al. (2009). "A Constant Flux of Diverse Thermophilic Bacteria into the Cold Arctic Seabed." *Science* **325**: 1541-1544.
- Jerosch, K., Schlüter, M., et al. (2007). "Spatial Distribution of Mud Flows, Chemoautotrophic Communities, and Biogeochemical Habitats at Håkon Mosby Mud Volcano." *Mar Geol* **243**: 1-17.
- Jørgensen, B. B. (1978). "A Comparison of Methods for the Quantification of Bacterial Sulfate Reductin in Coastal Marine Sediments I. Measurements with Radiotracer Techniques." *Geomicrobiol J* **1**: 11-27.
- Kallmeyer, J., Ferdeman, T. G., et al. (2004). "A Cold Chromium Distillation Procedure for Radiolabeled Sulfide Applied to Sulfate Reduction Measurements." *Limnol. Oceanogr.: Methods* **2**: 171-180.
- Kaul, N., Foucher, J. P., et al. (2006). "Estimating Mud Expulsion Rates from Temperature Measurements on Håkon Mosby Mud Volcano, Sw Barents Sea." *Mar Geol* **229**: 1-14.
- King, G. M. (2003). "Contributions of Atmospheric Co and Hydrogen Uptake to Microbial Dynamics on Recent Hawaiian Volcanic Deposits." *Appl Environ Microbiol* **69**: 4067-4075.

- Kopf, A. J. (2002). "Significance of Mud Volcanism." *Rev Geophys* **40**: 1005.
- Kruskal, J. B. (1964). "Nonmetric Multidimensional Scaling: A Numerical Method." *Psychometrika* **29**: 115-129.
- Kubo, K., Lloyd, K. G., et al. (2012). "Archaea of the Miscellaneous Crenarchaeotal Group Are Abundant, Diverse and Widespread in Marine Sediments." *ISME J* **6**: 1949-1965.
- Levin, L. A. (2005). Ecology of Cold Seep Sediments: Interactions of Fauna with Flow, Chemistry and Microbes. *Oceanography and Marine Biology: An Annual Review*. Gibson, R. N., Atkinson, R. J. A., et al., Taylor & Francis. **43**: 1-46.
- Lichtschlag, A., Felden, J., et al. (2010). "Geochemical Processes and Chemosynthetic Primary Production in Different Thiotrophic Mats of the Haakon Mosby Mud Volcano (Barents Sea)." *Limnol Oceanogr* **55**: 931-949.
- Lloyd, K. G., Schreiber, L., et al. (2013). "Predominant Archaea in Marine Sediments Degrade Detrital Proteins." *Nature* **496**: 215-218.
- Lösekan, T., Knittel, K., et al. (2007). "Diversity and Abundance of Aerobic and Anaerobic Methane Oxidizers at the Haakon Mosby Mud Volcano, Barents Sea." *Appl Environ Microbiol* **73**: 3348-3362.
- Lösekan, T., Robador, A., et al. (2008). "Endosymbioses between Bacteria and Deep-Sea Siboglinid Tubeworms from an Arctic Cold Seep (Haakon Mosby Mud Volcano, Barents Sea)." *Environ Microbiol* **10**: 3237-3254.
- Lustwerk, R. L. and Burdige, D. J. (1995). "Elimination of Dissolved Sulfide Interference in the Flow Injection Determination of by Addition of Molybdate." *Limnol Oceanogr*: 1011-1012.
- McCliment, E. A., Voglesonger, K. M., et al. (2006). "Colonization of Nascent, Deep-Sea Hydrothermal Vents by a Novel Archaeal and Nanoarchaeal Assemblage." *Environ Microbiol* **8**: 114-125.
- Meyer-Reil, L. A. (1983). "Benthic Response to Sedimentation Events During Autumn to Spring at a Shallow Water Station in the Western Kiel Bight." *Mar Biol* **77**: 247-256.
- Milkov, A. V., Sassen, R., et al. (2003). "Global Gas Flux from Mud Volcanoes: A Significant Source of Fossil Methane in the Atmosphere and the Ocean." *Geophys Res Lett* **30**: 1037.
- Morono, Y., Terada, T., et al. (2011). "Carbon and Nitrogen Assimilation in Deep Subseafloor Microbial Cells." *Proceedings of the National Academy of Sciences*.
- Nauhaus, K., Albrecht, M., et al. (2007). "In Vitro Cell Growth of Marine Archaeal-Bacterial Consortia During Anaerobic Oxidation of Methane with Sulfate." *Environ Microbiol* **9**: 187-196.
- Niemann, H. and Boetius, A. (2010). Mud Volcanoes. *Handbook of Hydrocarbon and Lipid Microbiology*. Timmis, K. N., Springer. **1**: 205-214.
- Niemann, H., Lösekan, T., et al. (2006). "Novel Microbial Communities of the Haakon Mosby Mud Volcano and Their Role as a Methane Sink." *Nature* **443**: 854-858.
- Oksanen, J., Blanchet, F. G., et al. (2012). "Vegan: Community Ecology Package."
- Orcutt, B. N., Bach, W., et al. (2011). "Colonization of Subsurface Microbial Observatories Deployed in Young Ocean Crust." *ISME J* **5**: 692-703.
- Pagé, A., Tivey, M. K., et al. (2008). "Temporal and Spatial Archaeal Colonization of Hydrothermal Vent Deposits." *Environ Microbiol* **10**: 874-884.
- Parkes, R. J., Webster, G., et al. (2005). "Deep Sub-Sea-floor Prokaryotes Stimulated at Interfaces over Geological Time." *Nature* **436**: 390-394.
- Perez-Garcia, C., Feseker, T., et al. (2009). "The Håkon Mosby Mud Volcano: 330 000 years of Focused Fluid Flow Activity at the Sw Barents Sea Slope." *Mar Geol* **262**: 105-115.

- Pop Ristova, P., Wenzhöfer, F., et al. (2012). "Bacterial Diversity and Biogeochemistry of Different Chemosynthetic Habitats of the Regab Cold Seep (West African Margin, 3160 M Water Depth)." *Biogeosciences* **9**: 5031-5048.
- Quince, C., Lanzen, A., et al. (2009). "Accurate Determination of Microbial Diversity from 454 Pyrosequencing Data." *Nat Meth* **6**: 639-641.
- Rassa, A. C., McAllister, S. M., et al. (2009). "Zeta-Proteobacteria Dominate the Colonization and Formation of Microbial Mats in Low-Temperature Hydrothermal Vents at Loihi Seamount, Hawaii." *Geomicrobiol J* **26**: 623-638.
- Roalkvam, I., Dahle, H., et al. (2012). "Fine-Scale Community Structure Analysis of Anme in Nyegga Sediments with High and Low Methane Flux." *Front Microbiol* **3**.
- Roberts, D. W. (2012). *Labdsv: Ordination and Multivariate Analysis for Ecology*.
- Ruff, S. E., Arnds, J., et al. (2013). "Microbial Communities of Deep-Sea Methane Seeps at Hikurangi Continental Margin (New Zealand)." *PLoS ONE* **8**: e72627.
- Schloss, P. D., Westcott, S. L., et al. (2009). "Introducing Mothur: Open-Source, Platform-Independent, Community-Supported Software for Describing and Comparing Microbial Communities." *Appl Environ Microbiol* **75**: 7537-7541.
- Schrenk, M. O., Huber, J. A., et al. (2010). "Microbial Provinces in the Subseafloor." *Annu Rev Mar Sci* **2**: 279-304.
- Sievert, S. M. and Vetriani, C. (2012). "Chemoautotrophy at Deep-Sea Vents: Past, Present, and Future." *Oceanography* **25**: 218-233.
- Sogin, M. L., Morrison, H. G., et al. (2006). "Microbial Diversity in the Deep Sea and the Underexplored "Rare Biosphere"." *Proc Natl Acad Sci USA* **103**: 12115-12120.
- Treude, T., Boetius, A., et al. (2003). "Anaerobic Oxidation of Methane above Gas Hydrates at Hydrate Ridge, Ne Pacific Ocean." *Marine Ecology-Progress Series* **264**: 1-14.
- Treude, T., Smith, C. R., et al. (2009). "Biogeochemistry of a Deep-Sea Whale Fall: Sulfate Reduction, Sulfide Efflux and Methanogenesis." *Mar Ecol Prog Ser* **382**: 1-21.
- Wang, F., Zhou, H., et al. (2009). "Geochip-Based Analysis of Metabolic Diversity of Microbial Communities at the Juan De Fuca Ridge Hydrothermal Vent." *Proceedings of the National Academy of Sciences* **106**: 4840-4845.
- Wegener, G. and Boetius, A. (2009). "An Experimental Study on Short-Term Changes in the Anaerobic Oxidation of Methane in Response to Varying Methane and Sulfate Fluxes." *Biogeosciences* **6**: 867-876.

## Chapter 5

## **Anaerobic methanotrophic community of a 5346 m-deep vesicomylid clam colony in the Japan Trench**

Janine Felden<sup>1,2\*</sup>, S. Emil Ruff<sup>1,3</sup>, Tobias Ertefai<sup>3</sup>,  
Fumio Inagaki<sup>4</sup>, Kai-Uwe Hinrichs<sup>3</sup>, Frank Wenzhöfer<sup>1</sup>

- 1: HGF-MPG Group for Deep Sea Ecology and Technology,  
Alfred Wegener Institute for Polar and Marine Research,  
Max Planck Institute for Marine Microbiology, Bremen, Germany
  - 2: MARUM Center for Marine Environmental Sciences,  
University Bremen, Bremen, Germany
  - 3: Department of Molecular Ecology,  
Max Planck Institute for Marine Microbiology, Bremen, Germany
  - 4: Kochi Institute for Core Sample Research,  
Japan Agency for Marine-Earth Science and Technology, Kochi, Japan
- \*corresponding author: J. Felden (jfelden@marum.de)

*In review at Geobiology*

Relevant contributions:

I processed, analyzed and visualized sequencing data  
and helped to write the manuscript

## Abstract

*Vesicomyidae* clams harbor sulfide-oxidizing endosymbionts and are typical members of cold seep communities associated with tectonic faults where active venting of fluids and gases takes place. We investigated a vesicomyid clam colony in the Japan Trench at 5346 m water depth to understand the main biogeochemical processes that support the locally restricted seep community. An integrated approach of biogeochemical and molecular ecological techniques was used combining *in situ* and *ex situ* measurements. In the upper sediment layer of the clam colony, low sulfate reduction (SR) rates (max. 128 nmol ml<sup>-1</sup> d<sup>-1</sup>) were measured which were coupled to the anaerobic oxidation of methane (AOM). SR and AOM were observed over a depth range of 15 cm, caused by active transport of sulfate due to bioturbation of the vesicomyid clams, yielding a depth integrated SR rate of 6 mmol m<sup>-2</sup> d<sup>-1</sup>. A distinct separation between the seep and the surrounding seafloor was shown by steep horizontal geochemical gradients and pronounced microbial community shifts. The sediment below the clam colony was dominated by anaerobic methanotrophic archaea of the clade ANME-2c and sulfate-reducing *Desulfobulbaceae* of the clades SEEP-SRB-3 and SEEP-SRB-4. Aerobic methanotrophic bacteria were not detected in the sediment whereas the oxidation of sulfide might be carried out chemolithoautotrophically by *Sulfurovum* species. Thus, major redox processes were mediated by distinct subgroups of seep-related microorganisms that might have been selected by this specific abyssal seep environment. Fluid flow and microbial activity was low but sufficient to support the clam community over decades and to build up high biomasses. Hence, the clams and their microbial communities adapted successfully to a low energy regime and may represent widespread chemosynthetic communities in the Japan Trench that are locally restricted but highly productive over long time periods.

## Introduction

Cold seep communities establish where tectonic or gravitational forces push free gas, methane-rich pore water and/or mud upward into sulfate-penetrated surface sediments (Judd & Hovland, 2007). High energy availability at and near the sediment surface thereby support enormous biomasses of chemosynthetic organisms such as siboglinid tubeworms, mytilid and vesicomyid bivalves, and giant sulfide-oxidizing bacteria (e.g. Danovaro et al., 2010; Grünke et al., 2012; Levin, 2005; Sahling et al., 2002; Sibuet & Olu, 1998). These organisms are well adapted to access and use reduced compounds in seep sediments. For instance, most vesicomyid clams have a reduced gut system and thus rely almost entirely on their autotrophic sulfide oxidizing-endosymbionts for nutrient and energy supply (Childress et al., 1993; Goffredi & Barry, 2002 and references therein). To access the sulfide, they dig with their foot several centimeters into the sediment (Dubilier et al., 2008), take the sulfide up and transport it with their blood to the endosymbionts (Childress et al., 1993). Some vesicomyid species are able to accumulate amounts of sulfide in their body that exceed ambient concentrations more than 60-fold (Barry & Kochevar, 1998; Childress et al., 1993) and are thus found in habitats with a wide range of sulfide concentrations (0.6-20 mM; e.g. Barry et al., 1997; Decker et al., 2012; Pop Ristova et al., 2012). Bioturbation by the clams' activity enhances the sulfate transport from the water column into the sediment resulting in sulfate reduction (SR) at sediment depths that otherwise would be sulfate limited (Levin et al., 2003; Treude et al., 2003; Wallmann et al., 1997). Hence, vesicomyid clams are able to populate seep sites of low geological activity, where sulfide is not found close to the sediment surface (Fischer et al., 2012).

In methane-enriched seep sediments, sulfide is a product of bacterial sulfate reduction (SR) that is often coupled to the anaerobic oxidation of methane (AOM) mediated by microbial consortia of anaerobic methanotrophic archaea (ANME) and sulfate-reducing bacteria (SRB) (Boetius et al., 2000). High densities of these microbial consortia have been described in seep sediments of all continental margins from shallow waters to the deep sea (Knittel & Boetius, 2009 and references therein). The occurrence, distribution and activity of the microbes involved in AOM have been intensively studied using different molecular ecological tools and biogeochemical measurements (Boetius et al., 2009; Knittel & Boetius, 2009). So far, there are three main ANME clades ANME-1, ANME-2 and ANME-3 (Hinrichs et al., 1999; Niemann et al., 2006b; Orphan et al., 2002), which contain several sub-clades, such as thermophilic ANME-1 (Holler et al., 2011),

ANME-2a-c (Orphan et al., 2001) and the recently described *Methanoperedenaceae* (Haroon et al., 2013). The involved SRB are close relatives of either *Desulfosarcina/Desulfococcus* or *Desulfobulbus* (Kleindienst et al., 2012; Knittel et al., 2003; Schreiber et al., 2010). The different ANME clades can be distinguished using methods based on nucleic acids (e.g. Knittel et al., 2005; Orphan et al., 2001; Pernthaler et al., 2008) and membrane lipids (Elvert et al., 2003; Hinrichs et al., 1999; Rossel et al., 2011).

In the last decade, the improvement of deep-sea technologies such as remotely operated vehicle or submersible enabled the scientific community to explore seep ecosystems in detail by performing focused sampling and *in situ* measurements. These *in situ* investigations have significantly increased our knowledge in small-scale variability of biodiversity and of biogeochemical activities within and between seep ecosystems (Boetius & Wenzhöfer, 2013; Jørgensen & Boetius, 2007 and references therein). However, only a few studies exist in water depths deeper than 4000 m because it is still a technological challenge to access these remote abyssal habitats for sampling and *in situ* measurements (Boetius & Wenzhöfer, 2009; Boetius & Wenzhöfer, 2013). It is known from the Nankai Trough or the Japan Trench that cold seeps occur frequently even down to water depths of at least 7500 m (Arakawa et al., 2005; Kobayashi, 2002 and reference therein). This tectonically active area hosts numerous seeps and the deepest known vesicomid clam colonies at 6437 m (Fujikura et al., 1999; Ogawa et al., 1996; Sibuet et al., 1988). Japan Trench seeps offer a unique opportunity to study microbial community structure and biogeochemical processes at abyssal seep ecosystems as most seep studies have been conducted at shallower sites (Boetius & Wenzhöfer, 2013; Sibuet et al., 1988), however due to the water depth and the comparably small seep size it difficult to access them.

Although chemosynthetic clam colonies at the Japan Trench are known for long and also well documented, detailed insights into the underlying biogeochemical processes and predominant microbial communities fueling these remote and high biomass seep communities are sparse.. Here, we combined analyses of sediment pore water chemistry, sediment-water interface exchange processes, methane and sulfate turnover rate measurements with community analyses based on 16S rRNA genes and intact polar lipids to thoroughly investigate the biogeochemistry and microbial community. To our knowledge this is the first and most comprehensive study on the functioning of an abyssal seep ecosystem using *in situ* activity measurements in the Japan Trench to date. Our main

hypotheses were (1) the key biogeochemical processes in the sediment that fuel the spatially restricted clam colony are similar to those found at shallow seeps and (2) the microbial community composition of this ecosystem differs from that of shallow seeps.

## Material & Methods

### *Seafloor observations and sampling*

During the cruise YK06-05 in 2006 with the RV *Yokosuka* to the Japan Trench, we investigated a clam colony inhabited by *Abyssogena phaseoliformis* (former known as *Calyptogena phaseoliformis*) and *Isorropodon fossajaponicum* (former known as *Calyptogena fossajaponica*) at 5346 m water depth. The names of both species were adapted according to the most recent taxonomic studies of the family *Vesicomysidae* (Krylova & Sahling, 2010 and references therein) and the accepted nomenclature in the World Register of Marine Species (<http://www.marinespecies.org/>). The targeted sampling and precise positioning of the *in situ* instruments were achieved with the manned research submersible *Shinkai 6500* (JAMSTEC, Japan). Beside the well-defined vesicomysid clam colonies present in this area of the Japan Trench, no other chemosynthetic communities, such as sulfide-oxidizing bacterial mats, were observed. The colonies, however, were associated with different groups of benthic organisms including actinaria, holothurians, and tube-dwelling polychaetes. Typically, the clam patches were round with diameters ranging from a few decimeters to two meters (Fig. 1). The distances between the widespread colonies were a few tens of meters and we observed several trails of moving clams during the dives. One large vesicomysid clam colony (Fig. 1; 39° 6.3560' N, 143° 53.5619' E) was studied in detail with microbiological and biogeochemical methods. In the following text, this particular Japan Trench clam colony is termed JTC colony. Sampling was first performed close to the rim of the JTC colony and then at the center (Fig.1) in order to collect undisturbed sediments. Immediately after sample recovery onboard, the sediment core was sub-sampled for *ex situ* rate measurements or preserved for later analyses.

### *Geochemistry*

*Ex situ* pore water concentrations of sulfate and dissolved inorganic carbon (DIC) were measured, along with the concentrations and isotopic compositions of dissolved methane, total organic carbon (TOC) content, and turnover rates of sulfate as well as methane. In addition, *in situ* benthic oxygen uptake rates were determined with a microprofiler and a benthic chamber module.

### *Ex situ measurements*

To measure the concentrations of pore water constituents, push cores were sub-sampled in one centimeter intervals and pore water was extracted via sediment squeezing (Reeburgh, 1967, 0.45  $\mu\text{m}$  Durapore Filter (Millipore, Bedford, USA)). For each sample depth, we obtained 1 - 5 ml pore water that was immediately preserved and stored at 4°C until the measurements were done in the home laboratory. To determine sulfate concentrations 0.5 - 1 ml pore water were fixed in 1 ml 2% zinc acetate (ZnAc) solution. Samples were diluted and filtered before concentrations were determined by non-suppressed anion exchange chromatography (Waters IC-Pak anion exchange column, Waters 430 conductivity detector).

For measuring dissolved inorganic carbon (DIC) concentrations, the pore water was preserved with 20  $\mu\text{L}$  saturated mercuric chloride ( $\text{HgCl}_2$ ) solution and stored headspace free. DIC content of the samples was measured by the flow injection method (detector VWR scientific model 1054) according to Hall and Aller (1992). Dissolved methane concentrations and isotopic compositions were determined with the headspace method according to Kvenvolden (1986) and Ertefai et al. (2010) using gas chromatography and isotope ratio mass spectrometry, respectively. Carbon isotope ratios are reported in the  $\delta$ -notation as per mil (‰) deviation from Vienna Pee Dee Belemnite standard (VPDB). Standard deviations of  $\delta^{13}\text{C}$  values were obtained from repeated measurements and were usually less than  $\pm 1.0\text{‰}$ .

Pyrite and carbonate content of the sediment was measured by X-ray refraction analysis as previously described (Ertefai et al., 2010). Total organic carbon (TOC) contents were measured from dry and homogenized sediment samples using a Leco CS 200 analyzer. Prior to the TOC analysis, the samples were treated with 12.5% hydrogen chloride (HCl) solution to remove any inorganic carbon. Sulfate reduction (SR) and anaerobic oxidation of methane (AOM) were measured *ex situ* by the whole core injection method (Jørgensen, 1978). We incubated the samples at *in situ* temperature (1.5°C) for 48 hours with either  $^{14}\text{CH}_4$  (dissolved in water, 2.5 kBq) or carrier-free  $^{35}\text{SO}_4$  (dissolved in water, 50 kBq). Sediment was fixed in 25 ml sodium hydroxide (NaOH) solution (2.5%, w/v) or 20 ml ZnAc solution (20%, w/v) for AOM or SR, respectively. Turnover rates were measured as previously described (Kallmeyer et al., 2004; Treude et al., 2003).

### *In situ measurements*

Total oxygen uptake (TOU) and dissolved oxygen uptake (DOU) were measured at the center and the rim of the JTC colony, respectively. The difference between TOU and DOU is commonly dedicated to faunal-mediated consumption, including bioirrigation and bioturbation as well as the animal respiration itself (Glud, 2008 and references therein). TOU of the JTC colony center was determined with a small cylindrical benthic chamber module (Boetius & Wenzhöfer, 2009; Boetius & Wenzhöfer, 2013), which enclosed a sediment area of 284 cm<sup>2</sup> (radius=9.5 cm) together with 15 cm of overlying bottom water (equivalent to approx. 5 l). Two Clark-type minielectrodes continuously recorded the oxygen concentration of the enclosed water body during the incubation (Treude et al., 2009). Sensors were calibrated against bottom water oxygen concentration (determined from Winkler titration) and a zero reading recorded at *in situ* temperature on board. TOU (mmol m<sup>-2</sup> d<sup>-1</sup>) was calculated from the initial linear change in oxygen concentration versus time (for more details see Wenzhöfer & Glud, 2002).

Oxygen penetration depth and DOU at the rim of the clam colony was measured with a small deep-sea microprofiler module (Treude et al., 2009), carrying 3 oxygen Clark-type microelectrodes (Revsbech et al., 1983) and one temperature sensor (Pt100, UST Umweltsensorentchnik GmbH, Germany). High-resolution microprofiles across the sediment-water interface were measured with a vertical resolution of 100 µm on a total length of 15 cm. Oxygen electrodes had a linear response to the oxygen concentration in seawater and were calibrated *in situ* using constant readings in the bottom water (oxygen concentration determined by Winkler titration) and the anoxic parts of the sediment (De Beer et al., 2006; Wenzhöfer et al., 2000). DOU (mmol m<sup>-2</sup> d<sup>-1</sup>) was calculated from the measured microprofiles and Fick's first law of diffusion with  $DOU = D_0 * (dC/dz)$ , where  $D_0$  (1.26 x 10<sup>-9</sup> m<sup>2</sup> s<sup>-1</sup>) is the molecular diffusion coefficient in water corrected for temperature and salinity (Li & Gregory, 1974), C (µM) is the solute concentration, and z (m) is the depth within the diffusive boundary layer (Rasmussen & Jørgensen, 1992).

### ***Microbial community analysis***

#### *16S rRNA gene analyses*

To analyze the microbial community composition we constructed archaeal and bacterial 16S rRNA gene libraries of sediments from the center and the rim of the JTC colony. On board, sediment cores were sectioned into 1-5 cm intervals and frozen at -20 °C. Total community DNA was retrieved from 5 g of sediment (pooled from the 0-10 cm depth

horizon) by chloroform extraction as described by Zhou et al. (1996) and purified using the Wizard DNA clean-up system (Promega, Madison, WI, USA). PCRs for 16S rRNA gene libraries were carried out using the Master Taq polymerase (Eppendorf, Hamburg, Germany), 26-30 cycles and the bacterial primers GM3/GM4 (Muyzer et al., 1995) or archaeal primers Arch20F/Uni1392R (Lane et al., 1985; Massana et al., 1997). Purification of PCR products, cloning reactions and the sequencing of inserts were performed as previously described (Niemann et al., 2006a) and chimeric sequences were removed using Mallard (Ashelford et al., 2006). The nucleotide sequence data reported in this paper have been archived in the EMBL nucleotide sequence database under the accession numbers HG425384-HG425704.

The 16S rRNA gene sequences were aligned with SILVA INcremental Aligner (SINA) (Prüsse et al., 2007) and manually optimized according to the secondary structure.. Phylogenetic classification was carried out using the ARB software package (Ludwig et al., 2004) based on the SILVA small subunit 16S rRNA reference sequence database (SSURef v111) (Quast et al., 2013). Phylogenetic trees were calculated with the maximum likelihood algorithm PHYML (100 bootstraps) and a positional variability filter as described before (Ruff et al., 2013). Operational taxonomic units at 97% 16S rRNA gene identity (OTU<sub>0.03</sub>) and Chao1 richness estimates were calculated using the software mothur v1.24 (Schloss et al., 2009).

#### *Intact polar lipid analyses*

Before intact and free cell membrane constituents were analyzed by liquid and gas chromatography, freeze dried sediment was spiked with internal standards and lipids extracted using a modified Bligh and Dyer method (Sturt et al., 2004). The total lipid extract was separated chromatographically on a glass column using 3 g of silica gel (60 mesh) into three fractions: a non-polar fraction (dichloromethane), a glycolipid fraction (acetone), and a phospholipid fraction (methanol). The phospholipid fractions were analyzed for intact polar lipids, which were measured by high performance liquid chromatography/electrospray ionization-multiple stage-mass spectrometry (HPLC/ESI-MS<sup>n</sup>) as previously described (Sturt et al., 2004). The non-polar fractions were further separated for gas chromatography analyses following standard protocols for separation, derivatization, and transesterification (e.g. Elvert et al., 2003; Elvert et al., 2000) described in detail by Ertefai et al. (2008).

## Results

### ***Sediment solid phase***

The recovered sediment cores were visually differentiated into upper (0-10 cm below seafloor - cmbsf), middle (10-25 cmbsf) and lower (>25 cmbsf) sections (Fig. 2A). The upper 10 cm showed a light brown color and was characterized by living vesicomid clams being partly buried into the slightly sandy sediment. The middle section of the core was black with broken shells and a sulfidic smell was noticed during subsampling. Below 25 cm depth, the sediment was of uniform grey color. The differentiation of the sediment into different horizons was also reflected in the pyrite, carbonate, and TOC contents of the sediment (Fig. 2B). In the upper sediment horizon (0-10 cm), pyrite ( $\text{FeS}_2$ ) was absent and carbonate was low (5-7 wt-%). In the middle section, the amount of pyrite and carbonate increased to up to 8 and 32 wt-%, respectively. The carbonate content declined again in the lower section in contrast to pyrite, which reached values of up to 12 wt-%. TOC content in the sediment was constant in the upper 15 cm (~1.7wt-%), decreased in the middle section of the core (14-18 cmbsf) and stayed constant again in the lower section (Fig. 2B).

### ***Sediment geochemistry***

#### *Pore water geochemistry*

In the center and at the rim of the JTC colony sulfate, DIC, and dissolved methane concentrations as well as the methane isotopic composition were determined. In the center of the clam patch, sulfate concentration decreased to less than 1 mM at 12 cmbsf (Fig. 3A). The DIC concentration profile showed an opposite behavior to the sulfate profile, as it first increased with depth and then stayed nearly constant at more than 100 mM below 10 cmbsf. In contrast, at the JTC colony rim, sulfate penetrated deeper into the sediment (18 cmbsf) as compared to the center (Fig. 3) and the maximum DIC concentration (~100 mM) was found at 31 cmbsf. Dissolved methane was analyzed in all three lithostratigraphic horizons (Fig. 3). Concentrations and isotopic compositions varied with sediment depth and showed differences between sampling spots. The center revealed higher dissolved methane concentrations than the rim with a maximum between 25 and 33 cmbsf (Fig. 3 A). At the center,  $\delta^{13}\text{C}$  values of dissolved methane ranged from -84 to -79‰. The most  $^{13}\text{C}$ -enriched values were found in the middle section of the core at 15-20 cmbsf. At the rim, the dissolved methane was less depleted in  $^{13}\text{C}$  (-72 to -66‰; Fig. 3B).

### *Methane oxidation and sulfate reduction rates*

Sulfate consumption was measured at the rim and the center of the JTC colony, whereas methane turnover could only be quantified in the rim sediment (Fig. 3). At the center, SR values were scattered over the investigated depth horizon and ranged from 16 to 128 nmol ml<sup>-1</sup> d<sup>-1</sup>. The averaged depth integrated SR rate (0-16 cm) was 6.3 mmol m<sup>-2</sup> d<sup>-1</sup>. At the colony rim, sulfate turnover was lower (1.4 - 64 nmol ml<sup>-1</sup> d<sup>-1</sup>) with a maximum at about five centimeter below seafloor and decreased with increasing sediment depth. Horizontal distribution of methane consumption at the rim was similar to SR rates with values ranging from 2 to 52 nmol ml<sup>-1</sup> d<sup>-1</sup>. The average depth (0-16 cm below seafloor) integrated turnover rates of methane and sulfate at the rim were in the same range with 2.4 (n=3) and 2.1 (n=3) mmol m<sup>-2</sup> d<sup>-1</sup>, respectively.

### *In situ oxygen uptake measurements*

The microprofiler module was placed at the sediment next to the JTC colony, since a direct placement of the fragile glass sensors in the JTC colony was not possible. Approximately 20 cm beside the colony rim, the average oxygen penetration depth was 1.64 cm (n=3) with an average diffusive oxygen uptake (DOU) of 1.9 mmol m<sup>-2</sup> d<sup>-1</sup> (Fig. 4). The temperature remained constant at about 1.3 °C for the entire profiling length and, thus no heat flow was observed. In contrast to the microprofiler, the benthic chamber was placed directly on the clams enclosing about 20 clams. A total oxygen uptake (TOU) of 21 mmol m<sup>-2</sup> d<sup>-1</sup> was measured, which is one order of magnitude higher than the DOU outside the colony. Assuming that the DOU represents the benthic oxygen consumption of the pelagic sediment in the Japan Trench at 5346 m, we calculated the oxygen consumption related to the benthic chemosynthetic community (CCOU) by subtracting DOU from TOU (CCOU = TOU – DOU). For our investigated JTC colony this resulted in a community consumption of 19 mmol O<sub>2</sub> m<sup>-2</sup> d<sup>-1</sup>. The chamber enclosed a sediment area of 0.0284 m<sup>2</sup>, populated by approximately 20 clams, which resulted in a clam density of ~ 700 clams m<sup>-2</sup>. Thus, one clam consumed about 27 μmol oxygen per day.

## ***Microbial community***

### *Biomarker analyses*

Analyses of microbial lipids as both intact polar membrane lipids and free lipids were performed using sediment from below the clams in the center of the JTC colony (Fig. 5). The HPLC-MS<sup>n</sup> analysis revealed phosphate-based intact polar lipids (IPLs) in the form of

hydroxyarchaeol (OH-Ar) with phosphatidylglycerol (PG) and phosphatidylserine (PS) as polar headgroups. Both IPL types increased with sediment depth from 5 to 141  $\mu\text{g kg}^{-1}$  dry sediment and were most abundant in the sediment horizon between 12 and 18 cm (141  $\mu\text{g kg}^{-1}$ ) before their concentration declined to 35  $\mu\text{g kg}^{-1}$  with sediment depth (Fig. 5). Bacterial dietherglycerolipids (DEG), occurring as phosphatidylethanolamine (PE) and PS, were absent in the upper 6 cm, but increased with sediment depth and peaked in the sediment horizon at 12 to 18 cm (27  $\mu\text{g kg}^{-1}$ ) and then declined to 4  $\mu\text{g kg}^{-1}$  dry sediment. The free extractable lipids included OH-Ar and monoalkyl glycerol ethers (MAGE) supporting the HPLC-MS analysis.  $\delta^{13}\text{C}$  values of free extractable lipids varied with sediment depth and the most strongly  $^{13}\text{C}$ -depleted lipids were present at 12-18 cm below seafloor (Fig. 5).

#### *Phylogenetic diversity*

Sequencing of selected clones from 16S rRNA gene libraries resulted in a total of 147 archaeal and 173 bacterial sequences (Fig. 6) from the surface sediment (0-10 cm) of the JTC colony center and the rim. The archaeal community of the center seemed to be extremely low in diversity (Fig. 7a), since we only obtained three OTU<sub>0.03</sub> and gene diversity was too little to reasonably estimate Chao1 richness. The OTU<sub>0.03</sub> belonged to the ANME-2c clade (88% of all clones), the ANME-2a clade (1%) and the *Methanococoides* (11%). The bacterial gene library of the center was dominated by deltaproteobacterial SRB of the orders *Desulfobacterales* (26%) and *Desulfarculales* (4%). The diversity of sulfate reducers was high, including members of the genus *Desulfarculaceae*, *Desulfobacula*, *Desulforhopalus* and *Desulfobacterium* (Fig. 7c). Interestingly, we did not detect sequences of the SEEP-SRB-1 clade, which is common at seep ecosystems, instead the SRB community seemed to be dominated by *Desulfobulbaceae* (20%), such as SEEP-SRB-3 and SEEP-SRB-4. The sulfur oxidizing community seemed to be dominated by chemolithoautotrophic *Sulfurovum* species (14%) within the *Epsilonproteobacteria*, whereas sequences of *Thiotrichales* (~1%) were rare.

The archaeal community of the JTC colony rim appeared to be more diverse than that of the center. Most sequences belonged to the genus *Methanococoides* (63%), followed by ANME-2c archaea (18%). In addition, we found members of Marine Benthic Group B (14%), Deep-Sea Hydrothermal Vent Group 6 (4%), and Marine Group 1 (~1%). The bacterial gene library of the rim sediment was greatly dominated by *Psychrobacter* (51%) of the order *Pseudomonadales* showing a high microdiversity (Fig. 7b). The

community also included *Desulfobacterales*. The 16S rRNA gene libraries from the center and rim sediments of the JTC colony indicated that the investigated microbial communities had a low diversity and estimated richness. Remarkably, the seep seemed to lack clades that are common to many seep sites worldwide, such as SEEP-SRB-1, *Methylococcales*, ANME-1 and *Thermoplasmatales*.

## Discussion

### *Seepage intensity at a Japan Trench clam colony*

The distribution of clams at seeps is strongly controlled by the biogeochemical processes in underlying sediments, which are influenced by the supply of methane-rich fluids from the subsurface. Upward flow of hydrocarbon-rich fluids through thrust faults (Kobayashi, 2002) at fracture zones of the Japan Trench has been described, where vesicomid clam colonies with sharp boundaries have often been detected (Juniper & Sibuet, 1987; Ogawa et al., 1996; Sibuet et al., 1988). Oxygen and temperature profiles at the JTC colony investigated in this study also point to a locally focused release of seep fluids. The measured oxygen penetration depth of 1.6 cm (Fig. 4) and the corresponding low benthic oxygen consumption rate indicated that sediments a few centimeters away from the colony rim were similar to non-seep influenced sediments (De Beer et al., 2006; Wenzhöfer & Glud, 2002). At typical cold seep habitats, oxygen penetration into the sediment is usually limited to the top few millimeters (Felden et al., 2013; Lichtschlag et al., 2010), even at vesicomid clam sites with bioturbating activity oxygen penetration depth is reduced (Levin et al., 2003). Moreover, a straight temperature profile was measured beside the rim of the clam colony (Fig. 4), indicating that fluid flow from the deep subsurface is not detectable next to the JTC colony rim. At active seep sediments, upward fluid flow is indicated by increasing temperatures with increasing depths (e.g. Feseker et al., 2008). Such temperature gradients have been recorded for numerous clam colonies, e.g. at the Nankai Trough (Kobayashi, 2002) and at the Peruvian margin (Olu et al., 1996). Unfortunately, we could not measure sediment temperature profiles directly below the clam patch. However, the concave-shaped sulfate concentration profile and the methane concentrations measured at the colony center (Fig. 3) indicated a low seepage activity nourishing the clam community. Methane  $\delta^{13}\text{C}$  values of less than -80‰ at the JTC colony center (Fig. 3) indicate biogenic methane formation from  $\text{CO}_2$  and  $\text{H}_2$  rather than a deep subsurface thermogenic origin (Whiticar, 1999). However, similar isotopic ratios and methane concentrations below 1 mM were also found at other clam sites, where methane rises from the deep subsurface (Olu et al., 2009).

Alternatively, the JTC colony could have also developed, because methane-rich and sulfate-free deep sediment layers were suddenly exposed to oxygenated and sulfate-rich bottom waters as proposed for the Monterey Canyon seep ecosystems (Paull et al.,

2005). There, chemosynthetic benthic communities are most common on steep slopes where seafloor erosion occurs and tectonically driven fluid flow is lacking (Paull et al., 2005). Erosion of the sediment in the Japan Trench might have happened when the upper sediment layer was removed during one of the regularly occurring earthquakes (Kawagucci et al., 2012; Kobayashi, 2002), however, our data and dive observations do not indicate such sediment instabilities for the investigated site.

### ***Biogeochemical processes in the Japan Trench clam colony sediment***

To investigate whether there are also similarities to shallow seeps concerning the underlying biogeochemical processes, we analyzed methane and sulfate consumption rates. Fluid flow and associated methane availability at the JTC colony were rather low, but sufficient to maintain a dense seep community of living clams. The depth integrated rates of AOM and SR have a ratio close to one, indicating a close coupling of methane consumption and sulfide production (Niemann et al., 2006b; Treude et al., 2003), which constantly nourished the clams and their chemosynthetic symbionts.

SR rates of clam patches at different seep ecosystems cover a wide range of turnover rates (Boetius & Suess, 2004; Pop Ristova et al., 2012; Treude et al., 2003), and seem to correlate with the methane availability in the sediment. Rates measured at the JTC colony are in the same range as those of a clam colony at the REGAB pockmarks (Pop Ristova et al., 2012). But these values are nearly two orders of magnitude lower compared to Hydrate Ridge off Oregon, where SR rates of up to 3000 nmol ml<sup>-1</sup> d<sup>-1</sup> in combination with methane concentration of up to 10 mM have been found (Boetius & Suess, 2004; Torres et al., 2002). In fact, even lower methane concentrations sustain clam habitats (Barry et al., 1997; Cambon-Bonavita et al., 2009; Wallmann et al., 1997), which underlines the capability of *Vesicomysidea* clams to adapt to different environmental conditions. Low methane concentrations are not only an indicator for low seepage rates, they also result in lower sulfide availability within the sediment. *Vesicomysidea* clams are able to inhabit sites with low sulfide concentrations simply due to their ability to enrich sulfide in their body fluids above ambient concentrations (Barry & Kochevar, 1998; Barry et al., 1997; Childress et al., 1993). A continuous supply of sulfide seems to be more important for these animals than the absolute concentration (Dubilier et al., 2008). Furthermore, *in situ* sulfide concentrations in close vicinity of the clam foot could be significantly higher similar to what has been described for vestimentiferan tubeworms (Cordes et al., 2005). These tubeworms were shown to build up high biomasses even in

seep sediments with sulfide concentration that were too low to maintain their growth. This is possible because the tubeworms supply the benthic microbial community close to their roots with sulfate and thus enhance locally the microbial sulfide production. An efficient sulfide uptake mechanism by the animal together with the microbially mediated biogeochemical reactions thus prevents the enrichment of sulfide in the sediment (Cordes et al., 2005). Furthermore, clams can move to sediments with higher sulfide concentrations as soon as sulfide is depleted at one location (Levin, 2005; Olu et al., 1996; Sibuet et al., 1988). In fact, such single moving clams were observed during our exploration. However, since the majority of clams were associated in patches (Fig. 1B), methane seepage and subsequent sulfide availability seemed to be sufficient to maintain the colonies.

At the JTC colony, the low methane concentrations in the surface sediments might not only be the result of low seepage activity but could have also resulted from efficient methane consumption by the benthic filter. Indeed, we measured SR rates of  $6.3 \text{ mmol m}^{-2} \text{ d}^{-1}$  in the sediment below the clam colony. If we assume that oxygen was used as the terminal electron acceptor for sulfide oxidation, which in turn is mainly produced by SR coupled to AOM, then TOU can be used to estimate the *in situ* methane consumption within the sediment. An oxygen uptake of  $21 \text{ mmol m}^{-2} \text{ d}^{-1}$  would correspond to a methane consumption rate of  $10.5 \text{ mmol m}^{-2} \text{ d}^{-1}$  based on the stoichiometric ratios of methane to sulfide (1:1) and of sulfide to oxygen (1:2). Methane efflux measurements at other clam habitats indicated that the uprising methane is completely oxidized in the sediment (Pop Ristova et al., 2012; Sommer et al., 2006). Therefore, the methane flux from the deep subsurface for the entire JTC colony (diameter  $1.8 \text{ m}^2$ ) would be  $19 \text{ mmol d}^{-1}$ , which corroborates that seepage was relatively low compared to other clam habitats (Boetius & Suess, 2004; Pop Ristova et al., 2012; Sommer et al., 2006; Torres et al., 2002). This could be either a temporal effect because fluid flow can slightly vary over time at seeps (Olu et al., 1996) or the seep community of the JTC colony is well adapted to efficiently use a low, but constant methane supply to build up the observed high biomasses.

### ***Chemosynthetic seep community at the Japan Trench clam colony***

#### ***Clams as bioengineers***

*Vesicomysid* clams rely on the biogeochemical processes in the sediment for their sulfide supply and at the same time strongly influence the benthic biogeochemical regime by bioirrigation and bioturbation (Fischer et al., 2012; Wallmann et al., 1997). Geochemical gradients (DIC, pyrite, calcium carbonate content) and turnover rates at the JTC colony

showed an active community performing SR and AOM in the upper 10 - 15 cm of the sediment. However, we did not find a distinct production zone at the JTC colony, which is usually present at seep habitats with other associated organisms (e.g. Felden et al., 2013; Felden et al., 2010; Treude et al., 2003). The activity was rather spread throughout the sediment, within a depth range that was affected by the clams, which had an average body length of 15-17 cm and were buried up to four fifths in the sediment. Clams and other seep-associated fauna, such as polychaete tubeworms are known to enhance the availability of electron acceptors in deeper sediment horizons by bioirrigation, which results in a lowering of the sulfate methane transition zone (Fischer et al., 2012; Levin et al., 2003; Ruff et al., 2013; Treude et al., 2003; Wallmann et al., 1997). By this mechanism, competing chemosynthetic surface organisms are separated from their energy source over time, which is a known phenomenon at cold seeps (Fischer et al., 2012; Pop Ristova et al., 2012). At the JTC colony, the clams seem to have successfully altered the sulfide availability within the sediment and thus other common members of cold seeps such as thiotrophic bacterial mats were not observed (Felden et al., 2013; Felden et al., 2010; Lichtschlag et al., 2010; Treude et al., 2003).

Using average growth rates of other vesicomid clam species (Barry & Kochevar, 1998) and the measured shell sizes, we estimated an average age of 10-15 years for the living clams at the JTC colony. The mixture of living clams and empty shells suggests that the clam colony existed for more than 15 years; consequently methane seepage has likely influenced this site at least for several decades. The reduced faunal diversity at the JTC colony dominated by only two clam species indicate relatively stable spatial and temporal environmental conditions (e.g. fluid flow), since it was shown that the reduction of ecological niches and thus diversity results from habitat stability (Sibuet & Olu-Le Roy, 2002). Although studies of seeps deeper than 5000 m are rare, the comparison between shallower seep ecosystems indicated a correlation between seep-fauna diversity as well as biomass and fluid flow rate variation on temporal but also spatial scales (Cordes et al., 2010; Sibuet & Olu-Le Roy, 2002).

#### *Benthic microbial community in a low seepage, abyssal clam habitat*

We demonstrated the presence of an active microbial community at the JTC colony that couples SR to AOM by biogeochemical measurements, lipid analyses and 16S rRNA gene analyses. In the sediment below the clams, the lipid analyses revealed diagnostic biomarkers for AOM specific archaeal and bacterial groups. The depth trend of IPL

concentrations indicated an increase of prokaryotic cell abundances at the depth of the geochemical reaction zone, where sulfate and methane were metabolized (Fig. 5). Archaeol-based lipids and high ratios of OH-Ar vs. Ar lipids strongly suggested a predominance of ANME-2 archaea in the center of the JTC colony (Niemann, 2008). The gene library results indicated that the dominant clade for anaerobic methane oxidation is ANME-2c, which is supported by previous findings (Vossmeyer et al., 2012). ANME-2c seems to preferentially occur in sediments bioirrigated by clams, e.g. at Hydrate Ridge in the Northeast Pacific and the REGAB pockmark in the Kongo Basin (Elvert et al., 2005; Knittel et al., 2005; Pop Ristova et al., 2012), and in low fluid flux regimes (Elvert et al., 2005; Wegener et al., 2008). Furthermore, the ANME-2c organisms that we found were closely related to those of other seeps worldwide, indicating a global distribution. Hence, the environmental niche of ANME-2c seemed to be determined by bioturbation and low methane seepage, rather than water depth and geographic location.

In contrast to other clam colonies (Cambon-Bonavita et al., 2009; Knittel et al., 2003), we did not detect ANME-1 or ANME-3 in sediments below vesicomyids (Fig. 7a). The absence of ANME-1 at the JTC colony was previously observed (Vossmeyer et al., 2012) and might be due to the environmental requirements of this organism. The top 10 cm of the sediment at the JTC colony were light brown (Fig. 2) and pyrite was absent, suggesting oxygenation of the sediment due to faunal activity. ANME-1 seem to be sensitive towards oxygen since they were absent at bioirrigated seeps at the Hikurangi margin (Ruff et al., 2013) and increased with increasing sediment depth and decreasing sediment irrigation at clam colonies (Knittel et al., 2005; Rossel et al., 2011). Moreover, ANME-1 appeared to also be more sensitive to cold temperatures than ANME-2 (Rossel et al., 2011). In contrast to our findings, the presence of ANME-3 in the JTC sediments was reported previously (Vossmeyer et al., 2012). However, the finding was based on T-RFLP fragments and it is very hard to distinguish ANME-3 and *Methanococcoides* spp. with this method because these two clades are closely related and include organisms that have the same *Hha1* restriction site (not shown). Hence, it is very likely that the detected TRFs belonged to *Methanococcoides* rather than ANME-3.

The presence of sulfate-reducing *Deltaproteobacteria*, which includes the partner SRB of ANME-2 was shown by the <sup>13</sup>C-depleted IPL-derived bacterial lipids and the high amounts of monoalkyl glycerol ethers (Ertefai et al., 2008; Hinrichs et al., 2000; Niemann, 2008) in the center of the JTC colony. Additionally, we retrieved many sequences that were affiliated to numerous clades of deltaproteobacterial SRB (Fig. 6, 7c). Remarkably,

we did not detect sequences of the SEEP-SRB1 or SEEP-SRB-2 clades, which are typically the syntrophic partner SRB of ANME-2 archaea and are found at seep sites worldwide (Schreiber 2010, Kleindienst 2012). Instead, we found many sequences of the clades SEEP-SRB-3 and SEEP-SRB-4 within the *Desulfobulbaceae* (Fig. 7c). These clades occur preferably as single cells in surface sediments of gas seeps that are covered by bacterial mats and clams (Kleindienst et al., 2012; Knittel et al., 2003) and decrease with increasing sediment depth (Knittel et al., 2003). SEEP-SRB-3 were also found at a clam colony in the Nankai trough (Li et al., 1999a) and both clades occurred in bioirrigated seeps at Hikurangi margin (Ruff et al., 2013). Hence, SEEP-SRB-3 and SEEP-SRB-4 might have an advantage over other SRB clades because they are adapted to bioturbated and thus oxygenated sediments, such as those at clam colonies. As SEEP-SRB-1 was not detected ANME-2c organisms may have been associated with other SRBs (Pernthaler et al., 2008), or occurred as aggregates or single cells without direct contact to SRBs (Knittel & Boetius, 2009), or performed AOM without a partner SRB (Milucka et al., 2012).

Unexpectedly, aerobic methylotrophic bacteria were not detected in the sediment of the JTC colony, although they are widespread in methane-rich ecosystems, especially at bioirrigated mud volcanoes and cold seeps (Inagaki et al., 2004b; Lösekann et al., 2007; Ruff et al., 2013; Tavormina et al., 2008) and contribute significantly to the benthic methane and oxygen consumption (Boetius & Wenzhöfer, 2013; Felden et al., 2013; Felden et al., 2010). Benthic oxygen consumption at the JTC colony was in the same range as sulfide production, suggesting that aerobic methane oxidation was very low. In contrast, at the REGAB clam colonies benthic oxygen consumption was up to three orders of magnitude higher than sulfide production rates (Decker et al., 2012; Pop Ristova et al., 2012), which was assigned to aerobic methanotrophy (Pop Ristova et al., 2012).

Sulfide oxidation at the JTC colony seemed to be performed not only by the chemosynthetic vesicomyids, but also by free-living sulfur-oxidizing bacteria. Sulfide oxidation seemed to be carried out mainly by *Sulfurovum* spp., which are sulfur oxidizers that were first isolated from hydrothermal vent sediments of the mid-Okinawa Trough (Inagaki et al., 2004a). Although we cannot exclude that elemental sulfur was present in the JTC colony sediments, this observation indicated that *Sulfurovum* organisms are also able to oxidize sulfide (Fang et al., 2006; Inagaki et al., 2002; Li et al., 1999a; Li et al., 1999b). It is also worth noting that members of the genera *Beggiatoa* and *Arcobacter*, which are sulfur-oxidizing bacteria commonly detected at cold seeps (Grünke et al., 2011;

Grünke et al., 2012; Omoregie et al., 2008), were not observed at the Japan Trench cold seep.

The microbial community at the rim of the JTC colony differed greatly from the one at the center, despite a distance of only 30 cm. The microbial community mirrored the sharp biogeochemical gradients and defined ecosystem boundaries. The sediment at the rim of the colony was dominated by psychrophilic *Gammaproteobacteria* and comprised clades that are common to deep-sea sediments, such as *Thaumarchaeota* (Durbin & Teske, 2011). However, sequences of the Marine Benthic Group B, *Desulfobacterales*, ANME-2c and many *Methanococoides* sequences, which occur in methane-rich subsurface sediments (Biddle et al., 2006; Inagaki et al., 2006), were also found indicating that methane is at least occasionally present. Nevertheless, there was little community overlap between the sediments on species-level (97% 16S rRNA gene identity) (Fig. 7a-c), pointing to distinct differences between these seafloor habitats.

## Conclusion

We could show that an abyssal clam colony in the Japan Trench is similar to the ones found at shallower depths, concerning the predominant biogeochemical processes, such as anaerobic oxidation of methane (AOM), sulfate reduction (SR) and benthic oxygen consumption. The tight coupling of AOM and SR rates indicate that also at the abyssal site the benthic methane filter is as efficient as at shallow clam seeps. The methanotrophic community was dominated by ANME-2c organisms, which also occur at shallow low-seepage clam colonies. These observations suggest that the environmental niche of ANME-2c is largely affected by bioturbation of the clams and low methane seepage rather than by pressure or by geographic location. However, other ecosystem functions such as sulfate reduction and thiotrophy are mediated by clades that are rarely found at shallow clam seeps, indicating environmental filtering at these extreme sites. To better understand these widespread and potential globally important ecosystems we need to repeat such in-depth studies of biogeochemical processes at other abyssal seep sites. This includes the investigation of the distribution and abundance of key functional clades as well as the *in situ* quantification of oxygen and methane fluxes.

## Acknowledgements

We thank the members of the shipboard crew of the RV Yokosuka, the *Shinkai 6500* team and the shipboard scientific party for the excellent support during cruise YK06-05. We are grateful for the technical support from Martina Alisch, Viola Beier, Xavier Prieto Mollar, Gabriele Schüßler, and especially Gabriele Eickert. Special thanks to the “SeaTechs” Axel Nordhausen, Marc Viehweger, Patrick Meyer and Volker Asendorf for building and maintaining the *in situ* instruments. We thank Antje Boetius and Katrin Knittel for very helpful discussions during the preparation of the manuscript. This work was performed in the framework of the GEOTECHNOLOGIEN project MUMM II (03G0608C) funded by the German Ministry of Education and Research (BMBF) and German Research Foundation (DFG) as well as the Max Planck Society.

## Figures

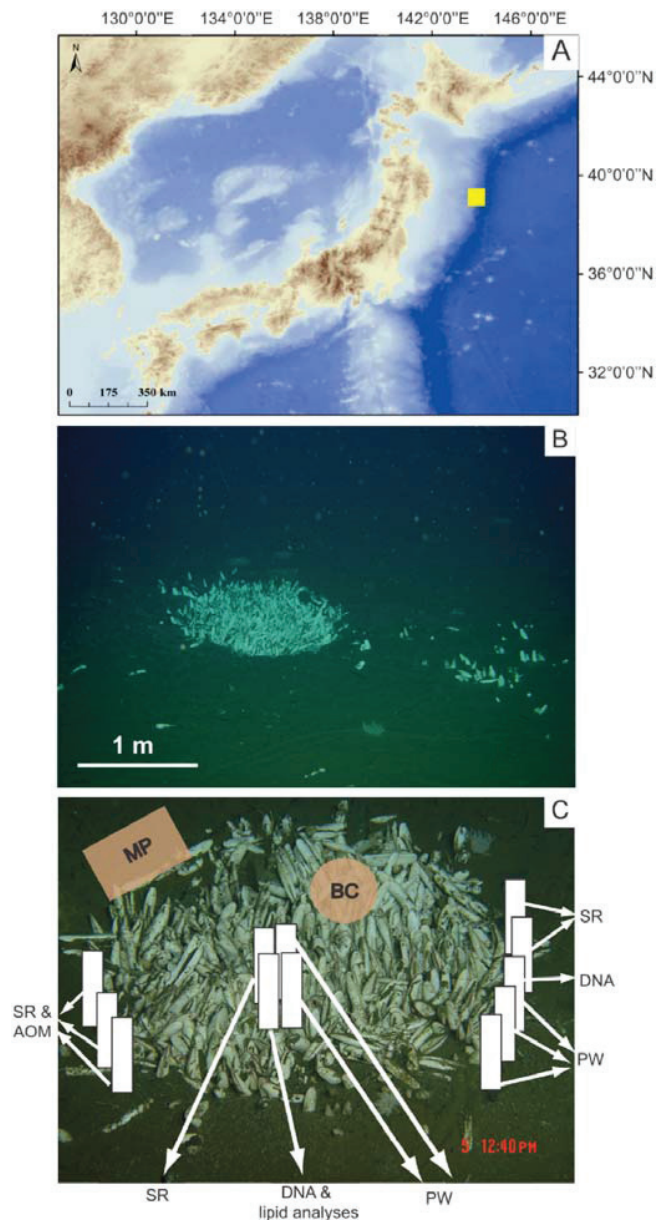


**Figure 1: Location of the *Vesicomysidae* colony and sampling scheme**

Sampling and *in situ* measurements were performed at a vesicomysid clam colony in the Japan Trench at a water depth of 5346 m (A, B). The relative positions of *in situ* measurements and pushcore sampling (white bars) at the investigated clam patch are indicated (C). (MP = microprofiler; BC = benthic chamber; DNA = 16S rDNA analyses; SR = sulfate reduction; AOM = anaerobic oxidation of methane; PW = pore water chemistry, methane concentration and isotopy; calcium carbonate, pyrite and total organic carbon content).

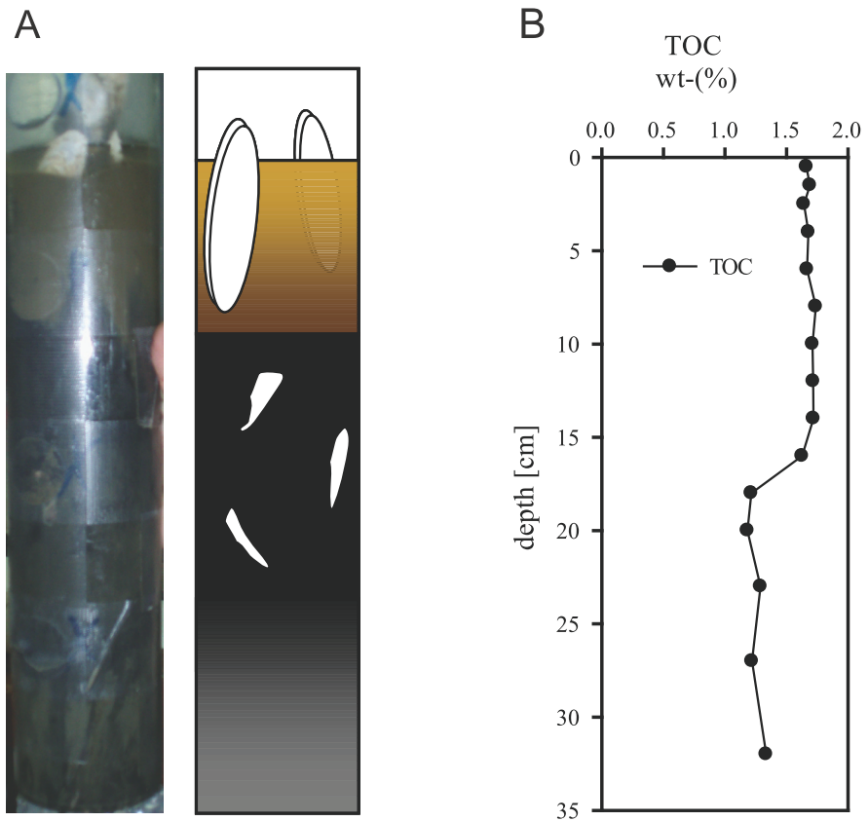


**Figure 2: Stratification of the center sediment**

Photograph and sketch of a push core sampled in the center of the Japan Trench clam colony (**A**). The upper part of the core was oxic/suboxic (brown layer with live clams), whereas the lower part was anoxic/sulfidic (black part with clam shells). Total organic carbon (TOC) content was constant in the upper part of the core and then dropped in the deeper layers (**B**)

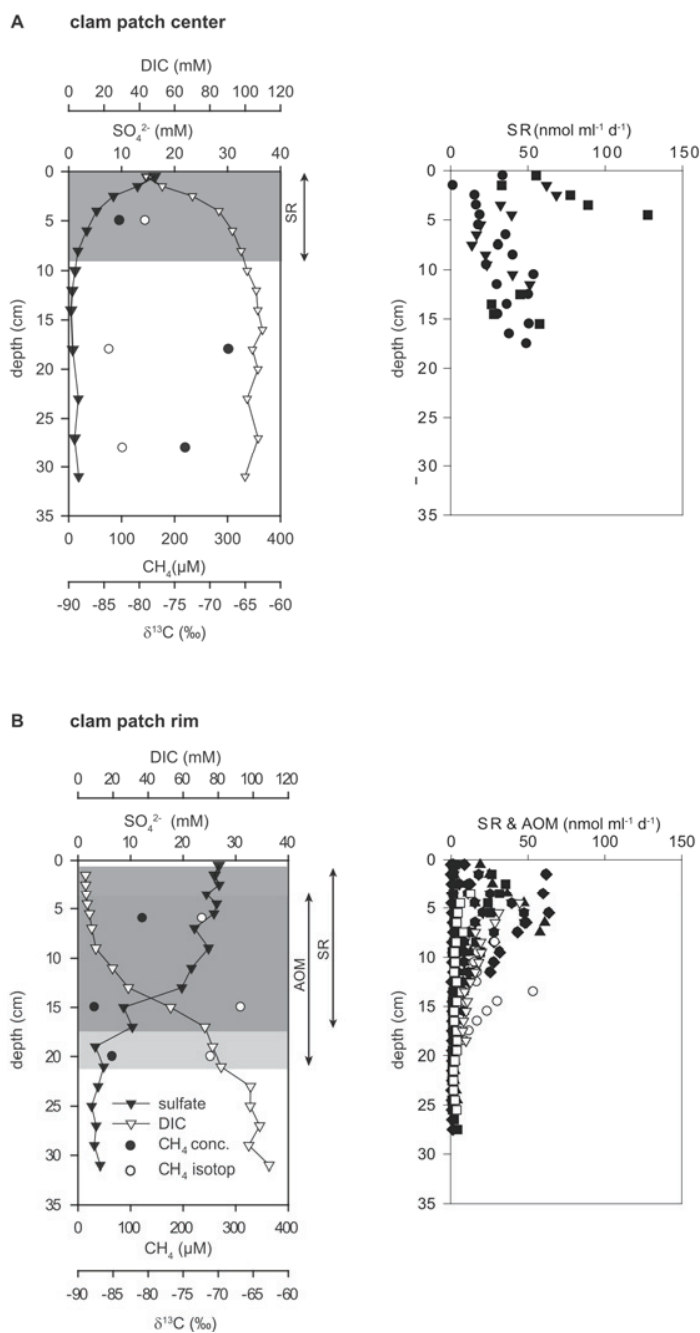


### Figure 3: Biogeochemistry

*Left panel:* Sulfate (black triangles) and DIC (white triangles) concentrations were measured in the pore water from the center (A) and the rim (B) of the JTC colony. Potential SR and AOM horizons according to pore water concentrations are highlighted. Furthermore, methane concentration (black dots) and isotopic composition (white dots) were determined at both locations. *Right panel:* SR rates (in black) and AOM (in white) rates from the center and the rim of the JTC colony. The different symbols represent replicates of turnover rate measurements.

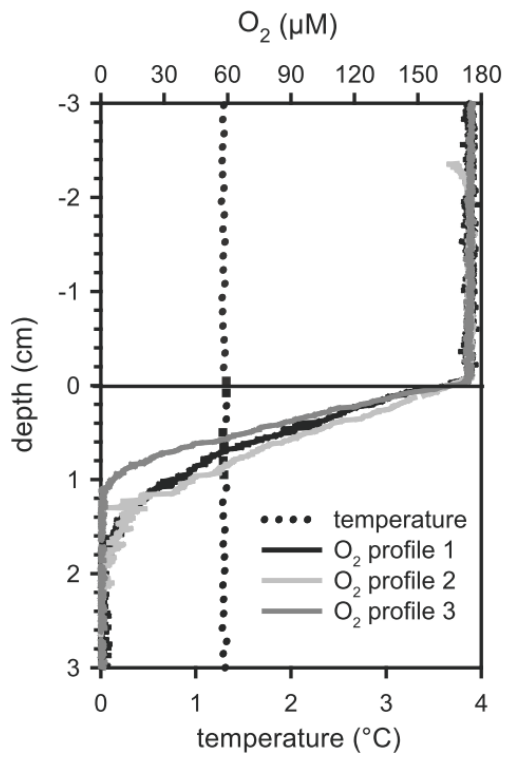


**Figure 4: Microsensor measurements**

High resolution microsensor measurements outside of the colony showed an oxygen penetration depth of > 1cm and constant temperature throughout the entire sediment layer.

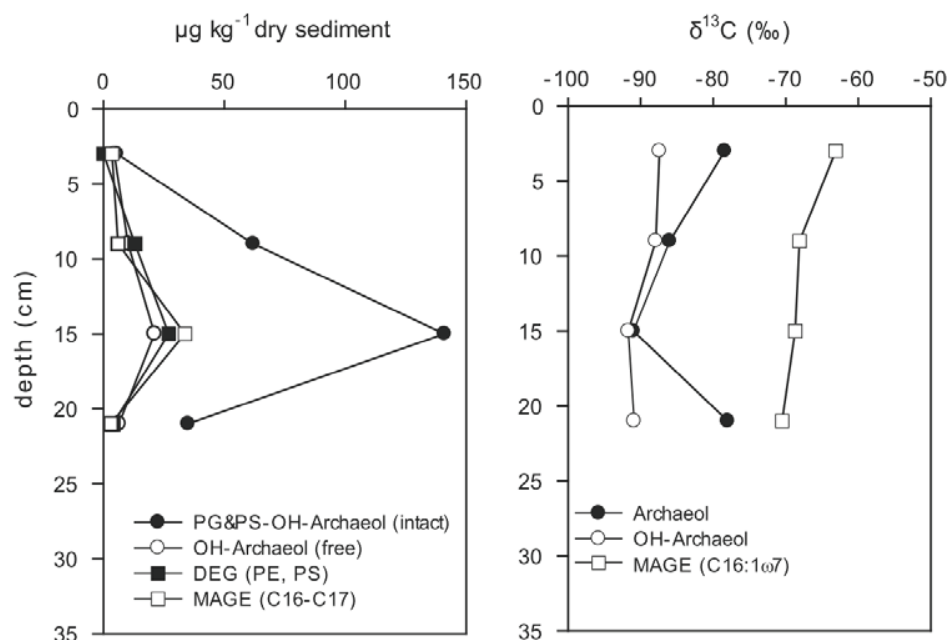


**Figure 5: Microbial lipid profiles in the center of the JTC colony**

Concentrations of archaeal and bacterial lipids are shown on the left and the isotopic compositions are on the right panel; abbreviations: PG&PS-OH-archaeol (intact): hydroxyarchaeol (OH-Ar) with phosphatidylglycerol (PG) and phosphatidylserine (PS) as polar headgroups; DEG (PE, PS): dietheryglycerolipid as phosphatidylethanolamine and PS; OH-archaeol (free): free extractable OH-Ar; MAGE (C16-C17): sum of monoalkyl glycerol ether C16 and C17; MAGE (C16:1 $\omega$ 7): monounsaturated C16-MAGE.

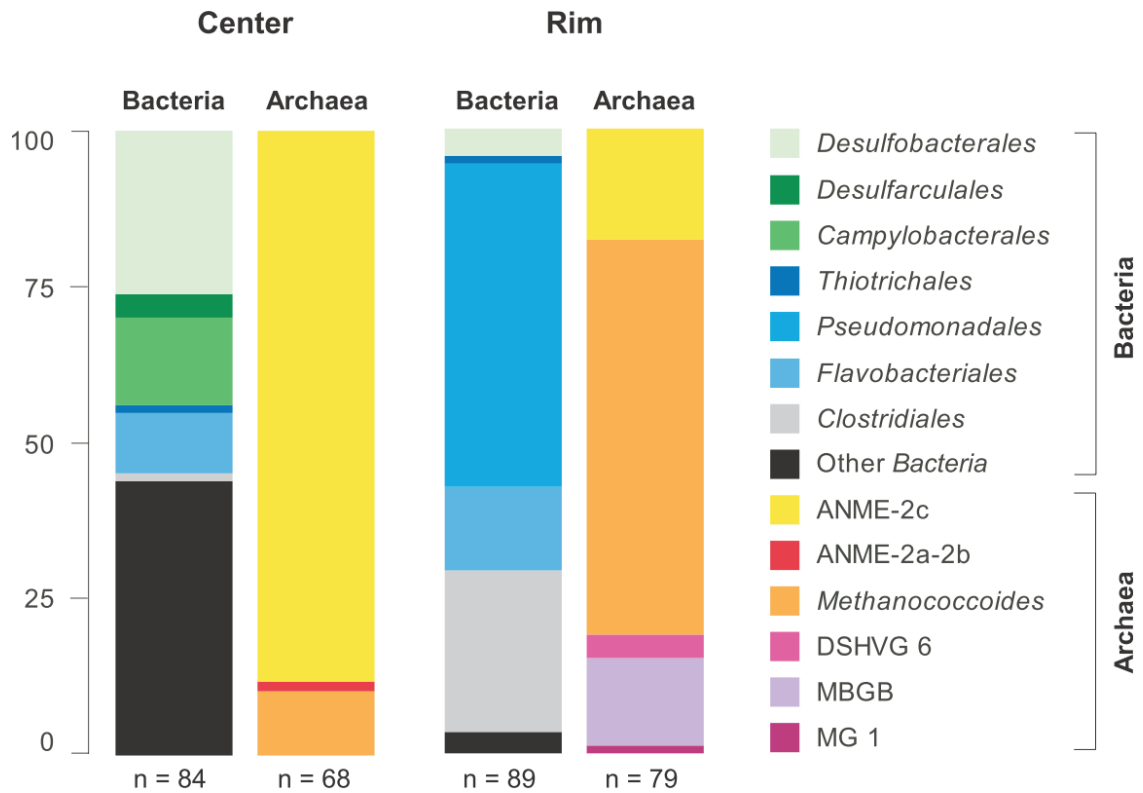
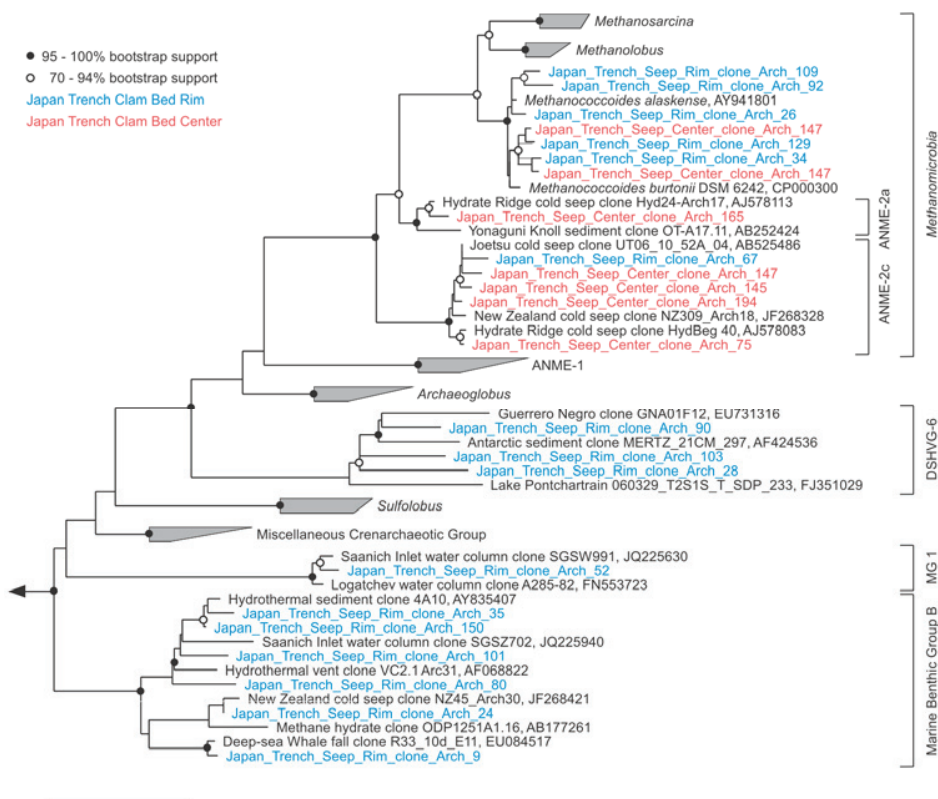
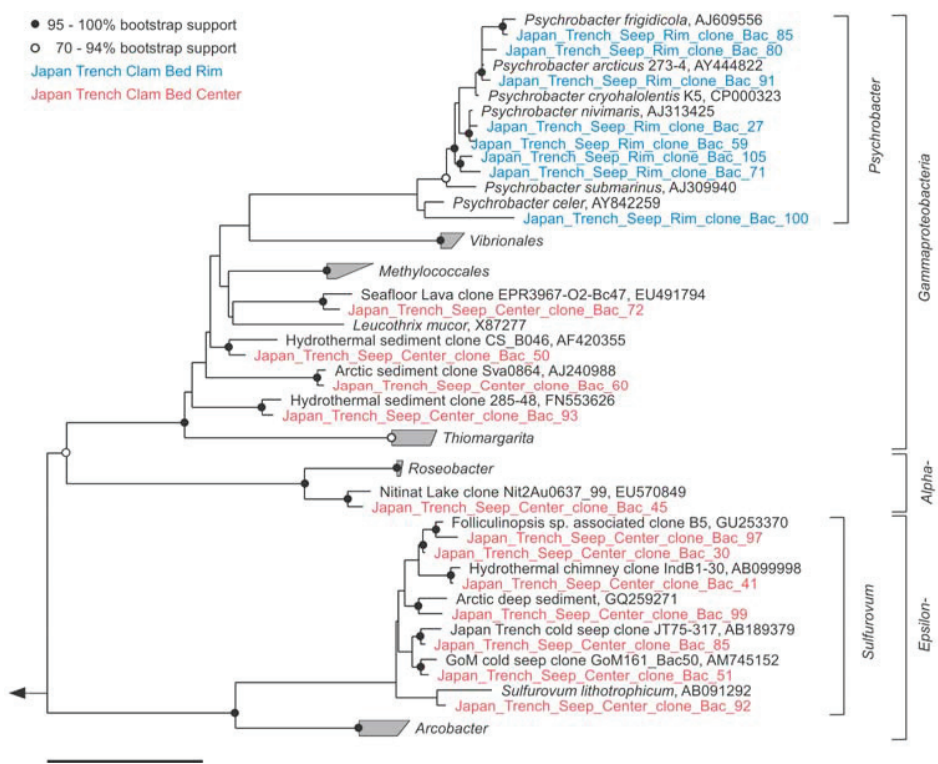


**Figure 6: Relative 16S rRNA gene frequencies**

Archaeal and bacterial diversity in the center and at the rim of the JTC colony. The scale bar represents relative 16S rRNA gene frequencies in percent. The total number of clones per gene library is indicated below the respective column. ANME = Anaerobic methane-oxidizing archaea, DSHVG = Deep Sea Hydrothermal Vent Group, MBGB = Marine Benthic Group B, MG1 = Marine Group 1



A



B

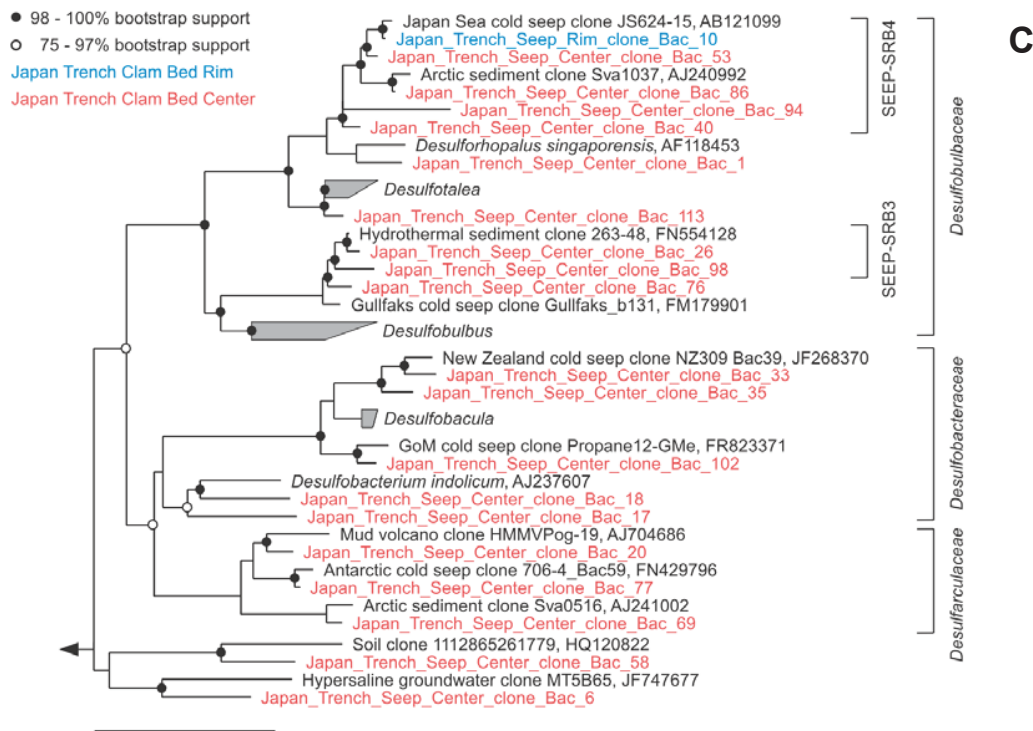


**Figure 7: Phylogenetic affiliation of microbial taxa**

Phylogeny of *Archaea* (A), *Alphaproteobacteria*, *Gammaproteobacteria*, *Epsilonproteobacteria* (B) and *Deltaproteobacteria* (C) in the sediments of the colony center (red) and the colony rim (blue) based on partial 16S rRNA gene sequences. The trees were calculated using the maximum likelihood algorithm RAXML as implemented in ARB (Ludwig et al., 2004). The scale bars represent 10% estimated sequence divergence.

## References

- Arakawa S, Sato T, Sato R, Zhang J, Gamo T, Tsunogai U, Hirota A, Yoshida Y, Usami R, Inagaki F, Kato C (2006) Molecular Phylogenetic and Chemical Analyses of the Microbial Mats in Deep-Sea Cold Seep Sediments at the Northeastern Japan Sea. *Extremophiles*, **10**, 311-319.
- Ashelford KE, Chuzhanova NA, Fry JC, Jones AJ, Weightman AJ (2006) New screening software shows that most recent large 16S rRNA gene clone libraries contain chimeras. *Appl. Environ. Microbiol.*, **72**, 5734-5741.
- Barry JP, Kochevar RE (1998) A tale of two clams: differing chemosynthetic life styles among vesicomyids in Monterey Bay cold seeps. *Cah. Biol. Mar.*, **39**, 329-331.
- Barry JP, Kochevar RE, Baxter CH (1997) The influence of pore-water chemistry and physiology on the distribution of vesicomyid clams at cold seeps in Monterey Bay: Implications for patterns of chemosynthetic community organization. *Limnol. Oceanogr.*, **42**, 318-328.
- Biddle JF, Lipp JS, Lever MA, Lloyd KG, Sorensen KB, Anderson R, Fredricks HF, Elvert M, Kelly TJ, Schrag DP, Sogin ML, Brenchley JE, Teske A, House CH, Hinrichs KU (2006) Heterotrophic Archaea dominate sedimentary subsurface ecosystems off Peru. *Proc. Natl. Acad. Sci. U S A*, **103**, 3846-3851.
- Boetius A, Holler T, Knittel K, Felden J, Wenzhöfer F (2009) The seabed as natural laboratory: lessons from uncultivated methanotrophs. In: *Uncultivated Microorganisms* (ed Epstein S). Springer Berlin / Heidelberg, pp. 59-82.
- Boetius A, Ravensschlag K, Schubert CJ, Rickert D, Widdel F, Gieseke A, Amann R, Jørgensen BB, Witte U, Pfannkuche O (2000) A marine microbial consortium apparently mediating anaerobic oxidation of methane. *Nature*, **407**, 623-626.
- Boetius A, Suess E (2004) Hydrate Ridge: a natural laboratory for the study of microbial life fueled by methane from near-surface gas hydrates. *Chem. Geol.*, **205**, 291-310.
- Boetius A, Wenzhöfer F (2009) In situ technologies for studying deep-sea hotspot ecosystems. *Oceanography*, **22**, 177-177.
- Boetius A, Wenzhöfer F (2013) Seafloor oxygen consumption fuelled by methane from cold seeps. *Nature Geosci.*, **6**, 725-734.
- Cambon-Bonavita MA, Nadalig T, Roussel E, Delage E, Duperron S, Caprais JC, Boetius A, Sibuet M (2009) Diversity and distribution of methane-oxidizing microbial communities associated with different faunal assemblages in giant pockmark of the Gabon continental margin. *Deep-Sea Res. II*, **56**, 2248-2258.
- Childress JJ, Fisher CR, Favuzzi JA, Arp AJ, Oros DR (1993) The role of a zinc-based, serum-borne sulfide-binding component in the uptake and transport of dissolved sulfide by the chemoautotrophic symbiont-containing clam *Calymene bairdii*. *J Exp Biol*, **179**, 131-158.
- Cordes EE, Arthur MA, Shea K, Arvidson RS, Fisher CR (2005) Modeling the mutualistic interactions between tubeworms and microbial consortia. *PLoS Biol*, **3**, 497-506.
- Cordes EE, Cunha MR, Galeron J, Mora C, Olu-Le Roy K, Sibuet M, Van Gaever S, Vanreusel A, Levin LA (2010) The influence of geological, geochemical, and biogenic habitat heterogeneity on seep biodiversity. *Mar. Ecol.*, **31**, 51-65.
- Danovaro R, Company JB, Corinaldesi C, D'Onghia G, Galil B, Gambi C, Gooday AJ, Lampadariou N, Luna GM, Morigi C, Olu K, Polymenakou P, Ramirez-Llodra E, Sabbatini A, Sarda F, Sibuet M, Tselepidis A (2010) Deep-Sea Biodiversity in the Mediterranean Sea: The Known, the Unknown, and the Unknowable. *PLoS One*, **5**.

- De Beer D, Sauter E, Niemann H, Kaul N, Foucher JP, Witte U, Schlüter M, Boetius A (2006) In situ fluxes and zonation of microbial activity in surface sediments of the Håkon Mosby mud volcano. *Limnol. Oceanogr.*, **51**, 1315-1331.
- Decker C, Caprais JC, Khripounoff A, Olu K (2012) First respiration estimates of cold-seep vesicomyid bivalves from in situ total oxygen uptake measurements. *C. R. Biol.*, **335**, 261-270.
- Dubilier N, Bergin C, Lott C (2008) Symbiotic diversity in marine animals: the art of harnessing chemosynthesis. *Nat. Rev. Microbiol.*, **6**, 725-740.
- Durbin AM, Teske A (2011) Microbial diversity and stratification of South Pacific abyssal marine sediments. *Environ. Microbiol.*, **13**, 3219-3234.
- Elvert M, Boetius A, Knittel K, Jørgensen BB (2003) Characterization of specific membrane fatty acids as chemotaxonomic markers for sulfate-reducing bacteria involved in anaerobic oxidation of methane. *Geomicrobiol. J.*, **20**, 403-419.
- Elvert M, Hopmans EC, Treude T, Boetius A, Suess E (2005) Spatial variations of methanotrophic consortia at cold methane seeps: implications from a high-resolution molecular and isotopic approach. *Geobiology*, **3**, 195-209.
- Elvert M, Suess E, Greinert J, Whiticar MJ (2000) Archaea mediating anaerobic methane oxidation in deep-sea sediments at cold seeps of the eastern Aleutian subduction zone. *Org. Geochem.*, **31**, 1175-1187.
- Ertefai TF, Fisher MC, Fredricks HF, Lipp JS, Pearson A, Birgel D, Udert KM, Cavanaugh CM, Gschwend PM, Hinrichs KU (2008) Vertical distribution of microbial lipids and functional genes in chemically distinct layers of a highly polluted meromictic lake. *Org. Geochem.*, **39**, 1572-1588.
- Ertefai TF, Heuer VB, Prieto-Mollar X, Vogt C, Sylva SP, Seewald J, Hinrichs KU (2010) The biogeochemistry of sorbed methane in marine sediments. *Geochim. Cosmochim. Acta*, **74**, 6033-6048.
- Fang JS, Shizuka A, Kato C, Schouten S (2006) Microbial diversity of cold-seep sediments in Sagami Bay, Japan, as determined by 16S rRNA gene and lipid analyses. *FEMS Microbiol. Ecol.*, **57**, 429-441.
- Felden J, Lichtschlag A, Wenzhöfer F, De Beer D, Feseker T, Ristova PP, De Lange G, Boetius A (2013) Limitations of microbial hydrocarbon degradation at the Amon mud volcano (Nile deep-sea fan). *Biogeosciences*, **10**, 3269-3283.
- Felden J, Wenzhöfer F, Feseker T, Boetius A (2010) Transport and consumption of oxygen and methane in different habitats of the Håkon Mosby Mud Volcano (HMMV). *Limnol. Oceanogr.*, **55**, 2366-2380.
- Feseker T, Foucher JP, Harmegnies F (2008) Fluid flow or mud eruptions? Sediment temperature distributions on Håkon Mosby mud volcano, SW Barents Sea slope. *Mar. Geol.*, **247**, 194-207.
- Fischer D, Sahling H, Nothen K, Bohrmann G, Zabel M, Kasten S (2012) Interaction between hydrocarbon seepage, chemosynthetic communities, and bottom water redox at cold seeps of the Makran accretionary prism: insights from habitat-specific pore water sampling and modeling. *Biogeosciences*, **9**, 2013-2031.
- Fujikura K, Kojima S, Tamaki K, Maki Y, Hunt J, Okutani T (1999) The deepest chemosynthesis-based community yet discovered from the hadal zone, 7326 m deep, in the Japan Trench. *Mar. Ecol. Prog. Ser.*, **190**, 17-26.
- Glud RN (2008) Oxygen dynamics of marine sediments. *Mar. Biol. Res.*, **4**, 243-289.
- Goffredi SK, Barry JP (2002) Species-specific variation in sulfide physiology between closely related Vesicomyid clams. *Mar. Ecol. Prog. Ser.*, **225**, 227-238.
- Grünke S, Felden J, Lichtschlag A, Girth AC, De Beer D, Wenzhöfer F, Boetius A (2011) Niche differentiation among mat-forming, sulfide-oxidizing bacteria at cold seeps of the Nile Deep Sea Fan (Eastern Mediterranean Sea). *Geobiology*, **9**, 330-348.

- Grünke S, Lichtschlag A, De Beer D, Felden J, Salman V, Ramette A, Schulz-Vogt HN, Boetius A (2012) Mats of psychrophilic thiotrophic bacteria associated with cold seeps of the Barents Sea. *Biogeosciences*, **9**, 2947-2960.
- Hall PO, Aller RC (1992) Rapid, small-volume, flow-injection analysis for Sigma-CO<sub>2</sub> and NH<sub>4</sub><sup>+</sup> in marine and fresh-waters. *Limnol. Oceanogr.*, **37**, 1113-1119.
- Haroon MF, Hu SH, Shi Y, Imelfort M, Keller J, Hugenholtz P, Yuan ZG, Tyson GW (2013) Anaerobic oxidation of methane coupled to nitrate reduction in a novel archaeal lineage. *Nature*, **500**, 567-+.
- Hinrichs KU, Hayes JM, Sylva SP, Brewer PG, Delong EF (1999) Methane-consuming archaeobacteria in marine sediments. *Nature*, **398**, 802-805.
- Hinrichs KU, Summons RE, Orphan V, Sylva SP, Hayes JM (2000) Molecular and isotopic analysis of anaerobic methane-oxidizing communities in marine sediments. *Org. Geochem.*, **31**, 1685-1701.
- Holler T, Widdel F, Knittel K, Amann R, Kellermann MY, Hinrichs K-U, Teske A, Boetius A, Wegner G (2011) Thermophilic anaerobic oxidation of methane by marine microbial consortia. *ISME J.*, **5**, 1946-1956.
- Inagaki F, Nunoura T, Nakagawa S, Teske A, Lever M, Lauer A, Suzuki M, Takai K, Delwiche M, Colwell FS, Nealson KH, Horikoshi K, D'hondt S, Jørgensen BB (2006) Biogeographical distribution and diversity of microbes in methane hydrate-bearing deep marine sediments, on the Pacific Ocean Margin. *Proc. Natl. Acad. Sci. U S A*, **103**, 2815-2820.
- Inagaki F, Sakihama Y, Inoue A, Kato C, Horikoshi K (2002) Molecular phylogenetic analyses of reverse-transcribed bacterial rRNA obtained from deep-sea cold seep sediments. *Environ. Microbiol.*, **4**, 277-286.
- Inagaki F, Takai K, Nealson KH, Horikoshi K (2004a) *Sulfurovum lithotrophicum* gen. nov., sp. nov., a novel sulfur-oxidizing chemolithoautotroph within the epsilon-Proteobacteria isolated from Okinawa Trough hydrothermal sediments. *Int. J. Syst. Evol. Microbiol.*, **54**, 1477-1482.
- Inagaki F, Tsunogai U, Suzuki M, Kosaka A, Machiyama H, Takai K, Nunoura T, Nealson KH, Horikoshi K (2004b) Characterization of C<sub>1</sub>-metabolizing prokaryotic communities in methane seep habitats at the Kuroshima Knoll, Southern Ryukyu Arc, by analyzing *pmoA*, *mmoX*, *mxoF*, *mcrA*, and 16S rRNA genes. *Appl. Environ. Microbiol.*, **70**, 7445-7455.
- Jørgensen BB (1978) A comparison of methods for the quantification of bacterial sulfate reductin in coastal marine sediments I. Measurements with radiotracer techniques *Geomicrobiol. J.*, **1**, 11-27.
- Jørgensen BB, Boetius A (2007) Feast and Famine - Microbial Life in the Deep-Sea Bed. *Nat. Rev. Micro.*, **5**, 770-781.
- Judd AG, Hovland M (2007) *Seabed fluid flow*, Cambridge University Press, Cambridge.
- Juniper SK, Sibuet M (1987) Cold seep benthic communities in Japan subduction zones - spatial-organization, trophic strategies and evidence for temporal evolution. *Mar. Ecol. Prog. Ser.*, **40**, 115-126.
- Kallmeyer J, Ferdelman TG, Weber A, Fossing H, Jørgensen BB (2004) A cold chromium distillation procedure for radiolabeled sulfide applied to sulfate reduction measurements. *Limnol. Oceanogr. Meth.*, **2**, 171-180.
- Kawagucci S, Yoshida YT, Noguchi T, Honda MC, Uchida H, Ishibashi H, Nakagawa F, Tsunogai U, Okamura K, Takaki Y, Nunoura T, Miyazaki J, Hirai M, Lin WR, Kitazato H, Takai K (2012) Disturbance of deep-sea environments induced by the M9.0 Tohoku Earthquake. *Sci. Rep.-UK*, **2**.

- Kleindienst S, Ramette A, Amann R, Knittel K (2012) Distribution and in situ abundance of sulfate-reducing bacteria in diverse marine hydrocarbon seep sediments. *Environ. Microbiol.*, **14**, 2689-2710.
- Knittel K, Boetius A (2009) Anaerobic oxidation of methane: progress with an unknown process. *Annu. Rev. Microbiol.*, **63**, 311-314.
- Knittel K, Boetius A, Lemke A, Eilers H, Lochte K, Pfannkuche O, Linke P, Amann R (2003) Activity, distribution, and diversity of sulfate reducers and other bacteria in sediments above gas hydrate (Cascadia margin, Oregon). *Geomicrobiol. J.*, **20**, 269-294.
- Knittel K, Lösekann T, Boetius A, Kort R, Amann R (2005) Diversity and distribution of methanotrophic archaea at cold seeps. *Appl. Environ. Microbiol.*, **71**, 467-479.
- Kobayashi K (2002) Tectonic significance of the cold seepage zones in the eastern Nankai accretionary wedge - an outcome of the 15 years' KAIKO projects. *Mar. Geol.*, **187**, 3-30.
- Krylova EM, Sahling H (2010) Vesicomidae (Bivalvia): Current Taxonomy and Distribution. *PLoS One*, **5**.
- Kvenvolden KA, McDonald, T. J. (1986) Organic geochemistry on the JOIDES Resolution - an essay. *ODP Tech. Note 6*.
- Lane DJ, Pace B, Olsen GJ, Stahl DA, Sogin ML, Pace NR (1985) Rapid-determination of 16S Ribosomal-RNA sequences for phylogenetic analyses. *Proc. Natl. Acad. Sci. U S A*, **82**, 6955-6959.
- Levin LA (2005) Ecology of cold seep sediments: Interactions of fauna with flow, chemistry and microbes. In: *Oceanography and Marine Biology - an Annual Review* (eds. Gibson RN, Atkinson RJA, Gordeon JDM). Taylor&Francis, pp. 1-46.
- Levin LA, Ziebis W, Mendoza GF, Growney VA, Tryon MD, Brown KM, Mahn C, Gieskes JM, Rathburn AE (2003) Spatial heterogeneity of macrofauna at northern California methane seeps: influence of sulfide concentration and fluid flow. *Mar. Ecol. Prog. Ser.*, **265**, 123-139.
- Li L, Guenzennec J, Nichols P, Henry P, Yanagibayashi M, Kato C (1999a) Microbial Diversity in Nankai Trough Sediments at a Depth of 3,843 m. *J Oceanogr*, **55**, 635-642.
- Li L, Kato C, Horikoshi K (1999b) Microbial diversity in sediments collected from the deepest cold-seep area, the Japan Trench. *Mar. Biotechnol.*, **1**, 391-400.
- Li YH, Gregory S (1974) Diffusion of ions in sea-water and in deep-sea sediments. *Geochim. Cosmochim. Acta*, **38**, 703-714.
- Lichtschlag A, Felden J, Brüchert V, Boetius A, De Beer D (2010) Geochemical processes and chemosynthetic primary production in different thiotrophic mats of the Håkon Mosby Mud Volcano (Barents Sea). *Limnol. Oceanogr.*, **55**, 931-949.
- Lösekann T, Knittel K, Nadalig T, Fuchs B, Niemann H, Boetius A, Amann R (2007) Diversity and abundance of aerobic and anaerobic methane oxidizers at the Håkon Mosby mud volcano, Barents Sea. *Appl. Environ. Microbiol.*, **73**, 3348-3362.
- Ludwig W, Strunk O, Westram R, Richter L, Meier H, Yadhukumar, Buchner A, Lai T, Steppi S, Jobb G, Forster W, Brettske I, Gerber S, Ginhart AW, Gross O, Grumann S, Hermann S, Jost R, König A, Liss T, Lussmann R, May M, Nonhoff B, Reichel B, Strehlow R, Stamatakis A, Stuckmann N, Vilbig A, Lenke M, Ludwig T, Bode A, Schleifer KH (2004) ARB: a software environment for sequence data. *Nucleic Acids Res.*, **32**, 1363-1371.
- Massana R, Murray AE, Preston CM, Delong EF (1997) Vertical distribution and phylogenetic characterization of marine planktonic Archaea in the Santa Barbara Channel. *Appl. Environ. Microbiol.*, **63**, 50-56.

- Milucka J, Ferdelman TG, Polerecky L, Franzke D, Wegener G, Schmid M, Lieberwirth I, Wagner M, Widdel F, Kuypers MMM (2012) Zero-valent sulphur is a key intermediate in marine methane oxidation. *Nature*, **491**, 541-+.
- Muyzer G, Teske A, Wirsén CO, Jannasch HW (1995) Phylogenetic-Relationships of Thiomicrospira Species and Their Identification in Deep-Sea Hydrothermal Vent Samples by Denaturing Gradient Gel-Electrophoresis of 16s Rdna Fragments. *Arch. Microbiol.*, **164**, 165-172.
- Niemann H, Duarte J, Hensen C, Omeregíe E, Magalhaes VH, Elvert M, Pinheiro LM, Kopf A, Boetius A (2006a) Microbial methane turnover at mud volcanoes of the Gulf of Cadiz. *Geochim. Cosmochim. Acta*, **70**, 5336-5355.
- Niemann H, Elvert, M. (2008) Diagnostic lipid biomarker and stable carbon isotope signatures of microbial communities mediating the anaerobic oxidation of methane with sulphate. *Org. Geochem.*, **39**, 1668-1677.
- Niemann H, Lösekann T, De Beer D, Elvert M, Nadalig T, Knittel K, Amann R, Sauter EJ, Schlüter M, Klages M, Foucher JP, Boetius A (2006b) Novel microbial communities of the Håkon Mosby mud volcano and their role as a methane sink. *Nature*, **443**, 854-858.
- Ogawa Y, Fujioka K, Fujikura K, Iwabuchi Y (1996) En echelon patterns of Calyptogena colonies in the Japan trench. *Geology*, **24**, 807-810.
- Olu K, Caprais JC, Galéron J, Causse R, Von Cosel R, Budzinsky H, Le Ménach K, Le Roux C, Levache D, Khripounoff A, Sibuet M (2009) Influence of seep emission on the non-symbiont-bearing fauna and vagrant species at an active giant pockmark in the Gulf of Guinea (Congo–Angolamargin). *Deep-Sea Res. II*, **56**, 2380-2393.
- Olu K, Duperret A, Sibuet M, Foucher JP, Fialamedioni A (1996) Structure and distribution of cold seep communities along the Peruvian active margin: relationship to geological and fluid patterns. *Mar. Ecol. Prog. Ser.*, **132**, 109-125.
- Omeregíe EO, Mastalerz V, De Lange G, Straub KL, Kappler A, Roy H, Stadnitskaia A, Foucher JP, Boetius A (2008) Biogeochemistry and community composition of iron- and sulfur-precipitating microbial mats at the Chefrén mud volcano (Nile Deep Sea fan, Eastern Mediterranean). *Appl. Environ. Microbiol.*, **74**, 3198-3215.
- Orphan VJ, Hinrichs KU, Ussler W, Paull CK, Taylor LT, Sylva SP, Hayes JM, Delong EF (2001) Comparative analysis of methane-oxidizing archaea and sulfate-reducing bacteria in anoxic marine sediments. *Appl. Environ. Microbiol.*, **67**, 1922-1934.
- Orphan VJ, House CH, Hinrichs KU, Mckeegan KD, Delong EF (2002) Multiple archaeal groups mediate methane oxidation in anoxic cold seep sediments. *Proc. Natl. Acad. Sci. U S A*, **99**, 7663-7668.
- Paull CK, Schlüning B, Ussler W, Paduan JB, Caress D, Greene HG (2005) Distribution of chemosynthetic biological communities in Monterey Bay, California. *Geology*, **33**, 85-88.
- Pernthaler A, Dekas AE, Brown CT, Goffredi SK, Embaye T, Orphan VJ (2008) Diverse syntrophic partnerships from deep-sea methane vents revealed by direct cell capture and metagenomics. *Proc. Natl. Acad. Sci. U S A*, **105**, 7052-7057.
- Pop Ristova P, Wenzhöfer F, Ramette A, Zabel M, Fischer D, Kasten S, Boetius A (2012) Bacterial diversity and biogeochemistry of different chemosynthetic habitats of the REGAB cold seep (West African margin, 3160 m water depth). *Biogeosciences*, **9**, 5031-5048.
- Prüsse E, Quast C, Knittel K, Fuchs BM, Ludwig WG, Peplies J, Glöckner FO (2007) SILVA: a comprehensive online resource for quality checked and aligned ribosomal RNA sequence data compatible with ARB. *Nucleic Acids Res.*, **35**, 7188-7196.

- Quast C, Pruesse E, Yilmaz P, Gerken J, Schweer T, Yarza P, Peplies J, Glockner FO (2013) The SILVA ribosomal RNA gene database project: improved data processing and web-based tools. *Nucleic Acids Res.*, **41**, D590-D596.
- Rasmussen H, Jørgensen BB (1992) Microelectrode Studies of Seasonal Oxygen-Uptake in a Coastal Sediment - Role of Molecular-Diffusion. *Mar. Ecol. Prog. Ser.*, **81**, 289-303.
- Reeburgh WS (1967) An improved interstitial water sampler. *Limnol. Oceanogr.*, **12**, 163-&.
- Revsbech NP, Jørgensen BB, Blackburn TH, Cohen Y (1983) Microelectrode studies of the photosynthesis and O<sub>2</sub>, H<sub>2</sub>S, and pH profiles of a microbial mat. *Limnol. Oceanogr.*, **28**, 1062-1074.
- Rossel PE, Elvert M, Ramette A, Boetius A, Hinrichs KU (2011) Factors controlling the distribution of anaerobic methanotrophic communities in marine environments: Evidence from intact polar membrane lipids. *Geochim. Cosmochim. Acta*, **75**, 164-184.
- Ruff SE, Arnds J, Knittel K, Amann R, Wegener G, Ramette A, Boetius A (2013) Microbial Communities of Deep-Sea Methane Seeps at Hikurangi Continental Margin (New Zealand). *PLoS One*, **8(9)**.
- Sahling H, Rickert D, Lee RW, Linke P, Suess E (2002) Macrofaunal community structure and sulfide flux at gas hydrate deposits from the Cascadia convergent margin, NE Pacific. *Mar. Ecol. Prog. Ser.*, **231**, 121-138.
- Schloss PD, Westcott SL, Ryabin T, Hall JR, Hartmann M, Hollister EB, Lesniewski RA, Oakley BB, Parks DH, Robinson CJ, Sahl JW, Stres B, Thallinger GG, Van Horn DJ, Weber CF (2009) Introducing mothur: Open-Source, Platform-Independent, Community-Supported Software for Describing and Comparing Microbial Communities. *Appl. Environ. Microbiol.*, **75**, 7537-7541.
- Schreiber L, Holler T, Knittel K, Meyerdierks A, Amann R (2010) Identification of the dominant sulfate-reducing bacterial partner of anaerobic methanotrophs of the ANME-2 clade. *Environ. Microbiol.*, **12**, 2327-2340.
- Sibuet M, Juniper SK, Pautot G (1988) Cold-seep benthic communities in the Japan subduction zones - geological control of community-development. *J Mar Res*, **46**, 333-348.
- Sibuet M, Olu-Le Roy K (2002) Cold seep communities on continental margins: structure and quantitative distribution relative to geological and fluid venting patterns. In: *Ocean Margin System* (eds Wefer G, Billett D, Hebbeln D, Jørgensen BB, Schlüter M, Van Weering TCE). Springer-Verlag, pp. 235-251.
- Sibuet M, Olu K (1998) Biogeography, biodiversity and fluid dependence of deep-sea cold-seep communities at active and passive margins. *Deep-Sea Res. II*, **45**, 517-567.
- Sommer S, Pfannkuche O, Linke P, Luff R, Greinert J, Drews M, Gubsch S, Pieper M, Poser M, Viergutz T (2006) Efficiency of the benthic filter: biological control of the emission of dissolved methane from sediments containing shallow gas hydrates at Hydrate Ridge. *Glob. Biogeochem. Cycles*, **20**.
- Sturt HF, Summons RE, Smith K, Elvert M, Hinrichs K-U (2004) Intact polar membrane lipids in prokaryotes and sediments deciphered by high-performance liquid chromatography/electrospray ionization multistage mass spectrometry—new biomarkers for biogeochemistry and microbial ecology. *Rapid Commun. Mass Sp.*, **18**, 617-628.
- Tavormina PL, Ussler W, Orphan VJ (2008) Planktonic and sediment-associated aerobic methanotrophs in two seep systems along the North American margin. *Appl. Environ. Microbiol.*, **74**, 3985-3995.

- Torres ME, Mcmanus J, Hammond DE, De Angelis MA, Heeschen KU, Colbert SL, Tryon MD, Brown KM, Suess E (2002) Fluid and chemical fluxes in and out of sediments hosting methane hydrate deposits on Hydrate Ridge, OR, I: Hydrological provinces. *Earth Planet. Sci. Lett.*, **201**, 525-540.
- Treude T, Boetius A, Knittel K, Wallmann K, Jørgensen BB (2003) Anaerobic oxidation of methane above gas hydrates at Hydrate Ridge, NE Pacific Ocean. *Mar. Ecol. Prog. Ser.*, **264**, 1-14.
- Treude T, Smith CR, Wenzhöfer F, Carney E, Bernardino AF, Hannides AK, Krüger M, Boetius A (2009) Biogeochemistry of a deep-sea whale fall: sulfate reduction, sulfide efflux and methanogenesis. *Mar. Ecol. Prog. Ser.*, **382**, 1-21.
- Vossmeyer A, Deusner C, Kato C, Inagaki F, Ferdelman T (2012) Substrate-specific pressure dependence of microbial sulfate reduction in deep-sea cold seep sediments of the Japan Trench. *Front. Microbiol.*, **3**.
- Wallmann K, Linke P, Suess E, Bohrmann G, Sahling H, Schlüter M, Dahlmann A, Lammers S, Greinert J, Von Mirbach N (1997) Quantifying fluid flow, solute mixing, and biogeochemical turnover at cold vents of the eastern Aleutian subduction zone. *Geochim. Cosmochim. Acta*, **61**, 5209-5219.
- Wegener G, Niemann H, Elvert M, Hinrichs K-U, Boetius A (2008) Assimilation of methane and inorganic carbon by microbial communities mediating the anaerobic oxidation of methane. *Environ. Microbiol.*
- Wenzhöfer F, Glud RN (2002) Benthic carbon mineralization in the Atlantic: a synthesis based on *in situ* data from the last decade. *Deep-Sea Res. I*, **49**, 1255-1279.
- Wenzhöfer F, Holby O, Glud RN, Nielsen HK, Gundersen JK (2000) In situ microsensor studies of a shallow water hydrothermal vent at Milos, Greece. *Mar. Chem.*, **69**, 43-54.
- Whiticar MJ (1999) Carbon and hydrogen isotope systematics of bacterial formation and oxidation of methane. *Chem. Geol.*, **161**, 291-314.
- Zhou JZ, Bruns MA, Tiedje JM (1996) DNA recovery from soils of diverse composition. *Appl. Environ. Microbiol.*, **62**, 316-322.

## Chapter 6

## **General discussion**

Marine methane seeps are locally restricted, yet highly productive oases of life in the sea bed. Substantial scientific effort was directed at these ecosystems in the past decades concerning the microbial and faunal communities, the biogeochemistry and their interaction (Sibuet and Olu, 1998; Levin, 2005; Reeburgh, 2007; Knittel and Boetius, 2009; Boetius and Wenzhöfer, 2013). Generally, the research was targeted at the detailed description of single ecosystems, such as seeps at Hydrate Ridge in the Northeast Pacific (Boetius et al., 2000; Boetius and Suess, 2004; Knittel et al., 2005), in the Japan Trench (Li et al., 1999; Inagaki et al., 2002), in the Gulf of Mexico (Joye et al., 2004; Joye et al., 2010; Lloyd et al., 2010), in the North Sea (Niemann et al., 2005; Wegener et al., 2008) and at Håkon Mosby mud volcano (Niemann et al., 2006; Lösekann et al., 2007; Felden et al., 2010), to name just a few. These studies yielded valuable knowledge about the microbial communities and processes at single ecosystems, however, a census of the microbial diversity at cold seeps on broad spatial scales was lacking. In addition, little is known about the ecological mechanisms that create and maintain microbial diversity at these ecosystems.

### **Microbial communities at methane seep ecosystems**

Based on numerous studies we hypothesized that despite large differences between single communities there might be a global metacommunity of key functional groups due to the outstanding and extreme habitats at seep ecosystems. To address this hypothesis I investigated seep sites on a local (Chapter 3, 4 and 5), regional (Chapter 3) and global scale (Chapter 2).

### ***Local microbial diversity at seep ecosystems***

In the course of this thesis I investigated 50 cold seep sediment samples from 23 seep sites of 15 areas using culture-independent techniques such as, community fingerprinting, pyrosequencing, gene libraries and fluorescence *in situ* hybridization. The communities greatly differed concerning the most frequent organisms, key functional clades and community structure and showed enormous differences in evenness, estimated richness and beta diversity (Chapter 2-5). The differences in microbial diversity were observed for both the dominant, key functional groups and also the background community. The spectrum ranged from simple communities that were dominated by a few organisms (e.g.

Håkon Mosby mud volcano – north of Norway in the Barents Sea) to some of the most complex marine microbial communities known to date (e.g. Quepos Slide – west of Costa Rica in the East Pacific Ocean). Accordingly, species diversity was poorly constrained at 97% 16S rRNA gene identity (Chapter 2, Figure S3) and novel microbial taxa can be expected for each additionally analyzed seep ecosystem.

#### *Microorganisms involved in the methane cycle*

The aerobic oxidation of methane (AeOM) is a long known process that is carried out by bacteria of several lineages, such as *Alphaproteobacteria*, *Betaproteobacteria*, *Gammaproteobacteria* and *Verrucomicrobia* (Hanson and Hanson, 1996; Op den Camp et al., 2009). However, at seep ecosystems we exclusively found type-I methanotrophs of the gammaproteobacterial order *Methylococcales* (Chapter 2-4) which confirms the findings of previous studies (Inagaki et al., 2004b; Yan et al., 2006; Lösekann et al., 2007; Tavormina et al., 2008; Wasmund et al., 2009). Aerobic cold seep methanotrophs clustered among at least three distinct groups that we termed Marine Methylophilic Group 1-3, of which two contain methanotrophic endosymbionts of marine invertebrates (Chapter 3, Figure 4) (Duperron et al., 2005; Lösekann et al., 2007). *Methylococcales* occurred at all seep sites that had access to oxygen, but seemed to vary greatly concerning their abundance. They dominated the oxic and suboxic sediments at ampharetid seeps of Hikurangi margin and at the center of HMMV, and seemed to be present in low abundances at siboglinid habitats (Chapter 3,4) (Lösekann et al., 2007), but were extremely rare at the clam patch of the Japan Trench (Chapter 5). The occurrence of aerobic methanotrophs in suboxic and even anoxic/sulfidic layers at cold seeps was reported before, but never commented (Lösekann et al., 2007; Pachiadaki et al., 2010; Roalkvam et al., 2011). However, their abundance and the bright CARD-FISH signals (Chapter 3, Figure 5) strongly indicated that they were active and hence adapted to high-sulfide low-oxygen conditions. This is supported by other studies where related type-I methanotrophs were active in suboxic waters of the Black Sea (Blumenberg et al., 2007), present in oxygen minimum zones of the Pacific Ocean (Hayashi et al., 2007) and in anoxic peat soils (Roslev and King, 1994) and survived prolonged anoxic conditions (Roslev and King, 1995).

The diversity of ANME archaea was very large with ANME-1 being the broadest clade and responsible for almost half of the ANME OTU<sub>0.03</sub> that we detected. ANME-2a/b comprised around one third, ANME-2c and ANME-3 together accounted for less than a quarter of all ANME OTU<sub>0.03</sub>. Similar to the total microbial diversity at seeps the ANME

diversity ranged from sites that hosted very few OTU<sub>0.03</sub>, e.g. hydrothermal sediments at Guaymas Basin, to sites, such as seeps on Hydrate Ridge that contained more than 25% of all globally observed ANME OTU<sub>0.03</sub>. However, despite the great diversity most sites seemed to be dominated by one clade (Chapter 2-5) (Michaelis et al., 2002; Knittel et al., 2005; Lloyd et al., 2006; Niemann et al., 2006; Wegener et al., 2008; Biddle et al., 2012), sometimes even by one OTU<sub>0.03</sub> (Chapter 4, 5). The most common ANME archaea belonged to the clade ANME-2a, which occurred at almost all sites, whereas the least common seemed to be *Candidatus Methanoperedenaceae* (Haroon et al., 2013). ANME-2a seemed to have an ecological advantage at sites where both sulfate and methane concentrations are high, e.g. above shallow hydrates (Knittel et al., 2005; Lösekann et al., 2007) and in enrichment cultures (Wegener pers. comm.), probably due to faster growth rates. ANME-2c occurred preferentially at clam impacted seeps, whereas ANME-1 seemed to be adapted to hot and deep environments. Methanogenic archaea also occurred at most cold seep samples, however due to their low relative sequence abundance of usually less than one percent it is likely that they were introduced from the subsurface where they are thought to be active members of the microbial community (Fry et al., 2008).

#### *Microorganisms involved in the sulfur cycle*

Cold seeps harbor both sulfide-reducing bacteria (SRB) and sulfur-oxidizing bacteria (SOB). Although the diversity of SRB in all marine sediments (e.g. Ravenschlag et al., 2001), including cold seeps, is usually very high as sulfate is the most ubiquitous electron acceptor, cold seeps were either dominated by *Desulfosarcina/Desulfococcus*-related or *Desulfobulbus*-related organisms (Chapter 2-5). SOB were found at all seep sediments that are oxic or suboxic and occurred at an astounding diversity. Most of the seep SOB were gammaproteobacterial *Thiotrichales*. However, seep SOB were also found in the epsilonproteobacterial *Campylobacteriales*, such as *Arcobacter* spp. (Omeregie et al., 2008) and *Sulfurovum* spp. (Inagaki et al., 2004a). It was proposed that temporal and spatial variations in the energy supply are responsible for the predominance of different SOB (Grünke et al., 2011). *Campylobacteriales*, for instance, occurred at many seeps, yet they only seemed to dominate habitats such as the Japan clam colony where *Beggiatoa* mats were absent. Whether this is caused by different niche-preferences of the clades or due to competitive advances of the *Beggiatoa* spp. remains to be elucidated.

The overall diversity of seep ecosystems is illustrated by the comparison of one sample from each of the well-characterized seeps of Chapter 3-5 (Table 1). These three sites harbored distinct aerobic and anaerobic methane oxidizers, sulfur oxidizers and sulfate reducers and differed concerning richness, evenness and total cell abundance.

Table 1: Microbial diversity at three cold seep ecosystems

|   |      | HMMV                    | NZ309                     | JAP957                   |
|---|------|-------------------------|---------------------------|--------------------------|
| Dominant ANME type  |      | ANME-3                  | ANME-2a                   | ANME-2c                  |
| Dominant SRB  |      | <i>Desulfobulbaceae</i> | <i>Desulfobacteraceae</i> | <i>Desulfobulbaceae</i>  |
| Aerobic sulfur oxidizers                                      |      | <i>Thiotrichales</i>    | <i>Thiotrichales</i>      | <i>Campylobacterales</i> |
| Aerobic methane oxidizers                                     |      | <i>Methylococcales</i>  | <i>Methylococcales</i>    | <i>Methylococcales</i> * |
| Estimated richness (Chao1)                                    | Arch | 136                     | 615                       | 577                      |
|   | Bac  | 1777                    | 3446                      | 2549                     |
| Evenness (Inverse Simpson)                                    | Arch | 1.2                     | 7.8                       | 6.1                      |
|   | Bac  | 35.3                    | 51.1                      | 120.8                    |
| Total cell number ( $\times 10^{10}$ cells ml <sup>-1</sup> ) |      | 1.9                     | 0.2                       | n.a.                     |
| Seep-associated organisms                                     |      | <i>Beggiatoa</i> mats   | Ampharetid tubeworms      | Vesicomylid clams        |

\* were extremely rare, as only few sequences were detected by deep sequencing, n.a not analyzed

#### *Other organisms potentially involved in AOM*

The anaerobic oxidation of methane coupled to sulfate reduction was a long standing geochemical enigma until it was shown that specific microorganisms mediate this process (Hinrichs et al., 1999; Boetius et al., 2000). In recent years, however, evidence accumulated that methane is oxidized anaerobically using manganese, iron or nitrate as electron acceptors (Beal et al., 2009; Wankel et al., 2012; Haroon et al., 2013) or via entirely new metabolic pathways (Ettwig et al., 2010). Our global survey of microbial diversity at cold seeps indicated additional clades that might potentially be involved in AOM, since their relative abundance at AOM habitats was significantly higher than at other non-seep ecosystems. These were *Spirochaetes*, which comprise enigmatic endosymbionts of marine oligochaetes (Blazejak et al., 2005) and sulfide-oxidizers that live in consortia with sulfate-reducing bacteria (Dubinina et al., 2011), *Deferribacteres*, which is a clade that was shown to include iron, sulfur and nitrate reducing organisms (Janssen et al., 2002; Gittel et al., 2012) and Hyd24-12, a candidate division with unknown function that was retrieved from a Hydrate Ridge cold seep (Knittel et al., 2003). Remarkably, candidate phylum JS1 was found at all investigated seep ecosystems. It was a significant indicator clade and correlated negatively with *Deltaproteobacteria*, indicating that JS1

might compete with sulfate reducers under certain conditions, such as high temperatures at Guaymas Basin ecosystems. At many cold seeps JS1 seemed to be much more abundant than in the deep biosphere, where they are frequently observed (Blazejak and Schippers, 2010) suggesting that they are an active part of the seep community being important for the ecosystem function and possibly linked to AOM. This hypothesis is supported by findings of earlier studies, as it was proposed that JS1 might be involved in AOM at cold seeps in the Marmara Sea (Chevalier et al., 2013) and in methane cycling at cold seeps of the South China Sea (Zhang et al., 2012). JS1 was very abundant in methane-hydrate bearing sediments (Inagaki et al., 2006), under anoxic sulfate-reducing conditions in slurries of marine sediments (Webster et al., 2006) and enrichment cultures of cold seep sediments (G. Wegener – pers. comm.). Hence, the role of JS1 at cold seep ecosystems is an interesting research topic for future studies.

### ***Regional differences between seep communities***

The microbial diversity does not seem to differ within sites only, but also to a certain extent within regions, since the communities of seeps within a region tended to be more similar than those of different regions. At Hikurangi margin we showed that although the seeps differ from each other they share commonalities that distinguish them from other seepage areas. Most obvious was the frequent occurrence of ampharetid polychaetes at the sediment surface and aerobic methanotrophs in the sediment below. Moreover we found ANME-3 at all investigated seeps, whereas ANME-1 was not detected by either 16S rRNA gene libraries, CARD-FISH or deep sequencing (Chapter 2,3). Additionally, the biogeochemistry was outstanding as it featured some of the highest fluid fluxes and total oxygen uptake rates that were measured at seeps (Sommer et al., 2010). Baco and colleagues (2010) suggested that Hikurangi margin might be a new cold seep province due to its distinct fauna. However, we can not tell if this is also the case for the microbial communities as we have just begun to investigate these ecosystems and lack comprehensive data.

Cold seeps in the Japan Trench are among the deepest that have been investigated so far. The microbial community at the clam colony seemed to be different compared to other seep types, but similar to vesicomid dominated seeps. ANME-2c was the most frequently detected ANME clade, which might be correlated to the vesicomid clams (Chapter 5) and *Desulfobulbaceae* seemed to be the dominant sulfate reducer. ANME-2a and relatives of *Desulfosarcina/Desulfococcus*, which are common at most seep

sites appeared to be very rare. Interestingly, a large number of detected sequences belonged to *Epsilonproteobacteria* of the genus *Sulfurovum*, which is a sulfur oxidizer that was isolated from the Okinawa Trough (Inagaki et al., 2004a). This organism seems to be abundant at seep ecosystems of the area (Arakawa et al., 2006; Nunoura et al., 2012), but less important at seeps elsewhere, with some exceptions, e.g. at Nyegga (Roalkvam et al., 2011). Aerobic methane oxidizers were extremely rare (Chapter 2) or not detected at Japan Trench abyssal seeps (Arakawa et al., 2006). Additionally, the background community seemed to be dominated by methanogenic and ammonia-oxidizing archaea and by psychrophilic bacteria such as *Psychrobacter* spp., the latter being common in deep waters of the Japan Trench (Maruyama et al., 2000) and sediments of the Japan Sea (Romanenko et al., 2004). It was suggested that these organisms originate from Antarctic water masses (Maruyama et al., 2000) that reach Japan via bottom water circulation (Kawabe and Fujio, 2010). However, it is unclear which factors caused the trends we observed, since the study was focused on one ecosystem.

Based on the global dataset it seemed as if samples from the same region, such as Guaymas Basin, Hydrate Ridge, Hikurangi Margin or the North Atlantic Ocean had similar community structures as they clustered in the same area of the NMDS ordination (Chapter 2, Figure 2). Moreover, samples from the same region seemed to have a similar microbial diversity. Samples from the Guaymas Basin or the Gulf of Mexico had high archaeal diversity, whereas samples from the North Atlantic had low archaeal diversity (Chapter 2, Figure 1). Microbial habitat connectivity within seeps of a region was shown for the Guaymas Basin (Meyer et al., 2013), however our observations need to be confirmed based on studies with suitable sampling strategies, since the necessary resolution to unambiguously investigate the observed patterns was lacking.

### ***Globally distributed populations of functional clades***

The findings in Chapter 2 indicated that the overall diversity of OTU<sub>0.03</sub> at cold seep is immense and the species accumulation curve impressively showed that with every new seep that we sampled, the number of species increased almost linearly. Instead, the microbial diversity on order level was more constrained and indicated that we have retrieved nearly all taxa at that level of phylogenetic resolution revealing a set of core clades that likely performed core functions. Due to the high average species turnover between cold seeps, however, we did not find any OTU<sub>0.03</sub> that was cosmopolitan, neither from ANME nor from other clades.

*Metapopulations and functional redundancy at cold seeps*

AOM was carried out by a multitude of ANME and SRB from different lineages, showing that consistent core function did not rely on a consistent core phylogeny, at least not at high phylogenetic resolution. This functional redundancy of microbial communities was already shown for other ecosystems, such as the human gut microbiome, where communities of different composition carried out similar functions (Turnbaugh et al., 2009). Furthermore, it seemed as if ANME clades did not necessarily out-compete each other, since some seeps were inhabited by many ANME OTU<sub>0.03</sub> and all ecosystems harbored at least two different ANME clades (Chapter 2). ANME-2a/2b occurred most often and comprised the single most read-abundant OTU<sub>0.03</sub>. The sequencing results also indicated that ANME-3 was more important on a global scale than previously assumed, whereas ANME-2c seemed to play a minor role. The ten most abundant ANME OTU<sub>0.03</sub> were responsible for 85% of all ANME reads and each of them was found at 15 seeps on average. Remarkably, similar trends were observed for aerobic methanotrophs, thiotrophs and sulfate reducers, suggesting that these globally important processes might be carried out by very few species-level taxa within these clades. Moreover, at least half of those ten most important phylotypes were SSO<sub>rel</sub> indicating that those populations are highly dynamic concerning their abundance.

### **Environmental heterogeneity at methane seep ecosystems**

The extent of environmental heterogeneity of an ecosystem determines the number of possible habitats and thus species niches that can be occupied. Hence the second hypothesis of this thesis was that environmental parameters such as geochemistry and faunal activity influenced the microbial communities at the investigated cold seeps.

### ***Environmental heterogeneity due to the activity of faunal communities***

At cold seep ecosystems the biogeochemistry and the benthic microbial and faunal communities are neatly connected and influence each other (e.g. Levin, 2005; Dattagupta et al., 2008; Bowden et al., 2013). This was also the case at the recently discovered ampharetid habitat, where aerobic methanotrophy was a major ecosystem function (Sommer et al., 2010; Thurber et al., 2013), because bioirrigation by the tubeworms seemed to create a niche for aerobic methylotrophs (Chapter 3). Our results confirmed a close trophic link between the tubeworms and the methylotrophs (Thurber et al., 2010) indicating that the animals might even actively “garden” the sediment and harvest the methylotrophs.

In the Japan Trench we investigated an abyssal seep ecosystem dominated by vesicomyid clams and similar to the ampharetid habitat it seemed as if the animals were creating a niche for specific clades of microorganisms (Chapter 5). Despite the great water depth and the spatial distance to other clam habitats we found ANME-2c and *Desulfobulbus*-related SRB clades that were previously found to be associated to clam seeps (Knittel et al., 2005; Kleindienst et al., 2012). This strongly suggested niche-based processes and a major influence of the animals on the underlying community possibly due to bioturbation of the sediment (Wallmann et al., 1997).

### ***Environmental heterogeneity due to geochemical and physical gradients***

The interaction of communities and environmental conditions within an ecosystem creates a multitude of ecological niches that establish along biogeochemical, spatial and temporal gradients (Finlay et al., 1997). These interactions also occurred at Håkon Mosby mud volcano, since shifts in microbial community structure in freshly exposed muds were linked to decreasing fluid flow, increasing exposure time and the presence of other microorganisms (Chapter 4). The succession was accompanied by an increase of microbial biomass and diversity (Chapter 4, Figure 3) and an increase in ecosystem functions (Figure 8). The link between communities and biogeochemistry was shown

nicely for the case of sulfide oxidation. Sulfide, which is normally not abundant in surface sediments of the seabed, was produced during AOM at HMMV and thus caused the emergence of thiotrophs. This niche is lacking at cold seeps, where oxygen is not available. Here, the sulfide may be oxidized abiotically using metals, which was shown at mud volcanoes in the Black Sea (Lichtsclag et al., 2012). Thus, microbial populations can create niches for other organisms depending on the environment, which may explain the variety of microbial communities that are sustained by methane as the main energy source. The finding that the lowest diversity was found at anoxic and or subsurface ecosystems (Chapter 2, Figure 1), while diversity peaked at subtropical and fairly shallow ecosystems, indicated that the availability of diverse electron donors and acceptors promoted ecological niches at seep ecosystems. Since species diversity and habitat diversity positively correlated in avian and plant ecology (Recher, 1969; Kohn and Walsh, 1994) it may be a general mechanism in ecology.

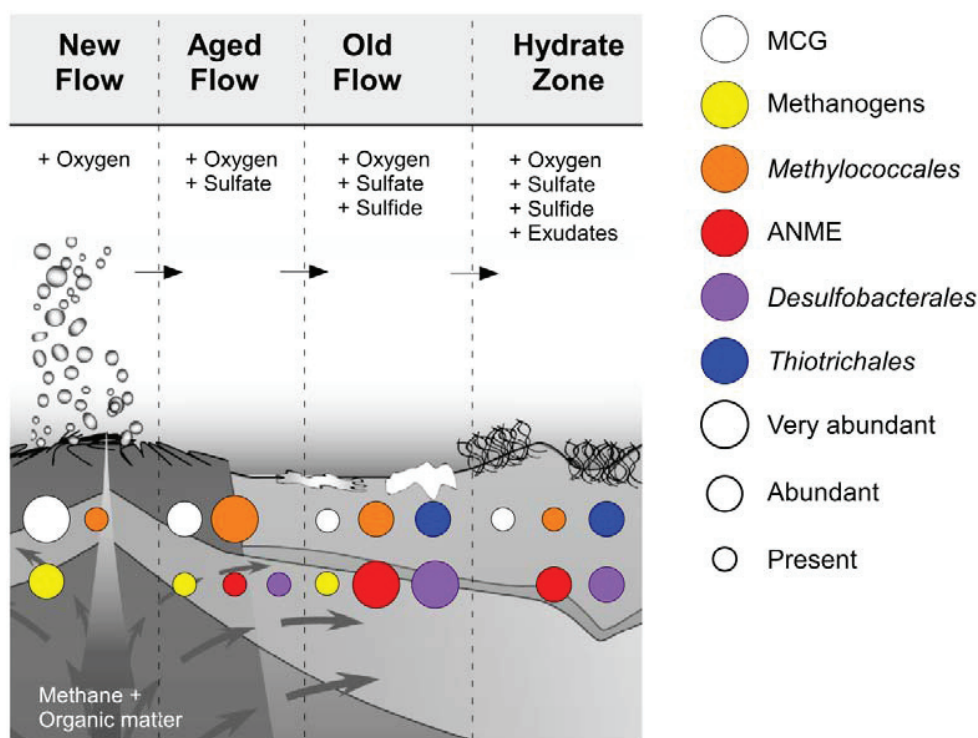


**Figure 8: Succession of functional clades at Håkon Mosby mud volcano**

This scheme depicts the succession of functional clades in the surface muds of HMMV. The circle color denotes clades and the circle size their relative sequence abundance based on pyrosequencing. Each of the inner zones was dominated by certain groups, whereas the community at the hydrate zone was more even and contained many other microbial clades. MCG - Miscellaneous Crenarchaeotic Group, ANME – Anaerobic methane oxidizing archaea

### **Microbial community assembly at methane seep ecosystems**

Microbial ecologists have just begun to approach the mechanisms that govern the assembly and maintenance of microbial communities using classical ecological theory and even ecosystems that are very well studied and easy to access, such as the human gut, are not yet fully understood (Costello et al., 2012). Hence, it is not surprising that little is known about the ecology of ecosystems in the deep sea. The last part of this thesis discusses possible ecological processes that might influence the microbial diversity at cold seep ecosystems.

### ***Cold seeps as discrete and permanent habitat patches in the deep sea***

The analysis of the microbial diversity of various benthic ecosystems during this thesis and also previous studies showed that cold seeps host very specific microbial habitats and communities (Chapter 2). Thus, following a description used in classical ecology, cold seeps may be perceived as assemblages of discrete, permanent habitat patches (Leibold et al., 2004), in other words, microbial islands in the deep-sea bed surrounded by very different microbial and faunal communities (Chapter 2) (Baker et al., 2010). This notion is supported by steep biogeochemical gradients between seep and non-seep sediments (Chapter 2-4) (Lloyd et al., 2010) and a high degree of endemism, as OTU<sub>0.03</sub> turnover between cold seeps and other seafloor realms and even between cold seeps themselves was extremely low. Only bacterial communities of hydrothermal vents had on average less species in common. Hydrothermal vents show great differences in temperature, chemistry and geology (Tivey, 2007), which likely causes the establishment of distinct microbial communities (Sievert and Vetriani, 2012) and thus endemism. Methane seeps do not seem to be as different, since the major energy source is always methane and still the high community turnover indicates a multitude of different ecological niches at each seep.

### ***Species sorting at cold seeps***

Organisms tend to enrich under environmental conditions that favor their proliferation. This selection of species is known as environmental filtering or species sorting (Leibold et al., 2004 and references therein). Species sorting is a key mechanism for the establishment of microbial communities at methane seeps, since their highly adapted and dominant functional clades are absent or rare in common deep-sea sediments. It was shown that geochemical settings shaped the seep communities (e.g. Grünke et al., 2011; Pop Ristova et al., 2012; Felden et al., 2013) and that high temperature (Meyer et al., 2013) and

pressure (Vossmeyer et al., 2012) might impact sulfate reduction. Although we could not resolve the niches of key functional groups in detail we confirmed that ANME-1 occurred predominantly in hot (Holler et al., 2011; Biddle et al., 2012) and deep sediments (Knittel et al., 2005; Vigneron et al., 2013). Other ANME clades occurred preferentially in sulfate-rich surface sediments that were anoxic and covered with SOB mats (ANME-2a) or oxic/suboxic and impacted by clam activity (ANME-2c) (Knittel et al., 2005; Vigneron et al., 2013) or influenced by cold water masses as observed for ANME-3. ANME-2a seemed to have the broadest niche as it dominates many different ecosystems, maybe due to faster growth rates. These patterns could be related to oxygen sensitivity or preferences of the ANME archaea, however, according to our findings they might also be related to the preferences of their partner SRB. Despite first insights into the diversity and distribution of the SRB (Schreiber et al., 2010; Kleindienst et al., 2012) there is still not enough information to exclude this possibility.

In addition to confirming previous findings we could for the first time observe environmental filtering of single ANME OTU<sub>0.03</sub> at cold seep sediments, since we monitored their development from being rare organisms to becoming abundant when the environmental conditions changed. This supported not only the importance of species sorting for the community assembly at seeps, but also the importance of rare organisms for ecosystem function (Campbell et al., 2011) and for the response of ecosystems under changing conditions (Sjöstedt et al., 2012; Hugoni et al., 2013). We have confirmed the importance of niche-based processes, but there are also stochastic processes, such as dispersal limitation, which cause endemism at microbial communities (Whitaker et al., 2003; Telford et al., 2006).

### ***Dispersal of main functional clades***

The presence of identical OTU<sub>0.03</sub> in distant cold seeps suggested that the dispersal of major functional clades was unlimited, which supports the long-standing theorem that microorganisms are everywhere because of their enormous population sizes and many ways of transmission (O'Malley, 2007). There seem to be four possible scenarios for the dispersal of functional clades between cold seeps as depicted in Figure 9. A: The communities are endemic, do not disperse and evolved at each cold seep or cold seep region. B: The cold seeps were once connected and the organisms could freely disperse between them. C: Organisms disperse through the watercolumn or D: organisms disperse through the sediment.

Scenario A would be reasonable if we find a very high degree of endemism at cold seeps and no OTU overlap between the functional groups at each seep. Indeed, with a mean value of shared OTUs of 4% for bacteria and 6% for archaea we found a very high degree of endemism. In contrast, we also found metapopulations of identical OTU<sub>0.03</sub> that connected seeps from different hemispheres, such as HMMV and Hikurangi margin. However, since it is impossible to tell organisms apart just based on their V6 region, we need to verify that these organisms indeed belong to the same species. Ideally, we should compare genomes of single cells or metagenomes from different seeps to actually pin down phylogenetic and genomic differences between the resident clades.

In scenario B the cold seeps would have been connected in the past, for instance because large parts of the oceans turned anoxic, so called anoxic oceanic events, which happened frequently throughout Earth history (Meyer and Kump, 2008). The overlap of ANME clades and similarity of ANME OTU<sub>0.03</sub> between seeps could be the result of an extremely low evolutionary pressure and long generation times of these organisms (Girguis et al., 2005; Nauhaus et al., 2007), whereas the differences might be due to speciation and extinction. Unfortunately we don't have a molecular clock (Bromham and Penny, 2003) for these organisms to relate phylogenetic distances to a time-scale.

Dispersal through the water column (scenario C) seems very likely for aerobic methylotrophs of the *Methylococcales*, since small amounts of methane are dissolved in water and we find close relatives of the sediment-dwelling methanotrophs in the watercolumn (Hayashi et al., 2007; Lesniewski et al., 2012) and as endosymbionts of marine invertebrates (Chapter 2,3) (Duperron et al., 2007). Moreover, the methanotrophs that inhabit cold seeps were different from the ones found in non-seep sediments of the deep sea (Wang et al., 2004; Hamdan et al., 2011). Aerobic sulfur oxidizers might also disperse through the water column, since they were found in upwelling zones (Lavik et al., 2009) and are quickly colonizing reduced habitats at the seafloor, such as whale and wood falls (Goffredi and Orphan, 2010; Bienhold et al., 2013).

Sulfate reducers and anaerobic methanotrophs however are likely transmitted differently, as they seem to be oxygen sensitive and were only found in waters that are anoxic, e.g. of the Black Sea (Schubert et al., 2006; Neretin et al., 2007) and occurred in subsurface sediments (Rossel et al., 2008). Dispersal through the sediment (D) could be achieved by these organisms either actively using a flagellum for which a complete set of genes was found in the ANME-3 genome (Ruff, Arnds, Boetius, Meyerdierks, Amann, Knittel, unpubl. results) or passively by transportation in aquifers, pore water or animals.

However, we did not detect ANME in the methane-rich subsurface of the center of HMMV, but in deep-sea surface sediments of a nearby site, which indicated that ANME were dispersed through the surface sediment or the benthic boundary layer rather than the deep subsurface. Transport in oxic waters might be achieved through temporal resistance to oxygen which was shown for the closely related *Methanosarcina* (Angel et al., 2012).

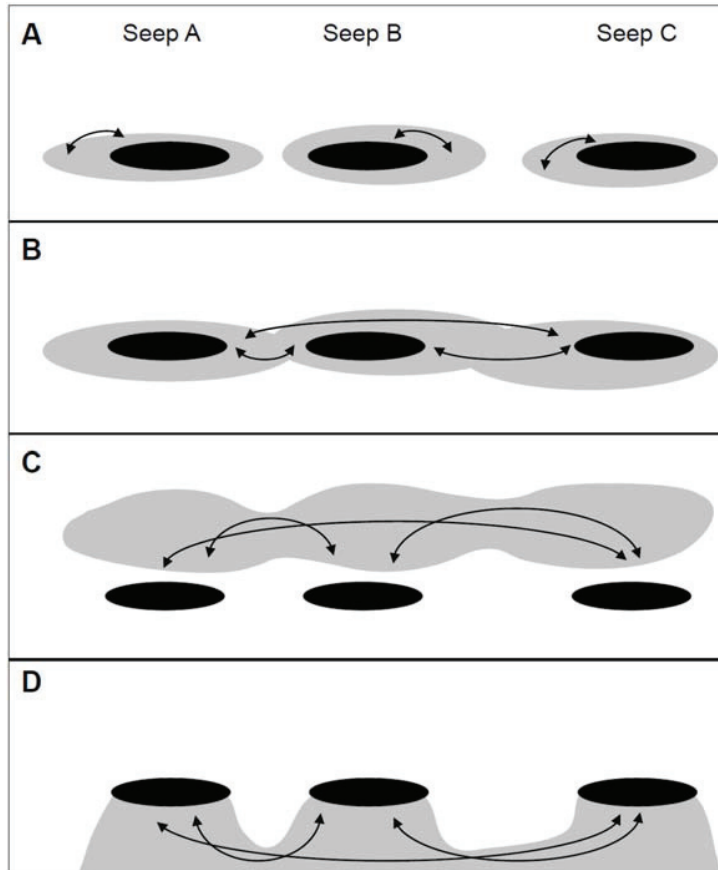


**Figure 9: Dispersal scenarios**

This scheme depicts four possible scenarios how micro-organisms may be transmitted between seep ecosystems. Seeps are shown as black patches and the grey areas represent the sources of micro-organisms that influence their local diversity. In **A** all seeps are isolated. In **B** the organisms freely disperse through space. They also could be transmitted exclusively through the water-column **C** or the sediment **D**.

### ***Thoughts on community assembly at cold seep ecosystems***

If we integrate the aforementioned findings, one possible mechanism that would explain many of the observations would be a community assembly according to the species sorting view of the metacommunity concept proposed by Leibold and colleagues (2004). Our data have shown that there are metapopulations of the main functional groups that seemed to occur worldwide. Nevertheless, they were not cosmopolitan as they were not present at all seeps and seemed to be selected by local abiotic and biotic conditions, similar to what was shown for community assembly of zooplankton in interconnected ponds (Cottenie et al., 2003). Thus local microbial diversity at seeps may be created by

the interplay of niche-based and neutral processes, such as species sorting and dispersal, which was already shown for soil microbial communities (Dumbrell et al., 2010). That means every island could be constantly invaded or contaminated by organisms, but most of them will not proliferate, which might explain the large amount of OTU<sub>0.03</sub> at most seeps despite the clear dominance of a few taxa. Similar mechanisms were proposed to describe the ecology of the human gut microbiome (Costello et al., 2012). Another reason for the wealth of functionally identical taxa could simply be their coexistence, which means that the same ecological niche is occupied by more than one organisms. This would violate Gause's axiom stating that two species can not inhabit the same niche (Leibold, 1995 and references therein), however coexistence was shown to be relevant for bacterial strains on agar plates and sulfate reducers in a bioreactor (Turner et al., 1996; Dar et al., 2007). Another way to increase diversity of an ecosystem is the packing of niches along resource or environmental gradients (MacArthur, 1970). Hence, the great diversity that we found and also the stratification of ANME populations along gradients that was observed at other cold seeps (Roalkvam et al., 2011) could be analogous to the establishment of plants along light gradients in forests (Whittaker, 1972). Furthermore, it seemed as if mass effects (Shmida and Wilson, 1985) played a role, since we detected microbial signatures at seeps that originated from the surrounding sediments (e.g. Chapter 3). Finally time impacted microbial community structure (Bell, 2010) which we showed in the mud volcano study (Chapter 4). We are aware that the suppositions put forward here are not based on sufficient data and are not thoroughly validated. Yet, they are a first humble step towards understanding the ecology of cold seeps based on empirical data and observations.

## Conclusion

We have just begun to investigate and understand fundamental mechanisms of microbial community assembly and maintenance. However the field of microbial ecology is gaining momentum especially concerning ecosystems that are difficult to access, for instance cold seeps in the deep sea, since technology is quickly developing. The investigations of remote cold seep ecosystems is rewarding in several ways: Firstly because they add to the growing body of knowledge concerning these globally important, yet enigmatic ecosystems, secondly because they harbor an immense diversity that likely contains new organisms and possibly new metabolic pathways and finally because these ecosystems are natural laboratories, which offer unique opportunities to study community development in situ. At HMMV we documented for the first time the development of microbial diversity and ecosystem functions of a cold seep ecosystem in detail. We indicated how tightly some microorganisms were linked to their ecological niche, showing the influence of deterministic processes and provided evidence for the role of dispersal between these ecosystems. This knowledge might be transferred to understand microbial community assembly at other marine and maybe even limnic ecosystems. Moreover, microbial communities of locally restricted ecosystems, such as cold seeps combined with high-throughput community analyses offer a unique opportunity to test hypothesis that cannot be resolved by classical ecology. Leibold and colleagues (2004) for instance report that it is difficult to apply theoretical definitions of metacommunities to real empirical situations mainly due to two reasons: i) Local communities do not have discrete boundaries and ii) different species may respond to processes at different scales. Both of these issues seem to be absent at cold seep communities, since i) their habitat has discrete boundaries and sharp gradients and ii) different microorganisms likely respond equally to ecological mechanism due to the similarity of their size and physical environment. If the strategies and scales of sampling in microbial ecology are adjusted to the hypotheses tested than it might even be feasible to develop new theories and step out of the comfortable shade that classical ecology casts.

## Outlook

Although this work has significantly improved our knowledge about microbial communities and habitat diversity at cold seeps, the mechanisms that shape the communities at these ecosystems are still not fully understood. There are several ways to optimize further studies, which can be summarized under the following four terms: species resolution, sampling strategy, sample metadata and theory development. Species resolution in surveys of microbial diversity needs to be improved, since we are using taxonomic markers that are not directly linked to function and physiology of the organisms. We can only describe niche differentiation, coexistence of species and species assembly once we connect the identity of organisms with their metabolic capabilities. We are currently trying to achieve this with two different approaches: i) by comparing draft genomes of the different ANME clades and ii) by comparing the microbial communities of several cold seep habitats based on fragments of genomes using metagenomics. With further advance of sequencing technologies it will soon be possible to compare ecosystems and metacommunities based on single cell genomes, which will greatly improve the resolution of ecological studies. In addition, we need to improve the sampling strategy, since it is essential for the outcome of an experiment to reconcile the experimental approach and the tested hypothesis. Detailed experiments under controlled conditions that are essential for the testing of hypothesis are missing in most surveys of microbial diversity. Another issue that needs to be considered is the comprehensive collection of metadata, since it is needed for determining niche-based processes. Lacking metadata was the biggest drawback in the large survey of Chapter 2, as we might have been able to explain much more of the variation, if a sufficient set of environmental parameters would have been available. Finally, it is rare in microbial ecology that new ecological concepts and theories are developed. However, there is tremendous potential in this regard, since it is fairly easy to obtain detailed insights into microbial communities and it may be possible to build artificial ecosystems in the lab for the targeted testing of hypotheses.

## References

- Allison, S. D. and Martiny, J. B. H. (2008). "Resistance, Resilience, and Redundancy in Microbial Communities." *Proc Natl Acad Sci USA* **105**: 11512-11519.
- Anderson, M. J., Crist, T. O., et al. (2011). "Navigating the Multiple Meanings of B Diversity: A Roadmap for the Practicing Ecologist." *Ecol Lett* **14**: 19-28.
- Angel, R., Claus, P., et al. (2012). "Methanogenic Archaea Are Globally Ubiquitous in Aerated Soils and Become Active under Wet Anoxic Conditions." *ISME J* **6**: 847-862.
- Arakawa, S., Sato, T., et al. (2006). "Molecular Phylogenetic and Chemical Analyses of the Microbial Mats in Deep-Sea Cold Seep Sediments at the Northeastern Japan Sea." *Extremophiles* **10**: 311-319.
- Arrhenius, O. (1921). "Species and Area." *J Ecol* **9**: 95-99.
- Arvidson, R. S., Morse, J. W., et al. (2004). "The Sulfur Biogeochemistry of Chemosynthetic Cold Seep Communities, Gulf of Mexico, USA." *Mar Chem* **87**: 97-119.
- Astorga, A., Oksanen, J., et al. (2012). "Distance Decay of Similarity in Freshwater Communities: Do Macro- and Microorganisms Follow the Same Rules?" *Global Ecol Biogeogr* **21**: 365-375.
- Baco, A. R., Rowden, A. A., et al. (2010). "Initial Characterization of Cold Seep Faunal Communities on the New Zealand Hikurangi Margin." *Mar Geol* **272**: 251-259.
- Baker, M. C., Ramirez-Llodra, E. Z., et al. (2010). Biogeography, Ecology, and Vulnerability of Chemosynthetic Ecosystems in the Deep Sea. *Life in the World's Oceans: Diversity, Distribution, and Abundance*. McIntyre, A. D., Wiley-Blackwell: 161-183.
- Barry, J. P. and Kochevar, R. E. (1998). "A Tale of Two Clams: Differing Chemosynthetic Life Styles among Vesicomysids in Monterey Bay Cold Seeps." *Cah Biol Mar* **39**: 329-332.
- Beal, E. J., House, C. H., et al. (2009). "Manganese- and Iron-Dependent Marine Methane Oxidation." *Science* **325**: 184-187.
- Bell, T. (2010). "Experimental Tests of the Bacterial Distance-Decay Relationship." *ISME J* **4**: 1357-1365.
- Bell, T., Ager, D., et al. (2005). "Larger Islands House More Bacterial Taxa." *Science* **308**: 1884.
- Biddle, J. F., Cardman, Z., et al. (2012). "Anaerobic Oxidation of Methane at Different Temperature Regimes in Guaymas Basin Hydrothermal Sediments." *ISME J* **6**: 1018-1031.
- Bienhold, C., Boetius, A., et al. (2011). "The Energy-Diversity Relationship of Complex Bacterial Communities in Arctic Deep-Sea Sediments." *ISME J* **6**: 724-732.
- Bienhold, C., Pop Ristova, P., et al. (2013). "How Deep-Sea Wood Falls Sustain Chemosynthetic Life." *PLoS ONE* **8**: e53590.

- Blazejak, A., Erséus, C., et al. (2005). "Coexistence of Bacterial Sulfide Oxidizers, Sulfate Reducers, and Spirochetes in a Gutless Worm (Oligochaeta) from the Peru Margin." *Appl Environ Microbiol* **71**: 1553-1561.
- Blazejak, A. and Schippers, A. (2010). "High Abundance of Js-1- and Chloroflexi-Related Bacteria in Deeply Buried Marine Sediments Revealed by Quantitative, Real-Time Pcr." *FEMS Microbiol Ecol* **72**: 198-207.
- Blumenberg, M., Seifert, R., et al. (2007). "Aerobic Methanotrophy in the Oxic-Anoxic Transition Zone of the Black Sea Water Column." *Org Geochem* **38**: 84-91.
- Boetius, A. (2005). "Microfauna-Macrofauna Interaction in the Seafloor: Lessons from the Tubeworm." *PLoS Biol* **3**: e102.
- Boetius, A. and Knittel, K. (2010). Habitats of Anaerobic Methane Oxidizers. *Handbook of Hydrocarbon and Lipid Microbiology*. Timmis, K. N., Springer: 2193-2202.
- Boetius, A., Ravensschlag, K., et al. (2000). "A Marine Microbial Consortium Apparently Mediating Anaerobic Oxidation of Methane." *Nature* **407**: 623-626.
- Boetius, A. and Suess, E. (2004). "Hydrate Ridge: A Natural Laboratory for the Study of Microbial Life Fueled by Methane from near-Surface Gas Hydrates." *Chem Geol* **205**: 291-310.
- Boetius, A. and Wenzhöfer, F. (2013). "Seafloor Oxygen Consumption Fuelled by Methane from Cold Seeps." *Nature Geosci* **6**: 725-734.
- Bolhuis, H. and Stal, L. J. (2011). "Analysis of Bacterial and Archaeal Diversity in Coastal Microbial Mats Using Massive Parallel 16s Rrna Gene Tag Sequencing." *ISME J* **5**: 1701-1712.
- Bowden, D. A., Rowden, A. A., et al. (2013). "Cold Seep Epifaunal Communities on the Hikurangi Margin, New Zealand: Composition, Succession, and Vulnerability to Human Activities." *PLoS ONE* **8**: e76869.
- Bray, J. R. and Curtis, J. T. (1957). "An Ordination of the Upland Forest Communities of Southern Wisconsin." *Ecol Monogr* **27**: 326-349.
- Brazelton, W. J., Ludwig, K. A., et al. (2010). "Archaea and Bacteria with Surprising Microdiversity Show Shifts in Dominance over 1,000-Year Time Scales in Hydrothermal Chimneys." *Proc Natl Acad Sci USA*.
- Bromham, L. and Penny, D. (2003). "The Modern Molecular Clock." *Nat Rev Genet* **4**: 216-224.
- Campbell, B. J., Yu, L., et al. (2011). "Activity of Abundant and Rare Bacteria in a Coastal Ocean." *Proc Natl Acad Sci USA*.
- Caporaso, J. G., Paszkiewicz, K., et al. (2012). "The Western English Channel Contains a Persistent Microbial Seed Bank." *ISME J* **6**: 1089-1093.
- Chao, A. (1984). "Nonparametric Estimation of the Number of Classes in a Population." *Scand J Stat* **11**: 265-270.
- Chave, J. (2004). "Neutral Theory and Community Ecology." *Ecol Lett* **7**: 241-253.
- Cheetham, A. H. and Hazel, J. E. (1969). "Binary (Presence-Absence) Similarity Coefficients." *J Paleontol* **43**: 1130-1136.
- Chevalier, N., Bouloubassi, I., et al. (2013). "Microbial Methane Turnover at Marmara Sea Cold Seeps: A Combined 16s Rrna and Lipid Biomarker Investigation." *Geobiology* **11**: 55-71.

- Colwell, R. K. and Rangel, T. F. (2009). "Hutchinson's Duality: The Once and Future Niche." *Proc Natl Acad Sci USA*.
- Cordes, E. E., Arthur, M. A., et al. (2005). "Modeling the Mutualistic Interactions between Tubeworms and Microbial Consortia." *PLoS Biol* **3**: e77.
- Cordes, E. E., Cunha, M. R., et al. (2010). "The Influence of Geological, Geochemical, and Biogenic Habitat Heterogeneity on Seep Biodiversity." *Mar Ecol* **31**: 51-65.
- Costello, E. K., Stagaman, K., et al. (2012). "The Application of Ecological Theory toward an Understanding of the Human Microbiome." *Science* **336**: 1255-1262.
- Cottenie, K., Michels, E., et al. (2003). "Zooplankton Metacommunity Structure: Regional Vs. Local Processes in Highly Interconnected Ponds." *Ecology* **84**: 991-1000.
- Curtis, T. P., Sloan, W. T., et al. (2002). "Estimating Prokaryotic Diversity and Its Limits." *Proc Natl Acad Sci USA* **99**: 10494-10499.
- D'Hondt, S., Jorgensen, B. B., et al. (2004). "Distributions of Microbial Activities in Deep Subseafloor Sediments." *Science* **306**: 2216-2221.
- Dar, S., Stams, A. M., et al. (2007). "Co-Existence of Physiologically Similar Sulfate-Reducing Bacteria in a Full-Scale Sulfidogenic Bioreactor Fed with a Single Organic Electron Donor." *Appl Microbiol Biotechnol* **75**: 1463-1472.
- Dattagupta, S., Arthur, M. A., et al. (2008). "Modification of Sediment Geochemistry by the Hydrocarbon Seep Tubeworm *Lamellibrachia Luymesii*: A Combined Empirical and Modeling Approach." *Geochim Cosmochim Acta* **72**: 2298-2315.
- De Beer, D., Sauter, E., et al. (2006). "In Situ Fluxes and Zonation of Microbial Activity in Surface Sediments of the Håkon Mosby Mud Volcano." *Limnol Oceanogr* **51**: 1315-1331.
- Decker, C., Olu, K., et al. (2013). "Phylogeny and Diversification Patterns among Vesicomysid Bivalves." *PLoS ONE* **7**: e33359.
- Dubilier, N., Bergin, C., et al. (2008). "Symbiotic Diversity in Marine Animals: The Art of Harnessing Chemosynthesis." *Nat Rev Micro* **6**: 725-740.
- Dubinina, G., Grabovich, M., et al. (2011). "Spirochaeta Perfilievii Sp. Nov., an Oxygen-Tolerant, Sulfide-Oxidizing, Sulfur- and Thiosulfate-Reducing Spirochaete Isolated from a Saline Spring." *Int J Syst Evol Microbiol* **61**: 110-117.
- Dumbrell, A. J., Nelson, M., et al. (2010). "Relative Roles of Niche and Neutral Processes in Structuring a Soil Microbial Community." *ISME J* **4**: 337-345.
- Duperron, S., Guezi, H., et al. (2011). "Relative Abundances of Methane- and Sulphur-Oxidising Symbionts in the Gills of a Cold Seep Mussel and Link to Their Potential Energy Sources." *Geobiology* **9**: 481-491.
- Duperron, S., Halary, S., et al. (2008). "Unexpected Co-Occurrence of Six Bacterial Symbionts in the Gills of the Cold Seep Mussel *Idas* Sp. (Bivalvia: Mytilidae)." *Environ Microbiol* **10**: 433-445.
- Duperron, S., Nadalig, T., et al. (2005). "Dual Symbiosis in a *Bathymodiolus* Sp. Mussel from a Methane Seep on the Gabon Continental Margin (Southeast Atlantic): 16s Rrna Phylogeny and Distribution of the Symbionts in Gills." *Appl Environ Microbiol* **71**: 1694-1700.

- Duperron, S., Sibuet, M., et al. (2007). "Diversity, Relative Abundance and Metabolic Potential of Bacterial Endosymbionts in Three Bathymodiulus Mussel Species from Cold Seeps in the Gulf of Mexico." *Environ Microbiol* **9**: 1423-1438.
- Elshahed, M. S., Youssef, N. H., et al. (2008). "Novelty and Uniqueness Patterns of Rare Members of the Soil Biosphere." *Appl Environ Microbiol* **74**: 5422-5428.
- Elvert, M., Hopmans, E. C., et al. (2005). "Spatial Variations of Methanotrophic Consortia at Cold Methane Seeps: Implications from a High-Resolution Molecular and Isotopic Approach." *Geobiology* **3**: 195-209.
- Epstein, S. S. (2013). "The Phenomenon of Microbial Uncultivability." *Curr Opin Microbiol* **In press**.
- Ettwig, K. F., Butler, M. K., et al. (2010). "Nitrite-Driven Anaerobic Methane Oxidation by Oxygenic Bacteria." *Nature* **464**: 543-548.
- Felden, J., Lichtschlag, A., et al. (2013). "Limitations of Microbial Hydrocarbon Degradation at the Amon Mud Volcano (Nile Deep-Sea Fan)." *Biogeosciences* **10**: 3269-3283.
- Felden, J., Wenzhöfer, F., et al. (2010). "Transport and Consumption of Oxygen and Methane in Different Habitats of the Håkon Mosby Mud Volcano (Hmmv)." *Limnol Oceanogr* **55**: 2366-2380.
- Feseker, T., Dählmann, A., et al. (2009). "In-Situ Sediment Temperature Measurements and Geochemical Porewater Data Suggest Highly Dynamic Fluid Flow at Isis Mud Volcano, Eastern Mediterranean Sea." *Mar Geol* **261**: 128-137.
- Fierer, N. and Lennon, J. T. (2011). "The Generation and Maintenance of Diversity in Microbial Communities." *Am J Bot* **98**: 439-448.
- Finlay, B. J. (2002). "Global Dispersal of Free-Living Microbial Eukaryote Species." *Science* **296**: 1061-1063.
- Finlay, B. J., Maberly, S. C., et al. (1997). "Microbial Diversity and Ecosystem Function." *Oikos* **80**: 209-213.
- Fischer, D., Sahling, H., et al. (2012). "Interaction between Hydrocarbon Seepage, Chemosynthetic Communities, and Bottom Water Redox at Cold Seeps of the Makran Accretionary Prism: Insights from Habitat-Specific Pore Water Sampling and Modeling." *Biogeosciences* **9**: 2013-2031.
- Flores, G. E., Shakya, M., et al. (2012). "Inter-Field Variability in the Microbial Communities of Hydrothermal Vent Deposits from a Back-Arc Basin." *Geobiology* **10**: 333-346.
- Folke, C., Carpenter, S., et al. (2004). "Regime Shifts, Resilience, and Biodiversity in Ecosystem Management." *Annu Rev Ecol Evol S* **35**: 557-581.
- Foucher, J.-P., Dupré, S., et al. (2010). "Changes in Seabed Morphology, Mud Temperature and Free Gas Venting at the Håkon Mosby Mud Volcano, Offshore Northern Norway, over the Time Period 2003 - 2006." *Geo-Mar Lett* **30**: 157-167.
- Fry, J. C., Parkes, R. J., et al. (2008). "Prokaryotic Biodiversity and Activity in the Deep Subseafloor Biosphere." *FEMS Microbiol Ecol* **66**: 181-196.
- Fuhrman, J. A., Steele, J. A., et al. (2008). "A Latitudinal Diversity Gradient in Planktonic Marine Bacteria." *Proc Natl Acad Sci USA* **105**: 7774-7778.

- Gaidos, E., Rusch, A., et al. (2010). "Ribosomal Tag Pyrosequencing of DNA and Rna from Benthic Coral Reef Microbiota: Community Spatial Structure, Rare Members and Nitrogen-Cycling Guilds." *Environ Microbiol* **13**: 1138-1152.
- Galand, P. E., Casamayor, E. O., et al. (2009). "Ecology of the Rare Microbial Biosphere of the Arctic Ocean." *Proceedings of the National Academy of Sciences* **106**: 22427-22432.
- García Martín, H. and Goldenfeld, N. (2006). "On the Origin and Robustness of Power-Law Species-Area Relationships in Ecology." *Proceedings of the National Academy of Sciences* **103**: 10310-10315.
- Gaston, K. J. and Chown, S. L. (2005). "Neutrality and the Niche." *Funct Ecol* **19**: 1-6.
- Gibbons, S. M., Caporaso, J. G., et al. (2013). "Evidence for a Persistent Microbial Seed Bank Throughout the Global Ocean." *Proc Natl Acad Sci USA* **110**: 4651-4655.
- Girguis, P. R., Cozen, A. E., et al. (2005). "Growth and Population Dynamics of Anaerobic Methane-Oxidizing Archaea and Sulfate-Reducing Bacteria in a Continuous-Flow Bioreactor." *Appl Environ Microbiol* **71**: 3725-3733.
- Girnth, A.-C., Grünke, S., et al. (2011). "A Novel, Mat-Forming Thiomargarita Population Associated with a Sulfidic Fluid Flow from a Deep-Sea Mud Volcano." *Environ Microbiol* **13**: 495-505.
- Gittel, A., Kofoed, M. V. W., et al. (2012). "Succession of Deferribacteres and Epsilonproteobacteria through a Nitrate-Treated High-Temperature Oil Production Facility." *Syst Appl Microbiol* **35**: 165-174.
- Gobet, A., Boer, S. I., et al. (2012). "Diversity and Dynamics of Rare and of Resident Bacterial Populations in Coastal Sands." *ISME J* **6**: 542-553.
- Goffredi, S. K. and Orphan, V. J. (2010). "Bacterial Community Shifts in Taxa and Diversity in Response to Localized Organic Loading in the Deep Sea." *Environ Microbiol* **12**: 344-363.
- Gotelli, N. J. and Colwell, R. K. (2001). "Quantifying Biodiversity: Procedures and Pitfalls in the Measurement and Comparison of Species Richness." *Ecol Lett* **4**: 379-391.
- Green, J. L., Holmes, A. J., et al. (2004). "Spatial Scaling of Microbial Eukaryote Diversity." *Nature* **432**: 747-750.
- Grinnell, J. (1917). "The Niche-Relationships of the California Thrasher." *Auk* **34**: 427-433.
- Grünke, S., Felden, J., et al. (2011). "Niche Differentiation among Mat-Forming, Sulfide-Oxidizing Bacteria at Cold Seeps of the Nile Deep Sea Fan (Eastern Mediterranean Sea)." *Geobiology* **9**: 330-348.
- Grünke, S., Lichtschlag, A., et al. (2012). "Mats of Psychrophilic Thiotrophic Bacteria Associated with Cold Seeps of the Barents Sea." *Biogeosciences* **9**: 2947-2960.
- Hamdan, L. J., Coffin, R. B., et al. (2013). "Ocean Currents Shape the Microbiome of Arctic Marine Sediments." *ISME J* **7**: 685-696.
- Hamdan, L. J., Gillevet, P. M., et al. (2011). "Diversity and Biogeochemical Structuring of Bacterial Communities across the Porangahau Ridge Accretionary Prism, New Zealand." *FEMS Microbiol Ecol* **77**: 518-532.

- Hanson, C. A., Fuhrman, J. A., et al. (2012). "Beyond Biogeographic Patterns: Processes Shaping the Microbial Landscape." *Nat Rev Micro* **10**: 497-506.
- Hanson, R. S. and Hanson, T. E. (1996). "Methanotrophic Bacteria." *Microbiol Rev* **60**: 439-71.
- Haroon, M. F., Hu, S., et al. (2013). "Anaerobic Oxidation of Methane Coupled to Nitrate Reduction in a Novel Archaeal Lineage." *Nature* **500**: 567-570.
- Harrison, B. K., Zhang, H., et al. (2009). "Variations in Archaeal and Bacterial Diversity Associated with the Sulfate-Methane Transition Zone in Continental Margin Sediments (Santa Barbara Basin, California)." *Appl Environ Microbiol* **75**: 1487-1499.
- Hayashi, T., Obata, H., et al. (2007). "Distribution and Phylogenetic Characteristics of the Genes Encoding Enzymes Relevant to Methane Oxidation in Oxygen Minimum Zones of the Eastern Pacific Ocean." *Res J Environ Sci* **1**: 275-284.
- Hilário, A., Capa, M., et al. (2011). "New Perspectives on the Ecology and Evolution of Siboglinid Tubeworms." *PLoS ONE* **6**: e16309.
- Hill, T. C. J., Walsh, K. A., et al. (2003). "Using Ecological Diversity Measures with Bacterial Communities." *FEMS Microbiol Ecol* **43**: 1-11.
- Hinrichs, K.-U., Hayes, J. M., et al. (1999). "Methane-Consuming Archaeobacteria in Marine Sediments." *Nature* **398**: 802-805.
- Hoehler, T. M. and Jørgensen, B. B. (2013). "Microbial Life under Extreme Energy Limitation." *Nat Rev Micro* **11**: 83-94.
- Hoekstra, J. M., Boucher, T. M., et al. (2005). "Confronting a Biome Crisis: Global Disparities of Habitat Loss and Protection." *Ecol Lett* **8**: 23-29.
- Holler, T., Widdel, F., et al. (2011). "Thermophilic Anaerobic Oxidation of Methane by Marine Microbial Consortia." *ISME J* **5**: 1946-1956.
- Horner-Devine, C. M., Leibold, M. A., et al. (2003). "Bacterial Diversity Patterns Along a Gradient of Primary Productivity." *Ecol Lett* **6**: 613-622.
- Horner-Devine, M. C., Lage, M., et al. (2004). "A Taxa-Area Relationship for Bacteria." *Nature* **432**: 750-753.
- Hovland, M., Gardner, J. V., et al. (2002). "The Significance of Pockmarks to Understanding Fluid Flow Processes and Geohazards." *Geofluids* **2**: 127-136.
- Hubbell, S. P. (1997). "A Unified Theory of Biogeography and Relative Species Abundance and Its Application to Tropical Rain Forests and Coral Reefs." *Coral Reefs* **16**: S9-S21.
- Huber, J. A., Mark Welch, D. B., et al. (2007). "Microbial Population Structures in the Deep Marine Biosphere." *Science* **318**: 97-100.
- Hugoni, M., Taib, N., et al. (2013). "Structure of the Rare Archaeal Biosphere and Seasonal Dynamics of Active Ecotypes in Surface Coastal Waters." *Proc Natl Acad Sci USA* **110**: 6004-6009.
- Hunt, D. E., Lin, Y., et al. (2013). "Relationship between Abundance and Specific Activity of Bacterioplankton in Open Ocean Surface Waters." *Appl Environ Microbiol* **79**: 177-184.
- Inagaki, F., Nunoura, T., et al. (2006). "Biogeographical Distribution and Diversity of Microbes in Methane Hydrate-Bearing Deep Marine Sediments on the Pacific Ocean Margin." *Proc Natl Acad Sci USA* **103**: 2815-2820.

- Inagaki, F., Sakihama, Y., et al. (2002). "Molecular Phylogenetic Analyses of Reverse-Transcribed Bacterial Rna Obtained from Deep-Sea Cold Seep Sediments." *Environ Microbiol* **4**: 277-286.
- Inagaki, F., Takai, K., et al. (2004a). "Sulfurovum Lithotrophicum Gen. Nov., Sp. Nov., a Novel Sulfur-Oxidizing Chemolithoautotroph within the E-Proteobacteria Isolated from Okinawa Trough Hydrothermal Sediments." *Int J Syst Evol Microbiol* **54**: 1477-1482.
- Inagaki, F., Tsunogai, U., et al. (2004b). "Characterization of C1-Metabolizing Prokaryotic Communities in Methane Seep Habitats at the Kuroshima Knoll, Southern Ryukyu Arc, by Analyzing Pmoa, Mmox, Mxaf, Mcra, and 16s Rna Genes." *Appl Environ Microbiol* **70**: 7445-7455.
- Jacob, M., Soltwedel, T., et al. (2013). "Biogeography of Deep-Sea Benthic Bacteria at Regional Scale (Lter Hausgarten, Fram Strait, Arctic)." *PLoS ONE* **8**: e72779.
- Janssen, P. H., Liesack, W., et al. (2002). "Geovibrio Thiophilus Sp. Nov., a Novel Sulfur-Reducing Bacterium Belonging to the Phylum Deferribacteres." *Int J Syst Evol Microbiol* **52**: 1341-7.
- Jones, S. E. and Lennon, J. T. (2010). "Dormancy Contributes to the Maintenance of Microbial Diversity." *Proc Natl Acad Sci USA* **107**: 5881-5886.
- Jørgensen, B. B. and Boetius, A. (2007). "Feast and Famine - Microbial Life in the Deep-Sea Bed." *Nat Rev Micro* **5**: 770-781.
- Jost, L. (2006). "Entropy and Diversity." *Oikos* **113**: 363-375.
- Joye, S. B., Boetius, A., et al. (2004). "The Anaerobic Oxidation of Methane and Sulfate Reduction in Sediments from Gulf of Mexico Cold Seeps." *Chem Geol* **205**: 219-238.
- Joye, S. B., Bowles, M. W., et al. (2010). "Biogeochemical Signatures and Microbial Activity of Different Cold-Seep Habitats Along the Gulf of Mexico Deep Slope." *Deep-Sea Res Pt II* **57**: 1990-2001.
- Judd, A. G. (2003). "The Global Importance and Context of Methane Escape from the Seabed." *Geo-Mar Lett* **23**: 147-154.
- Kallmeyer, J., Pockalny, R., et al. (2012). "Global Distribution of Microbial Abundance and Biomass in Subseafloor Sediment." *Proc Natl Acad Sci USA*.
- Kawabe, M. and Fujio, S. (2010). "Pacific Ocean Circulation Based on Observation." *J Oceanogr* **66**: 389-403.
- Kennicutt, M. C., Brooks, J. M., et al. (1985). "Vent-Type Taxa in a Hydrocarbon Seep Region on the Louisiana Slope." *Nature* **317**: 351-353.
- Kleindienst, S., Ramette, A., et al. (2012). "Distribution and in Situ Abundance of Sulfate-Reducing Bacteria in Diverse Marine Hydrocarbon Seep Sediments." *Environ Microbiol* **14**: 2689-2710.
- Knittel, K. and Boetius, A. (2009). "Anaerobic Oxidation of Methane: Progress with an Unknown Process." *Annu Rev Microbiol* **63**: 311-334.
- Knittel, K., Boetius, A., et al. (2003). "Activity, Distribution, and Diversity of Sulfate Reducers and Other Bacteria in Sediments above Gas Hydrate (Cascadia Margin, Oregon)." *Geomicrobiol J* **20**: 269-294.
- Knittel, K., Lösekann, T., et al. (2005). "Diversity and Distribution of Methanotrophic Archaea at Cold Seeps." *Appl Environ Microbiol* **71**: 467-479.

- Kohn, D. D. and Walsh, D. M. (1994). "Plant Species Richness--the Effect of Island Size and Habitat Diversity." *J Ecol* **82**: 367-377.
- Kubo, K., Lloyd, K. G., et al. (2012). "Archaea of the Miscellaneous Crenarchaeotal Group Are Abundant, Diverse and Widespread in Marine Sediments." *ISME J* **6**: 1949-1965.
- Lane, D. J., Pace, B., et al. (1985). "Rapid Determination of 16s Ribosomal Rna Sequences for Phylogenetic Analyses." *Proc Natl Acad Sci USA* **82**: 6955-6959.
- Lavik, G., Stührmann, T., et al. (2009). "Detoxification of Sulphidic African Shelf Waters by Blooming Chemolithotrophs." *Nature* **457**: 581-584.
- Lazar, C. S., L'Haridon, S., et al. (2011). "Archaeal Populations in Hypersaline Sediments Underlying Orange Microbial Mats in the Napoli Mud Volcano." *Appl Environ Microbiol* **77**: 3120-3131.
- Leibold, M. A. (1995). "The Niche Concept Revisited: Mechanistic Models and Community Context." *Ecology* **76**: 1371-1382.
- Leibold, M. A., Holyoak, M., et al. (2004). "The Metacommunity Concept: A Framework for Multi-Scale Community Ecology." *Ecol Lett* **7**: 601-613.
- Leibold, M. A. and McPeck, M. A. (2006). "Coexistence of the Niche and Neutral Perspectives in Community Ecology." *Ecology* **87**: 1399-1410.
- Lesniewski, R. A., Jain, S., et al. (2012). "The Metatranscriptome of a Deep-Sea Hydrothermal Plume Is Dominated by Water Column Methanotrophs and Lithotrophs." *ISME J* **6**: 2257-2268.
- Levin, L. A. (2005). Ecology of Cold Seep Sediments: Interactions of Fauna with Flow, Chemistry and Microbes. *Oceanography and Marine Biology: An Annual Review*. Gibson, R. N., Atkinson, R. J. A., et al., Taylor & Francis. **43**: 1-46.
- Levin, L. A., Ziebis, W., et al. (2013). "Ecological Release and Niche Partitioning under Stress: Lessons from Dorvilleid Polychaetes in Sulfidic Sediments at Methane Seeps." *Deep-Sea Res Pt II* **92**: 214-233.
- Levin, L. A., Ziebis, W., Ziebis, et al. (2003). "Spatial Heterogeneity of Macrofauna at Northern California Methane Seeps: Influence of Sulfide Concentration and Fluid Flow." *Mar Ecol Prog Ser* **265**: 123-139.
- Li, L., Kato, C., et al. (1999). "Microbial Diversity in Sediments Collected from the Deepest Cold-Seep Area, the Japan Trench." *Mar Biotechnol* **1**: 391-400.
- Lichtsclag, A., Felden, J., et al. (2010). "Methane and Sulfide Fluxes in Permanent Anoxia: In Situ Studies at the Dvurechenskii Mud Volcano (Sorokin Trough, Black Sea)." *Geochim Cosmochim Acta* **74**: 5002-5018.
- Lichtsclag, A., Kamyshny Jr, A., et al. (2012). "Intermediate Sulfur Oxidation State Compounds in the Euxinic Surface Sediments of the Dvurechenskii Mud Volcano (Black Sea)." *Geochim Cosmochim Acta* **105**: 130-145.
- Lipp, J. S., Morono, Y., et al. (2008). "Significant Contribution of Archaea to Extant Biomass in Marine Subsurface Sediments." *Nature* **454**: 991-994.
- Lloyd, K. G., Albert, D. B., et al. (2010). "Spatial Structure and Activity of Sedimentary Microbial Communities Underlying a *Beggiatoa* Spp. Mat in a Gulf of Mexico Hydrocarbon Seep." *PLoS ONE* **5**: e8738.

- Lloyd, K. G., Lapham, L., et al. (2006). "An Anaerobic Methane-Oxidizing Community of Anme-1b Archaea in Hypersaline Gulf of Mexico Sediments." *Appl Environ Microbiol* **72**: 7218-7230.
- Lloyd, K. G., Schreiber, L., et al. (2013). "Predominant Archaea in Marine Sediments Degrade Detrital Proteins." *Nature* **496**: 215-218.
- Lösekan, T., Knittel, K., et al. (2007). "Diversity and Abundance of Aerobic and Anaerobic Methane Oxidizers at the Haakon Mosby Mud Volcano, Barents Sea." *Appl Environ Microbiol* **73**: 3348-3362.
- Lösekan, T., Robador, A., et al. (2008). "Endosymbioses between Bacteria and Deep-Sea Siboglinid Tubeworms from an Arctic Cold Seep (Haakon Mosby Mud Volcano, Barents Sea)." *Environ Microbiol* **10**: 3237-3254.
- MacArthur, R. (1970). "Species Packing and Competitive Equilibrium for Many Species." *Theor Popul Biol* **1**: 1-11.
- Martiny, J. B. H., Eisen, J. A., et al. (2011). "Drivers of Bacterial B-Diversity Depend on Spatial Scale." *Proc Natl Acad Sci USA* **108**: 7850-7854.
- Maruyama, A., Honda, D., et al. (2000). "Phylogenetic Analysis of Psychrophilic Bacteria Isolated from the Japan Trench, Including a Description of the Deep-Sea Species Psychrobacter Pacificensis Sp. Nov." *Int J Syst Evol Microbiol* **50**: 835-46.
- Mende, D. R., Sunagawa, S., et al. (2013). "Accurate and Universal Delineation of Prokaryotic Species." *Nat Meth* **10**: 881-884.
- Menot, L., Galéron, J., et al. (2009). "Spatial Heterogeneity of Macrofaunal Communities in and near a Giant Pockmark Area in the Deep Gulf of Guinea." *Mar Ecol* **31**: 78-93.
- Merkel, A. Y., Huber, J. A., et al. (2012). "Detection of Putatively Thermophilic Anaerobic Methanotrophs in Diffuse Hydrothermal Vent Fluids." *Appl Environ Microbiol* **79**: 915-923.
- Meyer, K. M. and Kump, L. R. (2008). "Oceanic Euxinia in Earth History: Causes and Consequences." *Annu Rev Earth Pl Sci* **36**: 251-288.
- Meyer, S., Wegener, G., et al. (2013). "Microbial Habitat Connectivity across Spatial Scales and Hydrothermal Temperature Gradients at Guaymas Basin." *Front Microbiol* **4**.
- Michaelis, W., Seifert, R., et al. (2002). "Microbial Reefs in the Black Sea Fueled by Anaerobic Oxidation of Methane." *Science* **297**: 1013-1015.
- Milkov, A. V. (2000). "Worldwide Distribution of Submarine Mud Volcanoes and Associated Gas Hydrates." *Mar Geol* **167**: 29-42.
- Mills, H. J., Martinez, R. J., et al. (2004). "Identification of Members of the Metabolically Active Microbial Populations Associated with Beggiatoa Species Mat Communities from Gulf of Mexico Cold-Seep Sediments." *Appl Environ Microbiol* **70**: 5447-5458.
- Mills, H. J., Martinez, R. J., et al. (2005). "Characterization of Microbial Community Structure in Gulf of Mexico Gas Hydrates: Comparative Analysis of DNA- and Rna-Derived Clone Libraries." *Appl Environ Microbiol* **71**: 3235-3247.
- Mora, C., Tittensor, D. P., et al. (2011). "How Many Species Are There on Earth and in the Ocean?" *PLoS Biol* **9**: e1001127.
- Murray, B. R., Rice, B. L., et al. (1999). "Species in the Tail of Rank-Abundance Curves." *Ecology* **80**: 1806-1816.

- Muyzer, G. and Stams, A. J. M. (2008). "The Ecology and Biotechnology of Sulphate-Reducing Bacteria." *Nat Rev Microbiol* **6**: 441-454.
- Nauhaus, K., Albrecht, M., et al. (2007). "In Vitro Cell Growth of Marine Archaeal-Bacterial Consortia During Anaerobic Oxidation of Methane with Sulfate." *Environ Microbiol* **9**: 187-196.
- Nekola, J. C. and White, P. S. (1999). "The Distance Decay of Similarity in Biogeography and Ecology." *J Biogeogr* **26**: 867-878.
- Nemergut, D. R., Costello, E. K., et al. (2011). "Global Patterns in the Biogeography of Bacterial Taxa." *Environ Microbiol* **13**: 135-144.
- Nemergut, D. R., Schmidt, S. K., et al. (2013). "Patterns and Processes of Microbial Community Assembly." *Microbiol Mol Biol Rev* **77**: 342-356.
- Neretin, L. N., Abed, R. M. M., et al. (2007). "Inorganic Carbon Fixation by Sulfate-Reducing Bacteria in the Black Sea Water Column." *Environ Microbiol* **9**: 3019-3024.
- Niemann, H. and Boetius, A. (2010). Mud Volcanoes. *Handbook of Hydrocarbon and Lipid Microbiology*. Timmis, K. N., Springer. **1**: 205-214.
- Niemann, H., Elvert, M., et al. (2005). "Methane Emission and Consumption at a North Sea Gas Seep (Tommeliten Area)." *Biogeosciences* **2**: 335-351.
- Niemann, H., Fischer, D., et al. (2009). "Biogeochemistry of a Low-Activity Cold Seep in the Larsen B Area, Western Weddell Sea, Antarctica." *Biogeosciences* **6**: 2383-2395.
- Niemann, H., Linke, P., et al. (2013). "Methane-Carbon Flow into the Benthic Food Web at Cold Seeps - a Case Study from the Costa Rica Subduction Zone." *PLoS ONE* **8**: e74894.
- Niemann, H., Lösekann, T., et al. (2006). "Novel Microbial Communities of the Haakon Mosby Mud Volcano and Their Role as a Methane Sink." *Nature* **443**: 854-858.
- Nunoura, T., Takaki, Y., et al. (2012). "Microbial Diversity in Deep-Sea Methane Seep Sediments Presented by Ssu Rrna Gene Tag Sequencing." *Microbes Environ* **27**: 382-390.
- O'Malley, M. A. (2007). "The Nineteenth Century Roots of 'Everything Is Everywhere'." *Nat Rev Micro* **5**: 647-651.
- Olu-Le Roy, K., Caprais, J.-C., et al. (2007). "Cold-Seep Assemblages on a Giant Pockmark Off West Africa: Spatial Patterns and Environmental Control." *Mar Ecol* **28**: 115-130.
- Omeregíe, E. O., Mastalerz, V., et al. (2008). "Biogeochemistry and Community Composition of Iron- and Sulfur-Precipitating Microbial Mats at the Chefren Mud Volcano (Nile Deep Sea Fan, Eastern Mediterranean)." *Appl Environ Microbiol* **74**: 3198-3215.
- Op den Camp, H. J. M., Islam, T., et al. (2009). "Environmental, Genomic and Taxonomic Perspectives on Methanotrophic Verrucomicrobia." *Environ Microbiol Rep* **1**: 293-306.
- Orphan, V. J., Hinrichs, K. U., et al. (2001). "Comparative Analysis of Methane-Oxidizing Archaea and Sulfate-Reducing Bacteria in Anoxic Marine Sediments." *Appl Environ Microbiol* **67**: 1922-1934.

- Orphan, V. J., House, C. H., et al. (2002). "Multiple Archaeal Groups Mediate Methane Oxidation in Anoxic Cold Seep Sediments." *Proc Natl Acad Sci USA* **99**: 7663-7668.
- Pachiadaki, M. G., Lykousis, V., et al. (2010). "Prokaryotic Community Structure and Diversity in the Sediments of an Active Submarine Mud Volcano (Kazan Mud Volcano, East Mediterranean Sea)." *FEMS Microbiol Ecol* **72**: 429-444.
- Parkes, R. J., Wellsbury, P., et al. (2007). "Temperature Activation of Organic Matter and Minerals During Burial Has the Potential to Sustain the Deep Biosphere over Geological Timescales." *Org Geochem* **38**: 845-852.
- Paull, C. K., Hecker, B., et al. (1984). "Biological Communities at the Florida Escarpment Resemble Hydrothermal Vent Taxa." *Science* **226**: 965-967.
- Perez-Garcia, C., Feseker, T., et al. (2009). "The Håkon Mosby Mud Volcano: 330 000 years of Focused Fluid Flow Activity at the Sw Barents Sea Slope." *Mar Geol* **262**: 105-115.
- Pernthaler, A., Dekas, A. E., et al. (2008). "Diverse Syntrophic Partnerships from Deep-Sea Methane Vents Revealed by Direct Cell Capture and Metagenomics." *Proc Natl Acad Sci USA* **105**: 7052-7057.
- Pester, M., Bittner, N., et al. (2010). "A 'Rare Biosphere' Microorganism Contributes to Sulfate Reduction in a Peatland." *ISME J* **4**: 1591-1602.
- Petersen, J. M., Zielinski, F. U., et al. (2011). "Hydrogen Is an Energy Source for Hydrothermal Vent Symbioses." *Nature* **476**: 176-180.
- Pinero, E., Marquardt, M., et al. (2013). "Estimation of the Global Inventory of Methane Hydrates in Marine Sediments Using Transfer Functions." *Biogeosciences* **10**: 959-975.
- Pop Ristova, P., Wenzhöfer, F., et al. (2012). "Bacterial Diversity and Biogeochemistry of Different Chemosynthetic Habitats of the Regab Cold Seep (West African Margin, 3160 M Water Depth)." *Biogeosciences* **9**: 5031-5048.
- Preisler, A., de Beer, D., et al. (2007). "Biological and Chemical Sulfide Oxidation in a Beggiatoa Inhabited Marine Sediment." *ISME J* **1**: 341-353.
- Prosser, J. I., Bohannon, B. J. M., et al. (2007). "The Role of Ecological Theory in Microbial Ecology." *Nat Rev Micro* **5**: 384-392.
- Ramette, A. and Tiedje, J. (2007). "Biogeography: An Emerging Cornerstone for Understanding Prokaryotic Diversity, Ecology, and Evolution." *Microb Ecol* **53**: 197-207.
- Rappé, M. S. and Giovannoni, S. J. (2003). "The Uncultured Microbial Majority." *Annu Rev Microbiol* **57**: 369-394.
- Ravenschlag, K., Sahm, K., et al. (2001). "Quantitative Molecular Analysis of the Microbial Community in Marine Arctic Sediments (Svalbard)." *Appl Environ Microbiol* **67**: 387-395.
- Recher, H. F. (1969). "Bird Species Diversity and Habitat Diversity in Australia and North America." *Am Nat* **103**: 75-80.
- Reeburgh, W. S. (2007). "Oceanic Methane Biogeochemistry." *Chem Rev* **107**: 486-513.
- Ritt, B., Pierre, C., et al. (2011). "Diversity and Distribution of Cold-Seep Fauna Associated with Different Geological and Environmental Settings at Mud

- Volcanoes and Pockmarks of the Nile Deep-Sea Fan." *Mar Biol* **158**: 1187-1210.
- Roalkvam, I., Jørgensen, S. L., et al. (2011). "New Insight into Stratification of Anaerobic Methanotrophs in Cold Seep Sediments." *FEMS Microbiol Ecol* **78**: 233-243.
- Rogers, A. D., Tyler, P. A., et al. (2012). "The Discovery of New Deep-Sea Hydrothermal Vent Communities in the Southern Ocean and Implications for Biogeography." *PLoS Biol* **10**: e1001234.
- Romanenko, L. A., Lysenko, A. M., et al. (2004). "Psychrobacter Maritimus Sp. Nov. And Psychrobacter Arenosus Sp. Nov., Isolated from Coastal Sea Ice and Sediments of the Sea of Japan." *Int J Syst Evol Microbiol* **54**: 1741-1745.
- Roslev, P. and King, G. M. (1994). "Survival and Recovery of Methanotrophic Bacteria Starved under Oxic and Anoxic Conditions." *Appl Environ Microbiol* **60**: 2602-2608.
- Roslev, P. and King, G. M. (1995). "Aerobic and Anaerobic Starvation Metabolism in Methanotrophic Bacteria." *Appl Environ Microbiol* **61**: 1563-70.
- Rossel, P. E., Elvert, M., et al. (2011). "Factors Controlling the Distribution of Anaerobic Methanotrophic Communities in Marine Environments: Evidence from Intact Polar Membrane Lipids." *Geochim Cosmochim Acta* **75**: 164-184.
- Rossel, P. E., Lipp, J. S., et al. (2008). "Intact Polar Lipids of Anaerobic Methanotrophic Archaea and Associated Bacteria." *Org Geochem* **39**: 992-999.
- Rosselló-Móra, R. and Amann, R. (2001). "The Species Concept for Prokaryotes." *FEMS Microbiol Rev* **25**: 39-67.
- Roussel, E. G., Bonavita, M.-A. C., et al. (2008). "Extending the Sub-Sea-Floor Biosphere." *Science* **320**: 1046.
- Roy, H., Kallmeyer, J., et al. (2012). "Aerobic Microbial Respiration in 86-Million-Year-Old Deep-Sea Red Clay." *Science* **336**: 922-925.
- Ruamps, L. S., Nunan, N., et al. (2011). "Microbial Biogeography at the Soil Pore Scale." *Soil Biol Biochem* **43**: 280-286.
- Sanders, H. L. (1968). "Marine Benthic Diversity: A Comparative Study." *Am Nat* **102**: 243-282.
- Schauer, R., Røy, H., et al. (2011). "Bacterial Sulfur Cycling Shapes Microbial Communities in Surface Sediments of an Ultramafic Hydrothermal Vent Field." *Environ Microbiol* **13**: 2633-2648.
- Schreiber, L., Holler, T., et al. (2010). "Identification of the Dominant Sulfate-Reducing Bacterial Partner of Anaerobic Methanotrophs of the Anme-2 Clade." *Environ Microbiol* **12**: 2327-2340.
- Schubert, C. J., Coolen, M. J. L., et al. (2006). "Aerobic and Anaerobic Methanotrophs in the Black Sea Water Column." *Environ Microbiol* **8**: 1844-1856.
- Shmida, A. V. I. and Wilson, M. V. (1985). "Biological Determinants of Species Diversity." *J Biogeogr*: 1-20.

- Sibuet, M. and Olu, K. (1998). "Biogeography, Biodiversity and Fluid Dependence of Deep-Sea Cold-Seep Communities at Active and Passive Margins." *Deep-Sea Res Pt II* **45**: 517-567.
- Sievert, S. M. and Vetriani, C. (2012). "Chemoautotrophy at Deep-Sea Vents: Past, Present, and Future." *Oceanography* **25**: 218-233.
- Sjöstedt, J., Koch-Schmidt, P., et al. (2012). "Recruitment of Members from the Rare Biosphere of Marine Bacterioplankton Communities after an Environmental Disturbance." *Appl Environ Microbiol* **78**: 1361-1369.
- Sogin, M. L., Morrison, H. G., et al. (2006). "Microbial Diversity in the Deep Sea and the Underexplored "Rare Biosphere"." *Proc Natl Acad Sci USA* **103**: 12115-12120.
- Sommer, S., Linke, P., et al. (2010). "Benthic Respiration in a Seep Habitat Dominated by Dense Beds of Ampharetid Polychaetes at the Hikurangi Margin (New Zealand)." *Mar Geol* **272**: 223-232.
- Sommer, S., Linke, P., et al. (2009). "Seabed Methane Emissions and the Habitat of Frenulate Tubeworms on the Captain Arutyunov Mud Volcano (Gulf of Cadiz)." *Mar Ecol Prog Ser* **382**: 69-86.
- Sul, W. J., Oliver, T. A., et al. (2013). "Marine Bacteria Exhibit a Bipolar Distribution." *Proc Natl Acad Sci USA* **110**: 2342-2347.
- Sutcliffe, I. C., Trujillo, M. E., et al. (2012). "A Call to Arms for Systematists: Revitalising the Purpose and Practises Underpinning the Description of Novel Microbial Taxa." *Antonie van Leeuwenhoek* **101**: 13-20.
- Tavormina, P. L., Ussler, W., III, et al. (2008). "Planktonic and Sediment-Associated Aerobic Methanotrophs in Two Seep Systems Along the North American Margin." *Appl Environ Microbiol* **74**: 3985-3995.
- Telford, R. J., Vandvik, V., et al. (2006). "Dispersal Limitations Matter for Microbial Morphospecies." *Science* **312**: 1015.
- Teske, A., Hinrichs, K.-U., et al. (2002). "Microbial Diversity of Hydrothermal Sediments in the Guaymas Basin: Evidence for Anaerobic Methanotrophic Communities." *Appl Environ Microbiol* **68**: 1994-2007.
- Thurber, A. R., Kröger, K., et al. (2010). "Stable Isotope Signatures and Methane Use by New Zealand Cold Seep Benthos." *Mar Geol* **272**: 260-269.
- Thurber, A. R., Levin, L. A., et al. (2012). "Archaea in Metazoan Diets: Implications for Food Webs and Biogeochemical Cycling." *ISME J* **6**: 1602-1612.
- Thurber, A. R., Levin, L. A., et al. (2013). "Microbes, Macrofauna, and Methane: A Novel Seep Community Fueled by Aerobic Methanotrophy." *Limnol Oceanogr* **58**: 1640-1656.
- Tivey, M. K. (2007). "Generation of Seafloor Hydrothermal Vent Fluids and Associated Mineral Deposits." *Oceanography* **20**: 50.
- Treude, T., Smith, C. R., et al. (2009). "Biogeochemistry of a Deep-Sea Whale Fall: Sulfate Reduction, Sulfide Efflux and Methanogenesis." *Mar Ecol Prog Ser* **382**: 1-21.
- Tuomisto, H. (2012). "An Updated Consumer's Guide to Evenness and Related Indices." *Oikos* **121**: 1203-1218.
- Turnbaugh, P. J., Hamady, M., et al. (2009). "A Core Gut Microbiome in Obese and Lean Twins." *Nature* **457**: 480-484.

- Turner, P. E., Souza, V., et al. (1996). "Tests of Ecological Mechanisms Promoting the Stable Coexistence of Two Bacterial Genotypes." *Ecology* **77**: 2119-2129.
- Van Gaever, S., Galéron, J., et al. (2009a). "Deep-Sea Habitat Heterogeneity Influence on Meiofaunal Communities in the Gulf of Guinea." *Deep-Sea Res Pt II* **56**: 2259-2269.
- Van Gaever, S., Moodley, L., et al. (2009b). "Trophic Specialisation of Metazoan Meiofauna at the Håkon Mosby Mud Volcano: Fatty Acid Biomarker Isotope Evidence." *Mar Biol* **156**: 1289-1296.
- Vellend, M. (2010). "Conceptual Synthesis in Community Ecology." *Quart Rev Biol* **85**: 183-206.
- Vigneron, A., Cruaud, P., et al. (2013). "Archaeal and Anaerobic Methane Oxidizer Communities in the Sonora Margin Cold Seeps, Guaymas Basin (Gulf of California)." *ISME J* **7**: 1595-1608.
- Vossmeyer, A., Deusner, C., et al. (2012). "Substrate-Specific Pressure Dependence of Microbial Sulfate Reduction in Deep-Sea Cold Seep Sediments of the Japan Trench." *Front Microbiol* **3**.
- Walker, B., Kinzig, A., et al. (1999). "Plant Attribute Diversity, Resilience, and Ecosystem Function: The Nature and Significance of Dominant and Minor Species." *Ecosystems* **2**: 95-113.
- Wallmann, K., Linke, P., et al. (1997). "Quantifying Fluid Flow, Solute Mixing, and Biogeochemical Turnover at Cold Vents of the Eastern Aleutian Subduction Zone." *Geochim Cosmochim Acta* **61**: 5209-5219.
- Wang, P., Wang, F., et al. (2004). "Molecular Phylogeny of Methylotrophs in a Deep-Sea Sediment from a Tropical West Pacific Warm Pool." *FEMS Microbiol Ecol* **47**: 77-84.
- Wankel, S. D., Adams, M. M., et al. (2012). "Anaerobic Methane Oxidation in Metalliferous Hydrothermal Sediments: Influence on Carbon Flux and Decoupling from Sulfate Reduction." *Environ Microbiol* **14**: 2726-2740.
- Wasmund, K., Kurtböke, D. I., et al. (2009). "Microbial Diversity in Sediments Associated with a Shallow Methane Seep in the Tropical Timor Sea of Australia Reveals a Novel Aerobic Methanotroph Diversity." *FEMS Microbiol Ecol* **68**: 142-151.
- Webster, G., Watt, L. C., et al. (2006). "A Comparison of Stable-Isotope Probing of DNA and Phospholipid Fatty Acids to Study Prokaryotic Functional Diversity in Sulfate-Reducing Marine Sediment Enrichment Slurries." *Environ Microbiol* **8**: 1575-1589.
- Wegener, G., Shovitri, M., et al. (2008). "Biogeochemical Processes and Microbial Diversity of the Gullfaks and Tommeliten Methane Seeps (Northern North Sea)." *Biogeosciences* **5**: 1127-1144.
- Whittaker, R. J., Grogan, D. W., et al. (2003). "Geographic Barriers Isolate Endemic Populations of Hyperthermophilic Archaea." *Science* **301**: 976-978.
- Whittaker, R. H. (1972). "Evolution and Measurement of Species Diversity." *Taxon* **21**: 213-251.
- Whittaker, R. H., Levin, S. A., et al. (1973). "Niche, Habitat, and Ecotope." *Am Nat* **107**: 321-338.

- Willig, M. R., Kaufman, D. M., et al. (2003). "Latitudinal Gradients of Biodiversity: Pattern, Process, Scale, and Synthesis." *Annu Rev Ecol Evol S* **34**: 273-309.
- Witte, U., Aberle, N., et al. (2003). "Rapid Response of a Deep-Sea Benthic Community to Pom Enrichment: An in-Situ Experimental Study." *Mar Ecol Prog Ser* **251**: 27-36.
- Woese, C. R. and Fox, G. E. (1977). "Phylogenetic Structure of the Prokaryotic Domain: The Primary Kingdoms." *Proc Natl Acad Sci USA* **74**: 5088-5090.
- Worm, B., Barbier, E. B., et al. (2006). "Impacts of Biodiversity Loss on Ocean Ecosystem Services." *Science* **314**: 787-790.
- Yan, T., Ye, Q., et al. (2006). "Diversity of Functional Genes for Methanotrophs in Sediments Associated with Gas Hydrates and Hydrocarbon Seeps in the Gulf of Mexico." *FEMS Microbiol Ecol* **57**: 251-259.
- Yanagawa, K., Sunamura, M., et al. (2011). "Niche Separation of Methanotrophic Archaea (Anme-1 and -2) in Methane-Seep Sediments of the Eastern Japan Sea Offshore Joetsu." *Geomicrobiol J* **28**: 118-129.
- Yarza, P., Richter, M., et al. (2008). "The All-Species Living Tree Project: A 16s Rrna-Based Phylogenetic Tree of All Sequenced Type Strains." *Syst Appl Microbiol* **31**: 241-250.
- Zhang, Y., Su, X., et al. (2012). "Abundance and Diversity of Candidate Division Js1- and Chloroflexi-Related Bacteria in Cold Seep Sediments of the Northern South China Sea." *Front Earth Sci* **6**: 373-382.
- Zinger, L., Amaral-Zettler, L. A., et al. (2011). "Global Patterns of Bacterial Beta-Diversity in Seafloor and Seawater Ecosystems." *PLoS ONE* **6**: e24570.

## Acknowledgements

First of all I am deeply grateful to my supervisors Katrin Knittel, Antje Boetius, Rudi Amann and Alban Ramette. You gave me the opportunity to delve into a fascinating, new world and shared your invaluable experience like a hitchhikers guide. Our conversations and discussions were inspiring as they opened new perspectives, created new ideas and dismantled immature suppositions. Your support unfolded the urge and creativity that turned into what I now consider my passion and profession.

I am very thankful to Anke Meyerdierks, Ulrich Fischer, Bernhard Fuchs, Hanno Teeling, Marc Mußmann, Marc Strous and Casey Hubert that greatly influenced my work by their ideas and support during thesis committees, discussions and meetings. Moreover, I want to thank all the people that helped me with experiments in the lab and in the preparation of data, manuscripts, reports and presentations. For all your names please refer to the acknowledgements of each Chapter.

Then I am truly indebted to my office mates Nicole, Silke and Matze. Every day of work was a pleasure because of you! Big up also to my colleagues and friends, Daphne, Christina, Gerd, Gunter, Zwiebel and many more folks of the Molecol and Habitat groups for lunch, for parties, for beers, for everything!

Big thanks also to Hoof and Mouth. You guys helped me to escape from the day-to-day insanity. Practicing, recording, gigging and touring really spiced up my life. Unimaginable, how the last years would have been without you.

Finally and most importantly I thank my family and especially my six nieces, nephews and godchildren. You have been, you are and you will be the sun of my solar system that I revolve around because without you my world would be barren boredom.

## Appendix

## **Supporting information of Chapter 2**

## Supporting information of Chapter 2

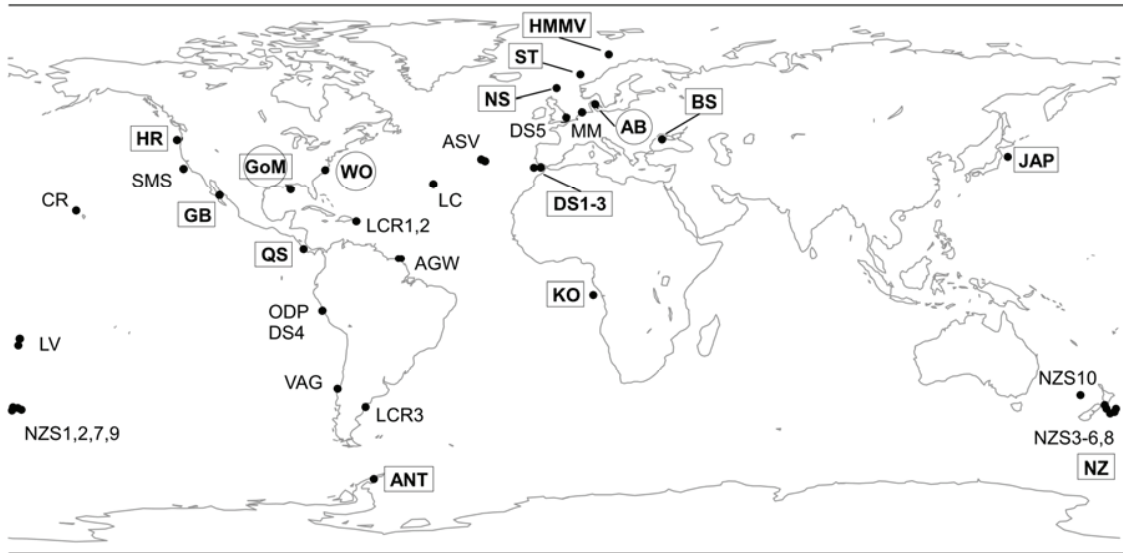


**Figure S1: Investigated sites**

Map of seafloor sampling sites investigated in this study (for details see Table S1-S3). Methane seeps (boxes) and subsurface sulfate methane transition zones (circles) are in bold letters. Studies with spatially distributed sites are numbered (LCR, DS and NZS).

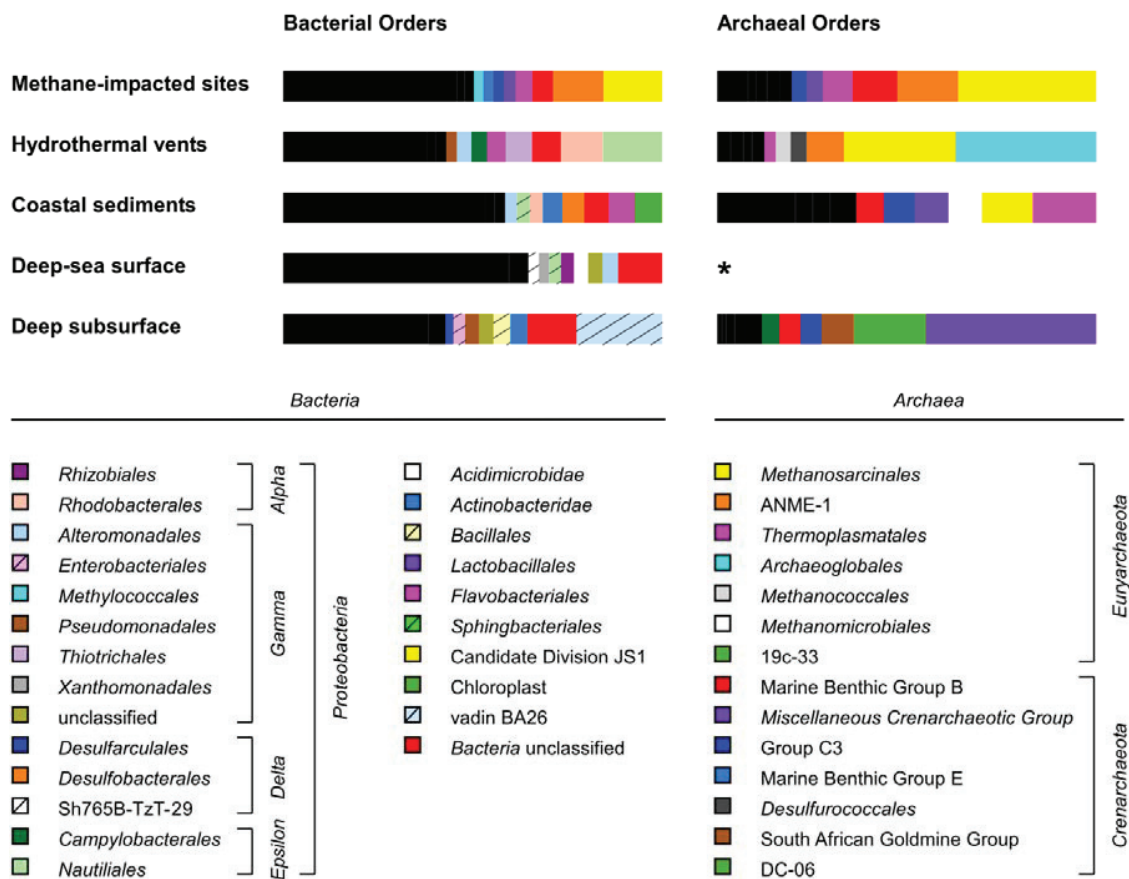


**Figure S2: Bacterial and archaeal orders present at investigated seafloor realms**

Relative read abundances of the eight most common bacterial and six most common archaeal orders that were retrieved from each seafloor realm. The bars represent the average of all samples from a certain realm. AOM habitats comprise 23 methane seeps and 4 SMTZ. The number of samples used for the analysis is given by the number behind each bar. The read abundance of other orders is depicted in black. The analysis is based upon samples from the ICoMM dataset. Unfortunately, no archaeal samples were obtained from deep sea surface sediments (asterisk).

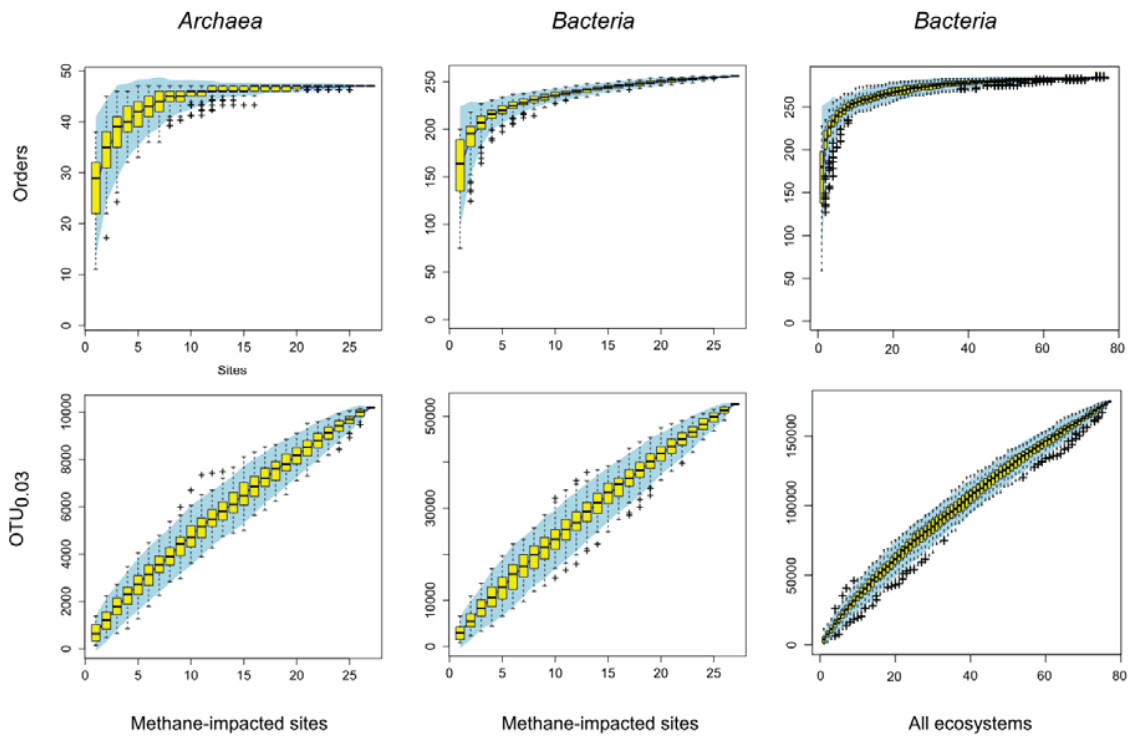


**Figure S3: Species accumulation curves of *Archaea* and *Bacteria***

Species accumulation curves based on archaeal and bacterial species (at 97% sequence identity) and order information of the 27 methane-impacted ecosystems (23 methane seeps and 4 SMTZ) as well as bacteria on species level for all 77 investigated ecosystems. The boxplots show a summary of 100 permutations that were calculated for each point using Chao1 richness and random subsampling. The blue area depicts the 95% confidence interval. Extrapolation of species richness using the Chao1 estimator based on the whole dataset indicated that around  $361000 \pm 1500$  ( $\pm$  standard error) bacterial and  $33000 \pm 470$  archaeal species inhabit the investigated seafloor habitats (not shown).

|   |            | Seeps | SMTZ | Coast | Surface | Subsurface |
|---|------------|-------|------|-------|---------|------------|
| Shared bacterial<br>phyla (%)               | SMTZ       | 88    |      |       |         |            |
|   | Coast      | 98    | 87   |       |         |            |
|   | Surface    | 94    | 86   | 96    |         |            |
|   | Subsurface | 81    | 83   | 82    | 82      |            |
|   | Vents      | 83    | 85   | 81    | 80      | 85         |
| Shared archaeal<br>OTU <sub>0.03</sub> (%)  | SMTZ       | 6     |      |       |         |            |
|   | Coast      | 6     | 7    |       |         |            |
|   | Surface    | NA    | NA   | NA    |         |            |
|   | Subsurface | 3     | 7    | 4     | NA      |            |
|   | Vents      | 2     | 1    | 1     | NA      | 1          |
| Shared bacterial<br>OTU <sub>0.03</sub> (%) | SMTZ       | 3     |      |       |         |            |
|   | Coast      | 6     | 2    |       |         |            |
|   | Surface    | 5     | 1    | 6     |         |            |
|   | Subsurface | 2     | 4    | 1     | 0.4     |            |
|   | Vents      | 2     | 1    | 3     | 2       | 2          |

**Figure S4:**

**Percentage of shared archaeal and bacterial taxa between seafloor realms**

Pairwise comparison of community similarity based on presence absence of phylum or OTU<sub>0.03</sub> data.

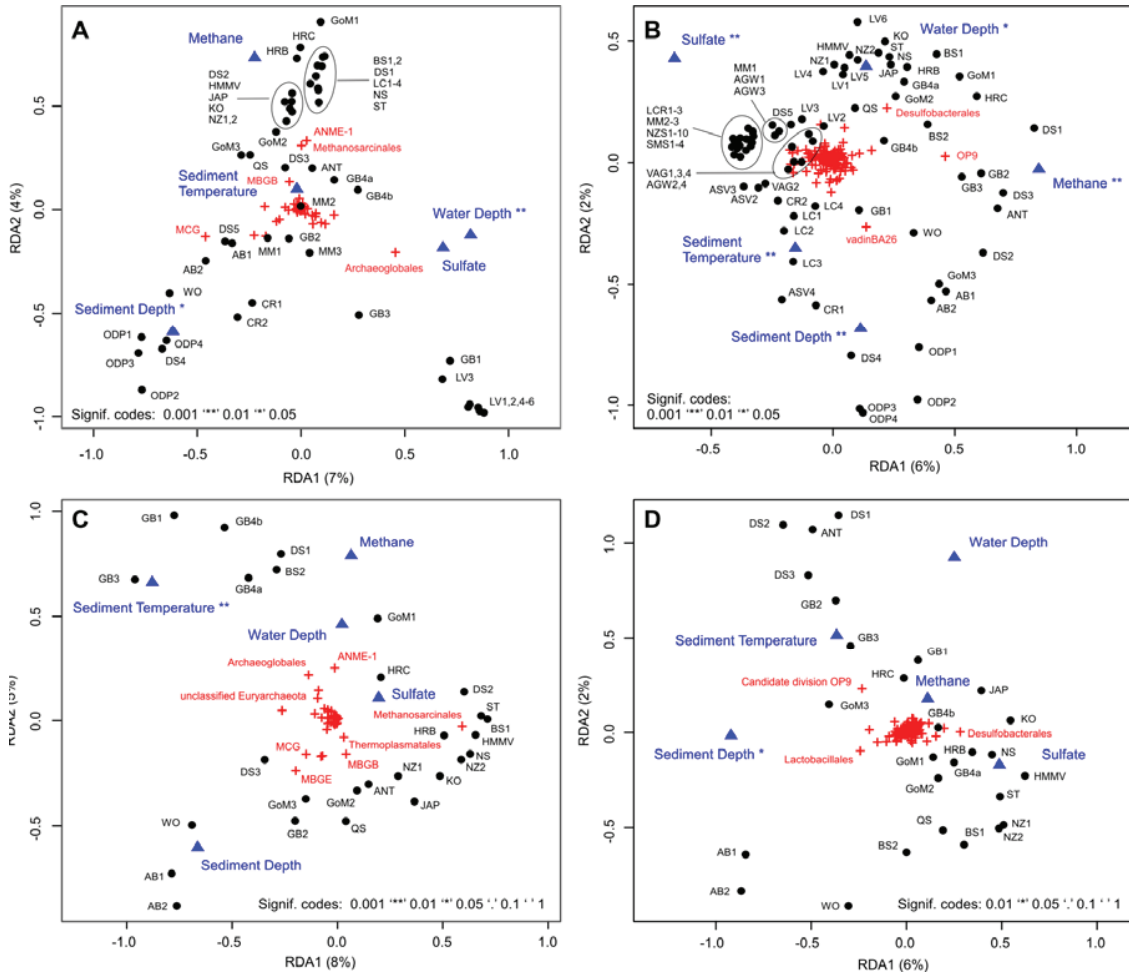


**Figure S5: Redundancy analysis of archaeal and bacterial diversity**

Redundancy analysis (RDA) based on relative abundance of archaeal (A,C) and bacterial (B,D) orders and five environmental parameters. A and B are based on all available samples, whereas C and D are based on the 27 methane-impacted ecosystems (23 methane seeps and 4 SMTZ). The plots show the full model considering all five parameters, which was highly significant for both domains. Black circles represent the microbial community of a given sample, environmental parameters are fitted to the ordination and represented as blue triangles. Microbial orders are depicted as red crosses. Note: In RDA plots environmental parameters and species are generally shown as centered arrows originating in point 0/0 (which represents the average and not zero). To simplify the plot we chose to show just the tips of the arrows as blue triangles or red crosses. Significance levels (marked by asterisks) were calculated for each parameter on its own using partial RDA. Total explained variation in case of the archaeal community is 15% in case of the bacterial community it is 11%. At methane-impacted ecosystems we could explain 16% of archaeal and 10% of bacterial variation.

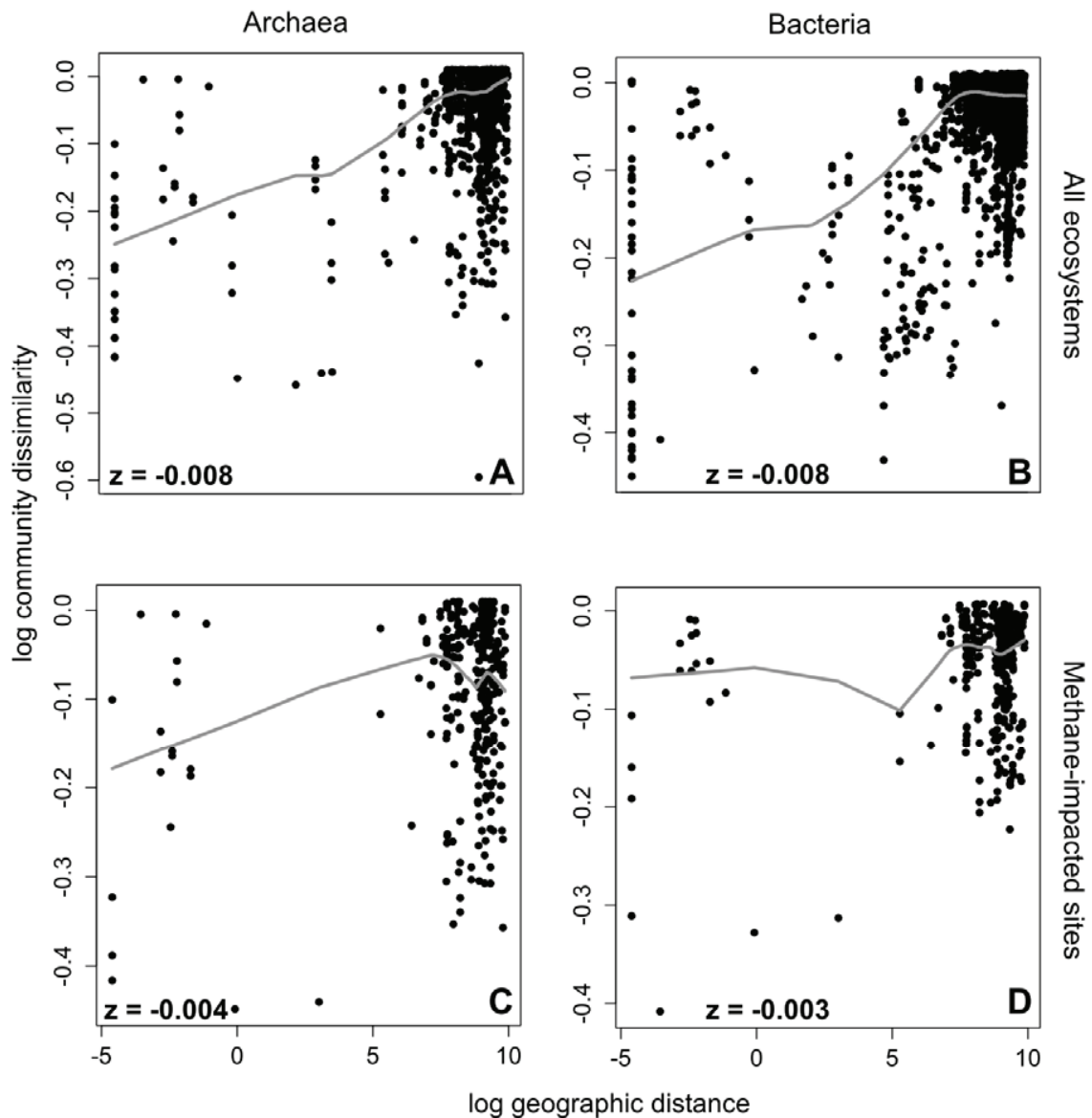


**Figure S6: Distance decay of microbial community similarity**

Distance decay (DD) of community similarity was calculated based on geographic and community distance matrices showing decreasing similarity of microbial communities (x-axis) with increasing geographic distance (y-axis). (A) and (C) show archaeal communities, (B) and (D) bacterial communities. The global dataset is shown in (A) and (B), whereas AOM habitats (23 methane seeps and four SMTZ) are represented by (C) and (D). The regression was calculated using a linear model. The slope  $z$  of each regression was highly significant ( $p > 0.001$ ) as determined by ANOVA and 1000 permutations.

**Table S1: Contextual data of methane-impacted samples**

| Site | Environment                  | Lat      | Lon       | Water depth (m) | Sediment depth (cmbsf) | T (°C) | CH <sub>4</sub> (cat) | SO <sub>4</sub> <sup>2-</sup> (cat) | Long-hurst Province | Long-hurst Biome | Prod index | Climate Zone | Sample Code | Sample Code |
|------|------------------------------|----------|-----------|-----------------|------------------------|--------|-----------------------|-------------------------------------|---------------------|------------------|------------|--------------|-------------|-------------|
|      |                              |          |           |                 |                        |        |                       |                                     |                     |                  |            |              | Bacteria    | Archaea     |
| GoM1 | Gulf of Mexico (in mat)      | 28.5147  | -88.2952  | 890             | 12.0                   | 5      | 4                     | 1                                   | CARB                | T                | 2          | ST           | GMS-0003    | GMS-0004    |
| GoM2 | Gulf of Mexico (outside mat) | 28.5147  | -88.2952  | 890             | 12.0                   | 5      | 2                     | 6                                   | CARB                | T                | 2          | ST           | GMS-0005    | GMS-0006    |
| ST   | Storegga Seep enrichment     | 65.5178  | 5.4747    | 721             | 5.0                    | -1     | 4                     | 6                                   | SARC                | P                | 3          | P            | GMS-0013    | GMS-0014    |
| BS2  | Black Sea nodule pink        | 44.7750  | 31.9922   | 225             | 0.1                    | 8      | 4                     | 5                                   | MEDI                | W                | 2          | TEM          | MET003      | MET004      |
| GB4a | Guaymas 4484 1cm             | 27.0065  | -111.4096 | 2000            | 1.0                    | 2      | 4                     | 6                                   | CAMR                | C                | 3          | ST           | GMS-0018    | GMS-0017    |
| GB4b | Guaymas 4484 4cm             | 27.0065  | -111.4096 | 2000            | 5.0                    | 50     | 4                     | 3                                   | CAMR                | C                | 3          | ST           | GMS-0020    | GMS-0019    |
| ANT  | Extinct Antarctic Seep       | -65.4350 | -61.4415  | 850             | 17.0                   | 2      | 1                     | 6                                   | APLR                | P                | 3          | P            | MET001      | MET002      |
| BS1  | Black Sea nodule black       | 44.7750  | 31.9922   | 225             | 0.1                    | 8      | 4                     | 5                                   | MEDI                | W                | 2          | TEM          | GMS-0015    | GMS-0016    |
| NS   | North Sea                    | 61.1733  | -2.2417   | 145             | 1.5                    | 8      | 5                     | 6                                   | NECS                | C                | 5          | P            | MET005      | MET006      |
| HMMV | Haakon Mosby Mud Volcano     | 72.0032  | 14.7205   | 1263            | 1.5                    | -1     | 4                     | 1                                   | SARC                | P                | 3          | P            | MET007      | MET008      |
| KO   | Kongo                        | 8.2083   | 11.5972   | 3172            | 3.0                    | 3      | 1                     | 5                                   | ETRA                | T                | 2          | T            | MET009      | MET010      |
| JAP  | Japan                        | 39.1059  | 143.8927  | 5347            | 5.0                    | 1      | 2                     | 3                                   | KURO                | W                | 2          | ST           | MET011      | MET012      |
| HRB  | Hydrate Ridge_Beg            | 44.5684  | -125.1468 | 777             | 4.0                    | 4      | 5                     | 4                                   | CCAL                | C                | 3          | TEM          | MET013      | MET014      |
| HRC  | Hydrate Ridge_Calyptogena    | 44.5698  | -125.1475 | 787             | 4.0                    | 4      | 5                     | 5                                   | CCAL                | C                | 3          | TEM          | MET015      | MET016      |
| CR   | Costa Rica                   | 8.8500   | -84.2148  | 400             | 5.0                    | 9      | 2                     | 3                                   | CAMR                | C                | 3          | T            | MET017      | MET018      |
| NZA  | New Zealand 309              | -41.7821 | 175.4020  | 1056            | 5.0                    | 4      | 3                     | 5                                   | NEWZ                | C                | 3          | TEM          | MET019      | MET020      |
| NZB  | New Zealand 315              | -41.8458 | 175.6347  | 1058            | 5.0                    | 4      | 3                     | 4                                   | NEWZ                | C                | 3          | TEM          | MET021      | MET022      |
| GB3  | Guaymas 4489                 | 27.0074  | -111.4089 | 2000            | 6.0                    | 85     | 4                     | 6                                   | CAMR                | C                | 3          | ST           | MET023      | MET024      |
| GB2  | Guaymas 4486                 | 27.0077  | -111.4088 | 2000            | 7.0                    | 25     | 4                     | 6                                   | CAMR                | C                | 3          | ST           | MET025      | MET026      |
| GB1  | Guaymas 4483                 | 27.0065  | -111.4087 | 2000            | 9.0                    | 15     | 4                     | 4                                   | CAMR                | C                | 3          | ST           | MET027      | MET028      |
| DS1  | Gulf of Cadiz                | 35.5617  | -9.5072   | 3860            | 87.5                   | 17     | 4                     | 1                                   | CNRY                | C                | 5          | ST           | CFU_01      | CFU_02      |
| DS2  | Gulf of Cadiz                | 35.6607  | -7.3342   | 1326            | 42.5                   | 17     | 4                     | 1                                   | CNRY                | C                | 5          | ST           | CFU_03      | CFU_04      |
| DS3  | Gulf of Cadiz                | 35.6616  | -7.3347   | 1326            | 67.5                   | 17     | 4                     | 1                                   | CNRY                | C                | 5          | ST           | CFU_05      | CFU_06      |
| WO   | White Oak River              | 34.7415  | -77.1241  | 2               | 24.0                   | 11     | 3                     | 2                                   | NWCS                | C                | 4          | ST           | GMS-0001    | GMS-0002    |
| GoM3 | Gulf of Mexico (deep/MC118)  | 28.5126  | -88.2940  | 890             | 212.0                  | 6      | 4                     | 1                                   | CARB                | T                | 2          | ST           | GMS-0007    | GMS-0008    |
| AB1  | Aarhus GC174_16              | 56.1179  | 10.3482   | 15              | 149.5                  | 8      | 2                     | 3                                   | NECS                | C                | 5          | TEM          | MET029      | MET030      |
| AB2  | Aarhus GC174_17              | 56.1179  | 10.3482   | 15              | 169.5                  | 8      | 3                     | 2                                   | NECS                | C                | 5          | TEM          | MET031      | MET032      |

Methane concentrations are presented in categories: 0: 0-0.001 mM; 1: 0.001-0.01 mM; 2: 0.01-0.1 mM; 3: 0.1-1 mM; 4: 1-10 mM; 5: 10-100 mM  
Sulfate concentrations are presented in categories: 1: 0-1 mM; 2: 1-2 mM; 3: 2-5 mM; 4: 5-10 mM; 5: 10-20 mM; 6: 20-30 mM  
The ICOMM contextual geospatial parameters are available on the web (VAMPS website: <http://vamps.mbl.edu>, MICROBIS website: <http://icommm.mbl.edu/microbis>).  
Additional data are from references: Longhurst et al. 1995; Knittel et al. 2007; Wegener et al. 2008; Niemann et al. 2009; Aquilina et al. 2010; Zinke et al. 2010; Lichtschlag et al. 2010; Lloyd et al. 2010; Sommer et al. 2011; Lloyd et al. 2011; Biddle et al. 2012; Pop Ristova et al. 2012; Ruff et al. 2013; Felden et al. submitted

**Table S2: Contextual data of reference sediments containing archaeal and bacterial V6 tags**

| Site | Environment           | Lat      | Lon       | Water depth (m) | Sediment depth (cmbsf) | T (°C) | CH <sub>4</sub> (cat) | SO <sub>4</sub> <sup>2-</sup> (cat) | Long-hurst Province | Long-hurst Biome | Prod index | Climate Zone | Sample Code Bacteria | Sample Code Archaea |
|------|-----------------------|----------|-----------|-----------------|------------------------|--------|-----------------------|-------------------------------------|---------------------|------------------|------------|--------------|----------------------|---------------------|
| LV1  | Lau Hydrothermal Vent | -20.3167 | -176.1363 | 2707            | 0.0                    | 3      | 1                     | 6                                   | SPSG                | T                | 1          | T            | ALR_01               | ALR_09              |
| LV2  | Lau Hydrothermal Vent | -20.3179 | -176.1374 | 2714            | 0.0                    | 3      | 1                     | 6                                   | SPSG                | T                | 1          | T            | ALR_02               | ALR_10              |
| LV3  | Lau Hydrothermal Vent | -22.1807 | -176.6012 | 1908            | 0.0                    | 3      | 1                     | 6                                   | SPSG                | T                | 1          | T            | ALR_04               | ALR_12              |
| LV4  | Lau Hydrothermal Vent | -20.0530 | -176.1337 | 2619            | 0.0                    | 3      | 1                     | 6                                   | SPSG                | T                | 1          | T            | ALR_08               | ALR_16              |
| LV5  | Lau Hydrothermal Vent | -20.3167 | -176.1363 | 2707            | 0.0                    | 3      | 1                     | 6                                   | SPSG                | T                | 1          | T            | ALR_17               | ALR_18              |
| LV6  | Lau Hydrothermal Vent | -20.3167 | -176.1363 | 2707            | 0.0                    | 3      | 1                     | 6                                   | SPSG                | T                | 1          | T            | ALR_19               | ALR_20              |
| DS4  | Peru Margin           | -11.0645 | -78.0778  | 262             | 3505.0                 | 15     | 2                     | 3                                   | CHIL                | C                | 2          | T            | CFU_07               | CFU_08              |
| DS5  | North Sea             | 51.8781  | 0.9335    | 1               | 2.5                    | 13     | 4                     | 4                                   | NECS                | C                | 5          | TEM          | CFU_11               | CFU_12              |
| MM1  | North Sea             | 53.4922  | 6.1399    | 0               | 0.3                    | 8      | 0                     | 6                                   | NECS                | C                | 5          | TEM          | CMM_02               | CMM_11              |
| MM2  | North Sea             | 53.4922  | 6.1399    | 0               | 0.3                    | 18     | 0                     | 6                                   | NECS                | C                | 5          | TEM          | CMM_05               | CMM_14              |
| MM3  | North Sea             | 53.4922  | 6.1399    | 0               | 0.3                    | 17     | 0                     | 6                                   | NECS                | C                | 5          | TEM          | CMM_08               | CMM_17              |
| CR1  | Oahu                  | 21.4667  | -157.8    | 1               | 1.0                    | 25     | 0                     | 6                                   | NPTG                | T                | 1          | ST           | CRS_01               | CRS_06              |
| CR2  | Oahu                  | 21.4667  | -157.8    | 1               | 50.0                   | 25     | 0                     | 6                                   | NPTG                | T                | 1          | ST           | CRS_04               | CRS_07              |
| LC1  | Lost City             | 30.124   | -42.1193  | 827             | 0.0                    | 7      | 1                     | 6                                   | NASW                | W                | 1          | ST           | LCY_01               | LCY_12              |
| LC2  | Lost City             | 30.124   | -42.1193  | 782             | 0.0                    | 73     | 1                     | 6                                   | NASW                | W                | 1          | ST           | LCY_03               | LCY_14              |
| LC3  | Lost City             | 30.124   | -42.1193  | 735             | 0.0                    | 81     | 1                     | 6                                   | NASW                | W                | 1          | ST           | LCY_05               | LCY_16              |
| LC4  | Lost City             | 30.124   | -42.1193  | 782             | 0.0                    | 73     | 1                     | 6                                   | NASW                | W                | 1          | ST           | LCY_07               | LCY_18              |
| ODP1 | Peru Margin           | -10.9833 | -77.95    | 150             | 250.0                  | 14     | 1                     | 5                                   | CHIL                | C                | 2          | T            | ODP_10               | ODP_09              |
| ODP2 | Peru Margin           | -10.9833 | -77.95    | 150             | 3015.0                 | 15     | 3                     | 1                                   | CHIL                | C                | 2          | T            | ODP_12               | ODP_11              |
| ODP3 | Peru Margin           | -10.9833 | -77.95    | 150             | 5035.0                 | 15     | 4                     | 1                                   | CHIL                | C                | 2          | T            | ODP_14               | ODP_13              |
| ODP4 | Peru Margin           | -10.9833 | -77.95    | 150             | 9145.0                 | 17     | 3                     | 1                                   | CHIL                | C                | 2          | T            | ODP_16               | ODP_15              |

Methane concentrations are presented in categories: 0: 0-0.001 mM; 1: 0.001-0.01 mM; 2: 0.01-0.1 mM; 3: 0.1-1 mM; 4: 1-10 mM; 5: 10-100 mM  
Sulfate concentrations are presented in categories: 1: 0-1 mM; 2: 1-2 mM; 3: 2-5 mM; 4: 5-10 mM; 5: 10-20 mM; 6: 20-30 mM  
The ICOMM contextual geospatial parameters are available on the web (VAMPS website: <http://vamaps.mbl.edu>, MICROBIS website: <http://icomm.mbl.edu/microbis>).  
Additional data are from reference: Longhurst et al. 1995

**Table S3: Contextual data of reference sediments containing bacterial V6 tags**

| Site  | Environment                 | Lat     | Lon      | Water depth (m) | Sediment depth (cmbsf) | T (°C) | CH <sub>4</sub> (log) | SO <sub>4</sub> <sup>2-</sup> (cat) | Long-hurst Province | Long-hurst Biome | Prod index | Climate Zone | Sample Code Bacteria |
|-------|-----------------------------|---------|----------|-----------------|------------------------|--------|-----------------------|-------------------------------------|---------------------|------------------|------------|--------------|----------------------|
| AGW1  | French Guiana Shallow Coast | 5.545   | -53.179  | 1               | 1.5                    | 28     | 0                     | 6                                   | GUIA                | C                | 5          | T            | AGW_0001             |
| AGW2  | French Guiana Shallow Coast | 5.545   | -53.179  | 1               | 8.5                    | 28     | 0                     | 6                                   | GUIA                | C                | 5          | T            | AGW_0002             |
| AGW3  | French Guiana Deep Coast    | 5.543   | -52.197  | 52              | 1.5                    | 28     | 0                     | 6                                   | GUIA                | C                | 5          | T            | AGW_0003             |
| AGW4  | French Guiana Deep Coast    | 5.543   | -52.197  | 52              | 8.5                    | 28     | 0                     | 6                                   | GUIA                | C                | 5          | T            | AGW_0004             |
| ASV1  | Azores Shallow Vent         | 37.724  | -25.319  | 7               | 0                      | 60     | 1                     | 6                                   | NASE                | W                | 1          | ST           | ASV_0007             |
| ASV2  | Azores Shallow Vent         | 37.724  | -25.319  | 6               | 0                      | 60     | 1                     | 6                                   | NASE                | W                | 1          | ST           | ASV_0008             |
| ASV3  | Azores Shallow Vent         | 38.233  | -26.633  | 20              | 0                      | 40     | 1                     | 6                                   | NASE                | W                | 1          | ST           | ASV_0015             |
| ASV4  | Azores Shallow Vent         | 38.233  | -26.633  | 20              | 0                      | 40     | 1                     | 6                                   | NASE                | W                | 1          | ST           | ASV_0016             |
| LCR1  | Caribbean Shallow Reef      | 17.939  | -67.048  | 2               | n.a.                   | 28     | 0                     | 6                                   | CARB                | T                | 2          | T            | LCR_0001             |
| LCR2  | Caribbean Deep Reef         | 17.876  | -67.040  | 50              | n.a.                   | 25     | 0                     | 6                                   | CARB                | T                | 2          | T            | LCR_0003             |
| LCR3  | South Argentina Intertidal  | -42.426 | -64.118  | 0               | 0                      | 10     | 0                     | 6                                   | FKLD                | C                | 4          | TEM          | LCR_0015             |
| NZS1  | New Zealand Deep Sea        | -43.288 | -175.553 | 644             | 1.5                    | 16     | 0                     | 6                                   | NEWZ                | C                | 3          | TEM          | NZS_0002             |
| NZS2  | New Zealand Deep Sea        | -42.782 | -176.714 | 1025            | 1.5                    | 16     | 0                     | 6                                   | NEWZ                | C                | 3          | TEM          | NZS_0003             |
| NZS3  | New Zealand Deep Sea        | -42.992 | 175.930  | 1197            | 1.5                    | 15     | 0                     | 6                                   | NEWZ                | C                | 3          | TEM          | NZS_0004             |
| NZS4  | New Zealand Deep Sea        | -42.992 | 178.992  | 530             | 1.5                    | 16     | 0                     | 6                                   | NEWZ                | C                | 3          | TEM          | NZS_0005             |
| NZS5  | New Zealand Deep Sea        | -44.126 | 178.645  | 516             | 1.5                    | 14     | 0                     | 6                                   | NEWZ                | C                | 3          | TEM          | NZS_0006             |
| NZS6  | New Zealand Deep Sea        | -44.485 | 177.141  | 1241            | 1.5                    | 13     | 0                     | 6                                   | NEWZ                | C                | 3          | TEM          | NZS_0007             |
| NZS7  | New Zealand Deep Sea        | -43.520 | -178.618 | 424             | 1.5                    | 15     | 0                     | 6                                   | NEWZ                | C                | 3          | TEM          | NZS_0009             |
| NZS8  | New Zealand Deep Sea        | -44.015 | 178.519  | 766             | 1.5                    | 14     | 0                     | 6                                   | NEWZ                | C                | 3          | TEM          | NZS_0010             |
| NZS9  | New Zealand Deep Sea        | -42.531 | -178.339 | 1400            | 1.5                    | 16     | 0                     | 6                                   | NEWZ                | C                | 3          | TEM          | NZS_0011             |
| NZS10 | New Zealand Deep Sea        | -38.620 | 167.526  | 482             | 1.5                    | 17     | 0                     | 6                                   | TASM                | W                | 2          | TEM          | NZS_0012             |
| SMS1  | East Pacific Station M      | 35.164  | -123.016 | 3953            | n.a.                   | 1      | 0                     | 6                                   | CCAL                | C                | 3          | TEM          | SMS_0007             |
| SMS2  | East Pacific Station M      | 35.164  | -123.016 | 3953            | n.a.                   | 1      | 0                     | 6                                   | CCAL                | C                | 3          | TEM          | SMS_0008             |
| SMS3  | East Pacific Station M      | 35.164  | -123.016 | 3953            | n.a.                   | 1      | 0                     | 6                                   | CCAL                | C                | 3          | TEM          | SMS_0010             |
| SMS4  | East Pacific Station M      | 35.164  | -123.016 | 3953            | n.a.                   | 1      | 0                     | 6                                   | CCAL                | C                | 3          | TEM          | SMS_0011             |
| VAG1  | Chilean Coastal Sands       | -36.690 | -73.070  | 15              | 2.5                    | 13     | 0                     | 6                                   | CHIL                | C                | 2          | TEM          | VAG_0009             |
| VAG2  | Chilean Coastal Sands       | -36.640 | -73.040  | 27              | 2.5                    | 11     | 0                     | 6                                   | CHIL                | C                | 2          | TEM          | VAG_0010             |
| VAG3  | Chilean Coastal Sands       | -36.600 | -73.000  | 35              | 2.5                    | 12     | 0                     | 6                                   | CHIL                | C                | 2          | TEM          | VAG_0011             |
| VAG4  | Chilean Coastal Sands       | -36.510 | -73.120  | 88              | 2.5                    | 10     | 0                     | 6                                   | CHIL                | C                | 2          | TEM          | VAG_0012             |

Methane concentrations are presented in categories: 0: 0-0.001 mM, 1: 0.001-0.01 mM, 2: 0.01-0.1 mM, 3: 0.1-1 mM, 4: 1-10 mM, 5: 10-100 mM  
Sulfate concentrations are presented in categories: 1: 0-1 mM, 2: 1-2 mM, 3: 2-5 mM, 4: 5-10 mM, 5: 10-20 mM, 6: 20-30 mM  
The ICOMM contextual geospatial parameters are available on the web (VAMPS website: <http://vammps.mbl.edu>, MICROBIS website: <http://fcomm.mbl.edu/microbis>).  
Additional data are from reference: Loughurst et al. 1995

**Table S4: Sequencing details of samples containing archaeal and bacterial data**

| Site | Quality Reads |       | OTU <sub>0.03</sub> |                       |      |                        | Inv Simpson |      | Chao1 |      |
|------|---------------|-------|---------------------|-----------------------|------|------------------------|-------------|------|-------|------|
|      | Bac           | Arch  | Bac                 | Bac <sub>3000</sub> * | Arch | Arch <sub>3000</sub> * | Bac         | Arch | Arch  | Bac  |
| WO   | 14375         | 16394 | 4190                | 1499                  | 953  | 421                    | 296.5       | 20.4 | 846   | 4217 |
| GoM1 | 17754         | 14365 | 2897                | 874                   | 336  | 164                    | 57.9        | 9.4  | 394   | 2762 |
| GoM2 | 14048         | 14622 | 4444                | 1575                  | 650  | 284                    | 370.6       | 19.4 | 687   | 5035 |
| GoM3 | 12364         | 6182  | 1206                | 588                   | 385  | 269                    | 28.5        | 18.2 | 501   | 1281 |
| ST   | 22912         | 15043 | 3498                | 990                   | 216  | 93                     | 97.4        | 1.7  | 159   | 2844 |
| BS2  | 17392         | 13739 | 1726                | 569                   | 134  | 57                     | 30.2        | 1.6  | 128   | 1497 |
| GB4a | 21617         | 9254  | 4510                | 1206                  | 726  | 401                    | 128.2       | 18.6 | 904   | 3838 |
| GB4b | 9018          | 12600 | 1515                | 817                   | 691  | 315                    | 86.5        | 10.0 | 578   | 1529 |
| LC1  | 8165          | 27510 | 492                 | 291                   | 192  | 64                     | 15.0        | 2.4  | 91    | 534  |
| LC2  | 3688          | 30829 | 263                 | 239                   | 195  | 54                     | 10.5        | 1.4  | 171   | 395  |
| LC3  | 14305         | 16469 | 380                 | 173                   | 239  | 73                     | 9.0         | 1.8  | 126   | 337  |
| LC4  | 6973          | 24435 | 625                 | 414                   | 193  | 59                     | 25.4        | 1.4  | 329   | 750  |
| ANT  | 27721         | 20516 | 1166                | 355                   | 397  | 133                    | 4.5         | 5.6  | 333   | 781  |
| BS1  | 20351         | 25498 | 1234                | 376                   | 302  | 108                    | 16.6        | 1.5  | 178   | 842  |
| NS   | 16765         | 25963 | 2099                | 690                   | 485  | 153                    | 67.5        | 2.1  | 325   | 1691 |
| HMMV | 53605         | 15385 | 3668                | 664                   | 217  | 78                     | 35.3        | 1.2  | 136   | 1777 |
| KO   | 12446         | 10074 | 1498                | 650                   | 333  | 177                    | 37.8        | 3.3  | 371   | 1600 |
| JAP  | 25785         | 21080 | 3856                | 921                   | 631  | 196                    | 120.8       | 6.1  | 577   | 2549 |
| HRB  | 30463         | 33665 | 5810                | 1131                  | 1199 | 257                    | 120.5       | 7.9  | 690   | 3850 |
| HRC  | 26048         | 30925 | 4340                | 947                   | 1149 | 296                    | 54.0        | 17.8 | 737   | 2726 |
| QS   | 16005         | 21950 | 5351                | 1613                  | 1386 | 420                    | 461.7       | 12.4 | 1106  | 5145 |
| NZ1  | 18425         | 24541 | 3947                | 1135                  | 1015 | 265                    | 51.1        | 7.8  | 615   | 3446 |
| NZ2  | 27493         | 22973 | 6626                | 1330                  | 585  | 181                    | 181.7       | 3.5  | 395   | 4207 |
| GB3  | 12074         | 22525 | 3167                | 1131                  | 1095 | 329                    | 31.7        | 11.0 | 809   | 4554 |
| GB2  | 20146         | 25446 | 3011                | 830                   | 1087 | 311                    | 11.4        | 12.2 | 831   | 2558 |
| GB1  | 19779         | 11865 | 955                 | 360                   | 440  | 174                    | 8.8         | 4.4  | 463   | 583  |
| AB1  | 19101         | 17460 | 1893                | 562                   | 699  | 245                    | 17.3        | 3.8  | 452   | 1760 |
| AB2  | 18755         | 22592 | 1553                | 480                   | 830  | 284                    | 5.2         | 7.6  | 739   | 1407 |
| LV1  | 21468         | 12267 | 1595                | 440                   | 402  | 186                    | 5.2         | 12.0 | 547   | 1065 |
| LV2  | 12080         | 9232  | 1014                | 439                   | 203  | 122                    | 14.2        | 1.9  | 221   | 1096 |
| LV3  | 16556         | 5135  | 1779                | 634                   | 236  | 178                    | 16.7        | 4.9  | 368   | 1886 |
| LV4  | 7212          | 15068 | 763                 | 477                   | 241  | 95                     | 19.4        | 1.5  | 223   | 1016 |
| LV5  | 18148         | 12756 | 1017                | 376                   | 387  | 154                    | 3.9         | 3.1  | 353   | 918  |
| LV6  | 25264         | 12488 | 1529                | 460                   | 512  | 203                    | 17.8        | 11.6 | 635   | 1027 |
| DS1  | 17217         | 18271 | 1040                | 331                   | 268  | 97                     | 11.2        | 1.8  | 183   | 973  |
| DS2  | 22472         | 9738  | 865                 | 279                   | 130  | 80                     | 6.8         | 1.9  | 186   | 616  |
| DS3  | 9578          | 23015 | 1540                | 711                   | 832  | 252                    | 7.6         | 10.5 | 538   | 2065 |
| DS4  | 12996         | 12822 | 1326                | 598                   | 383  | 161                    | 33.7        | 4.8  | 339   | 1240 |
| DS5  | 34012         | 16262 | 8973                | 1665                  | 1641 | 592                    | 524.1       | 44.9 | 1687  | 6138 |
| MM1  | 22933         | 5065  | 4945                | 1213                  | 1003 | 693                    | 186.0       | 58.2 | 1755  | 3844 |
| MM2  | 15528         | 3098  | 3224                | 1053                  | 509  | 502                    | 151.4       | 37.1 | 1265  | 2992 |
| MM3  | 19353         | 5327  | 4364                | 1252                  | 1203 | 812                    | 204.2       | 63.9 | 2617  | 3302 |
| CR1  | 10763         | 7711  | 1273                | 661                   | 898  | 553                    | 19.1        | 19.2 | 1028  | 1330 |
| CR2  | 12408         | 11287 | 3849                | 1546                  | 988  | 549                    | 188.3       | 52.4 | 996   | 4301 |
| ODP1 | 13391         | 24002 | 1937                | 842                   | 550  | 176                    | 99.1        | 9.3  | 348   | 1860 |
| ODP2 | 17006         | 15651 | 1791                | 676                   | 177  | 69                     | 69.7        | 3.7  | 151   | 1462 |
| ODP3 | 16565         | 16182 | 2201                | 909                   | 301  | 119                    | 119.6       | 6.0  | 250   | 1827 |
| ODP4 | 12336         | 7267  | 1629                | 726                   | 186  | 124                    | 67.9        | 11.0 | 257   | 1536 |

\* standardized numbers of OTU<sub>0.03</sub> based on resampling of 3000 sequences without replacement

**Table S5: Sequencing details of samples containing bacterial data**

| Site  | Quality Reads | OTU <sub>0.03</sub> |           |             |       |
|-------|---------------|---------------------|-----------|-------------|-------|
|       |               | OTU <sub>0.03</sub> | Resampled | Inv Simpson | Chao1 |
| ASV1  | 8456          | 1424                | 721       | 296.7       | 5729  |
| ASV2  | 17300         | 1958                | 620       | 180.1       | 5263  |
| ASV3  | 18023         | 2773                | 896       | 337.6       | 6377  |
| ASV4  | 17881         | 950                 | 331       | 214.0       | 5261  |
| AGW1  | 35557         | 9184                | 1662      | 80.3        | 2088  |
| AGW2  | 20162         | 5721                | 1573      | 23.3        | 1836  |
| AGW3  | 23538         | 7333                | 1726      | 145.6       | 2388  |
| AGW4  | 18389         | 5362                | 1597      | 7.5         | 793   |
| LCR1  | 15171         | 4704                | 1629      | 306.2       | 5275  |
| LCR2  | 4701          | 2607                | 1869      | 526.0       | 6264  |
| LCR3  | 25604         | 6465                | 1513      | 285.3       | 4474  |
| VAG1  | 18488         | 5385                | 1527      | 274.0       | 4742  |
| VAG2  | 17942         | 4730                | 1335      | 76.2        | 4710  |
| VAG3  | 14784         | 4220                | 1408      | 96.3        | 4147  |
| VAG4  | 19473         | 5450                | 1553      | 329.9       | 4637  |
| NZS1  | 17715         | 6348                | 1687      | 371.2       | 6297  |
| NZS2  | 25783         | 8483                | 1759      | 412.2       | 6865  |
| NZS3  | 20111         | 6223                | 1588      | 398.6       | 5482  |
| NZS4  | 26337         | 8652                | 1713      | 375.1       | 6078  |
| NZS5  | 33401         | 8572                | 1530      | 357.4       | 5268  |
| NZS6  | 25882         | 7854                | 1667      | 363.6       | 6317  |
| NZS7  | 20901         | 7310                | 1821      | 537.3       | 7681  |
| NZS8  | 19900         | 8710                | 1980      | 604.2       | 8409  |
| NZS9  | 33365         | 11671               | 1978      | 719.4       | 8848  |
| NZS10 | 28897         | 10157               | 1902      | 599.9       | 8286  |
| SMS1  | 27080         | 7926                | 1747      | 521.4       | 5831  |
| SMS2  | 18150         | 6223                | 1704      | 515.5       | 5571  |
| SMS3  | 27652         | 6881                | 1532      | 273.2       | 4620  |
| SMS4  | 21233         | 5551                | 1471      | 178.8       | 4702  |

\* standardized numbers of OTU<sub>0.03</sub> based on resampling of 3000 sequences without replacement

**Table S6: Indicator species for marine ecosystems**

| Bacterial taxa*<br>(class level and higher) | Seafloor<br>realm | Indicator<br>Value** | p Value | Archaeal taxa*<br>(class level and higher) | Seafloor<br>realm | Indicator<br>Value** | p Value |
|---|-------------------|----------------------|---------|--|-------------------|----------------------|---------|
| SAR202 ( <i>Chloroflexi</i> )               | 1                 | 0.80                 | 0.001   | Marine Group I                             | 2                 | 0.89                 | 0.003   |
| <i>Verrucomicrobia</i> unclassified         | 1                 | 0.74                 | 0.001   | <i>Methanobacteria</i>                     | 2                 | 0.85                 | 0.001   |
| JTB23 ( <i>Proteobacteria</i> )             | 1                 | 0.71                 | 0.001   | AK31 ( <i>Thaumarchaeota</i> )             | 2                 | 0.83                 | 0.001   |
| <i>Gemmatimonadetes</i>                     | 1                 | 0.67                 | 0.001   | Ancient Archaeal Group                     | 2                 | 0.81                 | 0.001   |
| KD4.96 ( <i>Chloroflexi</i> )               | 1                 | 0.66                 | 0.001   | pSL12 ( <i>Crenarchaeota</i> )             | 2                 | 0.78                 | 0.001   |
| OM190 ( <i>Planctomycetes</i> )             | 1                 | 0.64                 | 0.001   | South African Gold Mine Gp 1               | 2                 | 0.64                 | 0.002   |
| RB25 ( <i>Acidobacteria</i> )               | 1                 | 0.63                 | 0.001   | pMC2A209 ( <i>Crenarchaeota</i> )          | 2                 | 0.62                 | 0.002   |
| <i>Thermomicrobia</i>                       | 1                 | 0.57                 | 0.001   | Marine Benthic Group A                     | 2                 | 0.45                 | 0.04    |
| <i>Acidobacteria</i>                        | 1                 | 0.55                 | 0.001   | <i>Methanomicrobia</i>                     | 3                 | 0.41                 | 0.002   |
| Arctic97B.4 ( <i>Verrucomicrobia</i> )      | 1                 | 0.47                 | 0.002   | Soil Crenarchaeotic Group                  | 4                 | 0.62                 | 0.035   |
| <i>Acidimethylosilex</i>                    | 1                 | 0.46                 | 0.002   | <i>Methanopyri</i>                         | 5                 | 0.63                 | 0.007   |
| <i>Planctomycetacia</i>                     | 1                 | 0.43                 | 0.001   | Misc. Crenarchaeotic Group                 | 5                 | 0.58                 | 0.011   |
| Candidate division GOUTA4                   | 1                 | 0.42                 | 0.004   | <i>Thermococci</i>                         | 6                 | 0.59                 | 0.011   |
| ML602M.17 ( <i>Bacteroidetes</i> )          | 1                 | 0.42                 | 0.007   | Candidatus <i>Korarchaeum</i>              | 6                 | 0.57                 | 0.024   |
| <i>Holophagae</i>                           | 1                 | 0.42                 | 0.001   | <i>Archaeoglobi</i>                        | 6                 | 0.54                 | 0.047   |
| vadinHA49 ( <i>Planctomycetes</i> )         | 1                 | 0.42                 | 0.003   | <i>Methanococci</i>                        | 6                 | 0.50                 | 0.009   |
| Chloroplast                                 | 2                 | 0.79                 | 0.001   |  |                   |                      |         |
| OPB35 ( <i>Verrucomicrobia</i> )            | 2                 | 0.56                 | 0.003   |  |                   |                      |         |
| SM1A07 ( <i>Bacteroidetes</i> )             | 2                 | 0.53                 | 0.002   |  |                   |                      |         |
| Candidate division WS6                      | 2                 | 0.52                 | 0.008   |  |                   |                      |         |
| Candidate division Hyd24.12                 | 3                 | 0.69                 | 0.005   |  |                   |                      |         |
| Candidate phylum JS1                        | 3                 | 0.64                 | 0.004   |  |                   |                      |         |
| <i>Deltaproteobacteria</i>                  | 3                 | 0.35                 | 0.003   |  |                   |                      |         |
| GIF9 ( <i>Chloroflexi</i> )                 | 4                 | 0.86                 | 0.003   |  |                   |                      |         |
| <i>Chlorobia</i>                            | 4                 | 0.61                 | 0.003   |  |                   |                      |         |
| vadinBA26 ( <i>Chloroflexi</i> )            | 5                 | 0.75                 | 0.001   |  |                   |                      |         |
| MLE1.12 ( <i>Cyanobacteria</i> )            | 5                 | 0.58                 | 0.002   |  |                   |                      |         |
| <i>Epsilonproteobacteria</i>                | 6                 | 0.84                 | 0.002   |  |                   |                      |         |

Seafloor realms:

- 1: Deep-sea surface (lacking archaeal data)
- 2: Coastal sands
- 3: Methane seeps
- 4: SMTZ
- 5: Subsurface
- 6: Hydrothermal Vents

\* Taxonomy is based on ARB/SILVA (Quast et al. 2013)

\*\* Indicator Taxa are based on relative abundance and relative frequency of occurrence (Dufréne and Legendre 1997)

**Table S7: Comparison of culture independent methods**

| Cold seep  | Organism | V6 tag | 16S rRNA | FISH |
|--|----------|--------|----------|------|
| Haakon Mosby Mud Volcano<br><i>Beggiatoa</i> Mat | ANME-1   | -      | -        | -    |
|  | ANME-2   | +      | -        | -    |
|  | ANME-3   | +++    | +++      | +++  |
| Hydrate Ridge<br><i>Beggiatoa</i> Mat            | ANME-1   | ++     | ++       | ++   |
|  | ANME-2   | +++    | +++      | +++  |
|  | ANME-3   | +      | +        | n.d. |
| New Zealand<br><i>Beggiatoa</i> Mat              | ANME-1   | +      | -        | -    |
|  | ANME-2   | +++    | +++      | +++  |
|  | ANME-3   | ++     | ++       | +    |
| Gulfaks<br><i>Beggiatoa</i> Mat                  | ANME-1   | +      | -        | +    |
|  | ANME-2   | +++    | +++      | +++  |
|  | ANME-3   | +      | -        | -    |

- not detected, + present, ++ abundant, +++ dominant, n.d. not determined

**Table S8: Core bacterial orders of three seafloor realms in percent relative abundance**

| Bacterial Taxa* (order level and higher)     | Deep-Sea Surface | Deep Subsurface | Methane Seeps |
|--|------------------|-----------------|---------------|
| <i>Acidimicrobidae</i>                       | 3.8 **           | .               | .             |
| <i>Acidobacteriales</i>                      | 1.8              | .               | .             |
| <b><i>Actinobacteridae</i></b>               | 2.4              | 4.5             | 2.2           |
| <i>Alteromonadales</i>                       | 4.0              | .               | .             |
| <b><i>Bacillales</i></b>                     | 1.2              | 4.5             | 1.3           |
| BD2-11 ( <i>Gemmatimonadetes</i> )           | 2.0              | .               | .             |
| <i>Burkholderiales</i>                       | .                | 3.6             | .             |
| <b><i>Caldilineales</i></b>                  | .                | .               | 1.2           |
| <b>Candidate division JS1</b>                | .                | 2.0             | 16.9          |
| <i>Caulobacteriales</i>                      | 1.0              | .               | .             |
| <i>Chromatiales</i>                          | 2.5              | .               | .             |
| <b><i>Clostridiales</i></b>                  | 1.4              | 1.9             | 1.3           |
| <i>Desulfarculales</i>                       | .                | 2.3             | .             |
| <b><i>Desulfobacteriales</i></b>             | 1.9              | .               | 15.1          |
| <i>Desulfovibrionales</i>                    | .                | 1.5             | .             |
| <i>Desulfuromonadales</i>                    | 1.9              | .               | .             |
| <i>Enterobacteriales</i>                     | 1.3              | .               | .             |
| <b><i>Flavobacteriales</i></b>               | 2.3              | .               | 5.1           |
| <i>Gammaproteobacteria</i> unclassified      | 3.9              | 3.8             | .             |
| GIF3 ( <i>Chloroflexi</i> )                  | .                | 2.2             | .             |
| <i>Holophagales</i>                          | 1.2              | .               | .             |
| <b><i>Lactobacillales</i></b>                | .                | 2.2             | 3.0           |
| mle 1-8 ( <i>Phycisphaerae</i> )             | .                | 1.5             | .             |
| <i>Myxococcales</i>                          | 2.3              | .               | .             |
| <i>Nitrospirales</i>                         | 1.4              | .               | .             |
| <i>Oceanospirillales</i>                     | 2.3              | .               | .             |
| <i>Phycisphaerales</i>                       | 1.0              | .               | .             |
| <i>Planctomycetales</i>                      | 1.1              | .               | .             |
| <i>Proteobacteria</i> unclassified           | 1.1              | 2.2             | .             |
| <i>Pseudomonadales</i>                       | .                | 1.8             | .             |
| RB25 ( <i>Acidobacteria</i> )                | 1.8              | .               | .             |
| <i>Rhizobiales</i>                           | 3.3              | 1.2             | .             |
| <i>Rhodobacteriales</i>                      | 2.0              | .               | .             |
| <i>Rhodospirillales</i>                      | 2.4              | 2.1             | .             |
| Sh765B-TzT-29 ( <i>Deltaproteobacteria</i> ) | 2.7              | .               | .             |
| <b><i>Sphingobacteriales</i></b>             | 3.2              | .               | 2.5           |
| <b><i>Spirochaetales</i></b>                 | .                | .               | 1.1           |
| vadinBA26 ( <i>Chloroflexi</i> )             | .                | 22.7            | .             |
| <i>Xanthomonadales</i>                       | 2.8              | .               | .             |

\* Taxonomy is based on ARB-SILVA (Quast et al. 2013)

\*\* Boxes depict clades that occur exclusively or with a very high relative abundance in the respective realm  
Methane seep core taxa are in bold face

Table S9: Sequence read numbers of the most frequent key functional clades

**Table S9. Sequence read numbers of the most frequent methane seep key players**

| DS1   | DS2 | DS3 | GoM1 | GoM2 | ST    | BS2   | GB4a | GB4b | ANT   | BS1   | NS    | HMMV  | KO   | JAP  | HRB  | HRC  | QS   | NZ1  | NZ2   | GB3 | GB2 | GB1 | Total Reads | Clade              |
|-------|-----|-----|------|------|-------|-------|------|------|-------|-------|-------|-------|------|------|------|------|------|------|-------|-----|-----|-----|-------------|--------------------|
| 9     | 0   | 92  | 1930 | 2506 | 11246 | 26    | 0    | 0    | 122   | 20428 | 17370 | 75    | 545  | 415  | 8938 | 4203 | 4343 | 4371 | 11647 | 0   | 245 | 0   | 88511       | ANME2ab            |
| 46    | 0   | 8   | 577  | 447  | 4     | 0     | 0    | 0    | 883   | 0     | 7     | 13956 | 5455 | 29   | 6736 | 1885 | 13   | 6174 | 3395  | 0   | 27  | 0   | 39642       | ANME3              |
| 13189 | 44  | 883 | 2577 | 14   | 0     | 30    | 45   | 81   | 9     | 17    | 0     | 0     | 0    | 2    | 438  | 1511 | 0    | 0    | 0     | 0   | 0   | 0   | 18840       | ANME1              |
| 32    | 0   | 0   | 865  | 69   | 88    | 0     | 1    | 0    | 0     | 319   | 37    | 1     | 880  | 7022 | 3067 | 1359 | 114  | 133  | 18    | 0   | 56  | 0   | 14061       | ANME2c             |
| 0     | 0   | 538 | 890  | 111  | 0     | 10548 | 8    | 5    | 0     | 17    | 0     | 0     | 0    | 0    | 66   | 649  | 0    | 0    | 0     | 0   | 0   | 0   | 12832       | ANME1b             |
| 1     | 0   | 28  | 361  | 335  | 1570  | 4     | 0    | 27   | 23580 | 1941  | 25    | 32    | 32   | 1040 | 536  | 627  | 1590 | 637  | 1590  | 0   | 45  | 0   | 11411       | ANME2ab            |
| 106   | 0   | 492 | 3012 | 236  | 4     | 27    | 0    | 0    | 246   | 1     | 0     | 0     | 16   | 0    | 503  | 3811 | 0    | 1    | 0     | 0   | 0   | 0   | 8455        | ANME1b             |
| 5     | 0   | 3   | 0    | 0    | 0     | 1552  | 3336 | 0    | 0     | 0     | 0     | 0     | 0    | 0    | 40   | 21   | 0    | 0    | 0     | 1   | 0   | 2   | 4961        | ANME1              |
| 0     | 0   | 135 | 181  | 14   | 0     | 2329  | 1    | 0    | 0     | 0     | 0     | 0     | 0    | 0    | 13   | 194  | 0    | 0    | 0     | 0   | 0   | 0   | 2867        | ANME1b             |
| 2383  | 3   | 33  | 193  | 0    | 0     | 4     | 5    | 53   | 2     | 0     | 0     | 0     | 0    | 0    | 40   | 140  | 0    | 0    | 0     | 0   | 0   | 0   | 2856        | ANME1a             |
| 0     | 0   | 0   | 0    | 9    | 67    | 0     | 16   | 14   | 0     | 0     | 303   | 5488  | 114  | 73   | 130  | 61   | 2    | 2356 | 954   | 3   | 8   | 3   | 9601        | Methylococcales    |
| 0     | 0   | 0   | 0    | 0    | 0     | 0     | 0    | 0    | 0     | 0     | 0     | 3933  | 0    | 0    | 0    | 0    | 0    | 1    | 0     | 0   | 0   | 0   | 3934        | Methylococcales    |
| 0     | 0   | 0   | 1    | 26   | 98    | 0     | 6    | 15   | 0     | 0     | 826   | 11    | 51   | 149  | 122  | 54   | 5    | 110  | 329   | 1   | 2   | 0   | 1806        | Methylococcales    |
| 0     | 0   | 2   | 1    | 12   | 37    | 0     | 12   | 0    | 0     | 40    | 802   | 11    | 7    | 26   | 11   | 0    | 215  | 128  | 1     | 7   | 0   | 0   | 1312        | Methylococcales    |
| 0     | 0   | 0   | 0    | 0    | 50    | 0     | 0    | 0    | 0     | 0     | 816   | 35    | 34   | 16   | 8    | 0    | 0    | 157  | 91    | 1   | 0   | 44  | 1264        | Methylococcales    |
| 0     | 0   | 0   | 0    | 0    | 0     | 0     | 0    | 0    | 0     | 0     | 0     | 454   | 0    | 0    | 0    | 0    | 0    | 0    | 0     | 0   | 0   | 0   | 454         | Methylococcales    |
| 0     | 0   | 0   | 1    | 1    | 3     | 0     | 3    | 0    | 0     | 0     | 1     | 47    | 5    | 2    | 11   | 2    | 1    | 276  | 35    | 0   | 1   | 0   | 388         | Methylococcales    |
| 0     | 0   | 0   | 0    | 15   | 77    | 0     | 11   | 10   | 0     | 61    | 3     | 2     | 24   | 21   | 10   | 0    | 10   | 50   | 2     | 1   | 0   | 0   | 297         | Methylococcales    |
| 0     | 0   | 0   | 3    | 2    | 77    | 0     | 6    | 0    | 0     | 0     | 1     | 8     | 0    | 16   | 11   | 3    | 16   | 4    | 11    | 0   | 0   | 0   | 168         | Methylococcales    |
| 0     | 0   | 0   | 0    | 0    | 0     | 0     | 0    | 0    | 0     | 0     | 0     | 0     | 1    | 92   | 0    | 0    | 0    | 0    | 0     | 0   | 0   | 0   | 93          | Methylococcales    |
| 0     | 0   | 0   | 1126 | 127  | 423   | 21    | 0    | 0    | 0     | 405   | 223   | 2     | 24   | 615  | 497  | 208  | 99   | 54   | 835   | 1   | 1   | 0   | 4661        | Desulfobacteriales |
| 9     | 0   | 7   | 147  | 85   | 145   | 22    | 2    | 0    | 6     | 3133  | 192   | 0     | 3    | 79   | 191  | 124  | 117  | 12   | 94    | 76  | 85  | 121 | 4650        | Desulfobacteriales |
| 0     | 0   | 0   | 0    | 0    | 162   | 1     | 0    | 0    | 0     | 2738  | 1     | 567   | 0    | 3    | 44   | 4    | 0    | 0    | 62    | 0   | 0   | 0   | 3586        | Desulfobacteriales |
| 0     | 0   | 0   | 2    | 24   | 238   | 0     | 61   | 0    | 0     | 0     | 754   | 2     | 66   | 496  | 691  | 145  | 9    | 7    | 169   | 54  | 86  | 0   | 2804        | Desulfobacteriales |
| 0     | 0   | 35  | 150  | 16   | 328   | 218   | 802  | 335  | 0     | 3     | 0     | 0     | 0    | 0    | 106  | 704  | 3    | 0    | 0     | 5   | 3   | 20  | 2728        | Desulfobacteriales |
| 0     | 0   | 1   | 0    | 12   | 8     | 0     | 0    | 0    | 15    | 0     | 43    | 310   | 341  | 306  | 96   | 16   | 27   | 242  | 931   | 4   | 6   | 65  | 2423        | Desulfobacteriales |
| 0     | 0   | 0   | 0    | 0    | 0     | 0     | 0    | 0    | 0     | 0     | 0     | 2163  | 0    | 73   | 0    | 0    | 0    | 0    | 0     | 0   | 0   | 0   | 2236        | Desulfobacteriales |
| 0     | 0   | 0   | 0    | 0    | 0     | 0     | 1    | 0    | 0     | 0     | 28    | 980   | 14   | 10   | 468  | 45   | 21   | 268  | 50    | 0   | 3   | 26  | 1915        | Desulfobacteriales |
| 0     | 0   | 0   | 0    | 0    | 5     | 0     | 0    | 0    | 0     | 0     | 0     | 0     | 1459 | 71   | 0    | 0    | 0    | 0    | 1     | 1   | 0   | 0   | 1537        | Desulfobacteriales |
| 1     | 0   | 0   | 0    | 707  | 309   | 11    | 0    | 0    | 0     | 35    | 23    | 0     | 0    | 58   | 93   | 40   | 2    | 7    | 121   | 0   | 0   | 0   | 1486        | Desulfobacteriales |
| 0     | 0   | 2   | 5    | 71   | 598   | 0     | 4    | 0    | 0     | 0     | 221   | 47    | 129  | 500  | 474  | 275  | 39   | 78   | 139   | 85  | 106 | 0   | 2773        | Thiotrichales      |
| 0     | 0   | 0   | 0    | 0    | 0     | 0     | 288  | 223  | 0     | 0     | 0     | 0     | 0    | 0    | 0    | 0    | 0    | 0    | 0     | 1   | 1   | 13  | 536         | Thiotrichales      |
| 0     | 0   | 0   | 1    | 17   | 34    | 0     | 0    | 0    | 0     | 1     | 5     | 12    | 10   | 127  | 4    | 7    | 0    | 27   | 51    | 3   | 1   | 0   | 300         | Thiotrichales      |
| 0     | 0   | 0   | 0    | 0    | 17    | 123   | 0    | 0    | 0     | 0     | 12    | 3     | 3    | 11   | 40   | 18   | 2    | 0    | 15    | 6   | 6   | 0   | 257         | Thiotrichales      |
| 0     | 0   | 0   | 0    | 0    | 1     | 0     | 9    | 0    | 0     | 0     | 1     | 22    | 18   | 0    | 4    | 0    | 0    | 80   | 14    | 0   | 0   | 0   | 149         | Thiotrichales      |
| 0     | 0   | 0   | 0    | 2    | 32    | 0     | 2    | 0    | 0     | 0     | 2     | 0     | 0    | 16   | 26   | 4    | 1    | 15   | 4     | 7   | 0   | 0   | 114         | Thiotrichales      |
| 0     | 0   | 0   | 0    | 0    | 0     | 0     | 2    | 0    | 0     | 0     | 0     | 0     | 5    | 0    | 1    | 0    | 0    | 0    | 0     | 0   | 2   | 0   | 107         | Thiotrichales      |
| 0     | 0   | 0   | 0    | 0    | 0     | 0     | 0    | 0    | 0     | 0     | 0     | 1     | 2    | 31   | 2    | 1    | 0    | 58   | 6     | 0   | 1   | 0   | 102         | Thiotrichales      |
| 0     | 0   | 0   | 0    | 21   | 0     | 0     | 0    | 0    | 0     | 0     | 0     | 0     | 1    | 0    | 31   | 4    | 1    | 0    | 11    | 28  | 0   | 0   | 97          | Thiotrichales      |
| 0     | 0   | 0   | 0    | 0    | 5     | 0     | 3    | 0    | 0     | 0     | 0     | 0     | 0    | 6    | 2    | 3    | 27   | 1    | 7     | 3   | 7   | 20  | 85          | Thiotrichales      |

The numbers correspond to observed sequence reads per sample of the ten most frequent OTUs<sub>0.03</sub> of the respective order. Relative single sequence OTUs (SSO<sub>rel</sub>) are marked green.

## Supporting Material and Methods

### Sequence processing routine

Processing of the 454 pyrosequencing amplicons was performed according to the following routine modified from Pat Schloss (Schloss et al., 2011).

Step 1 - Extract data from binary file  
sffinfo(sff=Data.sff, flow=T)

Step 2 – Separate flowgrams  
trim.flows(flow=Data.flow, oligos=Data.oligos, pdiffs=2, bdiffs=1, processors=16)

Step 3 – Reducing sequencing error  
shhh.flows(file=Data.flow.files, processors=16)

Step 4 - Concatenate single files to make one file containing all samples:

```
cat *.trim.shhh.fasta > AllArch.fasta  
cat *.trim.shhh.names > AllArch.names  
cat *.trim.shhh.groups > AllArch.groups
```

Step 5 - Trim sequences using minlength=75 (for bacteria), 80 (for archaea):  
trim.seqs(fasta=All.fasta,name=All.names,oligos=Data.oligo,pdiffs=1,bdiffs=0,maxhomop=8,minlength=80,flip=F, processors=16)

Step 6 - Find unique sequences:  
unique.seqs(fasta=All.trim.fasta, name=All.trim.names)

Step 7 - Align sequences:  
align.seqs(fasta=All.trim.unique.fasta, reference=silva.archaea.fasta, processors=16)  
#for bacteria use (silva.bacteria.fasta)

Step 8 - Screen sequences:  
screen.seqs(fasta=All.trim.unique.align,name=All.trim.names,group=All.groups,optimize=start-end,criteria=90)

Step 9 - Filter dataset:  
filter.seqs(fasta=All.trim.unique.good.align, vertical=T, trump=., processors=16)

Step 10 - Simplify the dataset:  
unique.seqs(fasta=All.trim.unique.good.filter.fasta, name=All.trim.good.names)

Step 11 - Precluster:  
pre.cluster(fasta=All.trim.unique.good.filter.unique.fasta,name=All.trim.unique.good.filter.names,group=All.good.groups,diffs=0)

Step 12 - Chimera check:  
chimera.uchime(fasta=All.trim.unique.good.filter.unique.precluster.fasta,name=All.trim.unique.good.filter.unique.precluster.names,group=All.good.groups, processors=16)

Step 13 - Chimera removal:

```
remove.seqs(accnos=All.trim.unique.good.filter.unique.precluster.uchime.accnos,fasta=
All.trim.unique.good.filter.unique.precluster.fasta,name=All.trim.unique.good.filter.unique
.precluster.names,group=All.good.groups)
```

Step 14 - Classify sequences:

```
classify.seqs(fasta=All.trim.unique.good.filter.unique.precluster.pick.fasta,template=noga
p.archaea.fasta,taxonomy=silva.archaea.silva.tax) # for bacteria use
(nogap.bacteria.fasta,taxonomy=silva.bacteria.silva.tax)
```

Step 15 - Remove lineages:

```
remove.lineage(fasta=All.trim.unique.good.filter.unique.precluster.pick.fasta,name=All.tri
m.unique.good.filter.unique.precluster.pick.names,group=All.good.pick.groups,taxonomy
=All.trim.unique.good.filter.unique.precluster.pick.silva.taxonomy,taxon=Bacteria) # or
remove Eukarya/Archaea
```

Step 16 - Simplify names:

```
system(cp All.trim.unique.good.filter.unique.precluster.pick.silva.pick.taxonomy
All.taxonomy)
system(cp All.trim.unique.good.filter.unique.precluster.pick.pick.fasta All.fasta)
system(cp All.trim.unique.good.filter.unique.precluster.pick.pick.names All.names)
system(cp All.good.pick.pick.groups All.groups)
```

Step 17 - Distance matrix:

```
dist.seqs(fasta=All.fasta, cutoff=0.15, processors=16)
```

Step 18 - Cluster:

```
cluster(column=All.dist,name=All.names)
```

Step 19 - Get data for 0.03:

```
make.shared(list=All.an.list, group=All.groups, label=0.03)
```

Step 20 - Normalize the number of sequences in each sample:

```
count.groups() # subsample according to the smallest group size
sub.sample(shared=All.an.shared, size=smallest sample)
```

Step 21 - Consensus taxonomy for each OTU:

```
classify.otu(list=All.an.list, name=All.names, taxonomy=All.taxonomy, label=0.03,
cutoff=80)
```

Step 22 - OTU-based analysis Alpha diversity:

```
collect.single(shared=All.an.0.03.subsample.shared, calc=chao-invsimpson, freq=100)
summary.single(shared=All.an.0.03.subsample.shared,calc=nseqs-coverage-sobs-
invsimpson)
```

## References

- Aquilina, A., Knab, N. J., et al. (2010). "Biomarker Indicators for Anaerobic Oxidizers of Methane in Brackish-Marine Sediments with Diffusive Methane Fluxes." *Org Geochem* **41**: 414-426.
- Biddle, J. F., Cardman, Z., et al. (2012). "Anaerobic Oxidation of Methane at Different Temperature Regimes in Guaymas Basin Hydrothermal Sediments." *ISME J* **6**: 1018-1031.
- Dufrène, M. and Legendre, P. (1997). "Species Assemblages and Indicator Species: The Need for a Flexible Asymmetrical Approach." *Ecol Monogr* **67**: 345-366.
- Grünke, S., Lichtschlag, A., et al. (2010). "Novel Observations of Thiobacterium, a Sulfur-Storing Gammaproteobacterium Producing Gelatinous Mats." *ISME J* **4**: 1031-1043.
- Knittel, K., Lösekann, T., et al. (2005). "Diversity and Distribution of Methanotrophic Archaea at Cold Seeps." *Appl Environ Microbiol* **71**: 467-479.
- Lichtschlag, A., Felden, J., et al. (2010). "Geochemical Processes and Chemosynthetic Primary Production in Different Thiotrophic Mats of the Haakon Mosby Mud Volcano (Barents Sea)." *Limnol Oceanogr* **55**: 931-949.
- Lloyd, K. G., Albert, D. B., et al. (2010). "Spatial Structure and Activity of Sedimentary Microbial Communities Underlying a *Beggiatoa* Spp. Mat in a Gulf of Mexico Hydrocarbon Seep." *PLoS ONE* **5**: e8738.
- Lloyd, K. G., Alperin, M. J., et al. (2011). "Environmental Evidence for Net Methane Production and Oxidation in Putative Anaerobic Methanotrophic (Anme) Archaea." *Environ Microbiol* **13**: 2548-2564.
- Longhurst, A., Sathyendranath, S., et al. (1995). "An Estimate of Global Primary Production in the Ocean from Satellite Radiometer Data." *J Plank Res* **17**: 1245-1271.
- Niemann, H., Fischer, D., et al. (2009). "Biogeochemistry of a Low-Activity Cold Seep in the Larsen B Area, Western Weddell Sea, Antarctica." *Biogeosciences* **6**: 2383-2395.
- Pop Ristova, P., Wenzhöfer, F., et al. (2012). "Bacterial Diversity and Biogeochemistry of Different Chemosynthetic Habitats of the Regab Cold Seep (West African Margin, 3160 M Water Depth)." *Biogeosciences* **9**: 5031-5048.
- Quast, C., Pruesse, E., et al. (2013). "The Silva Ribosomal Rna Gene Database Project: Improved Data Processing and Web-Based Tools." *Nucleic Acids Res* **41**: D590-D596.
- Ruff, S. E., Arnds, J., et al. (2013). "Microbial Communities of Deep-Sea Methane Seeps at Hikurangi Continental Margin (New Zealand)." *PLoS ONE* **8**: e72627.
- Schloss, P. D., Gevers, D., et al. (2011). "Reducing the Effects of Pcr Amplification and Sequencing Artifacts on 16s Rrna-Based Studies." *PLoS ONE* **6**: e27310.
- Sommer, S., Linke, P., et al. (2010). "Benthic Respiration in a Seep Habitat Dominated by Dense Beds of Ampharetid Polychaetes at the Hikurangi Margin (New Zealand)." *Mar Geol* **272**: 223-232.
- Treude, T., Orphan, V., et al. (2007). "Consumption of Methane and Co2 by Methanotrophic Microbial Mats from Gas Seeps of the Anoxic Black Sea." *Appl Environ Microbiol* **73**: 2271-2283.
- Wegener, G., Shovitri, M., et al. (2008). "Biogeochemical Processes and Microbial Diversity of the Gullfaks and Tommeliten Methane Seeps (Northern North Sea)." *Biogeosciences* **5**: 1127-1144.

## Supporting information of Chapter 3

## Supporting information of Chapter 3

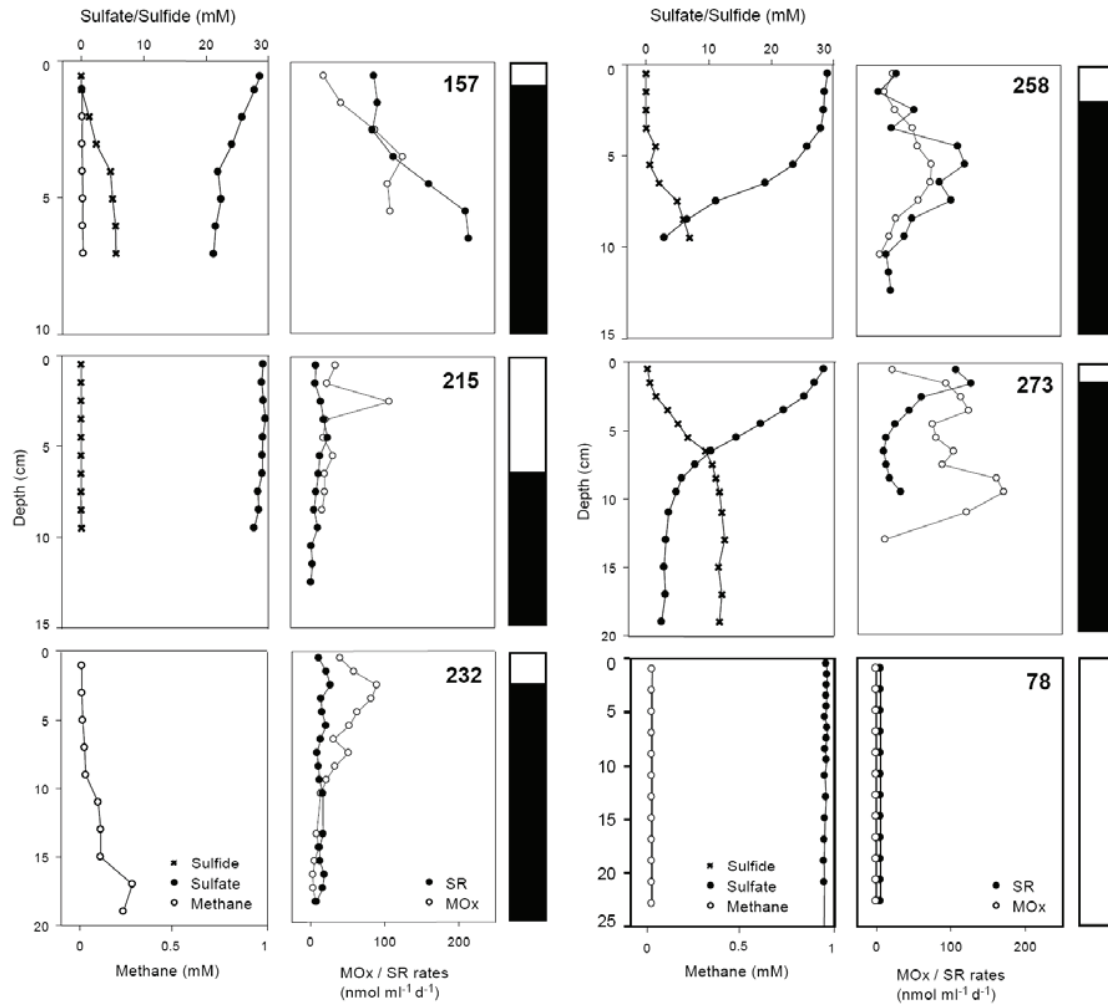
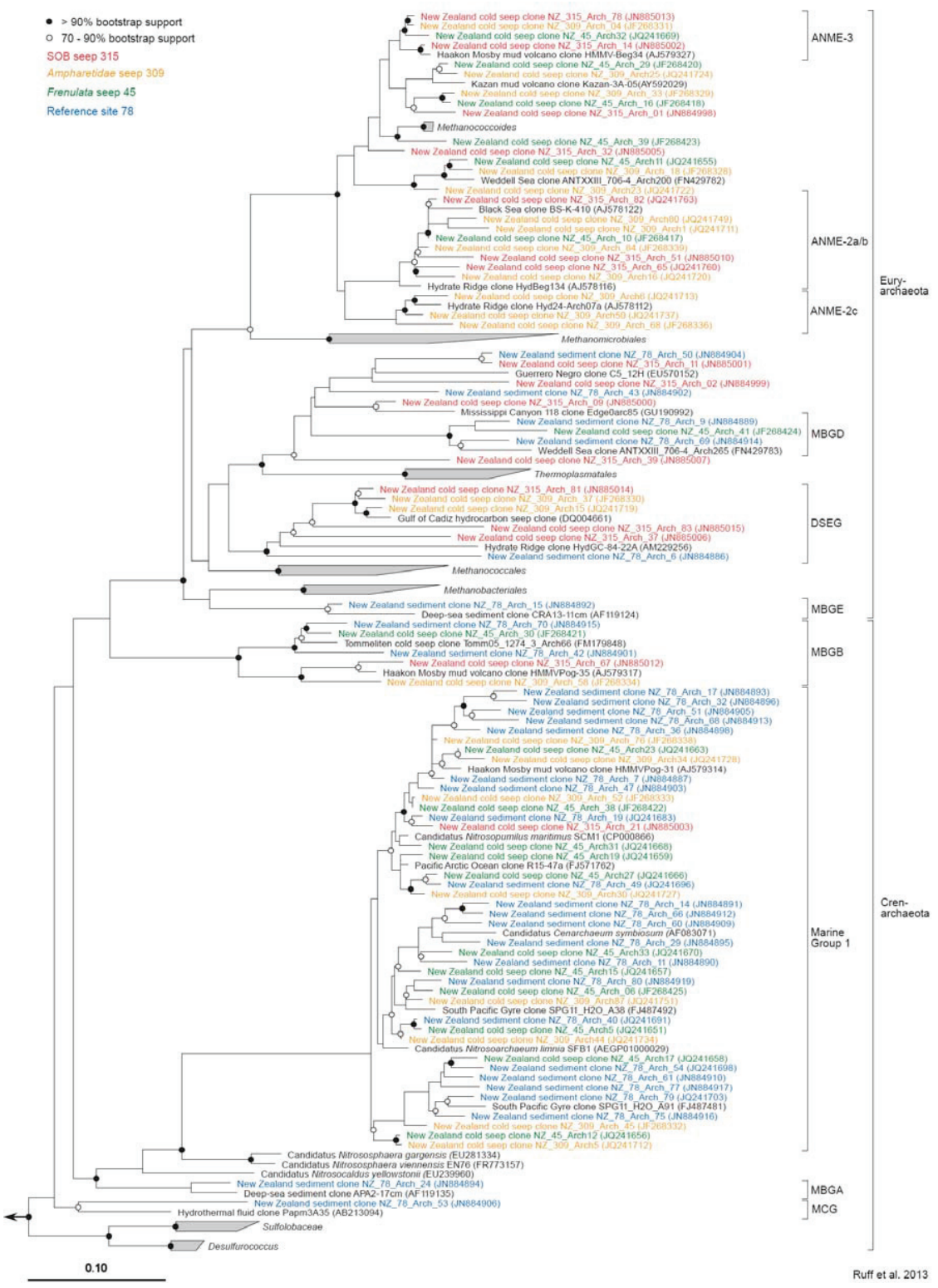


**Figure S1: Biogeochemistry of additional Hikurangi ecosystems**

Methane and sulfate concentrations, rates of methane oxidation (MOx) and sulfate reduction (SR), of five additional ampharetid habitats (157, 215, 232, 258 and 273) and a reference site (78) situated on Hikurangi margin. The bars on the side show the redox state of the sediment: White is the oxic/suboxic and black the anoxic/sulfidic zone. All sites show very low sulfide concentrations in the upper sediment horizons. Methane oxidation at these sites took place in the oxic and anoxic layers.

**Figure S2 (next page): Phylogeny of archaeal 16S rRNA**

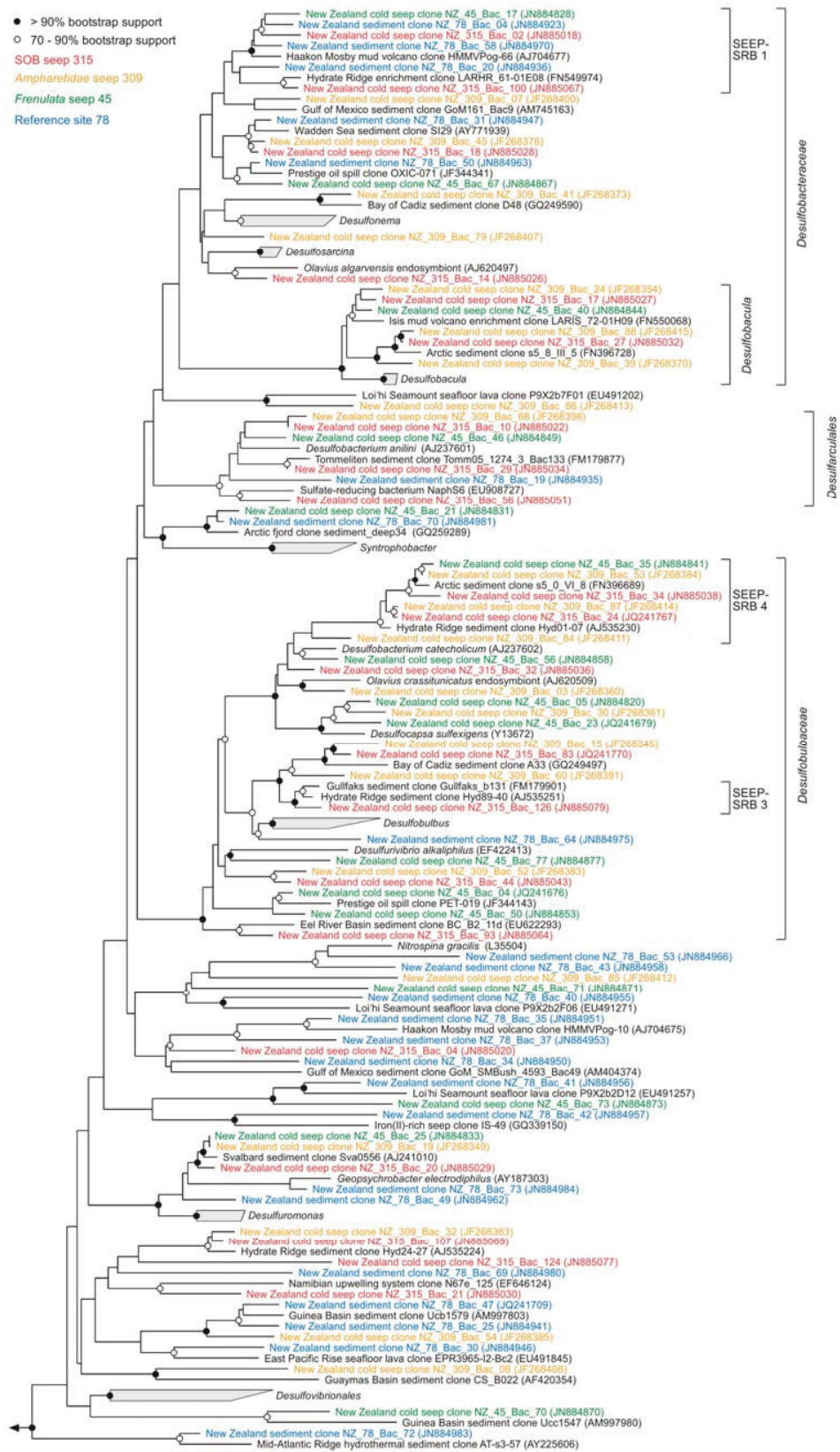
16S rRNA based phylogenetic tree showing archaeal sequences detected at the Hikurangi margin together with selected reference sequences of the domain *Archaea*. The tree is based on the RAxML algorithm as implemented in ARB [27]. Full-length sequences were obtained from the ampharetid site 309 (shown in red) and the frenulate site 45 (green). Partial sequences were retrieved from the SOB site 315 (yellow) and the reference site 78 (blue). Bar = 10% estimated sequence divergence.



**Figure S3 (next page): Phylogeny of deltaproteobacterial 16S rRNA**

16S rRNA based phylogenetic tree showing sequences of *Deltaproteobacteria* detected at the Hikurangi margin and selected reference sequences of that bacterial class. The tree is based on the RAxML algorithm as implemented in ARB [27]. Full-length sequences were obtained from the ampharetid site 309 (shown in red) and the frenulate site 45 (green). Partial sequences were retrieved from the SOB site 315 (yellow) and the reference site 78 (blue). Bar = 10% estimated sequence divergence.

- > 90% bootstrap support
- 70 - 90% bootstrap support
- SOB seep 315
- Ampharetidae seep 309
- Frenulata seep 45
- Reference site 78



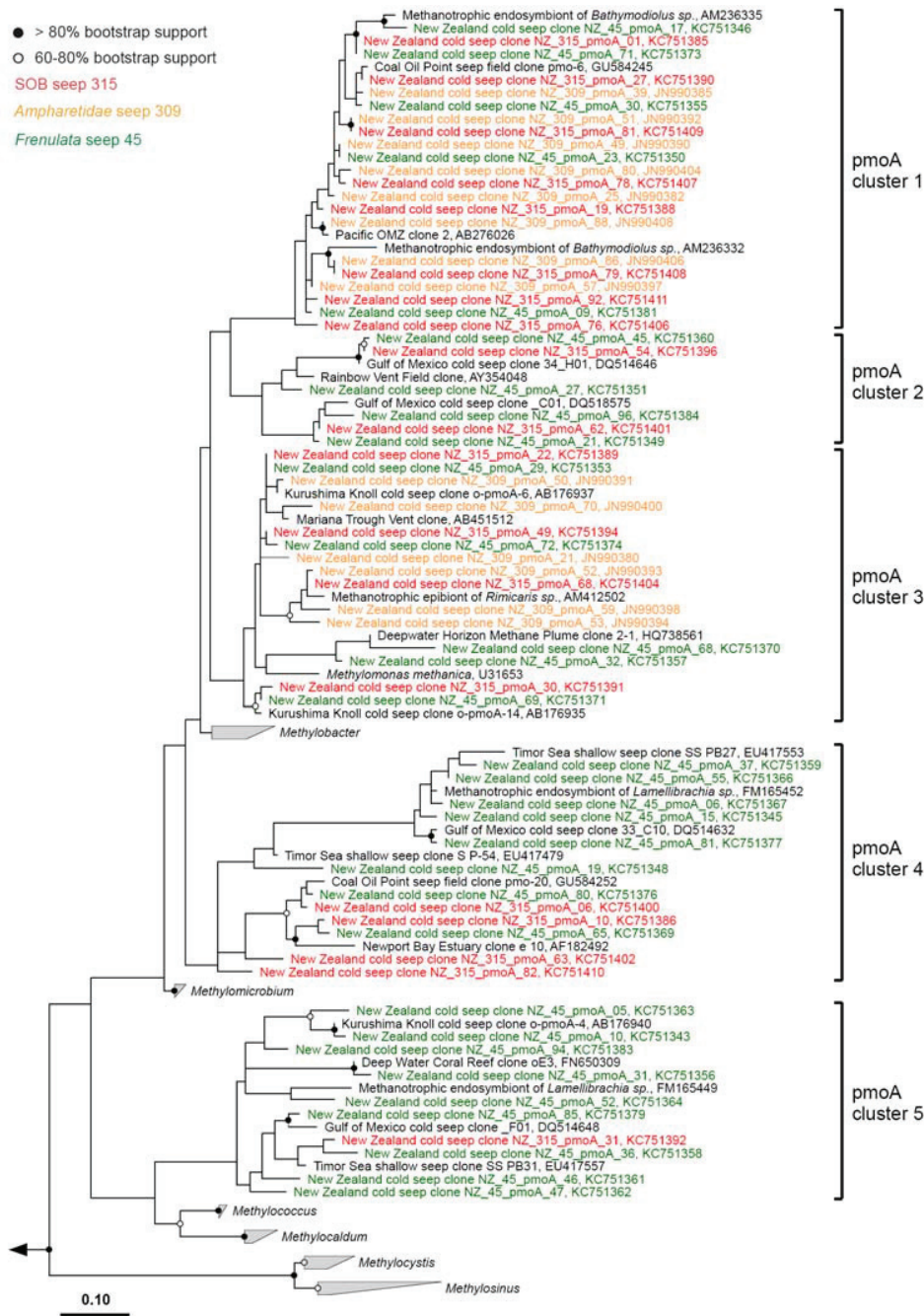


**Figure S4: Phylogeny of *pmoA* protein**

Phylogeny of the *pmoA* protein at the frenulate site 45, the ampharetid site 309 and the SOB site 315. The tree was calculated using 98 non-redundant, curated amino acid sequences, from the three habitats and 90 reference sequences. We used a maximum likelihood algorithm employing 100 bootstraps and a positional variability filter, excluding the highly variable regions. Bar = 10% estimated sequence divergence.

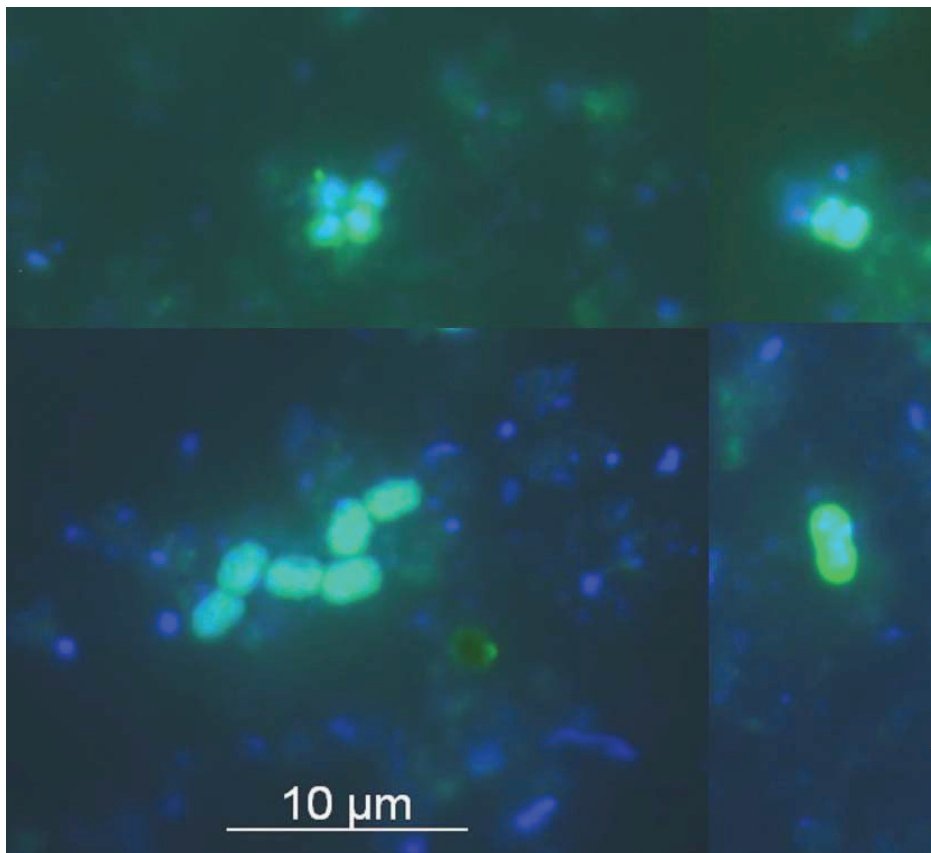


**Figure S5: Micrographs of MMG1 organisms related to *Bathymodiolus* sp. endosymbionts**

Aerobic methylotrophic organisms of the group MMG1 within the order *Methylococcales* (probe BMARm-345 - green) in surface sediment of the ampharetid habitat (site 309). The dual stain with probe and nucleic acid stain DAPI (blue) shows that some MMG1 cells were stained by a probe that is specific for the methanotrophic endosymbionts of *Bathymodiolus* spp.

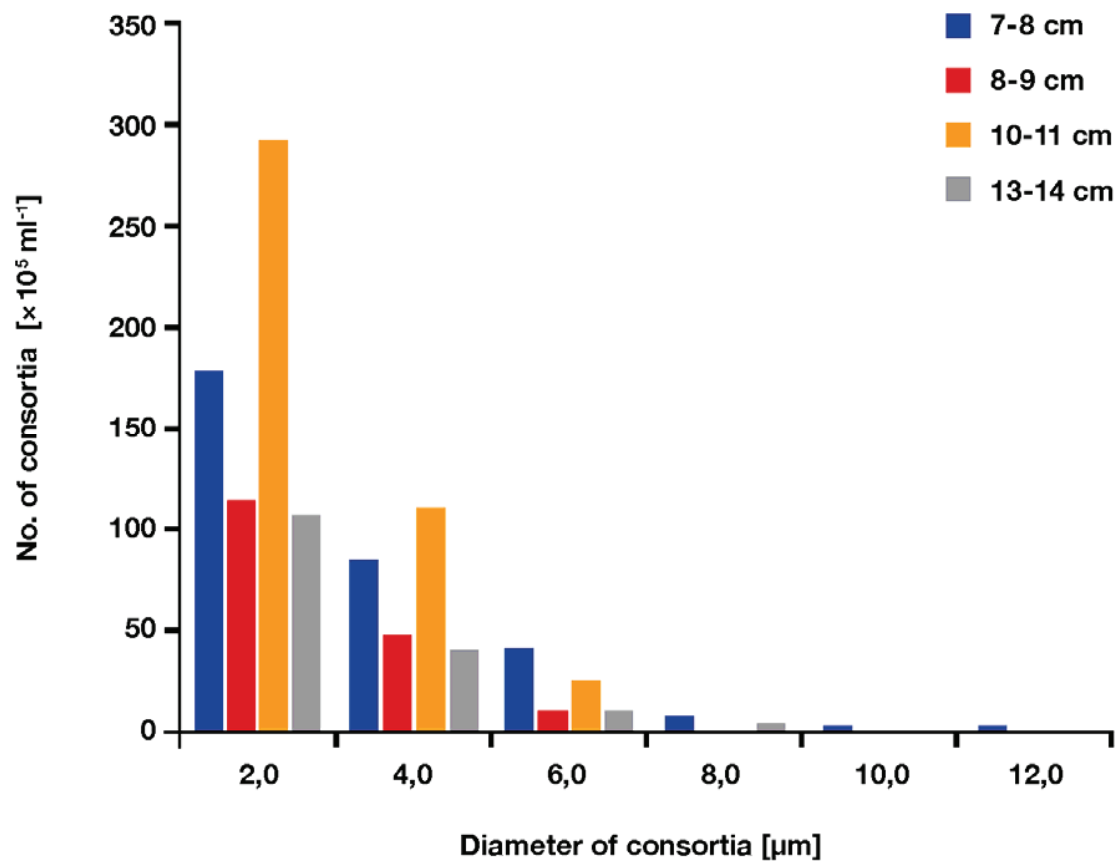


**Figure S6: Abundance and size distribution of AOM aggregates at site 124**

Abundance and size distribution of ANME-2a/SEEP-SRB-1a aggregates at ampharetid site 124. Bars of the same color represent consortia of different sizes in the same depth layer. In contrast to other seep sites the diameter of the aggregates is not normally distributed, instead the population is dominated by small aggregates.

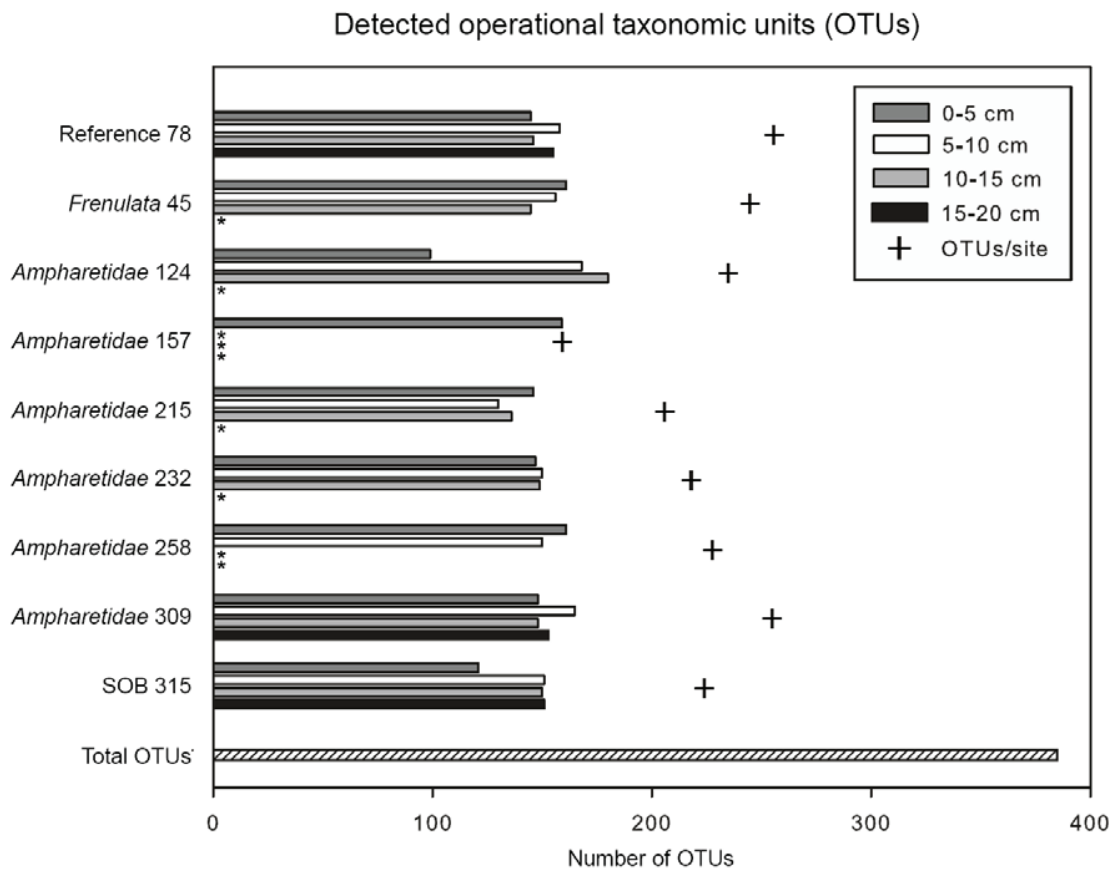
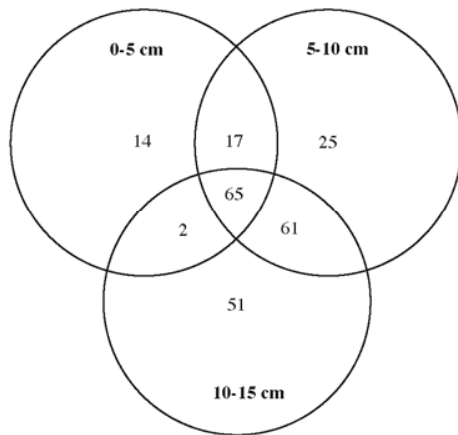


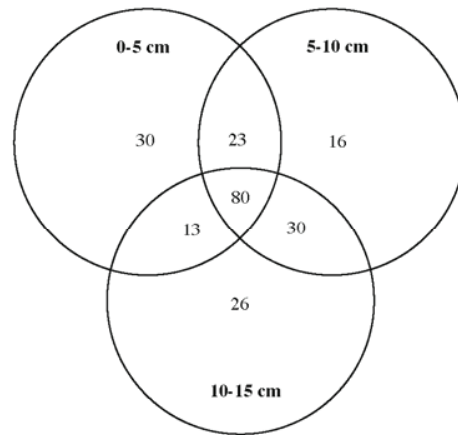
**Figure S7: Detected operational taxonomic units (OTUs)**

Total number of operational taxonomic units (OTUs) present in the investigated depth layers (horizontal bar) and in total for each sampling site (crosses) as detected by the DNA fingerprinting technique ARISA. \* denotes depth intervals that are missing due to shorter sediment cores. The striped bar (bottom of graph) represents the total number of unique OTUs detected on Hikurangi margin during this study.

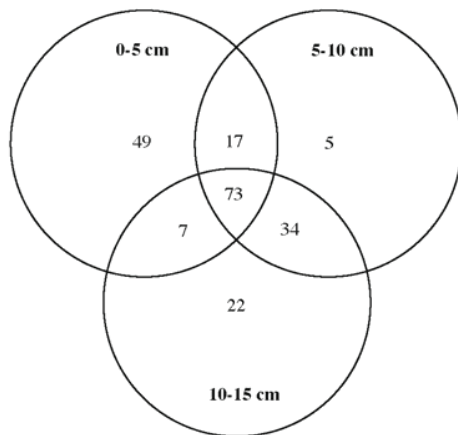
**Ampharetidae Site 124**



**Ampharetidae Site 232**



**Ampharetidae Site 215**



**Frenulata Site 45**

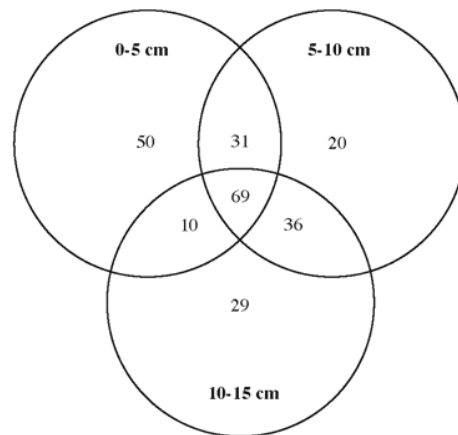
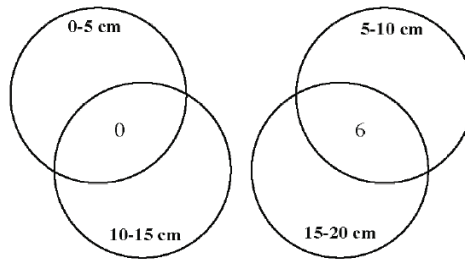
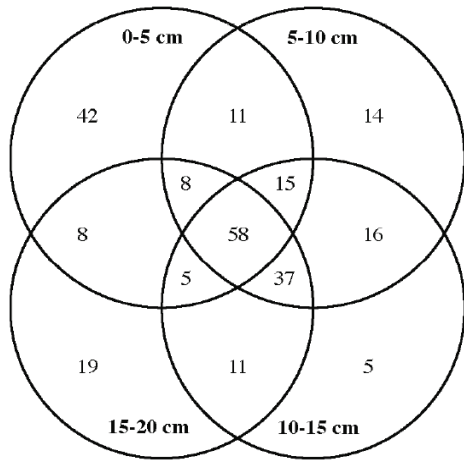


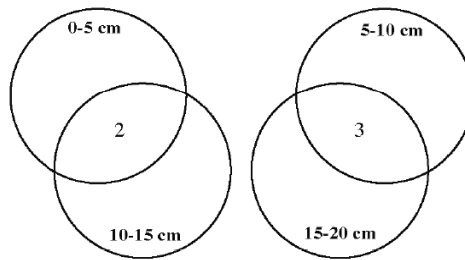
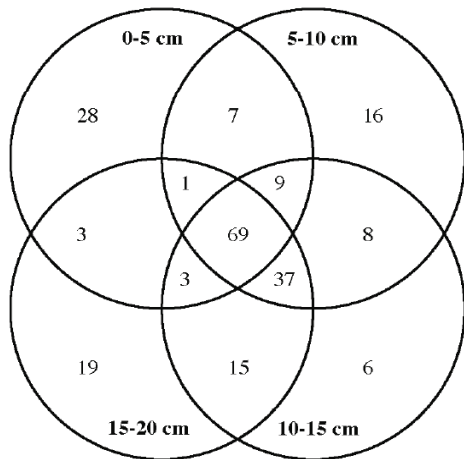
**Figure S8A: OTU partitioning plots for different depth layers.**

Sites 309, 315 and 78 include four depth layers, sites 124, 215, 232 and 45 only three sediment layers. Small circles to the right of each larger graph depict two further combinations that could not be visualized in the main graph. Numbers in circles and their intersections indicate OTUs that are shared between the respective layers. The sum of all numbers equals the total number of OTUs detected at the respective site (continuing on next page).

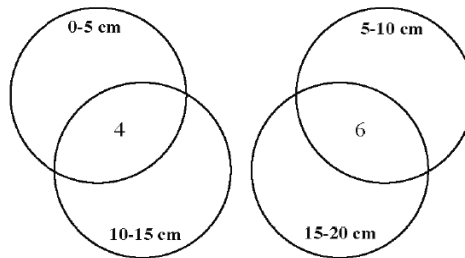
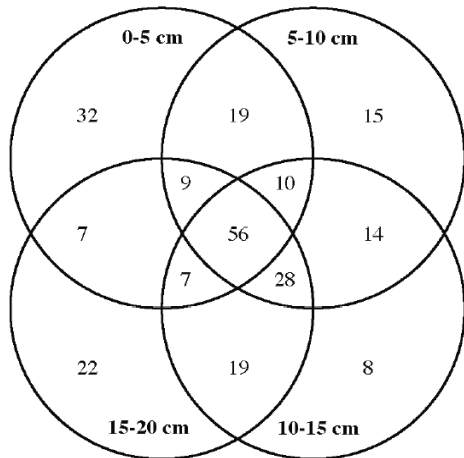
**Ampharetidae Site 309**



**SOB Site 315**



**Reference Site 78**



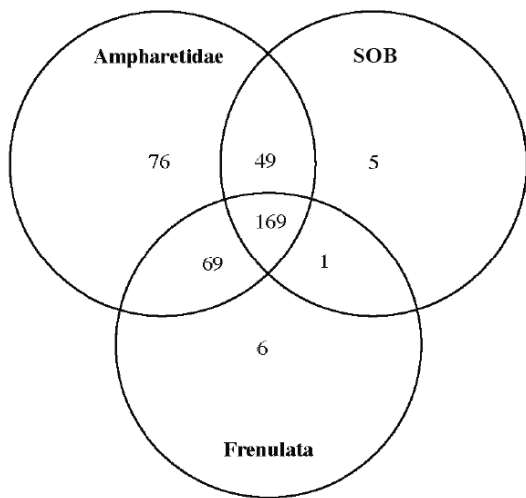


**Figure S8B: OTU partitioning according to the habitats**

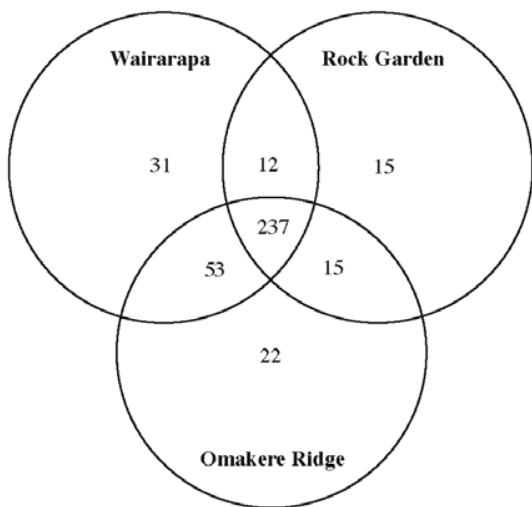


**Figure S8C: Grouping the dataset according to the sampling areas**

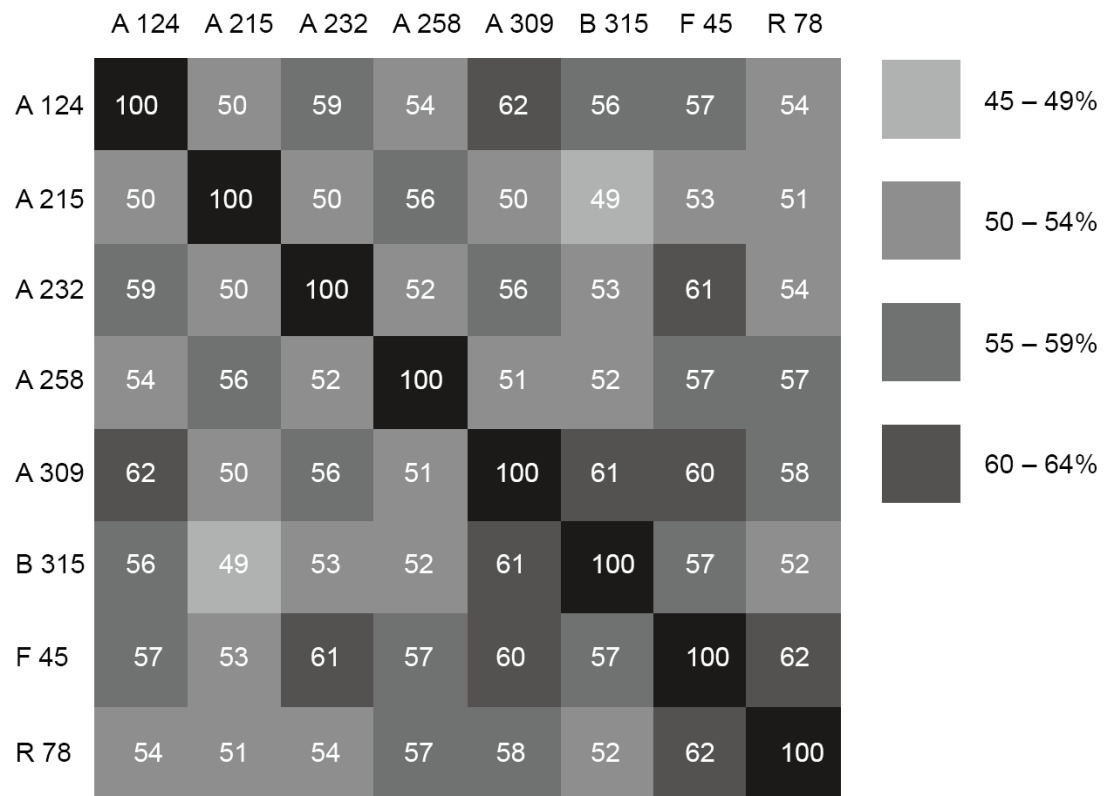


**Figure S9: Pairwise comparisons of shared OTUs**

Pairwise comparisons of shared OTUs in percent. The letter in front of the station number indicates the habitat type (A = *Ampharetidae*, B = SOB, F = *Frenulata*, R = Reference).

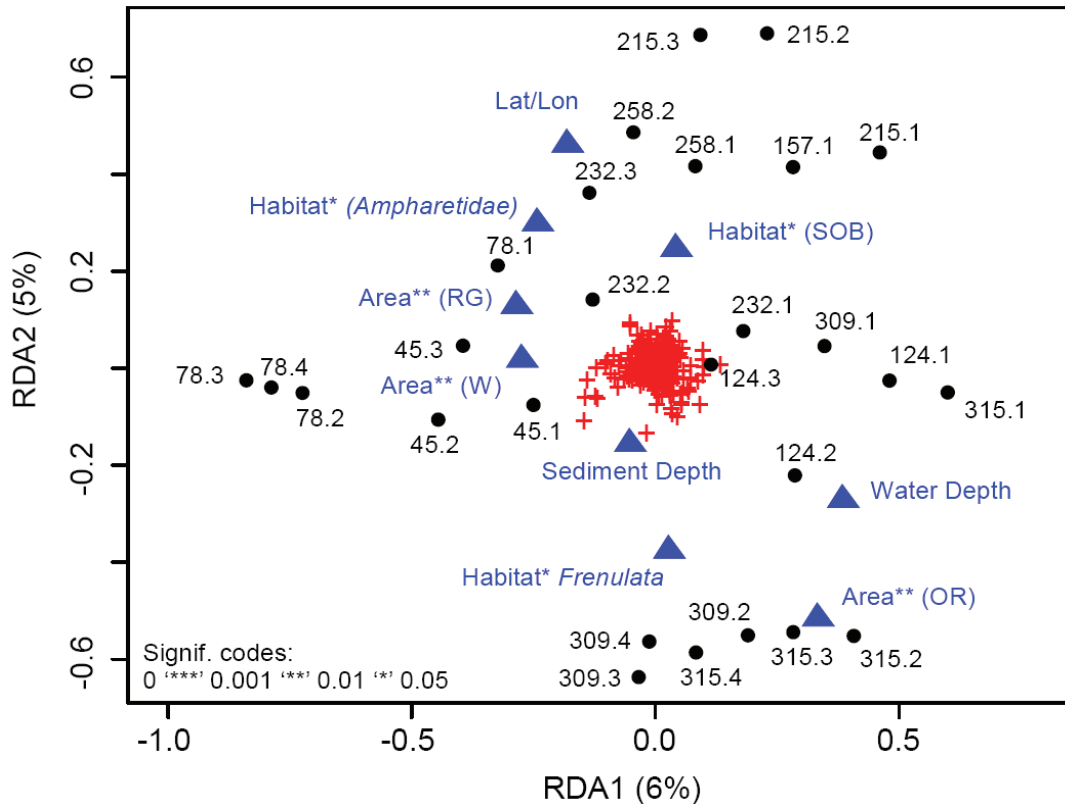


**Figure S10: Redundancy analysis of ARISA and environmental data**

Redundancy analysis based on the Hellinger-transformed ARISA dataset and environmental parameters. The plot shows the full model considering all parameters, which explained 23% of the total variation ( $p=0.001$ ). Black circles represent the microbial community of a given sampling site and depth layer (e.g. 124.1 = station 124, 0-5 cm; 124.2 = station 124, 5-10cm). Species are shown as red crosses, environmental parameters as blue triangles (OR: Omakere Ridge, RG: Rock Garden, W: Wairarapa). Note: In RDA plots environmental parameters and species are generally depicted as centered arrows originating in point 0/0 (which represents the average and not zero). To simplify the plot we chose to show just the tips of the arrows as crosses and triangles. Significance levels were calculated for each parameter using partial RDA and ANOVA. Only habitat type and seep area were significant on their own.

Table S1

Table S1: Total cell counts and relative abundance of methanotrophs at Hikurangi margin, Hydrate Ridge, Black Sea and Håkon Mosby mud volcano seep sites

|   | Total Cells<br>(10 <sup>6</sup> cm <sup>-3</sup> ) | <i>Methylococcales</i> | ANME-1 | ANME-2a/DSS<br>Consortia | ANME-2c/DSS<br>Consortia | ANME-3/DBB<br>Consortia |
|---|--|------------------------|--------|--------------------------|--------------------------|-------------------------|
| Hikurangi<br><i>Ampharetidae</i> (124)                  | 0.15   | +++                    | -      | +++                      | +                        | n.a.#                   |
| Hikurangi<br><i>Ampharetidae</i> (309)                  | 0.2  | +++                    | -      | ++                       | ++                       | n.a.#                   |
| Hikurangi<br><i>Frenulata</i> (45)                      | 0.13   | +                      | -      | +                        | -                        | +                       |
| Hikurangi<br>SOB (315)                                  | 1  | +                      | -      | +++                      | +                        | n.a.#                   |
| Hydrate Ridge<br><i>Beggiatoa</i> site                  | 4.2  | n.a.                   | +      | +++                      | +                        | -                       |
| Hydrate Ridge<br><i>Calyptogena</i> site                | 4.6  | n.a.                   | +      | +                        | +++                      | -                       |
| Black Sea<br>sediment P817                              | 2.7  | n.a.                   | +      | +++                      | +++                      | -                       |
| Black Sea P822<br>microbial mat,<br>top part of chimney | 30   | n.a.                   | +      | +++                      | +                        | -                       |
| Black Sea P822<br>microbial mat,<br>inside of chimney   | 1.4  | n.a.                   | +++    | +                        | +                        | -                       |
| HMMV<br><i>Beggiatoa</i> site                           | 1.9  | +                      | -      | -##                      | -##                      | +++                     |
| HMMV<br>tubeworm site                                   | 0.33   | -                      | +      | +++##                    | +++##                    | ++                      |

+present in low proportions ++high proportions +++dominant type n.a.: not assessed #present as 16S rRNA gene ## ANME-2/DSS

## References:

- Knittel et al. (2005) Diversity and Distribution of Methanotrophic Archaea at Cold Seeps. *Appl Environ Microbiol* 71: 467-479.  
 Niemann et al. (2006) Novel microbial communities of the Haakon Mosby mud volcano and their role as a methane sink. *Nature* 443: 854-858.  
 Lösekann et al. (2007) Diversity and Abundance of Aerobic and Anaerobic Methane Oxidizers at the Haakon Mosby Mud Volcano, Barents Sea. *Appl Environ Microbiol* 73: 3348-3362.  
 Schreiber et al. (2010) Identification of the dominant sulfate-reducing bacterial partner of anaerobic methanotrophs of the ANME-2 clade. *Environ Microbiol* 12: 2327-2340.28.  
 Arnds (2009) Molecular characterization of microbial populations in methane-rich marine habitats. Bremen: Universität Bremen. 158 p.  
 Knittel et al. (2003) Activity, distribution, and diversity of sulfate reducers and other bacteria in sediments above gas hydrate, (Cascadia Margin, Oregon). *Geomicrobiol J* 20: 269-294.

## Supporting Materials and Methods

### ARISA

ARISA was carried out according to Böer and colleagues [1] with the following modifications. Polymerase chain reactions (PCRs) (50 µl total volume) were conducted in triplicates containing 1× PCR buffer, 0.25 mM dNTP mix, 0.09 mg ml<sup>-1</sup> bovine serum albumin, 400 nM each of universal primer ITSF (Table S1), labeled with phosphoramidite dye FAM and bacterial ITSReub (Table S1), 0.05 units MasterTaq polymerase and 20-25 ng environmental DNA. PCR was carried out in an Eppendorf MasterCycler with an initial denaturation for 3 min at 94°C, followed by 30 cycles of 94°C for 45 sec, 55°C for 45 sec, 72°C for 90 sec and a final extension for 5 min at 72°C. PCR products were purified utilizing Sephadex G-50 Superfine, which is based on the principle of gel filtration by cross-linked dextran molecules. Sephadex was filled in the wells of a Multiscreen HV plate and soaked in 300 µl of HPLC-grade water per well for 3 h at RT, excess water was removed using an Eppendorf Centrifuge 5810R (910 × *g* for 5 min at RT), the wells were washed with 150 µl HPLC water and again centrifuged (as above). PCR products were loaded in the center of each well, centrifuged (as above) and collected in a sterile 96-well plate. A standardized amount of amplified DNA (100 ng) was mixed with a separation cocktail containing 0.5 µl (when <3 µl PCR products were used) or 1 µl (when ≥3 µl PCR products were used) of internal size standard Map Marker 1000 ROX (50-1000 bp), 0.5 µl tracking dye and 14 µl of deionized Hi-Di formamide. Discrimination of the PCR-amplified fragments via capillary electrophoresis was carried out on an ABI PRISM 3130xl Genetic Analyzer (Applied Biosystems) and the ARISA profiles were analyzed using the GeneMapper Software v3.7.

### **OTU partitioning and pairwise comparison**

OTU partitioning was used to determine the number of OTUs that are specific for a certain condition and was performed on the ARISA dataset using Microsoft Excel and a custom R script [2]. Pairwise OTU comparison was based on a custom R script.

### **Volume calculation and 3D animation of cell aggregates**

The three dimensional imaging was done using confocal laser scanning microscopy (C-LSM) and aggregate volume was calculated with PHLIP [3]. For the 3D animation of the AOM consortium (Movie\_S2.avi) we used *daim*e [4], the animation of the Methylococci aggregate (Movie\_S1.mpg) was calculated with IMARIS (v 7.1.1, Bitplane AG, Zürich, Switzerland). Both animations are based on C-LSM picture stacks that were processed and filtered (median filter, 2 pixels radius) with Image J v1.43 (<http://rsb.info.nih.gov/ij/index.html>) or deconvoluted with AutoQuant (v x2.2, Media Cybernetics, USA).

**Table S2: Oligonucleotide probes used in this study**

| Oligonucleotides | Specificity                              | Target Gene | Target Position | FA conc. (% v/v) | Annealing (°C) | Nucleotide Sequence 5'-3'      | Reference          |
|------------------|--|-------------|-----------------|------------------|----------------|--------------------------------|--------------------|
| A189F            | pmoA                                     | pmoA        | 189-206         | -                | 55             | GGN GAC TGG GAC TTC TGG        | [5]                |
| Arch20F          | most Archaea                             | 16S rRNA    | 20-38           | -                | 58             | TTC CGG TTG ATC CYG CCR G      | [6]                |
| GM3              | Bacteria                                 | 16S rRNA    | 8-23            | -                | 44             | AGA GTT TGA TCM TGG C          | [7]                |
| GM4              | Bacteria                                 | 16S rRNA    | 1492-1507       | -                | 44             | TAC CTT GTT ACG ACT T          | [7]                |
| ITSF FAM         | Universal                                | 16S rRNA    | 1423-1443       | -                | 55             | GTC GTA ACA AGG TAG CCG TA     | Modified after [8] |
| ITSREub          | Bacteria                                 | 23S rRNA    | 23-38           | -                | 55             | GCC AAG GCA TCC ACC            | [8]                |
| MB661R           | pmoA                                     | pmoA        | 661-679         | -                | 55             | CCG GMG CAA CGT CYT TAC C      | [9]                |
| Uni1392R         | Universal                                | 16S rRNA    | 1392-1406       | -                | 58             | ACG GGC GGT GTG TRC            | [10]               |
| ANME-1-350       | ANME-1                                   | 16S rRNA    | 350-367         | 40               | -              | AGT TTT CGC GCC TGA TGC        | [11]               |
| ANME-2a-647      | ANME-2a                                  | 16S rRNA    | 647-664         | 35               | -              | TCT TCC GGT CCC AAG CCT        | [12]               |
| ANME-2c-760      | ANME-2c                                  | 16S rRNA    | 760-777         | 50               | -              | CGC CCC CAG CTT TCG TCC        | [12]               |
| ANME-3-1249      | ANME-3                                   | 16S rRNA    | 1249-1266       | 30               | -              | TGC GAG TAG GGA CCC ATT        | [13]               |
| ANME-3-1249H3    | Helper                                   | 16S rRNA    | 1249-1266       | 30               | -              | GTC CCA ATC ATT GTA GCC GGC    | [14]               |
| ANME-3-1249H5    | Helper                                   | 16S rRNA    | 1249-1266       | 30               | -              | TTA TGA GAT TAC CAT CTC CTT    | [14]               |
| Arch915          | most Archaea                             | 16S rRNA    | 915-934         | 35               | -              | GTG CTC CCC CGC CAA TTC CT     | [15]               |
| BMARm-845        | Methanotrophic endosymbiont B. sp.       | 16S rRNA    | 845-862         | 30               | -              | GCT CCG CCA CTA AGC CTA        | [16]               |
| DS5658           | <i>Desulfosarcina/ Desulfococcus</i>     | 16S rRNA    | 658-675         | 50               | -              | TCC ACT TCC CTC TCC CAT        | [17]               |
| EelMS932         | ANME-2                                   | 16S rRNA    | 932-949         | 50               | -              | AGC TCC ACC CGT TGT AGT        | [11]               |
| EPS1682          | <i>Epsilonproteobacteria</i>             | 16S rRNA    | 682-700         | 20               | -              | CGG ATT TTA CCC CTA CAC M      | [18]               |
| Eub338-I         | most Bacteria                            | 16S rRNA    | 338-355         | 35               | -              | GCT GCC TCC CGT AGG AGT        | [19]               |
| Eub338-II        | most Planctomycetales                    | 16S rRNA    | 338-355         | 35               | -              | GCA GCC ACC CGT AGG TGT        | [20]               |
| Eub338-III       | most Verrucomicrobiales                  | 16S rRNA    | 338-355         | 35               | -              | GCT GCC ACC CGT AGG TGT        | [20]               |
| LEN338 *         | <i>Lentisphaerae</i>                     | 16S rRNA    | 338-355         | 35               | -              | GCA GCC TCC CGC AGG AGT        | This study         |
| Gam42a           | <i>Gammaproteobacteria</i>               | 23S rRNA    | 1027-1043       | 35               | -              | GCC TTC CCA CAT CGT TT         | [21]               |
| c-Gam42a         | Competitor                               | 23S rRNA    | 1027-1043       | 35               | -              | GCC TTC CCA CTT CGT TT         | [21]               |
| Gam660           | Potential sulfur-oxidizing Bacteria      | 16S rRNA    | 660-674         | 35               | -              | TCC ACT TCC CTC TAC            | [22]               |
| Met-I-444        | HMMV-type-I-Methanotrophs                | 16S rRNA    | 444-461         | 60               | -              | CCT GCC TGT TTT CCT CCC        | [13]               |
| MPH732           | <i>Methylophaga</i>                      | 16S rRNA    | 732-749         | 40               | -              | GTA ATG GCC CAG TGA GTC        | [13]               |
| MS1414           | <i>Methanosarcina /-cocoides /-lobus</i> | 16S rRNA    | 1414-1434       | 50               | -              | CTC ACC CAT ACC TCA CTC GGG    | [23]               |
| hMS1395          | MS1414-helper                            | 16S rRNA    | 1395-1412       | 50               | -              | GGT TTG ACG GGC GGT GTG        | [24]               |
| MTC-850          | <i>Methylococcales</i> clade MMG1/MMG2   | 16S rRNA    | 850-867         | 20               | -              | ACG TTA GCT CCG CCA CTA        | This study         |
| MTMC701          | most <i>Methylococcales</i>              | 16S rRNA    | 701-718         | 40               | -              | GTG TTC CTT CAG ATC TCT        | [11]               |
| c1-MTMC701       | Competitor                               | 16S rRNA    | 701-718         | 40               | -              | GTA TTC CTT CAG ATC TCT        | This study         |
| c2-MTMC701       | Competitor                               | 16S rRNA    | 701-718         | 40               | -              | GTG TTC CTC CAG ATC TCT        | This study         |
| NON338           | Nonsense probe                           | -           | -               | 35               | -              | ACT CCT ACG GGA GGC AGC        | [25]               |
| SEEP1a-473       | SEEP-SRB-1a                              | 16S rRNA    | 473-495         | 30               | -              | TTC AGT GAT ACC GTC AGT ATC CC | [26]               |

\* the LEN338 probe was combined with the general bacterial probe mix Eub338\_I,III for a more complete detection of bacterial clades in marine sediments

## References

1. Böer SI, Hedtkamp SIC, van Beusekom JEE, Fuhrman JA, Boetius A, et al. (2009) Time- and sediment depth-related variations in bacterial diversity and community structure in subtidal sands. *ISME J* 3: 780-791.
2. Ramette A (2009) Quantitative Community Fingerprinting Methods for Estimating the Abundance of Operational Taxonomic Units in Natural Microbial Communities. *Appl Environ Microbiol* 75: 2495-2505.
3. Mueller L, de Brouwer J, Almeida J, Stal L, Xavier J (2006) Analysis of a marine phototrophic biofilm by confocal laser scanning microscopy using the new image quantification software PHLIP. *BMC Ecology* 6: 1.
4. Daims H, Lüscher S, Wagner M (2006) daime, a novel image analysis program for microbial ecology and biofilm research. *Environmental Microbiology* 8: 200-213.
5. Holmes AJ, Costello A, Lidstrom ME, Murrell JC (1995) Evidence that particulate methane monooxygenase and ammonia monooxygenase may be evolutionarily related. *FEMS Microbiol Lett* 132: 203-208.
6. Massana R, Murray AE, Preston CM, DeLong EF (1997) Vertical distribution and phylogenetic characterization of marine planktonic Archaea in the Santa Barbara Channel. *Appl Environ Microbiol* 63: 50-56.
7. Muyzer G, de Waal EC, Uitterlinden AG (1993) Profiling of complex microbial populations by denaturing gradient gel electrophoresis analysis of polymerase chain reaction-amplified genes coding for 16S rRNA. *Appl Environ Microbiol* 59: 695-700.
8. Cardinale M, Brusetti L, Quatrini P, Borin S, Puglia AM, et al. (2004) Comparison of Different Primer Sets for Use in Automated Ribosomal Intergenic Spacer Analysis of Complex Bacterial Communities. *Appl Environ Microbiol* 70: 6147-6156.
9. Costello AM, Lidstrom ME (1999) Molecular Characterization of Functional and Phylogenetic Genes from Natural Populations of Methanotrophs in Lake Sediments. *Appl Environ Microbiol* 65: 5066-5074.
10. Lane DJ, Pace B, Olsen GJ, Stahl DA, Sogin ML, et al. (1985) Rapid determination of 16S ribosomal RNA sequences for phylogenetic analyses. *PNAS* 82: 6955-6959.
11. Boetius A, Ravensschlag K, Schubert CJ, Rickert D, Widdel F, et al. (2000) A marine microbial consortium apparently mediating anaerobic oxidation of methane. *Nature* 407: 623-626.
12. Knittel K, Lösekann T, Boetius A, Kort R, Amann R (2005) Diversity and Distribution of Methanotrophic Archaea at Cold Seeps. *Appl Environ Microbiol* 71: 467-479.
13. Niemann H, Lösekann T, de Beer D, Elvert M, Nadalig T, et al. (2006) Novel microbial communities of the Haakon Mosby mud volcano and their role as a methane sink. *Nature* 443: 854-858.
14. Lösekann T, Knittel K, Nadalig T, Fuchs B, Niemann H, et al. (2007) Diversity and Abundance of Aerobic and Anaerobic Methane Oxidizers at the Haakon Mosby Mud Volcano, Barents Sea. *Appl Environ Microbiol* 73: 3348-3362.
15. Stahl DA, Amann R (1991) Nucleic acid techniques in bacterial systematics. In: Stackebrandt E, Goodfellow M, editors. Chichester, England: John Wiley & Sons Ltd. pp. 205-248.
16. Duperron S, Bergin C, Zielinski F, Blazejak A, Pernthaler A, et al. (2006) A dual symbiosis shared by two mussel species, *Bathymodiolus azoricus* and *Bathymodiolus puteoserpentis* (Bivalvia: Mytilidae), from hydrothermal vents along the northern Mid-Atlantic Ridge. *Environ Microbiol* 8: 1441-1447.

17. Manz W, Eisenbrecher M, Neu TR, Szewzyk U (1998) Abundance and spatial organization of Gram-negative sulfate-reducing bacteria in activated sludge investigated by in situ probing with specific 16S rRNA targeted oligonucleotides. *FEMS Microbiol Ecol* 25: 43-61.
18. Moussard H, Corre E, Cambon-Bonavita M-A, Fouquet Y, Jeanthon C (2006) Novel uncultured Epsilonproteobacteria dominate a filamentous sulphur mat from the 13°N hydrothermal vent field, East Pacific Rise. *FEMS Microbiol Ecol* 58: 449-463.
19. Amann RI, Binder BJ, Olson RJ, Chisholm SW, Devereux R, et al. (1990) Combination of 16S rRNA-targeted oligonucleotide probes with flow cytometry for analyzing mixed microbial populations. *Appl Environ Microbiol* 56: 1919-1925.
20. Daims H, Brühl A, Amann R, Schleifer KH, Wagner M (1999) The domain-specific probe EUB338 is insufficient for the detection of all Bacteria: development and evaluation of a more comprehensive probe set. *Syst Appl Microbiol* 22: 434-444.
21. Manz W, Amann R, Ludwig W, Wagner M, Schleifer K-H (1992) Phylogenetic Oligodeoxynucleotide Probes for the Major Subclasses of Proteobacteria: Problems and Solutions. *Syst Appl Microbiol* 15: 593-600.
22. Ravensschlag K, Sahm K, Amann R (2001) Quantitative Molecular Analysis of the Microbial Community in Marine Arctic Sediments (Svalbard). *Appl Environ Microbiol* 67: 387-395.
23. Raskin L, Stromley JM, Rittmann BE, Stahl DA (1994) Group-specific 16S rRNA hybridization probes to describe natural communities of methanogens. *Appl Environ Microbiol* 60: 1232-1240.
24. Crocetti G, Murto M, Björnsson L (2006) An update and optimisation of oligonucleotide probes targeting methanogenic Archaea for use in fluorescence in situ hybridisation (FISH). *J Microbiol Meth* 65: 194-201.
25. Wallner G, Amann R, Beisker W (1993) Optimizing fluorescent in situ hybridization with rRNA-targeted oligonucleotide probes for flow cytometric identification of microorganisms. *Cytometry* 14: 136-143.
26. Schreiber L, Holler T, Knittel K, Meyerdierks A, Amann R (2010) Identification of the dominant sulfate-reducing bacterial partner of anaerobic methanotrophs of the ANME-2 clade. *Environ Microbiol* 12: 2327-2340.
27. Ludwig W, Strunk O, Westram R, Richter L, Meier H, et al. (2004) ARB: a software environment for sequence data. *Nucl Acids Res* 32: 1363-1371.

## Supporting information of Chapter 4

## Supporting information of Chapter 4

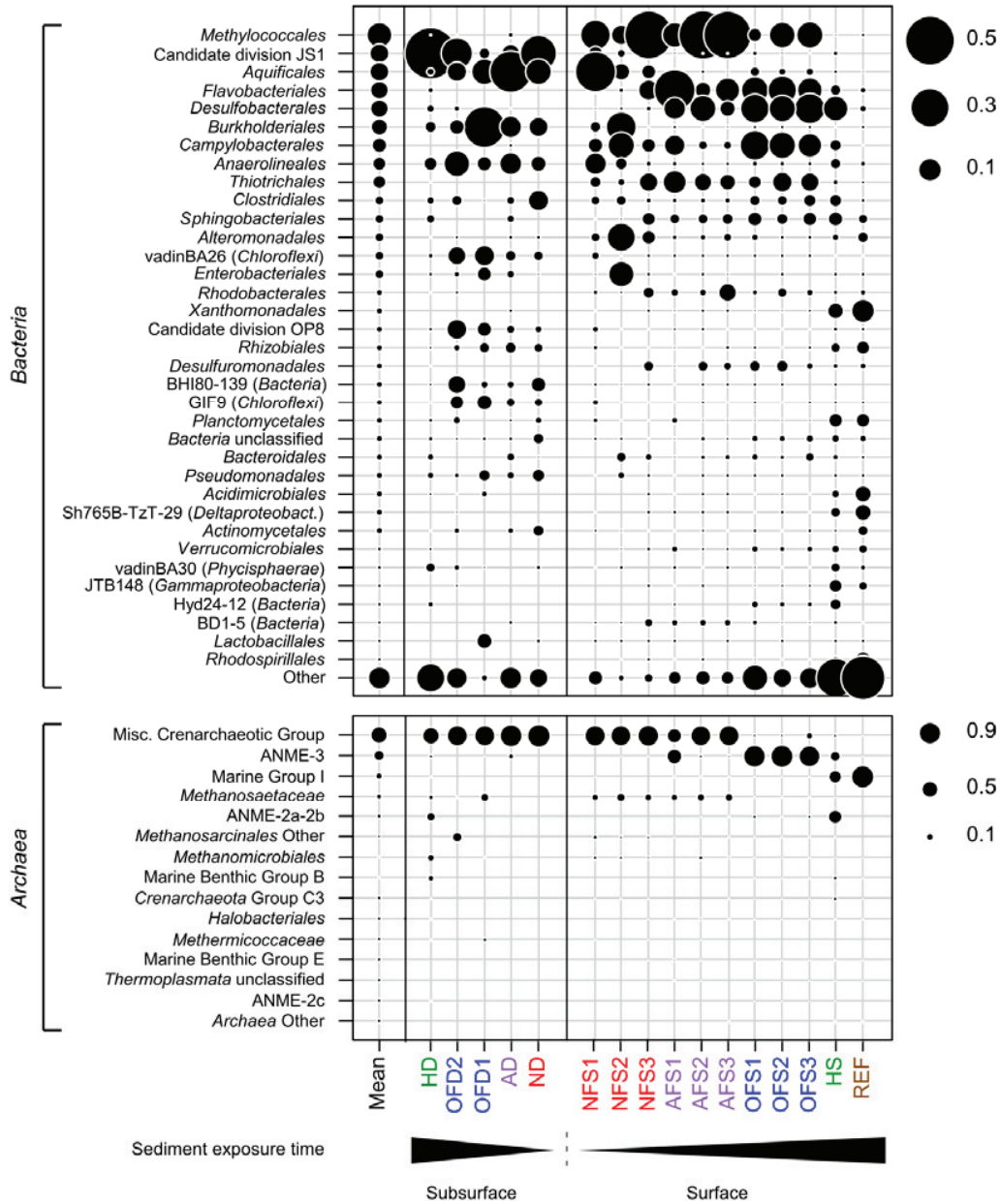


**Figure S1: Relative abundance of microbial clades**

The relative sequence abundance of microbial clades is represented by the size of the dots. The clades are sorted according to their average relative abundance in all investigated sediments. NF = new flow, AF = aged flow, OF = old flow, H = hydrate zone, REF = reference.

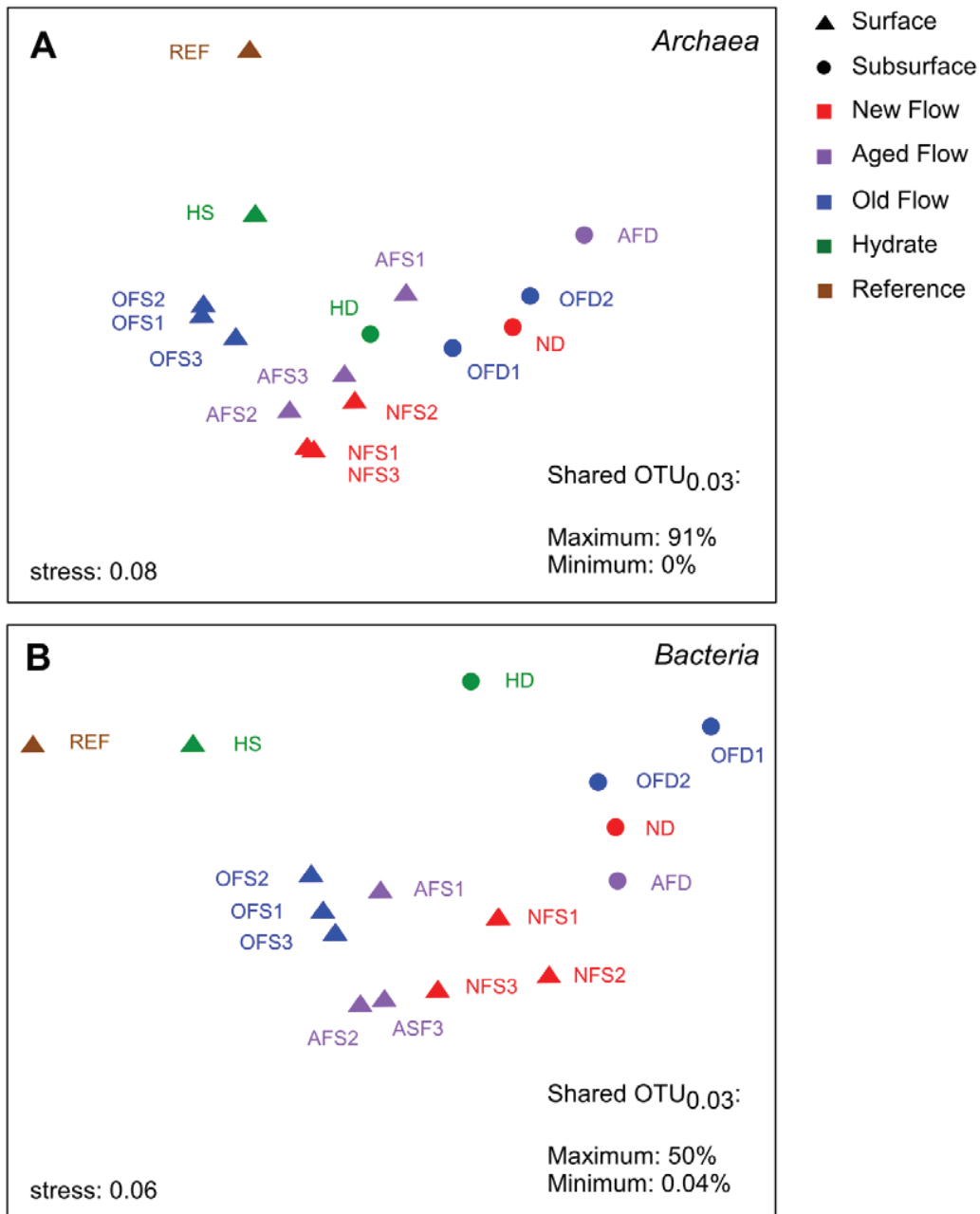


**Figure S2: Community structure of HMMV sediments**

The archaeal (**A**) and bacterial (**B**) community structure of HMMV sediments was visualized using non-metric multi dimensional scaling (NMDS) of Bray-Curtis dissimilarity matrices based on OTU<sub>0.03</sub> relative abundance data. The percentages of shared OTU<sub>0.03</sub> were determined based on presence absence data. The color coding indicates the succession of mud flows (red = new mud flow after eruption, purple = aged mud flow before eruption; blue = old mud flow; green= hydrate zone; brown = reference).

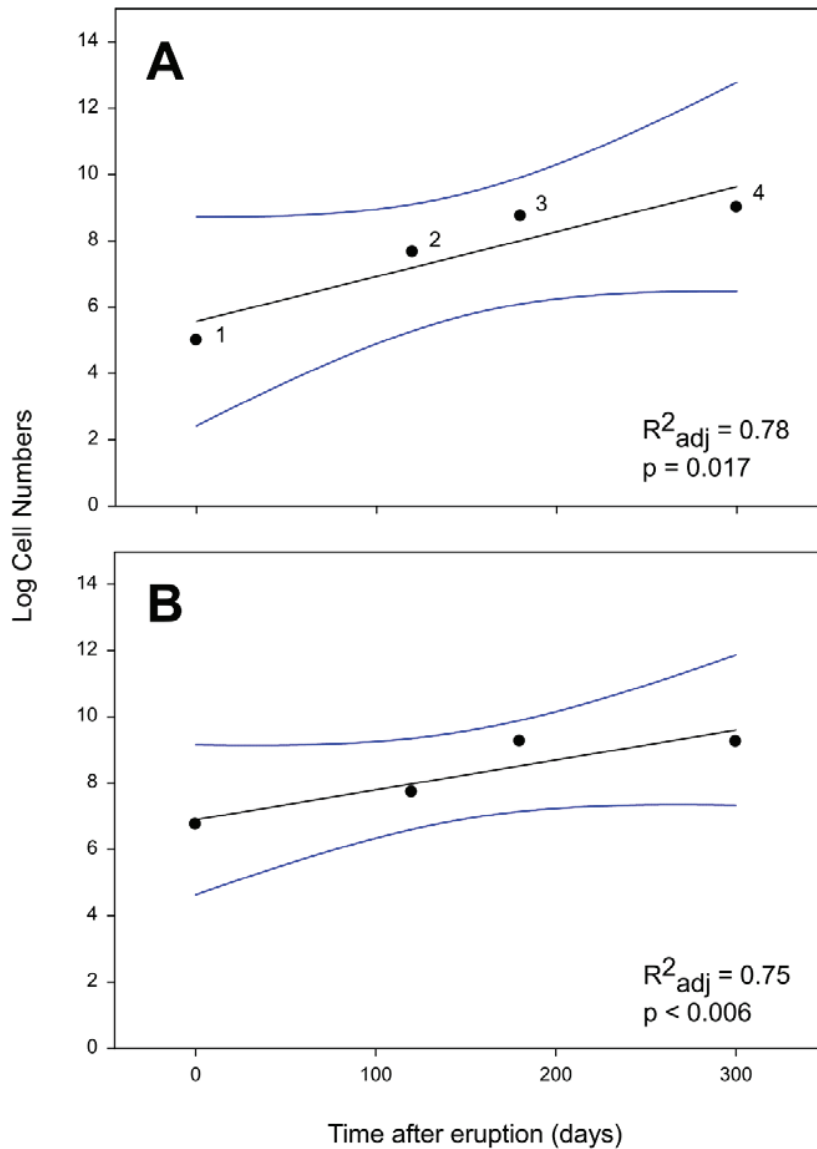


**Figure S3: Growth of microorganisms in mud flows**

Growth of *Methylococcales* (A) and *Bacteria* (B) in mud flows at Håkon Mosby mud volcano based on cell numbers per ml sediment (probe MTMC-701). We estimated a transport rate of 0.5 m per day and then used the distances of each sample to the active center to calculate the time between eruption and sampling, i.e. the number of days that the muds were exposed to ambient conditions. Cell numbers were log transformed. The blue lines show the 95% confidence band. 1:NFS2, 2: NFS2, 3: AFS2, 4: ASF3. Note: As we had to make several assumptions the trends are just indicative and need to be carefully repeated using more samples.

**Table S1: Station and sample overview.**

Sediment samples for sequencing were collected between 2003-2010 in the various HMMV habitats. Additionally, biogeochemical measurements had been performed to describe further the different sampling sites. More details about the biogeochemical methods and results can be found in Niemann et al., 2006 and Felden et al. 2010. Detailed results of the geochemical characterization are available via the Data Publisher for Earth & Environmental Science PANGAEA (<http://www.pangaea.de/>).

| Sample | Sediment<br>Depth<br>(m below<br>sea floor) | Habitat              | Event Label<br>(PANGAEA) | Year | °N       | °E        |
|--------|---|----------------------|--------------------------|------|----------|-----------|
| NFS1   | 0 - 0.2                                     | new flow surface     | PS74/169-1_puc-3         | 2009 | 72°0'18" | 14°43'35" |
| NFS2   | 0 - 0.2                                     | new flow surface     | PS74/168-1               | 2009 | 72°0'17" | 14°43'27" |
| NFS3   | 0 - 0.2                                     | new flow surface     | MSM16/2_838-1            | 2010 | 72°0'17" | 14°43'34" |
| NFD    | >2  | new flow deep        | PS64/332-1               | 2003 | 72°0'17" | 14°43'34" |
| AFS1   | 0 - 0.2                                     | aged flow surface    | PS64/312-1               | 2003 | 72°0'15" | 14°43'29" |
| AFS2   | 0 - 0.2                                     | aged flow surface    | MSM16/2_847-1            | 2010 | 72°0'15" | 14°43'37" |
| AFS3   | 0 - 0.2                                     | aged flow surface    | MSM16/2_855-1            | 2010 | 72°0'15" | 14°43'47" |
| AFD    | >2  | aged flow deep       | PS64/372-1               | 2003 | 72°0'16" | 14°43'36" |
| OFS1   | 0 - 0.2                                     | old flow surface     | PS64/317_puc-17          | 2003 | 72°0'09" | 14°43'53" |
| OFS2   | 0 - 0.2                                     | old flow surface     | PS74/172-1_puc-131       | 2009 | 72°0'19" | 14°43'34" |
| OFS3   | 0 - 0.2                                     | old flow surface     | MSM16/2_823-1            | 2010 | 72°0'10" | 14°43'57" |
| OFD1   | >2  | old flow deep        | PS64/371-1               | 2003 | 72°0'12" | 14°43'53" |
| OFD2   | >2  | old flow deep        | PS64/373-1               | 2003 | 72°0'12" | 14°43'40" |
| HS     | 0 - 0.2                                     | hydrate zone surface | PS64/326_puc-12          | 2003 | 72°0'04" | 14°43'08" |
| HD     | >2  | hydrate zone deep    | PS64/336-1               | 2003 | 72°0'01" | 14°43'34" |
| REF    | 0 - 0.2                                     | reference surface    | MSM16/2_809-1            | 2010 | 72°0'24" | 14°44'52" |

**Table S2: Sample overview**

*Archaea*

| Sample | Quality Reads |       | OTU <sub>0.03</sub> |    | Inverse Simpson |     | Chao1 Richness |    |
|--------|---------------|-------|---------------------|----|-----------------|-----|----------------|----|
|        | 1             | 2     | 1                   | 2  | 1               | 2   | 1              | 2  |
| Run *  |               |       |                     |    |                 |     |                |    |
| HD     | 2480          | 712   | 21                  | 14 | 3.2             | -   | 25             | -  |
| OFD2   | 106           | 34    | 3                   | 2  | -               | -   | -              | -  |
| OFD1   | 512           | 139   | 7                   | 5  | -               | -   | -              | -  |
| AFD    | 18            | 10    | 2                   | 2  | -               | -   | -              | -  |
| NFD    | 136           | 28    | 1                   | 1  | -               | -   | -              | -  |
| NFS1   | 20500         | 4884  | 32                  | 16 | 1.4             | 1.4 | 15             | 14 |
| NFS2   | 5467          | 1391  | 8                   | 7  | 1.5             | 1.6 | 5              | 8  |
| NFS3   | 21039         | 5761  | 32                  | 21 | 1.4             | 1.3 | 20             | 50 |
| AFS1   | 971           | 282   | 17                  | 13 | -               | -   | -              | -  |
| AFS2   | 23994         | 6062  | 93                  | 50 | 1.7             | 1.6 | 40             | 48 |
| AFS3   | 4781          | 1225  | 33                  | 20 | 1.5             | 1.4 | 19             | 21 |
| OFS2   | 37204         | 10769 | 163                 | 68 | 1.1             | 1.1 | 25             | 21 |
| OFS1   | 38273         | 11541 | 91                  | 33 | 1.1             | 1.1 | 5              | 14 |
| OFS3   | 30163         | 8656  | 113                 | 47 | 1.3             | 1.3 | 74             | 29 |
| HS     | 30106         | 8655  | 156                 | 91 | 4.7             | 4.6 | 54             | 54 |
| REF    | 33797         | 10323 | 219                 | 94 | 1.9             | 1.8 | 35             | 43 |

*Bacteria*

| Sample | Quality Reads |      | OTU <sub>0.03</sub> |      | Inverse Simpson |     | Chao1 Richness |      |
|--------|---------------|------|---------------------|------|-----------------|-----|----------------|------|
|        | 1             | 2    | 1                   | 2    | 1               | 2   | 1              | 2    |
| Run *  |               |      |                     |      |                 |     |                |      |
| HD     | 8828          | 3068 | 343                 | 228  | 3.0             | 3.3 | 250            | 303  |
| OFD2   | 1889          | 645  | 136                 | 96   | -               | -   | -              | -    |
| OFD1   | 425           | 165  | 35                  | 28   | -               | -   | -              | -    |
| AFD    | 6878          | 2370 | 353                 | 184  | 8               | 9   | 455            | 307  |
| NFD    | 3853          | 1431 | 183                 | 114  | 12              | -   | 360            | -    |
| NFS1   | 18834         | 6510 | 911                 | 475  | 10              | 10  | 528            | 477  |
| NFS2   | 19677         | 7495 | 375                 | 242  | 11              | 11  | 248            | 284  |
| NFS3   | 16681         | 5375 | 1001                | 505  | 10              | 11  | 729            | 655  |
| AFS1   | 15789         | 5289 | 1079                | 550  | 9               | 10  | 919            | 733  |
| AFS2   | 21739         | 7345 | 1006                | 583  | 9               | 11  | 761            | 641  |
| AFS3   | 17483         | 5881 | 715                 | 415  | 9               | 10  | 677            | 538  |
| OFS1   | 21611         | 8187 | 2319                | 1266 | 62              | 69  | 1567           | 1589 |
| OFS2   | 15604         | 5458 | 1340                | 724  | 31              | 37  | 817            | 1053 |
| OFS3   | 20064         | 7098 | 1723                | 975  | 43              | 48  | 1283           | 1318 |
| HS     | 20219         | 7693 | 3421                | 1937 | 266             | 226 | 2179           | 2469 |
| REF    | 24651         | 9247 | 5788                | 2999 | 263             | 215 | 3907           | 3623 |

\* To confirm the observed species richness and evenness we sequenced each sample twice (run 1 and run 2) using the same DNA and methods

**Table S3: Oligonucleotide probes used in this study**

| Oligonucleotides | Specificity  | Target Gene | Target Position | FA conc. (% v/v) | Nucleotide Sequence 5'-3'   | Reference |
|------------------|--|-------------|-----------------|------------------|-----------------------------|-----------|
| ANME-3-1249      | ANME-3   | 16S rRNA    | 1249-1266       | 30               | TCG GAG TAG GGA CCC ATT     | [1]       |
| ANME-3-1249H3    | Helper   | 16S rRNA    | 1249-1266       | 30               | GTC CCA ATC ATT GTA GCC GGC | [2]       |
| ANME-3-1249H5    | Helper   | 16S rRNA    | 1249-1266       | 30               | TTA TGA GAT TAC CAT CTC CTT | [2]       |
| Arch915          | most <i>Archaea</i>                                | 16S rRNA    | 915-934         | 35               | GTG CTC CCC CGC CAA TTC CT  | [3]       |
| DSS658           | <i>Desulfosarcina/ Desulfococcus</i> and relatives | 16S rRNA    | 658-675         | 50               | TCC ACT TCC CTC TCC CAT     | [4]       |
| Eub338-I         | most <i>Bacteria</i>                               | 16S rRNA    | 338-355         | 35               | GCT GCC TCC CGT AGG AGT     | [5]       |
| Eub338-II        | most <i>Planctomycetales</i>                       | 16S rRNA    | 338-355         | 35               | GCA GCC ACC CGT AGG TGT     | [6]       |
| Eub338-III       | most <i>Verrucomicrobiales</i>                     | 16S rRNA    | 338-355         | 35               | GCT GCC ACC CGT AGG TGT     | [6]       |
| MTMC701          | most <i>Methylococcales</i>                        | 16S rRNA    | 701-718         | 40               | GTG TTC CTT CAG ATC TCT     | [7]       |
| c1-MTMC701       | Competitor   | 16S rRNA    | 701-718         | 40               | GTA TTC CTT CAG ATC TCT     | [8]       |
| c2-MTMC701       | Competitor   | 16S rRNA    | 701-718         | 40               | GTG TTC CTC CAG ATC TCT     | [8]       |
| NON338           | Nonsense probe                                     | -           | -               | 35               | ACT CCT ACG GGA GGC AGC     | [9]       |

**Table S4: Percentage of shared OTUs between HMMV habitats**

|                 | New Flow  | Aged Flow | Old Flow | Hydrate |    |
|-----------------|-----------|-----------|----------|---------|----|
| <i>Archaea</i>  | Aged Flow | 15        |          |         |    |
|                 | Old Flow  | 5         | 13       |         |    |
|                 | Hydrate   | 4         | 5        | 6       |    |
|                 | Reference | 1         | 1        | 1       | 8  |
| <i>Bacteria</i> | Aged Flow | 13        |          |         |    |
|                 | Old Flow  | 15        | 15       |         |    |
|                 | Hydrate   | 20        | 20       | 19      |    |
|                 | Reference | 18        | 19       | 18      | 21 |

## References

1. Niemann, H.; Lösekann, T., et al. (2006). "Novel microbial communities of the Haakon Mosby mud volcano and their role as a methane sink." *Nature*, **443**: 854-858.
2. Lösekann, T.; Knittel, K., et al. (2007). "Diversity and Abundance of Aerobic and Anaerobic Methane Oxidizers at the Haakon Mosby Mud Volcano, Barents Sea." *Appl Environ Microbiol*, **73**: 3348-3362.
3. Stahl, D.A. and Amann, R. (1991). "Nucleic acid techniques in bacterial systematics." Stackebrandt, E. and Goodfellow, M., John Wiley & Sons Ltd.: 205-248.
4. Manz, W.; Eisenbrecher, M., et al. (1998). "Abundance and spatial organization of Gram-negative sulfate-reducing bacteria in activated sludge investigated by in situ probing with specific 16S rRNA targeted oligonucleotides." *FEMS Microbiol Ecol*, **25**: 43-61.
5. Amann, R.I.; Binder, B.J., et al. (1990). "Combination of 16S rRNA-targeted oligonucleotide probes with flow cytometry for analyzing mixed microbial populations." *Appl Environ Microbiol*, **56**: 1919-1925.
6. Daims, H.; Brühl, A., et al. (1999). "The domain-specific probe EUB338 is insufficient for the detection of all Bacteria: development and evaluation of a more comprehensive probe set." *Syst Appl Microbiol*, **22**: 434-444.
7. Boetius, A.; Ravensschlag, K., et al. (2000). "A marine microbial consortium apparently mediating anaerobic oxidation of methane." *Nature*, **407**: 623-626.
8. Ruff, S.E.; Arnds, J., et al. (2013). "Microbial Communities of Deep-Sea Methane Seeps at Hikurangi Continental Margin (New Zealand)." *PLoS ONE*, **8**: e72627.
9. Wallner, G.; Amann, R., et al. (1993). "Optimizing fluorescent in situ hybridization with rRNA-targeted oligonucleotide probes for flow cytometric identification of microorganisms." *Cytometry*, **14**: 136-143.

## Miscellaneous

## **Additional contributions to scientific publications and projects**

Hankeln, W., N. J. Wendel, J. Gerken, J. Waldmann, P. L. Buttigieg, I. Kostadinov, R. Kottmann, P. Yilmaz and F. O. Glöckner (2011). "CDinFusion - Submission-Ready, On-Line Integration of Sequence and Contextual Data." PLoS ONE **6**: e24797.

Contribution: Advice on usability and beta-testing of the new tool using 16S rRNA gene libraries that were constructed from cold seep sediment of Hikurangi margin, New Zealand.

Kuhfuss, H. (2013). „Investigations on AOM-mediating microorganisms at a shallow water methane gas seep in the Mediterranean Sea.” Magisterarbeit, Fakultät für Biologie, Albert-Ludwigs-Universität Freiburg im Breisgau. p. 124

Contribution: Assistance with gene libraries, sequence processing and phylogenetic tree reconstruction

Angelov, B. (2013). “Mud Volcanoes: A Window to the Deep Biosphere. Investigating succession and functional shifts in marine deep subsurface microbial communities exposed to mud volcanism.” Master Thesis, Fachbereich 2 Biologie/Chemie, Universität Bremen. p. 49.

Contribution: Co-supervision

## Curriculum Vitae

### Personal

Name: Sebastian Emil Ruff  
Date of Birth: 22.08.1981  
Place of Birth: Waiblingen, Germany  
Nationality: German  
Address: Falkenbergerstrasse 28, 28215 Bremen

### Education

- 09/2010 - 09/2013 Dissertation at Max Planck Institute for Marine Microbiology, Bremen  
**Microbial community ecology of marine methane seeps**
- 11/2009 – 08/2010 Diploma thesis at Max Planck Institute for Marine Microbiology, Bremen  
**Microbial communities of marine methane seeps at Hikurangi Margin (New Zealand)**
- 10/2003 – 08/2010 Studies of Technical Biology at Universität Stuttgart
- 11/2007 – 07/2008 Bachelor thesis at Max Planck Institute for Solid State Research, Stuttgart  
**Metallization of tobacco mosaic viruses to produce ferrofluids with enhanced magnetoviscosity**

### Science Outreach (selection)

- 11.10.2012 Klima Orakel – Section in the weekly *Handelsblatt* online  
Author – „Wie Mikroorganismen das Klima beeinflussen“
- 02.06.2012.1.1.1 Lange Nacht der Wissenschaft – Max Planck Science Gallery, Berlin  
Speaker – „Mikroben der Tiefsee - Leben am Energielimit“
- 16.02.2012 H<sub>2</sub>B – Studieren, forschen, leben in Bremen und Bremerhaven  
Interview for a PR-Supplement in the weekly newspaper *Die Zeit*
- 20.05.2011 Happy Hour – Radiostation Bremen 4  
Interview – „Junge Forscher der marinen Mikrobiologie in Bremen“
- 02/2011 – Ozeaneum – Deutsches Meeresmuseum, Stralsund  
Scientific advice for an exhibit on the Census of Marine Life
- 05/2006 – 08/2010 Museum of Natural History, Stuttgart  
Tour guide for school classes, families and adults
- 05/2009 – 07/2010 Wilhelma – Zoological Botanical Gardens, Stuttgart  
Tour guide for school classes

### Teaching Experience (selection)

- 09/2012-04/2013 Max Planck Institute for Marine Microbiology, Bremen  
Supervision – Master thesis in molecular ecology
- 04-05/2012 Max Planck Institute for Marine Microbiology, Bremen  
Supervision – Student project in molecular ecology
- 02/2011 Max Planck Institute for Marine Microbiology, Bremen  
Graduate assistant – Molecular ecology course for MarMic students

### Oral Presentations (selection)

- 21.08.2012 “Microbial communities of marine methane seeps: Sketching the big picture.”  
ISME Conference, Copenhagen, Denmark
- 21.03.2012 “Microbial communities of marine methane seeps: Sketching the big picture.”  
Annual Conference of the Association for General and Applied Microbiology (VAAM), Tübingen, Germany
- 29.07.2011 “Aerobic and anaerobic methanotrophs of marine methane seep sediments.”  
Girguis Laboratory, Harvard, Boston, USA
- 06.04.2011 “Life in the cold, dark south - Microbial communities of marine methane seeps at Hikurangi margin (New Zealand).”  
Annual Conference of the Association for General and Applied Microbiology (VAAM), Karlsruhe, Germany

### Awards

Poster Award at Gordon Research Conference – Marine Microbes 2012, Barga, Italy  
MarMic Teaching Award – Best Practical Course 2011, Bremen, Germany  
4<sup>th</sup> price at MBL Scientific Photography Contest 2011, Woods Hole, MA, USA

### Publications

Wu, Z.; Müller, A.; Degenhard, S.; **Ruff, S. E.**; Geiger, F.; Bittner, A. M.; Wege, C.; Krill, C. E. (2010). „Enhancing the magnetoviscosity of ferrofluids by the addition of biological nanotubes”. *ACS Nano*, **4**, 4531-4538.

Wu, Z.; Zierold, R.; Müller, A.; **Ruff, S. E.**; Ma, C.; Khan, A. A.; Geiger, F.; Sommer, B. A.; Knez, M.; Nielsch, K.; Bittner, A. M.; Wege, C.; Krill, C. E. (2010). „Preparation and magneto-viscosity of nanotube ferrofluids by viral scaffolding and ALD on porous templates.” *Physica Status Solidi B*, **247**, 2412-2423.

Name: Sebastian Emil Ruff

Bremen, den

Anschrift: Falkenbergerstrasse 28, 28215 Bremen

## **Erklärung**

Hiermit erkläre ich, dass ich die Doktorarbeit mit dem Titel:

### **Microbial community ecology of marine methane seeps**

selbstständig verfasst und geschrieben habe und außer den angegebenen Quellen keine weiteren Hilfsmittel verwendet habe.

Ebenfalls erkläre ich hiermit, dass es sich bei den von mir abgegebenen Arbeiten um drei identische Exemplare handelt.

Unterschrift

